AD-A154 711 THREE-DIMENSIONAL PHOTOCHEMICAL MACHINING WITH LASERS (U) BATTELLE COLUMBUS LABS OH R E SCHWERZEL ET AL. 28 DEC 84 AFOSR-TR-85-0456 F49620-82-C-0077

1/3

UNCLASSIFIED F/G 13/8 NL

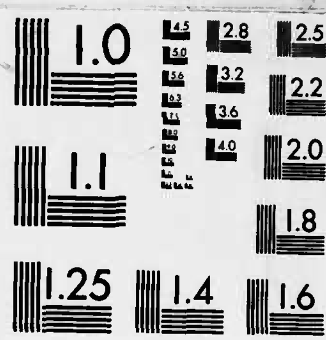

MICROCOPY RESOLUTION TEST CHART
NATIONAL BUREAU OF STANDARDS-1963-A

AFOSR-TR. 85-0456

Battelle
Columbus Laboratories

AD-A154 711

Report

THREE-DIMENSIONAL PHOTOCHEMICAL
MACHINING WITH LASERS

to

U.S. AIR FORCE
OFFICE OF SCIENTIFIC RESEARCH

December, 1984

FINAL TECHNICAL REPORT

on

THREE-DIMENSIONAL PHOTOCHEMICAL MACHINING WITH LASERS

to

U.S. AIR FORCE
OFFICE OF SCIENTIFIC RESEARCH

December, 1984

Principal Investigator: Robert E. Schwerzel
Project Team Members: William A. Ivancic, Dean R. Johnson, Vincent D. McGinniss, and Van E. Wood
Project Consultants: Jerry A. Jenkins, Steven Kramer, and Wyn Kelly Swainson

BATTELLE
Columbus Laboratories
505 King Avenue
Columbus, OH 43201

Battelle
Columbus Laboratories
505 King Avenue
Columbus, Ohio 43201-2693
Telephone (614) 424-6424
Telex 24-5454

February 11, 1985

Capt. Kevin Malloy
AFOSR/NE
Directorate of Electronics
And Materials Science
Building 410
Bolling AFB, DC 20332

Dear Kevin:

Re: DARPA Contract No. F49620-82-C-0077

I am pleased to submit for your consideration the enclosed three (3) copies of the Final Report for the subject contract, entitled "Three-Dimensional Photochemical Machining With Lasers". I apologize for the delay in getting this report to you, and hope that you have not been inconvenienced as a result. The report describes our work during the past two years in some detail, and I trust that it will be satisfactory to you.

Our research efforts have been directed primarily toward the development of novel photoinitiator systems that will trigger the desired polymerization reactions only when irradiated with two laser beams of different colors, not by either beam alone. This work has led to the synthesis of several promising new compounds, and has succeeded in identifying a number of new polymer/initiator combinations which exhibit the desired behavior to some degree. Several of these compositions may have promise as high-resolution photoresists, as well. A new concept for a rapidly focusing optical system, to help move the focal point of the laser beams within the photosensitive material, has also been developed during this project.

Much work remains to be done, despite these successes, before a truly viable prototype system can be built. In particular, problems still remain with the photosensitive polymers studied to date, in that some residual "single-beam" polymerization still tends to occur along one or the other beam path, with a corresponding loss of resolution at the focal point. We feel that this difficulty can be overcome with further improvements in the photoinitiator molecules, on the basis of the known spectroscopy of the best photosensitizers we have found, but this will require some effort. Further development also needs to be done on the optical system to focus and direct the laser beams, and on a computer interface to control the whole photochemical machining system. It is my hope that research on these tasks can be carried out with funding from the private sector in the near future.

As you know, we have had a number of requests for detailed information about our work on this program from companies, both in the United States and abroad, which are considering possible participation in the future development of this field. May we have your permission to distribute copies of this report to those who have requested it? I would appreciate your guidance on this, as it is my understanding that the report cannot be distributed to the public (and to foreign companies, in particular) without your approval.

I anticipate that I will be in Washington next Wednesday, February 20th, and would be pleased to stop in at your convenience to review the report with you on an informal basis if you wish. Also, please feel free to call me at (614) 424-5637 should you have any questions about our work. It has been a pleasure to work with you, Harry Winsor, and Steve Wax on this project for the past two years, and I hope we will have the opportunity to assist you with your research needs again in the future.

Best regards,

Bob

Robert E. Schwerzel, Ph.D.
Senior Research Scientist
Organic and Polymer Chemistry

RES:lnl
Encl.

cc: Director, Advanced Research Projects Agency (2 copies)
ATTN: Maj. Steven Wax, Program Manager
Materials Sciences Division
1400 Wilson Blvd.
Arlington, VA 22209

Mr. Frank M. Clark (2 copies)
Contracting Officer
AFOSR
Building 410
Bolling AFB, DC 20332

JNCLASSIFIED
RITY CLASSIFICATION OF THIS PAGE

REPORT DOCUMENTATION PAGE

EPORT SECURITY CLASSIFICATION UNCLASSIFIED	1b. RESTRICTIVE MARKINGS NONE
ECURITY CLASSIFICATION AUTHORITY NONE	3. DISTRIBUTION/AVAILABILITY OF REPORT Approved for public release; distribution unlimited. UNRESTRICTED
DECLASSIFICATION/DOWNGRADING SCHEDULE NONE	
ERFORMING ORGANIZATION REPORT NUMBER(S)	5. MONITORING ORGANIZATION REPORT NUMBER(S) AFOSR-TR- 85-0456
NAME OF PERFORMING ORGANIZATION ttelle Memorial Institute lumbus Laboratories 6b. OFFICE SYMBOL (If applicable)	7a. NAME OF MONITORING ORGANIZATION Air Force Office of Scientific Research/Directorate of Electronics & Materials Science
ADDRESS (City, State, and ZIP Code) 5 King Avenue lumbus, Ohio 43201	7b. ADDRESS (City, State, and ZIP Code) Building 410 Bolling AFB, DC 20332
NAME OF FUNDING/SPONSORING ORGANIZATION ef. Adv. Res. Proj. Agency 8b. OFFICE SYMBOL (If applicable)	9. PROCUREMENT INSTRUMENT IDENTIFICATION NUMBER Contract No. F49620-82-C-0077
ADDRESS (City, State, and ZIP Code) aterials Sciences Division 400 Wilson Blvd. rlington, VA 22209	10. SOURCE OF FUNDING NUMBERS PROGRAM ELEMENT NO. 61102F; PROJECT NO. 2306; TASK NO. B2; WORK UNIT ACCESSION NO.

TITLE (Include Security Classification)

hree-Dimensional Photochemical Machining With Lasers

PERSONAL AUTHOR(S)

obert E. Schwerzel, William A. Ivancic, Dean R. Johnson, Vince D. McGinniss & Van E. Wood

. TYPE OF REPORT	13b. TIME COVERED	14. DATE OF REPORT (Year, Month, Day)	15. PAGE COUNT
inal Technical Report	FROM 6/1/82 TO 9/30/84	1984, Dec. 28	112 + Appendix

SUPPLEMENTARY NOTATION

COSATI CODES			18. SUBJECT TERMS (Continue on reverse if necessary and identify by block number)
FIELD	GROUP	SUB-GROUP	Photochemical Machining, Lasers, Polymers, Photoinitiators, Photosensitizers, Porphyrins, Prototypes, Investment Casting.

ABSTRACT (Continue on reverse if necessary and identify by block number)

The primary objective of this research has been to evaluate the technical feaibility of three-dimensional photochemical machining with lasers, or PCM. PCM is a concept for the rapid fabrication of high-precision three-dimensional solid objects by spatially selective photopolymerization (or, alternatively, de-polymerization) at the intersection point of two intersecting laser beams. To obtain true spatially selective photochemistry, it is necessary to develop systems in which the first laser beam (Beam 1) will pump a photoinitiator or photosensitizer to an unreactive, and spontaneously reversible, metastable intermediate with an energy content less than that required to initiate the desired reaction. The second laser beam (Beam 2) then selectively pumps the intermediate species to an energy level above that required to fragment the photoinitiator and trigger the reaction. In this way, the photochemical reaction can be confined to the intersection point, with no reaction occurring in either beam above. cont keywords include:

. DISTRIBUTION/AVAILABILITY OF ABSTRACT ☒ UNCLASSIFIED/UNLIMITED ☐ SAME AS RPT. ☐ DTIC USERS	21. ABSTRACT SECURITY CLASSIFICATION UNCLASSIFIED
a. NAME OF RESPONSIBLE INDIVIDUAL Kevin J Malloy, Capt, USAF	22b. TELEPHONE (Include Area Code) (202) 767-4931 — 22c. OFFICE SYMBOL NE

D FORM 1473, 84 MAR — 83 APR edition may be used until exhausted. All other editions are obsolete.

SECURITY CLASSIFICATION OF THIS PAGE

UNCLASSIFIED

he research performed during the course of this project has confirmed the technical easibility of the PCM concept, and has demonstrated the occurrence of selective and/or nhanced photopolymerization for several combinations of photosensitizers, photoinitiators, and polymers. The most promising systems examined to date appear to be those ased on porphyrin sensitizers (such as meso-tetraphenyl porphyrin), benzoin ether or etone/amine photoinitiators, and crosslinking acrylic polymers. Some of these materials ay have promise as high-contrast photoresists, as well. A preliminary design for a apid-focus optical system for PCM has also been developed during this project, and U.S. atent applications have been filed for this and the photopolymer system described above.

considerable amount of further research is required to fully develop a working PCM ystem, however. Problems still remain with single-beam polymerization in several of the ore promising polymer systems, resulting from two-photon events occurring in a single aser beam because of overlap in the absorption spectra of the ground-state photosensiizer and the intermediate species. Much work also remains to be done in developing uitable optics and computer interfacing for controlling the motion of the intersection oint within the polymer material. Despite this, however, the process appears to be easible, and there appear to be no fundamental barriers to developing an operational PCM ystem.

ABSTRACT

The fabrication of objects having complex, three-dimensional shapes frequently requires a substantial expenditure of time, labor, and capital. This is particularly true of manufacturing techniques such as investment casting, where a wax or plastic replica of the finished object must be made before an actual metal casting can be produced. Because this process necessarily employs much skilled hand labor, many weeks or months may be required to proceed from design specifications to a prototype casting. Clearly, much cost and effort could be saved if it were possible to fabricate a complex plastic pattern directly from design data without the intermediacy of a hand-made metal mold or die.

The research program described in this report has been designed to evaluate a novel technology which has the potential to revolutionize the casting industry. The key to this new technology, which may be referred to as "Photochemical Machining", or PCM, is the computer-assisted fabrication of a plastic pattern directly from design specifications, by the selective, three-dimensional modification of a plastic material which is exposed simultaneously to two different laser beams which are focused onto a single point within the volume of the material.

If the chemical composition of a plastic material were designed properly, the solubility and hardness of the plastic could, in principle, be altered selectively at the point of intersection of the two beams without being affected by either beam alone. Given such a material, a three-dimensional object of any desired complexity could be fabricated directly by appropriate movements of the two laser beams (and thus of the intersection point) throughout the volume of the material. The softer, more soluble portions of the plastic could then be removed selectively, leaving a hard, rigid plastic piece having the desired shape.

Ideally, this piece would be suitable for immediate use for investment casting, electroplating, and so on, with minimal finishing being required. In this way, for example, prototype designs could easily be subjected to "real-world" test conditions and then modified easily and inexpensively by repeating the PCM process described above as often as needed to fully optimize the design. This could result in dramatic sav-

ings of time, labor, and cost. In addition, the complete three-dimensional flexibility provided by the PCM concept could lead to the casting of complex shapes which are at present difficult to fabricate, and make possible the production of precise castings which require minimal subsequent machining or finishing.

The research conducted on this project during the past two years has been successful in confirming the technical feasibility of the PCM concept, in developing a theoretical framework for relating optical and materials properties to the performance of a PCM system, and in designing and synthesizing several novel photosensitive compounds whose spectroscopic properties make them attractive candidates for use in a PCM system. These compounds are capable of initiating selective and/or enhanced polymerization when they are irradiated with laser beams of two different wavelengths.

The most promising systems studied to date appear to be those based on porphyrin sensitizers, benzoin ether or ketone/amine photoinitiators, and crosslinking acrylic polymers. Some of these materials may have promise as high-contrast photoresists, as well. A preliminary design for a rapid-focus optical system for PCM has also been developed during the project.

A considerable amount of further research is required to fully develop a working PCM system, however. Problems still remain with single-beam polymerization in several of the more promising polymer systems, resulting from two-photon events occurring in a single laser beam because of overlap in the absorption spectra of the ground-state photosensitizer and the intermediate species. Much work also remains to be done in developing suitable optics and computer interfacing for controlling the motion of the intersection point within the polymer material. Despite this, however, the process appears to be feasible, and there appear to be no fundamental barriers to developing an operational PCM system.

TABLE OF CONTENTS

APPENDIX

LIST OF FIGURES

TABLE OF CONTENTS
(Continued)

TABLE OF CONTENTS
(Continued)

LIST OF TABLES

FINAL TECHNICAL REPORT

on

THREE-DIMENSIONAL PHOTOCHEMICAL MACHINING WITH LASERS

to

U.S. AIR FORCE
OFFICE OF SCIENTIFIC RESEARCH

from

BATTELLE
Columbus Laboratories

December, 1984

INTRODUCTION

The production of castings having complex, three-dimensional shapes is so commonplace in today's technology that the enormous amount of painstaking manual effort involved is easily overlooked. Skilled artisans must labor for days or months to transform a set of blueprints and specifications into a "real" object, or to create the dies used to fabricate stamped or molded objects. Similarly, the duplication of an existing object may require the production of a mold from which a replica can be cast, or the fabrication of a replica by hand. While the gradual introduction of computer-assisted design and manufacturing techniques has increased the speed and flexibility of certain processes, a great deal of manual, artistic skill is still required. Furthermore, many of the potential advantages of computer-assisted design and manufacturing are lost because of the intrinsic limitations of the conventional manufacturing techniques to which the computer is applied.

Conventional manufacturing technology requires not only the use of multiple tools--lathes for the generation of cylindrical ribbed or round forms, drills for holes, milling machines for flat surfaces, and so on, but it requires also the application of great force for the removal or displacement of the material being worked. And it combines this need for force with the need for precision.

Even where advanced numerical control (NC) techniques are used, great inefficiency occurs in the course of proceeding from original design concepts through blueprinting or other design documentation, to model-making and the preparation of NC control tapes or programs specifying the semiautomatic sequence of operations on separate lathes, milling machines, drills, and the like which are required to fabricate a finished piece.

Clearly, much time, effort, and expense could be saved if the capabilities of the computer could be used to assist in the production of three-dimensional phototypes directly in the design and fabrication stages. The same techniques could permit the replication of objects in nearly any desired size, given a computer-compatible description of the original. For instance, such diverse objects as automotive or aircraft parts, models for wind-tunnel tests, intricate three-dimensional models for architecture or structural engineering design studies, or prototype artificial prosthetic devices could all be described by the appropriate computer-compatible notation, and the design features optimized as much as possible by computer calculations. If the computer could then control directly the production of a prototype object, utilizing the optimized design parameters, the design could be evaluated immediately by examination or by experimental means. Given the appropriate computerized description, entire complex clusters, made of disposable pattern material and ready for casting, could be automatically generated, tested, and then remade by simple changes in the computer program for the correction of gates and sprue routing, proportion, size, quantity, and the like.

In such a system, there would be direct and efficient interaction between the design engineer and the actual manipulable object generated. The effect would be as though the design and manufacturing system operated as a perfectly flexible machine tool, capable of creating an infinite choice of complex shapes -- carburetor housings, gears, turbine blades, anthropomorphic forms, reentrant-shaped surfaces or holes, and so on.

It is the purpose of this report to describe the results of Battelle's efforts to date in evaluating and developing a novel concept which could form the basis for truly implementing the futuristic technology envisioned above. The key to this new concept, which may be referred to as "Photochemical Machining", or PCM, is the computer-assisted fabrication of a plastic pattern directly from design specifications by the selective, three-dimensional modification of a plastic material which is exposed simultaneously to two laser beams focused onto a single point within the volume of the material. If the chemical composition of the plastic is designed properly, the solubility and hardness of the plastic can, in principle, be altered selectively at the point of intersection of the two beams without being affected by either beam alone.

Given such a material, a three-dimensional object of any desired complexity could be fabricated directly by appropriate movements of the two laser beams (and thus of the intersection point) within the volume of the material. The softer, more soluble portions of the plastic could then be removed selectively by a variety of means, leaving a hard, rigid plastic piece having the desired shape. This piece could then be used directly for investment casting, electroforming, or other end-use applications, as desired.

While the PCM concept as summarized above seems in some respects to be particularly well suited to investment casting by "lost wax" techniques, in Battelle's view this new technology could provide major benefits to all facets of the casting industry and could, if fully developed and exploited, bring about a major change in the way manufacturing technology is perceived and practiced today.

Description of the Photochemical Machining Concept

The essential features of a conceptual PCM system for the computer-assisted photochemical fabrication of three-dimensional precision patterns are depicted in Figure 1. As mentioned above, the pattern is formed from a polymer which can either be photochemically crosslinked

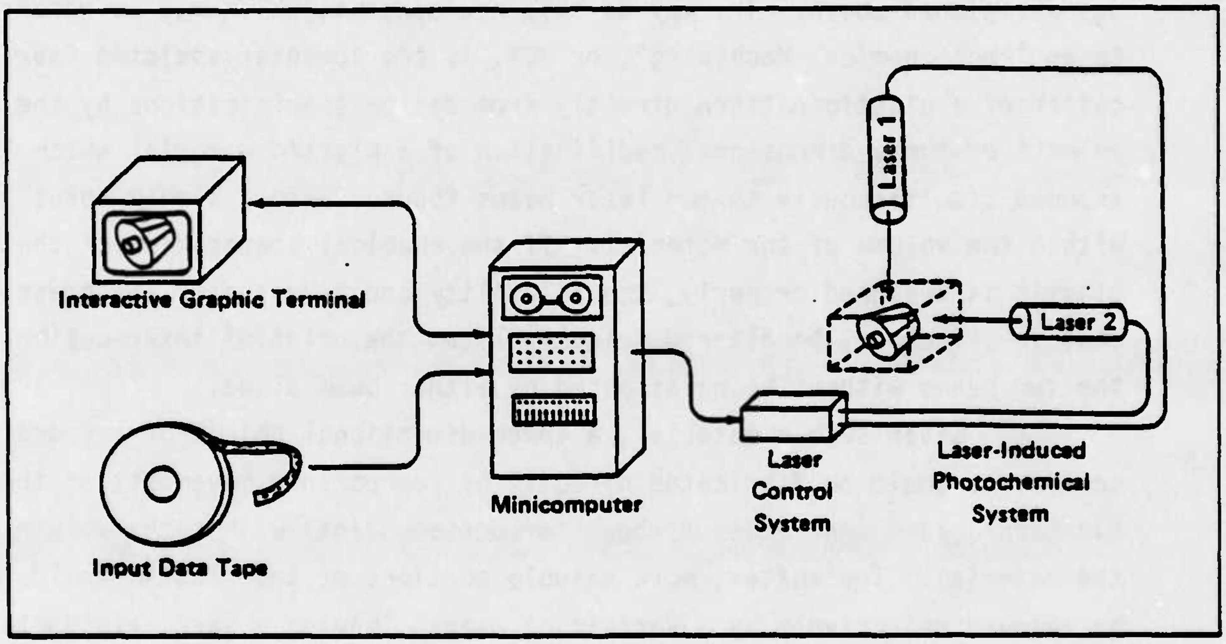

FIGURE 1. SCHEMATIC ILLUSTRATION OF A COMPUTER-ASSISTED PHOTOCHEMICAL MACHINING (PCM) SYSTEM

(made hard and insoluble) or degraded (made soft and easily dissolved or vaporized), depending on its chemical composition, by simultaneous exposure to the intersecting laser beams. In effect, the point of intersection of the laser beams serves as an infinitely flexible machine tool;

because the formation of the plastic pattern is achieved by means of photochemical reactions which occur only at the intersection point, the speed and efficiency of the process are affected only slightly by the complexity of the shape being produced.

In this conceptual PCM system, the minicomputer accepts input describing the size and shape of the object to be made, either from an interactive graphic terminal (which allows the operation the flexibility of drawing and modifying the design before a solid object is made) or from previously recorded data obtained elsewhere. It then generates the set of coordinates which will control the actual pattern-forming process. Such computerized input and data processing systems have been dramatically improved during the past several years and many machines of this type are now available commercially. Thus, the essential computer techniques already exist, for the most part, and relatively little effort should be required to modify them for use with the proposed PCM system.

Possible Modes of Operation

Depending on the properties of the polymer system and the requirements of the object to be formed, the PCM system can, in principle, be designed to operate in either of two modes:

- "Synthetic" Mode - In this mode, a rigid, crosslinked, insoluble polymer is formed by the photochemical crosslinking of a soluble, low molecular weight polymer precursor. The finished pattern is then "freed" by dissolving or vaporizing the uncrosslinked precursor.

- "Sculpting" Mode - In this mode, which is the converse of the synthetic mode, the precursor is a rigid, crosslinked polymer. The unwanted polymer is degraded at the reaction point, leaving the desired object unchanged; the degraded polymer may then be dissolved or vaporized, as above.

In both cases, the photochemical reactions which result in the formation of the object must occur only at the reaction point, and not in either beam alone. To achieve this, the chemical composition of the plastic must be designed in such a way that two photons (particles of light) are required to initiate the key photochemical reactions. A number of photochemical materials are amenable to this two-photon approach, and the choice of the reactions actually used will depend heavily on the properties desired in the final pattern. In general, however, the photochemical reactions will rely on the sequential absorption of two photons by the plastic material. The first photon will produce a reactive intermediate chemical species, and the second will cause an irreversible photochemical reaction of that intermediate. As the reactive intermediate will in general have absorption properties quite different from those of the precursor, there will be little chance of having the reaction occur in the presence of either beam alone. Thus, one laser beam will be of a color absorbed strongly by the original material, while the second beam will be of a color which is absorbed strongly by the reactive intermediate. As mentioned above, it is anticipated that the uncrosslinked portions of the plastic material will be removed either by dissolving them with an appropriate solvent or by vaporizing the material, leaving behind the hard, rigid plastic pattern. Note that the entire volume of the pattern need not be fully polymerized; it may be sufficient to simply harden a shell with a few internal supports in key locations.

While many of the components required for PCM have been developed to a significant extent, the commercial feasibility of developing an operational PCM system has not yet been demonstrated. It remains to fully evaluate the chemical and optical constraints on the operation of a PCM system, to develop and optimize the various system components which will be required, and to construct and evaluate a fully operational device which will be suitable for the fabrication of patterns for precision casting applications. Our research effort in this program has been directed toward these goals.

Anticipated Benefits of a PCM System

We envision that a PCM system, once developed, would offer its users significant benefits in speed, convenience, precision, and cost as compared to conventional techniques. The novel capabilities which a PCM system would offer include the following:

- Rapid Computer-Assisted Fabrication. The fabrication of the plastic pattern would be accomplished under computer control, using coordinates generated by the computer from the optimized design information. This would eliminate much of the costly, time-consuming hand labor which is now required for the fabrication of patterns, and could reduce the time required to produce a prototype casting from several months to several days or less.

- Design Optimization. Through the use of interactive input, the user could, if desired, design optimized shapes for a variety of cast metal or plastic objects, using the computer and the PCM system to fabricate prototype castings which could then be evaluated under actual test conditions. This process would avoid much of the time-consuming manual trial-and-error process currently involved in the design and fabrication of prototype cast parts, particularly for those parts which can be made by investment casting techniques. The application of the PCM concept to investment casting seems particularly attractive in this context, as in principle the plastic piece could be used directly in a "lost wax" process.

- Precise Scaling. The size of the objects produced could be scaled up and down easily by adjusting the output parameters of the computer control system.

- Reduced Need for Subsequent Machining. The objects produced will be hard, dry, and ready for examination, plating, or other uses as desired. In addition, because of the ease with which a PCM system will be able to fabricate complex shapes, it should be possible to produce castings with complex curvatures, internal holes or structures, and even prethreaded holes for screws or other fittings. Thus, castings produced by the PCM method should require less subsequent machining than those produced by conventional techniques.

Background Information

The concept for photochemical machining described above has its origins in research performed independently during the past decade by scientists at Battelle's Columbus Laboratories and at the Formigraphic Engine Corporation, a small company located in Oakland, California. The original patent application, which describes all of the essential features of a PCM system, was filed in 1967 by Mr. W. K. Swainson, now president of the Formigraphic Engine Corporation and a consultant to Battelle for this research program. This was followed by other patent applications by Mr. Swainson which described specific components and applications of the PCM concept in more detail. Meanwhile, scientists at Battelle's Columbus Laboratories independently filed patent applications describing their work on a three-dimensional real-time fluorescent display system (that is, a "3-D oscilloscope"). This research involved the use of intersecting light beams to produce an isolated fluorescent spot, which could be moved in three dimensions as the point of intersection of the beams was moved. Thus,the 3-D fluorescent display system encompassed many of the concepts which are implicit in photochemical machining.

These patent applications eventually led to the issuance of U.S. Patents 3,609,706 and 3,829,838 to Battelle, and U.S. patents 4,041,476 and 4,078,229 to the Formigraphic Engine Corporation. The Formigraphic patents may have priority over some of the claims in the Battelle patents, by virtue of their earlier filing date.

Although this research and development program has been conducted at Battelle's Columbus Laboratories, Formigraphic Engine Corporation has assisted Battelle in a consulting capacity. Because PCM technology is still very much in the formative stages, a relatively large research effort may be required to bring the PCM concept to commercialization if the results of the proposed feasibility evaluation indicate that such effort is warranted. Battelle would therefore welcome the participation of industrial co-sponsors in sharing the costs and benefits of this effort, so as to assist the Government in the transfer of this new technology to the industrial sector.

Program Objectives

The principal objectives of this research program have been:

- To evaluate in detail the technical feasibility of developing a photochemical machining (PCM) system suitable for the fabrication of patterns for precision casting applications, and

- To develop the individual chemical and optical components which will be required to evaluate realistically the feasibility of a prototype PCM system.

These objectives have been directed toward conducting the evaluation of PCM technology as efficiently as possible, and toward providing AFOSR with a logical progression of decision points by which the progress of the project can be evaluated in the context of DOD's own interests and constraints. The results which have been obtained during this research effort are described in the following sections of this report. Detailed experimental procedures can be found in the Appendix, which contains the M.S. Thesis of Mr. Dean R. Johnson (Ohio State University), who performed the bulk of the polymerization and sensitization experiments conducted during this period.

RESULTS AND DISCUSSION

Theoretical Considerations

In any practical photochemical machining system, there are obviously a number of design tradeoffs among such factors as laser power, workpiece size, surface finish, and fabrication time to be considered. It is helpful to work through a simple model of the system at the outset, in order to get a general idea of what the tradeoffs are, and of what is going to be required of the chemicals for the system to have a chance to work. We describe such a model calculation in this section.

Let us consider, for the sake of definiteness, a cubical sample volume, 10 cm on a side. Within this volume, we wish to be able to address spots 10 μm on a side with orthogonally propagating laser beams. These numbers are consistent with present-day beam-shaping and scanning equipment. The sample volume thus contains 10^{12} addressable spots. To produce a useful item, say a release mold outline, let us assume that we have to polymerize 10% of the sample volume, or, roughly, that we have to produce polymer in 10^{11} spots forming a connected surface and nowhere else within the sample volume.

We will assume that the polymer is produced by chain extension, cross-linking, or some similar process, stimulated by the presence of some photoproduced "initiator" molecular species. We will not focus on the details of the polymerization process at this time, but rather will simply consider as one goal of the calculation an estimate of the amount of polymerization required per significant photochemical event. One possible molecular-energy-level model for the initiation part of the process is shown in Figure 2. In this representation, straight arrows indicate radiative transitions, and wavy arrows indicate primarily non-radiative transitions (although D_s and D_t include a small spontaneous radiation component). The singlet ground state of a "sensitizer" molecule is pumped

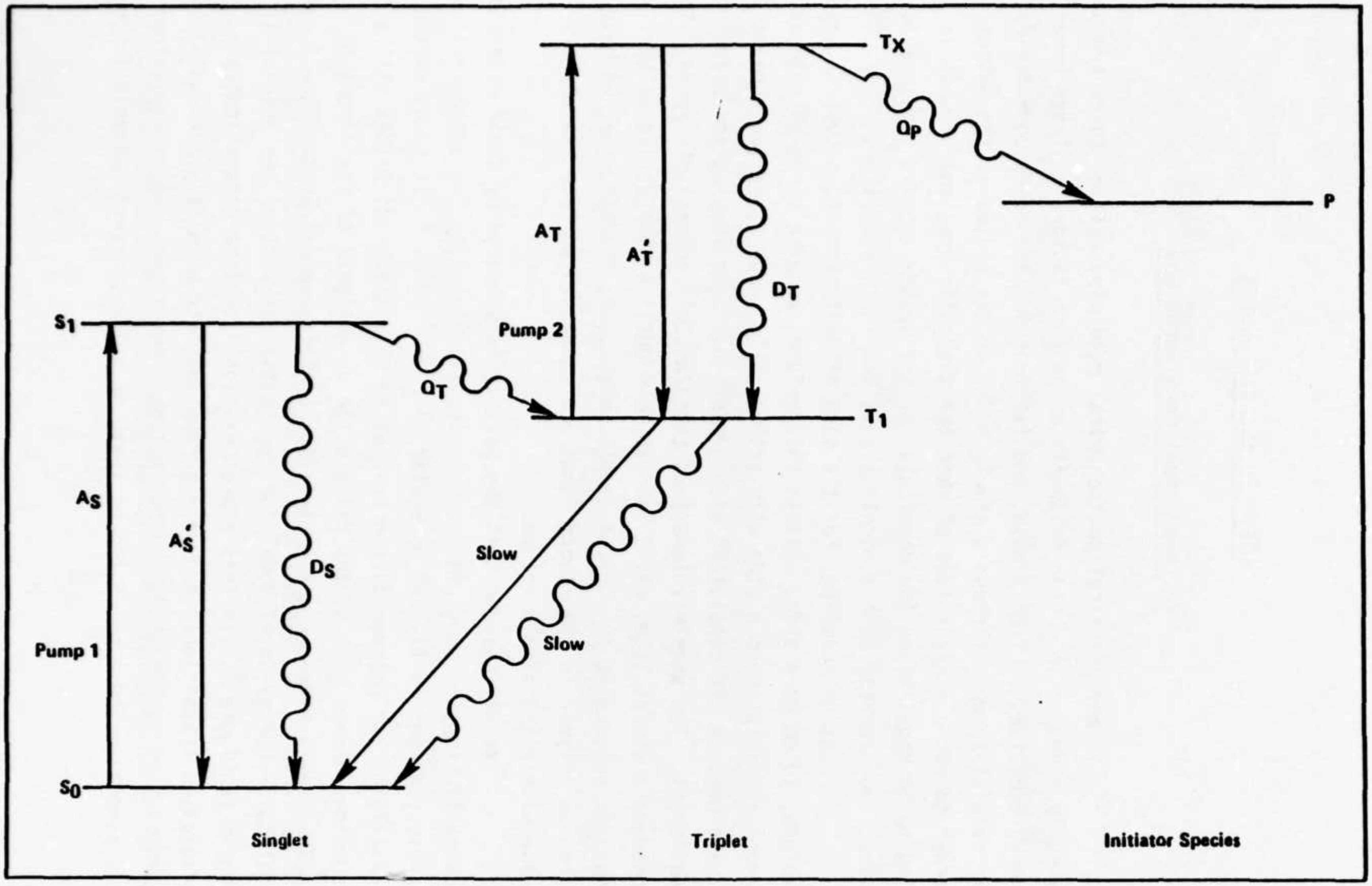

FIGURE 2. ONE POSSIBLE MOLECULAR ENERGY-LEVEL DIAGRAM FOR PRODUCTION OF INITIATOR SPECIES FOR CHAIN EXTENSION OR CROSS-LINKING OF POLYMERS

by the first laser beam to the excited state S_1. Some of the S_1-state molecules decay nonradiatively to the metastable triplet state T_1. Molecules in this state are pumped by the second, orthogonal, laser beam to the excited state T_x, from which some of them can react with each other or with other species present in solution to form the initiator species indicated schematically on the diagram at the level P.

The transfer rates indicated in Figure 2 are identified as follows: A_S is the rate at which molecules are excited from the ground-state level S_0 to S_1; it equals $I_1 \sigma_S$, where I_1 is the intensity (photons per unit area per second) of laser beam 1 and σ_S is the cross-section for the absorption process at the wavelength of beam 1. The stimulated decay rate from S_1 is indicated as A_S'; since the molecular excited state will generally be structurally altered from the ground state, the Einstein relations do not necessarily hold; that is, A_S' is not necessarily equal to A_S. In the calculations, we have assumed that stimulated decays from S_1 and T_x can both be neglected; trial calculations including them show that this is a very good approximation. D_S represents the combined rate of nonradiative and spontaneous radiative decay processes from S_1 to S_0, while Q_T is the rate of transfer from S_1 to the lowest triplet level T_1. The transfer rates for the triplet-state processes are defined in a similar way, except that Q_P is the rate of production of initiator species. As indicated on the diagram, decay rates from the lowest triplet state to the ground state are assumed to be slow; the associated time constants will be milliseconds or longer, so these processes can be ignored in the dynamic analysis.

With these definitions and assumptions given, it is now easy to write down the rate equations describing the model system:

$$dn_{So}/dt = -A_S n_{So} + D_S n_{S_1} \quad ; \qquad (1)$$

$$dn_{S_1}/dt = A_S n_{So} - (D_S + Q_T) n_S \quad ; \qquad (2)$$

$$dn_{T_1}/dt = Q_T n_{S_1} - A_T n_{T_1} + D_T n_{T_x} \quad ; \qquad (3)$$

$$dn_{T_x}/dt = A_T n_{T_1} - (D_T + Q_p) n_{T_x} \quad ; \qquad (4)$$

$$dn_p/dt = Q_p n_{T_x} \quad . \qquad (5)$$

In these equations, n_{S_0} indicates the number of molecules per unit volume in state S_0, and so forth. The initial conditions may be taken to be

$$n_{S_0}(0) = N_S \ , \qquad (6)$$

where N_S is of course the initial concentration of sensitizer molecules, with all other states initially empty.

It is possible to give a general solution to this system of equations, but such a solution is fairly complicated and not really necessary for the present model calculations. Rather, we will introduce some additional assumptions which simplify the physical picture while neither leading to any unwarranted mathematical approximations nor involving unlikely physical embodiments of the apparatus.

First, we shall assume that the singlet and triplet pumps are at decidedly different wavelengths, so that neither absorption process substantially affects the other. This situation should not be too difficult to obtain experimentally, although there may be a tradeoff to consider between broader absorption bands, which are more likely to have useful absorption coefficients at available laser wavelengths, and narrower absorption bands, which are less likely to overlap.

Second, we limit the discussion to the case of sequential excitation, in which the singlet pump laser 1 is turned on for a time τ_1 and then turned off while the triplet pump laser is turned on for a time τ_2. This assumption simplifies the mathematics while being very conservative in regard to attainable operating conditions.

Third, we simplify the boundary conditions by neglecting the small number of molecules transferred from S_1 to T_1 after beam 1 is turned off, and by neglecting the depletion of the ground state. Although a number of cycles of sequential excitation might be necessary fully to polymerize a given location, the calculations will show that the ground-state depletion is insignificant. Neglecting the singlet-triplet transfer after beam 1 is extinguished is again a "conservative" or worst-case assumption.

With these assumptions, solution of the rate equations (1)-(5) degenerates into the solution of two independent and formally identical simple problems, one represented by the first two equations and the other by the last three. The right-hand side of Eq. (3) contains only the first term while the singlet pump is active, and only the other two terms when the triplet pump is on. We have solved these equations by the Laplace transform method. The results have the considerable advantage that they are simple enough in form that it is not difficult to see how changes in the various parameters affect the rate of initiator molecule production. As is usual in such circumstances, the same combinations of parameters recur frequently in the results; so it is helpful to introduce some notation for these combinations.

First we introduce in the usual way the overall decay times characterizing the excited states:

$$\tau_S = (D_S + Q_T)^{-1} ; \qquad (7)$$

$$\tau_T = (D_T + Q_P)^{-1} . \qquad (8)$$

In terms of these decay times, we can define the fractional intersystem transfer probabilities by

$$f_S = Q_T \tau_S ; \qquad (9)$$

$$f_T = Q_P \tau_T . \tag{10}$$

Similarly, we can define fractional excitation-to-decay ratios for each subsystem by

$$g_S = A_S \tau_S ; \tag{11}$$

$$g_T = A_T \tau_T . \tag{12}$$

Normalized illumination times are defined by

$$\rho_S = \tau_1 /(2 \tau_S) ; \tag{13}$$

$$\rho_T = \tau_2 /(2 \tau_T) . \tag{14}$$

Other parameters which appear frequently are

$$R_S = [(1+g_S)^2 - 4f_S g_S]^{1/2} \tag{15}$$

and R_T which is defined similarly. Finally, we define N_T as the number of sensitizer molecules per unit volume transferred to the T_1 state after one cycle of the singlet-state pump, and N_P as the number of these molecules transferred to the initiator state P after one cycle of each pump. We will denote by N_S^* the number of sensitizer molecules left in the ground state after the singlet-state pump cycle.

Then, in terms of the dimensionless variables we have defined, the fractions of sensitizer molecules left in the ground state, transferred to the lowest triplet state, and transferred to the initiator configuration, per cycle of singlet-state and triplet-state pump in a given location, are given by Equations 16-18 as follows:

$$\frac{N_S^*}{N_S} = \frac{1}{2R_S}\left[(1-G_S + R_S)e^{-(1G_S-R_S)\rho_S} - (1-G_S-R_S)e^{-(1+G_S+R_S)\rho_S}\right] \; ; \qquad (16)$$

$$\frac{N_T}{N_S} = \frac{2F_S G_S}{R_S}\left[\frac{1-e^{-(1+G_S-R_S)\rho_S}}{1+G_S-R_S} - \frac{1-e^{-(1+G_S+R_S)\rho_S}}{1+G_S+R_S}\right] ; \qquad (17)$$

and

$$\frac{N_p}{N_T} = \frac{2F_T G_S}{R_T}\left[\frac{1-e^{-(1+G_T-R_T)\rho_T}}{1+G_T-R_T} - \frac{1-e^{-(1+G_T+R_T)\rho_T}}{1+G_T+R_T}\right] ; \qquad (18)$$

respectively.

To evaluate these expressions, it is necessary to make more specific assumptions about the system. Suppose we aim for a total laser-beam dwell time at each addressed spot of one μsec. Then to polymerize 10^{11} points will require 10^5 seconds, or a little over a day, neglecting the time for moving the beams around.

Next we should consider desirable attenuation characteristics of the beams. The singlet-state pump absorption should be moderate, so that reduction of available intensity at remote points in the sample does not result in a requirement of greatly increased exposure times at these points. If for instance the power attenuation coefficient $\alpha_S = 0.2 \text{ cm}^{-1}$, then a beam at the center of the sample is attenuated by a factor of 1/e, or 0.36, which should be tolerable. We shall assume we can adjust the singlet-pump attenuation to something like this value. The triplet-state absorption should of course be as high as possible in order to maximize the transfer to initiator states.

To relate the absorption coeficients to the parameters previously defined, we recall that

$$\sigma_S = \alpha_S / N_S \; ; \qquad (19)$$

so that

$$G_S = I_1 \alpha_S \tau_S / N_S , \qquad (20)$$

and similarly for G_T. In evaluating these expressions, we have naturally assumed that the molecular-species densities in the denominator do not change during the operative cycle time, since σ is the fundamental physical parameter and since the absorption coefficients are measured when the lower states are well-populated. Since the singlet-state absorption coefficient is low, the corresponding laser power must be large, even if the larger part of the dwell period is devoted to the ground state excitation. Suppose we take the singlet state pump as the 514.5 nm line of an argon laser, and assume that we can devise a molecule with suitable absorption at this wavelength. Suppose the laser power is 20 W, not out of the question with present-day equipment, and let us take this power to be focused sufficiently uniformly within one 10-μm-square cross-section of one addressable volume element. Then the incident radiation density I_1 equals 5.18×10^{29} photons m^{-2} s^{-1}. To estimate N_S, we shall assume a 5 atomic percent doping of the original material with sensitizer molecules; of course this doping level cannot be too high or it is likely to interfere with the polymerization. If the sensitizer particles have a molecular weight of around 125, and the overall specific gravity is around 1, then $N_S \approx 2.4 \times 10^{26}$ m^{-3}. The decay time of S_1 will ordinarily be short compared to the cycle time; let us take $\tau_S = 1$ ns. Then we find $G_S = 4.3 \times 10^{-5}$. Generally G_S will be much less than unity; this permits some simplifications in Eq. (17), but these are not worth discussing here except to note that as long as G_S is small, the exact value of τ_S is immaterial.

In favorable cases, the fractional transfer probabilities might be as high as 0.8, which value we shall adopt for both the S-to-T and the T-to-P transfer processes. For the singlet-state pumping time, 0.98 μs turns out to be a satisfactory value, and with these parameters we find that after this time has elapsed

$$N_T / N_S = 0.0332, \quad (21)$$

or $N_T = 8.0 \times 10^{24}$ triplet-state molecules per m^3 when the triplet state pump is turned on. At this time, also, $N_S^*/N_S = 0.9668$; so clearly several pump cycles could be provided if necessary to overcome beam attenuation effects without seriously depleting the ground state.

For the triplet-state pump, we will assume a laser operating at 647.1 nm with a power of 2 W. This might be a krypton laser or a dye laser. An examination of available triplet absorption spectra indicates the absorption coefficient at this wavelength might be in the range 100 to 500 cm^{-1}. We have used the value 127 cm^{-1}, which gives $g_T = 0.50$ with the other parameters stated. Using such a value along with $f_T = 0.8$ and $\rho_T = 10$, corresponding to τ_T also equal to 1 ns, we find from Eq. (18) that $N_P \approx N_T$; that is, practically all the lowest-triplet-state molecules are transferred to the initiator state, so there are about 8.0×10^9 initiator molecules per beam-interaction spot 10 μm on a side. If the remaining 95 atomic percent of the starting material is all monomer with a molecular weight of 100, there are about 5.7×10^{12} of these molecules per spot at the outset. Thus to polymerize the entire spot in one cycle, each initiator site will have to link up, on the average, some 720 monomer units. It should be clear from the discussion that the operating conditions could be varied quite substantially without markedly affecting this ratio.

With the high laser powers involved in the processes described here, it is natural to wonder about the temperature changes that might result from the absorption of the beams. We can estimate upper limits for these effects in a very simple way by assuming that all the energy absorbed is converted to heat and that none of this energy is transported away from the beam interaction region. Then

$$I_{abs}\ \tau = C_m N_m\ \Delta T, \quad (22)$$

where I_{abs} is the power absorbed from the pump beam in question within a suitable absorption volume, C_m is a suitably averaged molar heat capacity of the material, N_m is the number of moles affected, and ΔT is the temperature rise. For C_m we shall adopt a typical value of 20 J (mole K)$^{-1}$. To treat the singlet-state pump, let us assume that all 20 W are absorbed for 0.98 μs in the 10 cm long, 10 μm square rectangular parallelopiped in which we assume the laser beam intercepts the working volume. Then we find the average temperature rise in this region is around 1 K. Of course the calculated temperature rise near the entrance face will be somewhat greater. For the triplet-state pump, we have 2 W for 0.02 μs deposited in a cube 10 μm on a side; in this case the calculated temperature rise is about 19 K. Since we expect that only a relatively small portion of the absorbed energy will in fact be converted into heat, we conclude that heating effects are not likely seriously to interfere with system operation, at least when the operating conditions are normal.

Finally, it is of interest to try to make a rough estimate of the probability of an excited triplet state reacting with an initiator molecule, to promote polymer chain formation or extension, before it decays back to the ground state. While this is probably not a major concern with systems which utilize a reactive photosensitizer molecule (in which the initiator moiety is attached covalently to the sensitizer moiety), it is of critical importance in the design of systems which rely on energy transfer from the excited photosensitizer to a separate photoinitator molecule. In the above calculation of the required rate of polymerization events per incident photon pair, we assumed that this probability was 0.8, which considering the exothermic nature of the reaction is not unreasonable <u>if</u> there are enough initiators sufficiently close to excited triplets that the reaction can occur. What we wish to do here is to make a very simple estimate of what "enough" close initiator molecules might mean in the context of the present work. We shall use a "magic radius" or "hot zone" model, where the probability of reaction is <u>unity</u> if at least one initiator molecule (IM) is within a certain distance of the upper excited triplet (ET), and zero if no IM is within the specified distance. Since molecular diffusion rates are likely to be fairly low in a viscous medium of the type envisioned for photochemical machining, and since the ET lifetime is less than a nanosecond, we will assume that the IM must be already present in the triplet molecule's vicinity when the latter is excited. We will also make the drastic assumptions that all the molecules in the system, whether luminophors, initiators or oligomers are roughly the same size, that they are fairly spherical and hard, and that the liquid can be instantaneously represented as a random packing of these spheres. Departure from these assumptions not only greatly complicates the theory, but also requires further assumptions which are also not easy to justify.

If we let r be the radius of a molecule and r_m be the distance from the center of an ET within which reaction is assumed (the "magic radius"), then the total number of molecules within the sphere of radius r_m is given approximately by $N_h = p(r_m/r)^3$, where p is the packing fraction for spheres at random, which on the basis of experiments(1) we can take as around 0.63. The question we now wish to ask is, assuming we have an ET sensitizer at the center of the sphere of radius r_m, what is the probability that at least one of the $[N_h-1]$ other molecules in the "hot zone" is an IM? (The notation [ ] is used to mean the integer part of N_h). To find this, we proceed in the usual way to find the probability that all the molecules in the hot zone are either sensitizers or oligomers and subtract this from unity. Let us call the fraction of sensitizers in the solution a, of IM's b, and of oligomers c. We neglect any other species (or lump them in with the oligomers), so a + b + c = 1. Then, with completely random mixing, the probability that a given molecule is either a sensitizer or oligomer is a + c, and the probability that the $[N_h-1]$ noncentral molecules in the hot zone are all either a or c is $(a + c)^{[N_h-1]}$, assuming that the total number of each type of molecule in the solution is much greater than N_h. Since a + c = 1 - b, we may write the reaction probability as

$$P_r = 1-(1 - b)^{[N_h-1]} \quad . \tag{23}$$

The minimum possible value of r_m/r is 3; for this value $[N_h-1]$ equals 16. Actually, no more than 12 identical spheres can simultaneously touch a sphere of the same radius(2). Since we might want to allow for some molecules of slightly smaller radius, though, perhaps we should consider both these values. If we say that an initiator molecule must be in "contact" with an ET for reaction to occur, several questions may be posed.

First, what is the probability of reaction, based on this model, for conditions similar to those in our experiments? Assuming most of the polymerizable species in our solution have a molecular weight of around 150, we estimate the relative numbers of sensitizers, initiators, and oligomers as 1:22:66,000. Thus, $b \approx 1/3000$, and the reaction probability P_r is around 0.5% if $[N_h-1]$ equals 16 and around 0.4% if it equals 12.

Second, how do these probabilities vary if we extend the "hot zone" out further, say to $r_m/r = 5$; or alternatively, consider that there is a high probability that a molecule in the second coordination sphere can jump into a near-neighbor position during the lifetime of the excited state? Just considering the random packing case now, and proceeding as before, we find $P_r = 43\%$, a remarkable increase, and probably not an overestimate, since for this large a hot zone, the number of molecules (85) that could be fitted in by close packing(3-5) exceeds the random packing estimate (77).

Finally, assuming that close proximity is required for reaction, what sort of IM concentration is needed to bring the reaction probability up to 80%? If the number of close molecules $[N_h-1]$ is 16, the required molecular concentration b is 9.6%, while for $[N_h-1] = 12$, it is 12.6%. Thus an increase in the number of IM's in the solution by a factor of around 260 to 330 would be needed to obtain an 80% probability of reaction.

While this model is very crude, the conclusion is clear: there must be a very large excess, on the order of a 200-300 fold mole ratio, of IM's to ensure a high probability of reaction with an ET. On the other hand, although the IM's are probably less massive than the polymer precursors, adding upwards of 10% of IM's to the mix may inhibit the formation of fully solid polymer. Some additional adjustment in overall reaction rates might be obtained by changing the ET concentration as a result of changing that of the sensitizers, which has not been really optimized either; still, this concentration cannot be increased beyond the point of reasonably homogeneous absorption in the singlet state, and of course, it does not have any strong direct effect on the reaction probability we have been discussing in this section. In short, it would appear that the use of chemically distinct sensitizer and initiator molecules, while experimentally convenient, can succeed only within relatively narrowly defined concentration ratios, and that the development of combined sensitizer-initiator molecules will be required if high-efficiency photochemical machining reactions are to be achieved in practice.

There are a number of obvious ways that calculations of the type reported here could be modified and extended. At the present level of understanding, though, it is sufficient that they indicate a possibility that feasible operating conditions might conceivably be found; and more to the point than detailed numerical work is a conceptual study of ways the model we have developed indicates the system might fail to operate properly. We have just indicated, for instance, that heating effects of the laser beams can probably be dismissed.

Design of New Photoinitiator Molecules

The research conducted during the past two years has been focused on the design and development of new photoinitiator materials, as this is a crucial requirement for the successful operation of a PCM system. After considering a number of possible strategies for the design of a selective two-beam photoinitiator, the strategy shown schematically in Figure 3 was adopted as being the approach most likely to succeed. In this approach, as noted in the preceding section, a molecule is excited to its lowest excited singlet state (S_1) with photons from beam 1 having an energy below the dissociation threshold of the molecule and then rapidly undergoes intersystem crossing to its lowest triplet excited state (T_1). It is important that T_1 be transparent to light of the wavelength of beam 1, so no further excitation of the system can occur; in the absence of beam 2, therefore, the system will be inert, and T_1 will eventually decay harmlessly back to the ground state of the photoinitiator (S_0) with no chemical reaction taking place.

In the presence of beam 2, however, which is of a wavelength absorbed strongly by T_1 but not absorbed by the ground state, the photoinitiator will be excited to an upper triplet state, T_2, with an energy content above the dissociation threshold for fragmentation of the molecule into reactive radicals (or ions). These species then initiate the actual polymer crosslinking process.

The development of a successful photoinitiator molecule for PCM thus depends on the combination of two distinct functional groups: a light-absorbing moiety, or chromophore, with spectroscopic properties of the type just described, and a labile initiating group that can be fragmented with high efficiency once sufficient energy is contained in the molecule.

For this program, we have chosen to utilize two proven initiator groups for our candidate materials; these are the aryl sulfonyl chlorides

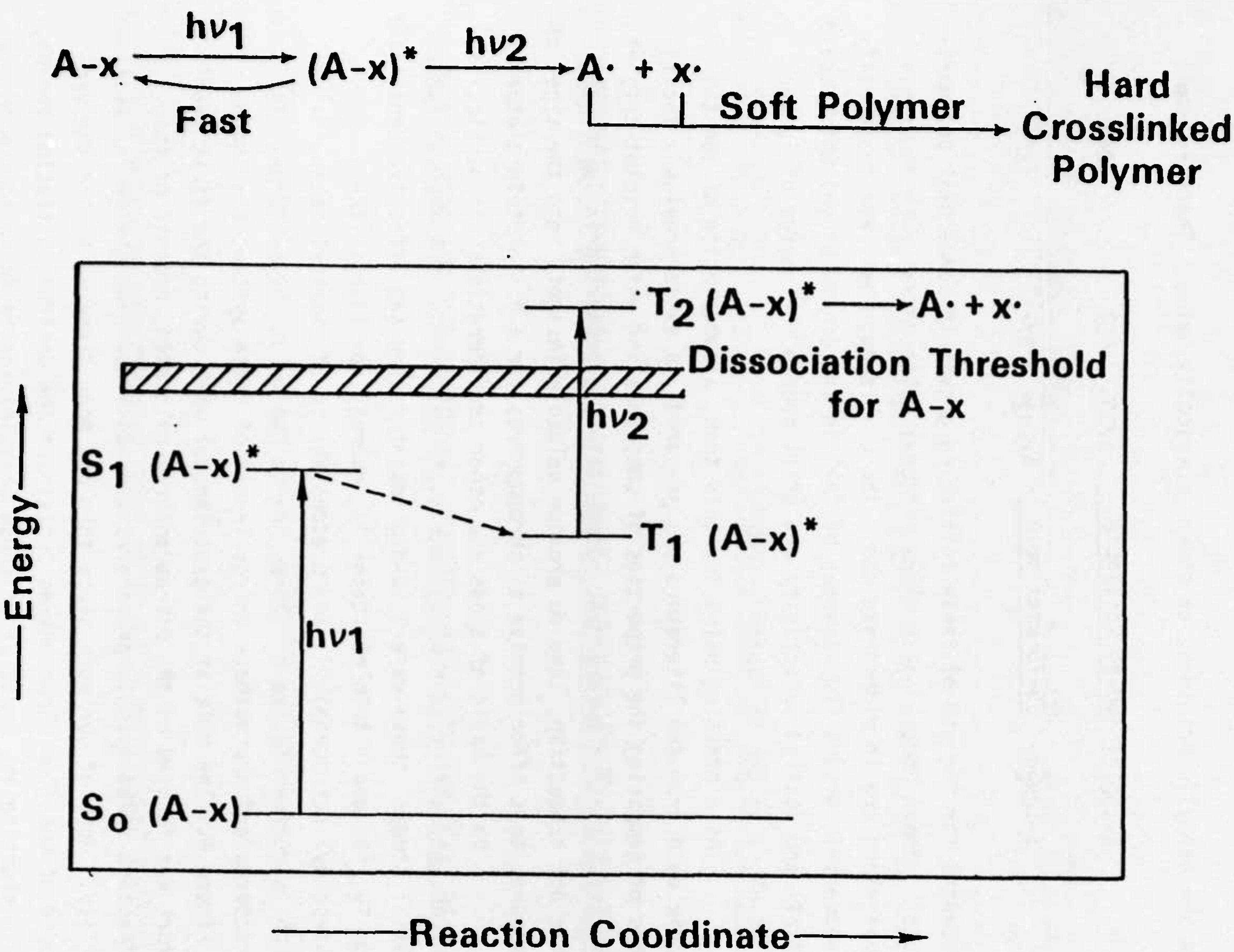

FIGURE 3. GENERAL STRATEGY FOR PHOTOINITIATOR DESIGN

and the benzylic bromides, as shown generically below. There is ample

$$Ar\text{-}SO_2Cl \xrightarrow{\text{60-65 kcal/mole}} ArSO_2\cdot + Cl\cdot \qquad (24)$$

$$Ar\text{-}CH_2Br \xrightarrow{\text{65-70 kcal/mole}} ArCH_2\cdot + Br\cdot \qquad (25)$$

precedent for the use of these initiating groups in commercial polymerization systems; both 2-napthalene sulfonyl chloride and 2-bromomethylnaphthalene are in widespread use. The challenge, then, was to identify chromophoric groups (represented by "Ar" in the scheme above) which would exhibit the desired selectivity and still couple the energy of T_2 effectively into the initiator group.

As a starting point for this task, a compilation of spectroscopic data from the literature was prepared, so as to provide a facile means of comparing the properties of compounds for which triplet-triplet absorption spectra were known. These data are presented in Tables 1-3. While not exhaustive, they do provide valuable insights into the types of compounds that offer promise as chromophores for a PCM photoinitiator.

On the basis of these and other considerations (in particular, availability and/or ease of synthesis) three chromophores were chosen for initial study: these were 9,10-dibromoanthracene (an effective sensitizer from T_2, its upper triplet state[7]); rubrene, or (5,6,11,12-tetraphenyl tetracene)[8]; and protoporphyrin IX dimethyl ester,[9,10] which is representative of the porphyrin family of chromophores. The structures and approximate energy levels of these systems are shown in Figure 4. The bulk of the experimental work during the first year's effort was focused on the dibromoanthracene system, because of its attractive spectroscopic properties and its widespread commercial availability. Much of our work since then has been directed toward the synthesis of modified chromophores containing the desired initiating groups, and evaluating the behavior of these photoinitiators in various monomers and polymers, paticularly methyl methacrylate. Dibromoanthracene

TABLE 1. SUMMARY OF SPECTROSCOPIC DATA[a]

ompound	E_S (kcal/mole)	E_S (nm)	E_{T_1} (kcal/mole)	E_{T_2} (kcal/mole)	$E_{T_1-T_2}$ (kcal/mole)	$E_{T_1-T_2}$ (nm)	ϵ_{T-T}	ϕ_{isc}
ene	40.6	704	30,9	--	--	--	--	--
il	59.0	485	53.4	128.6 112.2	·75.2 58.8	380.2 486.4	--	0.92
Butanedione iacetyl)	65.3	438	56.3	----See Table 2-------			--	1.00
horquinone	∿55	520	50	----See Table 2-------			--	1.00
renone	63.2	452	53.3	97.6	44.3	645.2	--	0.93
)-Dichloro- :hracene	71.1	402	40.4	108.9	68.5	422.8	51,000	0.50
·Benzopyrene	70.8	403	42.0	98.8	56.8	503.8	--	--
:aphene	67.5	423	48.4	--	--	--	--	--
lene	65.8	435	35.1	137.2 93.4	102.1 58.3	280 490	14,300	0.005
alene	60.7	471	29.3	89.3	60.0	476.2	60,000	--

From Reference 6, pp 316-327.

TABLE 2. TRIPLET-TRIPLET ABSORPTION SPECTRA OF CARBONYL COMPOUNDS[a]

Compound	E_{T-T} (kK)	(kcal/mole)	(nm)	ϵ_{T-T}
Benzaldehyde	32.50	92.92	307.69	(0.86)
	31.25	89.34	320.00	(1.00)
	27.40	78.34	364.96	(0.18)
	23.30	66.61	429.18	(0.11)
1-Naphthaldehyde	25.84	73.88	387.00	
	25.77	73.68	388.05	
	24.69	70.59	405.02	
	24.25	69.33	412.37	
	23.53	67.27	424.99	
	22.73	64.99	439.95	
	20.20	57.75	495.05	
Acetone	33.11	94.66	302.02	
Acetophenone	37.60	107.50	265.96	
	35.53	101.58	281.45	
Benzophenone	31.55	90.20	316.96	(1.00)
	23.98	68.56	417.01	(0.10)
	22.22	63.53	450.05	(0.14)
	20.20	57.75	495.05	(0.46)
	19.01	54.35	526.04	(0.68)
4-Aminobenzophenone	21.50	61.47	465.12	(1.00)
	15.62	44.66	640.20	(1.00)
3-Aminobenzophenone	21.99	62.87	454.75	(0.87)
	17.86	51.06	559.91	(1.00)
4-Hydroxybenzophenone	27.78	79.42	359.97	(1.00)
	19.42	55.52	514.93	(0.78)
Benzoin	27.03	77.28	369.96	(1.00)
	21.01	60.07	475.96	(0.95)
Fluorenone	30.50	87.20	327.87	(1.00)
	27.00	77.19	370.37	(0.36)
	25.80	73.76	387.60	(0.56)
	24.00	68.62	416.67	(0.82)
	23.20	66.33	431.03	(0.90)
	22.00	62.90	454.55	(0.70)
	18.10	51.75	552.49	(0.18)
	16.70	47.75	598.80	(0.22)
	15.50	44.31	645.16	(0.25)
	13.50	38.60	740.74	(0.10)
	11.00	31.45	909.09	(0.08)
2-Acetonaphthone	23.26	66.50	429.92	10,500
1-Acetylanthracene	22.90	65.47	436.68	(0.45)
	21.60	61.75	467.96	(0.70)
	21.00	60.04	476.19	(0.90)
	20.00	57.18	500.00	(1.00)
	18.20	52.03	549.45	(0.45)

TABLE 2. (Continued)

Compound	E_{T-T} (kK)	E_{T-T} (kcal/mole)	E_{T-T} (nm)	ε_{T-T}	
iacetyl	45.45	129.94	220.02		
	32.26	92.23	309.98	5,160	in Benzene (RT)
	30.30	86.63	330.03		
	13.89	39.71	719.94		
	12.56	35.91	796.18		
	10.92	31.22	915.75		
	9.45	27.02	1058.20		
amphorquinone	50.00	142.95	200.0		
	35.71	102.09	280.00		
	31.65	90.49	315.96		
	20.00	57.18	500.00		
	16.95	48.46	589.97		
	15.67	44.80	638.16		
	14.18	40.54	705.22		
	12.56	35.91	796.18		
	10.92	31.22	915.75		
	9.35	26.73	1069.52		
Benzil	26.30	75.19	380.23		
	20.56	58.78	486.38		
Acetylacetone	20.83	59.55	480.08	>>60	
	19.23	54.98	520.02		
Trifluoroacetylacetone	26.32	75.25	379.94	>>30	
	22.22	63.53	450.05		
Hexafluoroacetylacetone	25.64	73.30	390.02	1,000	
	21.28	60.84	469.92		
3-Phenylacetylacetone	20.40	58.32	490.20	>3,000	
Dibenzoylmethane	20.83	59.55	480.08		
	16.67	47.66	599.88		
	15.87	45.37	630.12	>1,500	
	13.51	38.80	736.92		
Benzoylacetone	24.39	69.73	410.0		
	22.83	65.27	438.02	>1,500	
	20.83	59.55	480.08		
	18.87	53.95	529.94		
	16.39	46.86	610.13		
Trifluorobenzoylacetone	17.24	49.29	580.05		
	15.80	45.17	632.91	18,000	
Duroquinone	21.80(a)	62.33	458.72		
	20.40(a)	58.32	490.20	5,330(b)	
					(a) Liq Paraffin, RT
					(b) Cyclohexane, RT

TABLE 2. (Continued)

Compound	E_{T-T} (kK)	(kcal/mole)	(nm)	ϵ_{T-T}
Anthraquinone	27.03	77.28	369.96	(1.00)
	24.69	70.59	405.02	(0.50)
	21.74	62.15	459.98	(0.28)
	19.05	54.46	524.93	(0.15)
	17.70	50.60	564.97	(0.12)
	16.26	46.49	615.01	(0.15)
	15.15	43.31	660.07	(0.16)
	14.81	42.34	675.22	(0.18)
Chloranil	20.83	59.55	480.08	
	20.00	57.18	500.00	
	18.52	52.95	539.96	
1,3,6',8'-Tetramethyl-	30.00	85.77	333.33	
Bianthrone	20.60	58.90	485.44	26,000
Benzoic Acid	31.25	89.34	320.00	
2-Aminobenzoic Acid	25.30	72.33	395.26	(0.90)
	23.00	65.76	434.78	(0.85)
	21.20	60.61	471.70	(1.00)
3-Aminobenzoic Acid	27.50	78.62	363.64	(0.85)
	24.30	69.47	411.52	(1.00)
3-Methylaminobenzoic Acid	27.50	78.62	363.64	(1.00)
	24.70	70.62	404.86	(0.55)
	23.00	65.76	434.78	(0.80)
3-Dimethylaminobenzoic	28.00	80.05	357.14	(1.00)
Acid Methylester	25.60	73.19	390.63	(0.30)
	24.30	69.47	411.52	(0.40)
	23.00	65.76	434.78	(0.40)
Benzamide	33.30	95.20	300.3	
	19.80	56.61	505.05	
2-Anthroic Acid	24.39	69.73	410.00	
	23.10	66.04	432.90	
Tetrachlorophthalic	25.50	72.90	392.16	
Anhydride	20.50	58.61	487.80	
	16.30	46.60	613.50	
Pyromellitic Dianhydride	25.70	73.48	389.11	
	20.20	57.75	495.05	
	18.50	52.89	540.54	

(a) From Reference 6, pp 326-327.

TABLE 3. TRIPLET-TRIPLET ABSORPTION SPECTRA OF ORGANIC DYESTUFFS[(a)]

	E_{T-T}			
Compound	(kK)	(kcal/mole)	(nm)	ε_{T-T}
Fluorescein	31.00a	89.75	318.57	4500a
	27.00a	78.17	365.76	8000a
	21.30a	61.66	463.65	9500a
	19.60b	56.74	503.86	6000a
	18.20b	52.69	542.62	
	15.75b	45.60	627.03	6500a
	13.50b	39.08	731.53	
	12.65b	36.62	780.68	
	10.65b	30.83	927.29	4000a
	9.20b	26.63	1073.44	
	8.75a	25.33	3267.43	13500a
	6.00b	17.37	1645.94	
Dibromofluorescein	19.76	57.21	499.78	18000
	30.80	89.17	320.64	
	23.20	67.16	425.67	
	21.80	63.11	453.01	28000
	18.50	53.56	533.82	
	17.00	49.22	580.92	
Erythrosin	19.01	55.03	519.50	26000
Proflavin	48.50	140.41	203.62	14000
	47.50	137.51	207.91	12000
	42.50	123.04	232.37	11500
	38.00	110.01	259.89	SH
	35.80	103.64	275.86	47000
	28.50	82.51	346.51	6500
	25.00	72.38	395.03	4000
	18.20	52.69	542.62	12500
	14.80	42.85	667.27	9000
	10.65	30.83	927.29	13000
	10.10	29.24	977.29	4000
	9.10	26.34	1085.24	65000
9-Phenylproflavin	48.50	138.7	206.2	30000
	41.80	119.5	239.2	17500
	35.50	101.5	281.7	47000
	29.00	82.9	344.8	6000
	26.00	74.3	384.6	8000
	25.40	72.6	393.7	9000
	17.40	49.7	574.7	12000
	16.00	45.7	625.0	10000
	14.50	41.5	689.7	11000
	10.00	28.59	1000.0	8000
	8.40	24.0	1190.5	40000

(a) EtOH/Ether (90°K)
(b) PMMA (77°K)

TABLE 3. (Continued)

Compound	E_{T-T} (kK)	(kcal/mole)	(nm)	ϵ_{T-T}	
Acridine Orange(a)	48.50	140.41	203.62	16000	(a) EtOH/Ether, 90°K
	41.00	118.70	240.87	17000	
	35.20	100.6	284.1	56000	
	28.50	81.5	350.9	5000	
	25.50	72.9	392.2	4000	
	18.60	53.2	537.6	10000	
	17.40	49.8	574.7		
	16.60	47.5	602.4	9500	
	15.50	44.3	645.2	10000	
	14.60	41.7	684.9		
	13.60	38.9	735.3		
	12.80	36.6	781.3		
	12.30	35.2	813		
	11.20	32.0	892.9		
	10.80	30.9	925.9	2500	
	9.60	27.4	1041.7		
	9.20	26.3	1087		
	8.60	24.6	1162.8	15500	
	8.10	23.2	1234.6	SH	
	7.90	22.6	1265.8	54000	
Acridine Yellow	16.50	47.2	606.0	(0.20)	
	10.00	28.59	1000.0	(1.00)	
Trypaflavin(b)	19.80	56.6	505		(b) PMMA, 77°K
	18.90	54.0	529	(0.32)	
	18.00	51.5	555.6		
	15.40	44.0	649.4	(0.29)	
	12.50	35.7	800.0		
	10.65	30.4	938.9		
	8.27	26.5	1078.7		
	8.40	24.0	1190.5	(1.00)	
	7.70	22.0	1298.7		
Benzoflavin	13.35	38.2	749		
	10.50	30.0	952.4		
	9.10	26.0	1098.9		
	8.34	23.8	1199		
	7.70	22.0	1298.7		
	6.07	17.35	1647.4		
Thionine (pH=1)	26.70	76.3	374.5	14000	
	15.30	43.7	653.6	15500	
Thionine (pH=8)	24.10	68.9	414.9	11500	
	15.60	44.6	641.0	6300	
	13.10	37.5	763.4	9200	

TABLE 3. (Continued)

Compound	E_{T-T} (kK)	E_{T-T} (kcal/mole)	E_{T-T} (nm)	ϵ_{T-T}
Auramine	14.30	40.9	699.3	
	9.20	26.3	1086.9	
	8.35	23.9	1197.6	
	7.70	22.0	1298.7	
Methyl Violet	18.50	52.9	540.5	
	15.90	45.5	628.9	
	8.10	23.2	1234.6	
Ethyl Violet	19.00	54.3	526.3	
	16.10	46.0	621.1	
	8.90	25.4	1123.6	
Crystal Violet	18.60	53.2	537.6	
	16.00	45.7	625	
	9.00	25.7	1111.1	
	8.00	22.9	1250.0	
Malachite Green	12.80	36.6	781.3	
Methylene Blue (pH=2)	26.70	76.3	374.5	
	23.80	68.0	420.2	
	21.30	60.9	469.5	
Methylene Blue (pH=7)	35.46	101.5	281.7	
	23.80	68.0	420.2	
	19.23	54.9	520.0	
	14.39	41.1	694.9	
	13.70	39.2	729.9	
	13.07	37.4	765.1	
	12.66	36.2	789.9	
	11.56	33.1	865.1	
Methylene Green	24.40	69.8	409.8	
	19.25	55.0	519.5	
	13.15	37.6	760.5	
	12.65	36.2	790.5	
Novomethylene Blue	23.80	68.0	420.2	
	12.80	36.6	781.2	
Safranine T (pH=9)	26.30	75.2	380.2	
	13.30	38.0	751.9	
Safranine T (pH=5)	25.60	73.2	390.6	
	15.40	44.0	649.4	
	13.90	39.7	719.4	
Phenosafranine (pH=9)	26.00	74.3	384.6	
	13.70	39.2	729.9	

TABLE 3. (Continued)

Compound	E_{T-T} (kK)	E_{T-T} (kcal/mole)	E_{T-T} (nm)	ϵ_{T-T}
Phenosafranine (pH=5)	25.30	72.3	395.3	
	16.25	46.5	615.4	
	15.05	43.0	664.5	
Rhodamine B	16.00	45.7	625	13500
Cyanine Dyes:				
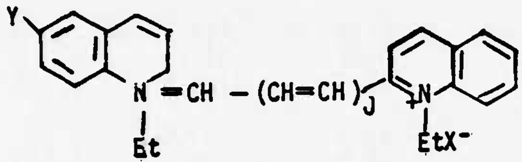				
J=0, X=I, Y=H	15.80	45.2	632.9	
J=0, X=I, Y=Br	15.40	44.0	649.3	
	20.00	57.2	500.0	
J=0, X=I, Y=I	15.00	42.9	666.7	
	14.90	42.6	671.1	
J=1, X=Cl, Y=H	13.50	38.6	740.7	
Thiacyanine Dyes:				
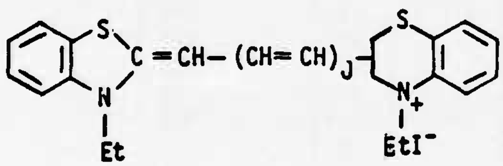				
	17.70	50.6	564.9	(0.16)
J=0	16.00	45.7	625	(1.00)
	15.00	42.9	666.7	(0.85)
	14.10	40.3	709.2	(0.85)
	11.50	32.9	869.6	(0.53)
J=1	11.00	31.4	909	(0.88)
	10.75	30.7	930	(1.00)
J=2	10.20	29.2	980.4	(0.45)
	9.85	28.2	1015.2	(1.00)
Biological Interest Compounds:				
Thymine	30.08	85.99	332.4	
Orotic Acid	27.40	78.34	364.9	
	23.20	66.3	431.0	
All trans-β-Carotene	22.20	63.47	450.5	66500
	20.80	59.47	480.8	107000
	19.60	56.0	510.20	130000

TABLE 3. (Continued)

Compound	E_{T-T} (kK)	(kcal/mole)	(nm)	ϵ_{T-T}
Biological Interest Compounds (Cont.)				
All *trans*-Lycopene	21.90	62.61	456.62	39000
	20.50	58.61	487.80	152000
	19.25	55.04	519.48	390000
	19.00	54.32	526.32	258000
	18.00	51.46	555.56	78000
Cis/*trans*-Lycopene	19.20	54.89	520.83	
Retinene	22.22	63.53	450.05	75800
Pheophytin-a	30.00	85.77	333.33	50000
	24.50	70.05	408.16	63000
	19.00	54.32	526.32	17800
	14.80	42.31	675.68	4700
Pheophytin-b	23.80	68.04	420.17	71000
	21.00	60.04	476.19	31500
	15.30	43.74	653.59	5700
Chlorophyll-a	21.70	62.04	460.83	32000
	18.90	54.04	529.10	17800
	16.40	46.89	609.76	
	15.20	43.46	657.89	
Chlorophyll-b	26.30	75.19	380.23	19700
	22.50	64.33	444.44	26000
	20.65	59.04	484.26	34700
	18.20	52.03	549.45	21500
	16.55	47.32	604.23	12000
	15.50	44.31	645.16	
Zr-Chlorophyll-a	22.20	63.47	450.45	
Chlorophylline	21.30	60.90	469.48	
	19.22	54.95	520.29	
Bacteriochlorophyll	24.40	69.76	409.84	22200
	20.00	57.18	500.00	10000
	16.15	46.17	619.20	11500
	15.25	43.60	655.74	9300
Methylchlorophyllide	21.30	60.90	469.48	
	19.22	54.95	520.29	
Pheophorbide	20.85	59.61	479.62	
	17.25	49.32	579.71	

TABLE 3. (Continued)

Compound	E_{T-T} (kK)	(kcal/mole)	(nm)	ϵ_{T-T}
Biological Interest Compounds (Cont.)				
Tetraphenylporphin	29.00	82.91	344.83	33000
	25.65	73.33	389.86	42000
	23.25	66.47	430.11	83000
	14.50	41.46	689.66	3500
	12.80	36.60	781.25	6000
Zn-Tetraphenylphorphin	25.00	71.48	400.00	42000
	21.30	60.90	469.48	74000
	13.42	38.37	745.16	5300
	11.85	33.88	843.88	8200
Photoporphyrin	28.60	81.77	349.65	(0.90)
	23.80	68.04	420.17	(1.00)
	(19.80)	56.61	505.05	(0.22)
	(18.90)	54.04	529.10	(0.15)
	(17.25)	49.32	579.71	(0.06)
	(15.90)	45.46	628.93	(0.08)
Zn-Protoporphyrin	22.00	62.90	454.55	(1.00)
	(18.55)	53.03	539.08	(0.13)
	(17.10)	48.89	584.80	(0.09)
	(15.65)	44.74	638.98	(0.08)
Mesoporphyrin	22.20	63.47	450.45	
Tetraphenylchlorin	21.30	60.90	469.48	
	(19.25)	55.04	519.48	
Coproporphyrin Dimethyl Ester	27.80	79.48	359.71	(0.75)
	25.60	73.19	390.63	(1.00)
	23.60	67.47	423.73	(0.90)
	20.00	57.18	500.00	(0.27)
Mg-Phthalocyanine	25.00	71.48	400.00	(1.00)
	21.30	60.90	469.48	(0.78)
Rubrene	23.90	68.33	418.41	(0.25)
	19.25	55.04	519.48	(1.00)
	18.60	53.18	537.63	(0.58)

(a) From Reference 6, p 335.

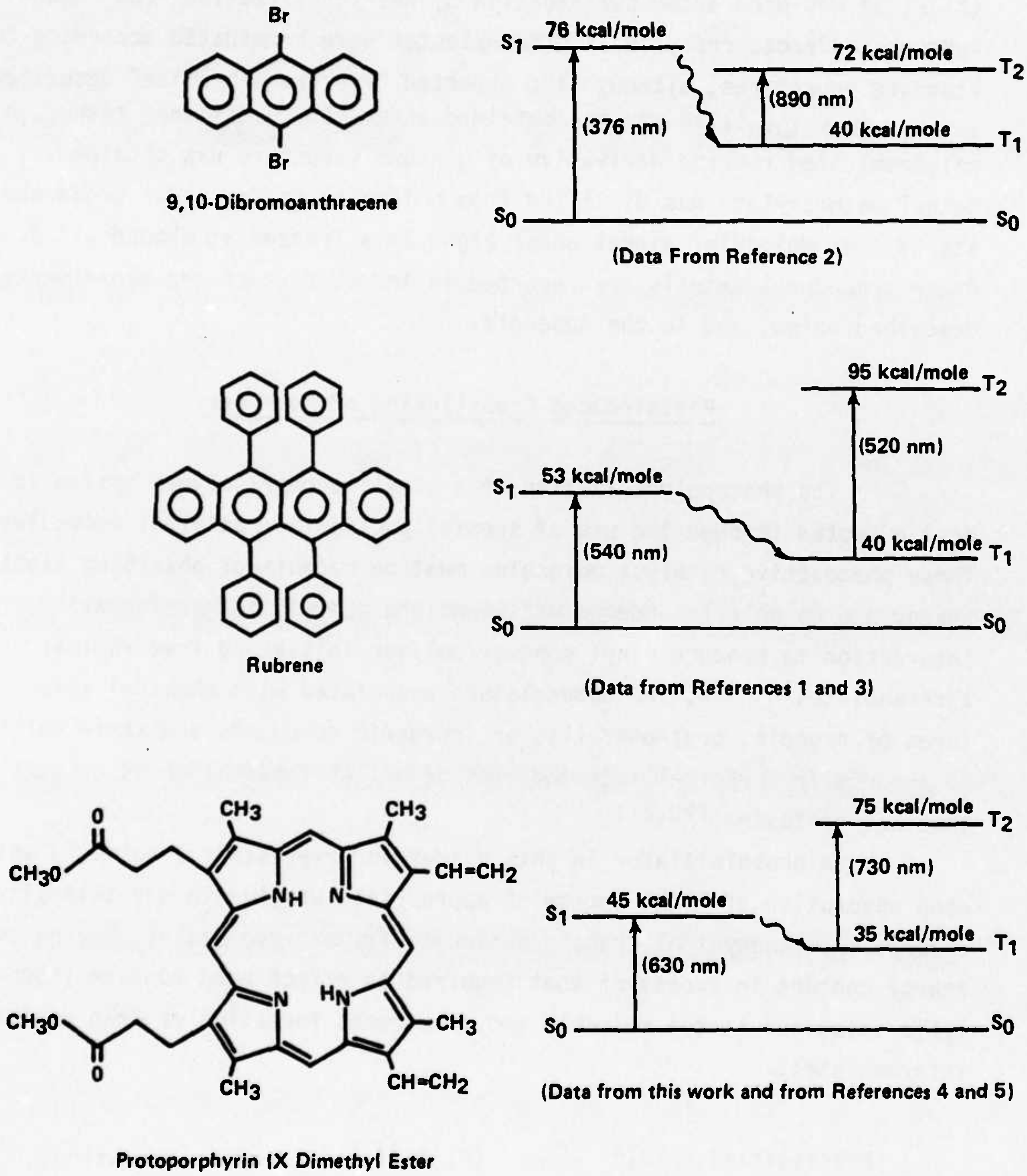

FIGURE 4. EXCITED-STATE ENERGETICS FOR INITIAL PHOTOSENSITIZER SYSTEMS

(Aldrich) was used after purification by recrystallization from ethanol. Rubrene and protoprophyrin IX dimethylester were brominated according to standard procedures, although the expected "rubrene dibromide" described in the literature[11]B was not obtained under our conditions; rather, a polybrominated rubrene derivative of unknown structure was obtained. Methyl methacrylate was distilled from molecular series under argon and stored over molecular sieves under argon in a freezer at around -10 C. Other procedural details are reported in the context of the experiments described below, and in the Appendix.

Photoinduced Crosslinking of Polymers

The photopolymerization of a vinyl monomer/polymer system is best effected through the use of special photoactive catalyst molecules. These photoactive catalyst molecules must be capable of absorbing light energy and be able to undergo efficient photochemical transformation or interaction to produce vinyl monomer/polymer-initiating free radical intermediates[12-19]. The nomenclature associated with chemical structures of organic, organometallic or inorganic compounds and their ability to produce free radical intermediates upon light absorption is presently somewhat confusing.[20,21]

A photoinitiator in this discussion represents a molecule which, upon absorption of light energy of appropriate wavelength and intensity, undergoes photophysical transformation to its excited states, having total energy content in excess of that required to effect bond rupture (homolytic scission) in the molecule and subsequent formation of free radical intermediates.

$$\text{Photoinitiator (PI)} \xrightarrow{h\nu} \text{(PI)* (excited state formation)} \quad (26)$$

$$\text{(PI)*} \xrightarrow{\text{bond rupture}} \text{PI (free radical intermediates)} \quad (27)$$

A photosensitizer can be a compound which upon absorption of light energy undergoes photophysical transformation to its excited states followed by inter- or intramolecular energy transfer to another compound, monomer or initiator (photo or thermal) which then results in the production of free radical intermediates.

$$\text{Photosensitizer (PS)} \xrightarrow{h\nu} (\text{PS})^* \quad \text{(excited states)} \tag{28}$$

$$(\text{PS})^* + \text{monomer or initiator (photo or thermal)} \longrightarrow \text{free radical formation} + \text{PS (ground state)} \tag{29}$$

The basic difference between both free radical intermediate generating systems is that, in one case, the photoinitiator is physically changed or destroyed while, in the other case, the photosensitizer is not consumed but acts only as an energy transfer agent.[20-23]

Photoreduction is another method by which a photosensitizer can produce active free radical intermediates. In this type of reaction an excited state photosensitizer molecule interacts with a ground state substrate containing an active hydrogen atom. The net result is that the photosensitizer becomes partially reduced to form a free radical intermediate and the substrate containing the donor hydrogen atom is also transformed into a free radical intermediate species.[24,25]

$$\text{PS} \longrightarrow (\text{PS})^* \quad \text{(excited states)} \tag{30}$$

$$\underset{\text{(hydrogen donor compound)}}{(\text{PS})^* + \text{SH}} \longrightarrow \cdot\text{PSH} + \text{S}\cdot \tag{31}$$

Another important process, in which a photosensitizer (specifically, aromatic carbonyl derivatives) can undergo electron-transfer complex formation resulting in photoreduction and subsequent formation of free radical intermediates, is as follows:

$$R_1R_2C{=}O + R_1-CH_2-\ddot{N}-R_2R_3 \xrightarrow{h\nu} [R_1R_2-\dot{C}-\overset{-}{O}\ \underset{R_2\ \ R_3}{\overset{+}{N}}\!\!\cdot\!-CH_2-R_1]^* \tag{32}$$

$$[R_1R_2\!-\!\dot{C}\!-\!\bar{O}\;\overset{+}{\underset{R_2\;\;R_3}{\dot{N}}}\!-\!CH_2R_1]^* \longrightarrow R_1R_2\!-\!\dot{C}\!-\!OH + R_1\!-\!\dot{C}H\ddot{N}R_2R_3 \qquad (33)$$

Each of the mechanisms for free radical intermediate production (photoinitiation, energy transfer, photoreduction, electron-transfer complex formation) will be discussed in the following sections.

Light Absorption. The first step in any photochemical reaction is the absorption of light energy, emitted from a given source, by the reacting molecule (in this case the photoinitiators or photosensitizers are the absorbing species). Since the light absorption process of a molecule is fundamental to photochemical reaction efficiency it is important to select photoinitiator and photosensitizer chemical structures that have light energy absorption bands which overlap the emission spectra of the light source used in the photochemical process. The probability of light absorption by a molecule is governed by the arrangement of atoms in the molecule and their surrounding environments.[26-29]

The basic UV and visible absorption spectra of aromatic ketones and mixed aromatic-aliphatic ketone structures associated with photoinitiator or photosensitizer compounds involves electronic transition between π (bonding) and π^* (antibonding) molecular orbitals characteristic of aromatic molecules as well as n (non-bonding) to π^* transitions associated with various carbonyl compounds.[30-33] The probability of absorption is measured or related to an experimental absorption coefficient or extinction coefficient (ε). By definition here, ε refers to the molar decadic (base 10) extinction coefficient; ε has units of $\ell\ mol^{-1}\ cm^{-1}$. Aromatic structures undergoing π-π^* transitions usually have large values for ε, while n-π^* transitions are usually forbidden because of symmetry but are observable through vibronic coupling; they have relatively low values for ε.(30-34)

A list of typical photoactive parent organic molecules, photo-initiators, photosensitizers and their extinction coefficients is given in Table 4.(34) In Fig. 5 are shown representative absorption spectra (presented as log ε versus wavelength) for a series of aromatic ketone photosensitizers.(35-36)

TABLE 4. MOLECULAR STRUCTURE-EXTINCTION COEFFICIENT RELATIONSHIPS[a]

Molecule	Extinction Coefficient, ε		
tosensitive Parent Molecule	λ = 254 nm	λ = 313 nm	λ = 366 nm
tone	7	3	0
tophenone	10^3	4×10^1	5
zophenone	$1{\cdot}7 \times 10^4$	5×10^1	7×10^1
'-Bis(N,N-dimethyl mino)benzophenone	$1{\cdot}3 \times 10^4$	$1{\cdot}1 \times 10^4$	$2{\cdot}8 \times 10^4$
zene	9×10^1	0	0
uene	$1{\cdot}7 \times 10^2$	0	0
thone	1×10^4	3×10^3	2×10^2
tosensitizer	λ = 318-320 nm	λ = 340-345 nm	
zoin	310	--	
ethylbenzoin	200	--	
ydroxymethyl benzoin	--	150	
zoin isopropyl ether	--	230	
zoin phenyl ether	--	250	

From Reference 34.

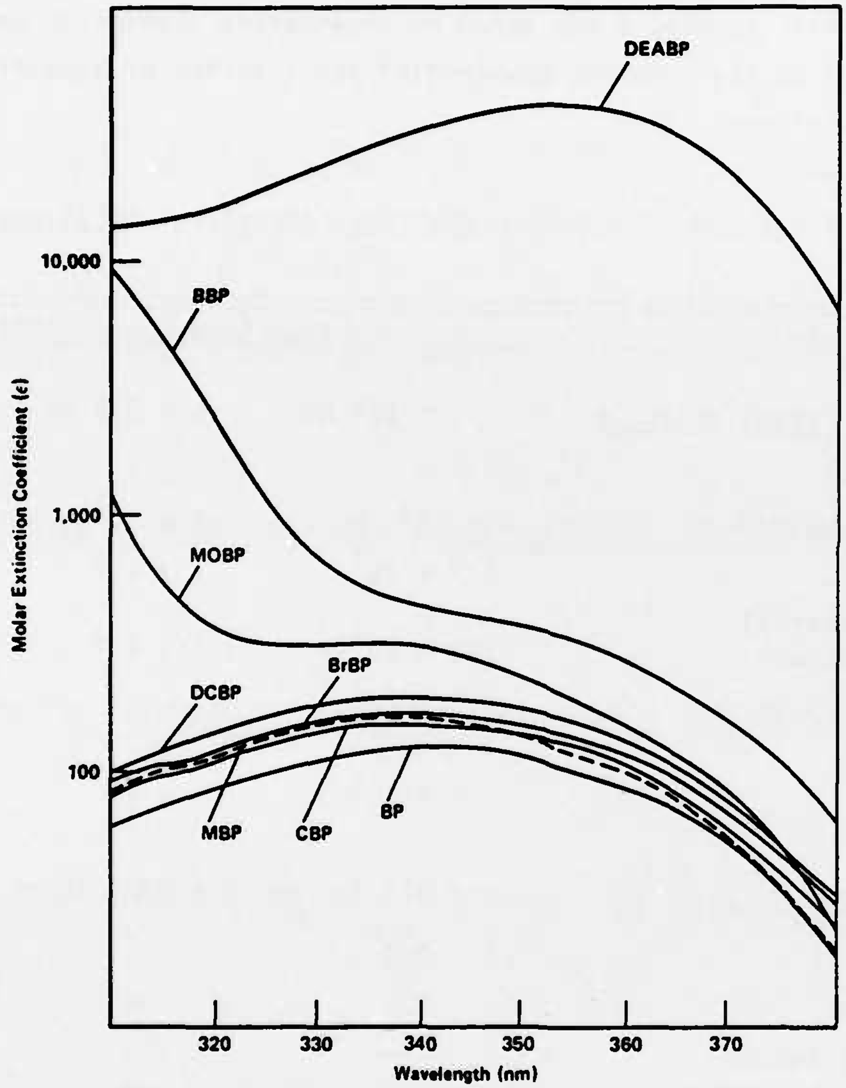

FIGURE 5. EXTINCTION COEFFICIENT (ε) AND λ_{max} VALUES FOR THE FOLLOWING SERIES OF p-SUBSTITUTED BENZOPHENONE DERIVATIVES:BENEZOPHENONE (BP), BISDIETHYLAMINOBENZOPHENONE (DEABP), BENZOYLBENZOPHENONE (BBP), METHOXYBENZOPHENONE (MOBP), DICHLOROBENZOPHENONE (DCBP), BROMOBENZOPHENONE (BrBP), METHYLBENZOPHENONE (MBP) AND CHLOROBENZOPHENONE (CBP).

Photophysical Processes

After absorption of light energy, followed by changes in electron distribution, the excited molecules can undergo various types of photophysical or photochemical deactivation pathways (Fig. 6).

Most organic molecules have paired electrons in their ground state (S_0) and upon absorption of light energy a change in electron distribution takes place in which electrons are promoted to upper singlet level (S_1, S_2) excited states with conservation of their electron spin configurations. Loss of this absorbed energy without molecular rearrangement can result from internal conversion or through fluorescence radiative processes.

A second process, especially important to aliphatic or aromatic carbonyl compounds, is the ability of an excited state molecule (S_1, S_2 energy levels) to undergo a change in electron spin configuration through intersystem crossing a lower triplet energy level excited state. Emission of light energy from the triplet level results in phosphorescence radiative processes.

Another factor to consider is the efficiency with which the incident radiation on the absorbing molecules is converted to the triplet excited state. This efficiency can be defined in the following manner:

$$\phi_p \text{ (quantum yield of phosphorescence)} = \frac{\text{number of triplet states which emit light}}{\text{number of photons absorbed by the molecules}} \tag{34}$$

Photoinitiators or photosensitizers having chemical structures that facilitate intersystem crossing processes and enhance ϕ_p would be expected to exhibit efficient free radical intermediate generating capabilities[31,34,37].

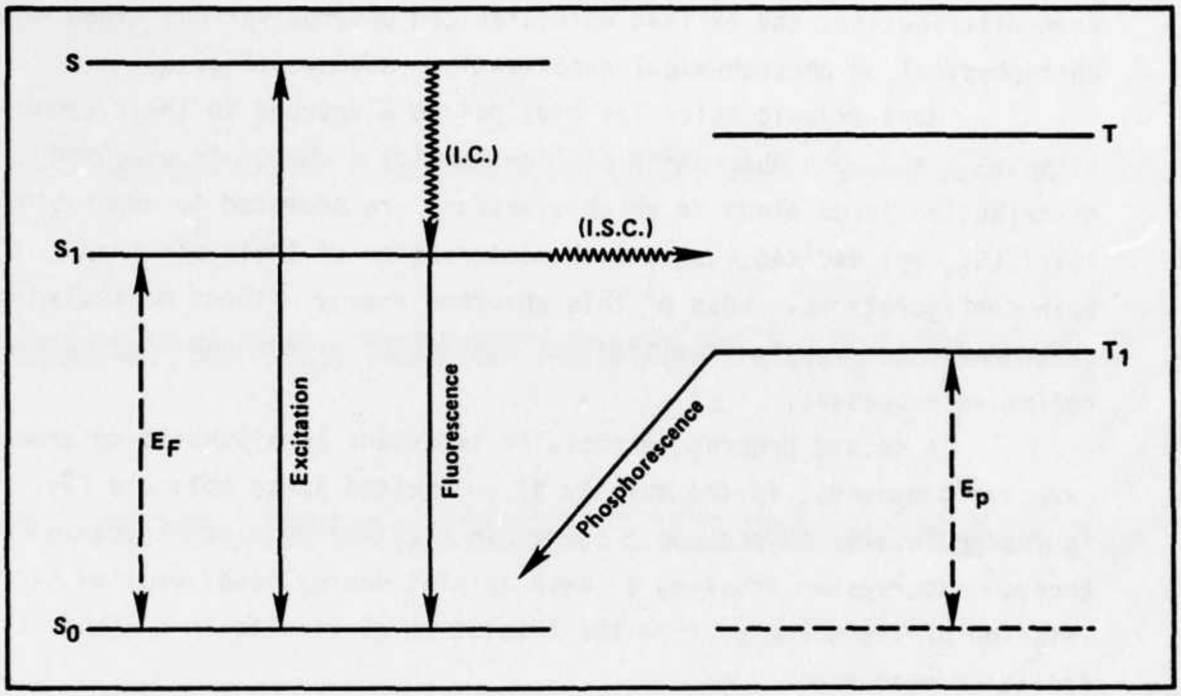

FIGURE 6. SCHEMATIC JABLONSKI DIAGRAM FOR A TYPICAL ORGANIC MOLECULE. S_0 = GROUND STATE; S = UPPER SINGLET LEVEL; S_1 = LOWEST SINGLET LEVEL; E_F = ENERGY OF LOWER SINGLET STATE; T_1 = LOWEST TRIPLET LEVEL; T = UPPER TRIPLET LEVEL; E_p = ENERGY OF LOWEST TRIPLET STATE; I.C. = RADIATIONLESS INTERNAL CONVERSION PROCESS; I.S.C. = RADIATIONLESS INTERSYSTEM CROSSING PROCESS

The energy and reactivity of the triplet states of a photoinitiator or photosensitizer are also important considerations, since most excited state photochemical reactions (molecular rearrangement, free radical intermediate formation and hydrogen abstraction reactions) occur from the triplet energy levels of these types of chemical structures. If the triplet lifetime of the photoinitiator or photosensitizer is short, then the chance of reaction, formation of free radical inermediates or undergoing hydrogen abstraction processes is less than if the triplet lifetime were long. If the triplet energy levels for photoinitiators or photosensitizers are low, it is possible that other chemical molecules in the photoreactive system (oxygen or certain monomer chemical structures) will cause quenching of the triplet excited state which subsequently lowers the ability of a photoinitiator or photosensitizer to effect free radical generation processes.(17,38) Examples of typical triplet lifetimes and triplet energies for aromatic and aromatic-aliphatic carbonyl compounds are listed in Table 5.(35)

TABLE 5. MOLECULAR STRUCTURE-TRIPLET ENERGY RELATIONSHIPS

Photosensitive Parent Molecule	Triplet Energy (kcal/mol)	Triplet Lifetime in Solution (μs)
Acetone	79-82	0·94
Acetophenone	73-4	3·50
Benzophenone	68-9	12·0
4,4'-Bis(N,N-dimethylamino)benzophenone	62	27
Xanthone	74	50

Mechanisms For Photochemical Production of Free Radical Intermediates

In order to describe the mechanism of a photochemical reaction it is necessary to evaluate and quantify the following processes:

1. light absorption;
2. radiative decay (fluorescence);
3. intersystem crossing efficiency;
4. phosphorescence;
5. molecular rearrangement; and
6. quenching.

For photoinitiators (PI) the primary photochemical reactions are as follows

$$PI + h\nu \xrightarrow{I_0\epsilon} (PI)_S^* \text{ (light absorption)} \tag{35}$$

$$(PI)_S^* \xrightarrow{k_f} PI + h\nu \text{ (fluorescence)} \tag{36}$$

$$(PI)_S^* \xrightarrow{k_{ST}} (PI)_T^* \text{ (intersystem crossing)} \tag{37}$$

$$(PI)_T^* \xrightarrow{k_p} PI + h\nu \text{ (phosphorescence)} \tag{38}$$

$$(PI)_S^* \text{ or } (PI)_T^* + M \xrightarrow{k_{qn}^{ST}} \text{(non-radical products)} \tag{39}$$

$$(PI)_S^* \text{ or } (PI)_T^* + M \xrightarrow{k_{qt}^{ST}} \text{(radical products--non-initiating or incapable of starting kinetic chains)} \tag{40}$$

$$(PI)_S^* \text{ or } (PI)_T^* \xrightarrow{k_r^{ST}} PI_1\cdot + PI_2\cdot \text{ (initiating and non-initiating radical intermediates)} \tag{41}$$

The optimum efficiency of photoinitiation is achieved if all fragment radical inermediates (PI_1 and PI_2) react rapidly with a monomer (M) and start the growth of kinetic chains (primary initiation).

$$PI_1^{\cdot} \text{ or } PI_2^{\cdot} + M \xrightarrow[\text{(2)propagation}]{\text{(1)primary initiation}} \text{(polymer)} \tag{42}$$

Another expression representing radical formation efficiency can be defined in the following manner:

$$\text{Rate of radical production} = \alpha_{PI} = (PI)^{*}_{ST}k_r^{ST} \tag{43}$$

If we assume $(PI)_T$ is more important than $(PI)_S$ for the formation of radical intermediates then

$$\alpha_{PI} = (PI)^{*}_{T}k_r^{T} \tag{44}$$

The rationale for this expression is that most photoinitiator molecules are composed of aromatic carbonyl chemical structures having long-lived triplet excited states, high k_{st} values and low k_f efficiencies, hence

$$d(PI)^{*}_{T}/dt = (PI)^{*}_{S}k_{ST} - (PI)^{*}_{T}k_p - (PI)^{*}_{T}[M]k^{T}_{qn} - (PI)^{*}_{T}[M]k^{T}_{qr} - (PI)^{*}_{T}k^{T}_{r} \tag{45}$$

Invoking steady state kinetic analysis conditions for $(PI)_S$ and $(PI)_T$ leads to

$$(PI)^{*}_{S} = \frac{[PI]I_0\varepsilon}{k_f+K_{ST} + [M]k^{S}_{qn} + [M]k^{S}_{qr} + k^{S}_{r}} \tag{46}$$

$$(PI)_T^* = \frac{(PS)_S^*}{k_p+[M]k_{qn}^T + [M]k_{qr}^T + k_r^T} \qquad (47)$$

If we assume $k_{ST} = 1$, $k_f = 0$ and

$$k_{qn}^S = k_{qr}^S = k_r^S \ll k_{qn}^T = k_{qr}^T = k_q \qquad (48)$$

then

$$(PI)_T^* = \frac{[PI]I_0\varepsilon}{k_p + [m]k_q + k_r^T} \qquad (49)$$

Substitution of eqn (48) into eqn (44) results in

$$\alpha_{PI} \text{ (rate of radical production)} = \frac{[PI]I_0\varepsilon k_r^T}{k_p+[M]k_q+k_r^T} \qquad (50)$$

If the rate constants for phosphorescence (k_p) and quenching (k_q) are larger than the radical formation rate constant (k_r) then the rate of radical production (α_{PI}) will be very small and inefficient. It is desirable to design photoinitiator molecules whose chemical structures enhance the t_r rate constant over the deactivation pathways.[39-42]

A similar reaction scheme can also be derived for photosensitizers (PS):

$$PS + h\nu \xrightarrow{I_0\varepsilon} (PS)_S^* \text{ (light absorption)} \qquad (51)$$

$$(PS)_S^* \xrightarrow{k_f} PS^* + h\nu \text{ (fluorescence)} \qquad (52)$$

$$(PS)_S^* \xrightarrow{k_{ST}} (PS)_T^* \text{ (intersystem crossing)} \qquad (53)$$

$$(PS)^*_S \xrightarrow{k_p} PS + h\nu \text{ (phosphorescence)} \tag{54}$$

$$(PS)^*_S \text{ or } (PS)^*_T + M \xrightarrow{k_q^{ST}} \text{(non-radical products or radical products which are incapable of starting kinetic chain lengths)} \tag{55}$$

$$(PS)^*_S \text{ or } (PS)^*_T + I \text{ (photo or thermal initiator) } \xrightarrow{k_I^{ST}} I\cdot\text{(free radical formation)} + PS \tag{56}$$

$$(PS)^*_S \text{ or } (PS)^*_T + SH \text{ (hydrogen donor substrate) } \xrightarrow{k_{SH}^{ST}} PSH\cdot + S\cdot \tag{57}$$

(photoreduction and initiating or non-initiating radical formation)

If we assume similar arguments apply as derived for photoinitiators then

$$\alpha_{PS} \text{ (rate of free radical production)} = (PS)^*_T[I]k_I^T \tag{58}$$

$$\alpha_{PS} \text{ (rate of free radical production)} = (PS)^*_T[SH]k_{SH}^T \tag{59}$$

$$\alpha_{PS} = \frac{[PS]I_o\varepsilon[I]K_I^T}{k_p + k_q[M] + [I]K_I^T} \tag{60}$$

$$\alpha_{PS} = \frac{[PS]I_o\varepsilon[SH]k_{SH}^T}{k_p + k_q[M] + [SH]k_{SH}^T} \tag{61}$$

It should be noted that not all free radical intermediates produced through photochemical reactions are primary initiators, in that certain structures may be incapable of starting kinetic chain growth of a vinyl monomer:

$$PI \xrightarrow{h\nu} PI_1\cdot + PI_2\cdot \tag{62}$$

$$PI_1\cdot + M \longrightarrow \text{(polymer formation)} \tag{63}$$

$$PI_2\cdot + M \not\longrightarrow \text{(no reaction)} \tag{64}$$

$$PS + SH \longrightarrow PSH\cdot + S\cdot \tag{65}$$

$$S\cdot + M \longrightarrow \text{(polymer formation)} \tag{66}$$

$$PSH\cdot + M \not\longrightarrow \text{(no reaction)} \tag{67}$$

It should also be noted that solvent factors and the actual chemical structure of the vinyl monomer (M) may ultimately determine whether or not a primary radical intermediate undergoes initiation or termination kinetic processes.

In some cases a certain free radical intermediate chemical structure may only participate in termination reactions with a growing polymer chain.[17,35,43,44]

$$\text{Growing polymer radical (GPR}\cdot\text{)} + PI_2\cdot \text{ or } PSH\cdot \longrightarrow GPR\text{—}PI_2 \text{ or } GPR\text{—}PSH \text{ (termination)} \tag{68}$$

All of the above factors must be considered when designing and selecting photoinitiators or photosensitizers for use in photopolymerization reactions.

Photopolymerization

The function of a photoinitiator or photosensitizer molecule is to provide primary initiating free radical intermediates in a photopolymerization reaction system. The greater the efficiency for primary radical production as well as the minimum competitive interactions between primary radicals and vinyl monomer determines the overall rate of photopolymerization.

$$PI \xrightarrow{h\nu} PI_1\cdot + PI_2\cdot \text{ (primary radical formation)} \tag{69}$$

$$PI_1\cdot \text{ or } PI_2\cdot + M \longrightarrow \text{(polymer, desired reaction)} \tag{70}$$

$$PI_1\cdot + PI_2\cdot \longrightarrow \text{(products, competitive reactions)} \tag{71}$$

$$PS + I \xrightarrow{h\nu} I\cdot + PS \text{ (primary radical formation)} \tag{72}$$

$$I\cdot + M \longrightarrow \text{(polymer)} \tag{73}$$

$$PS + SH \xrightarrow{h\nu} PSH\cdot + S\cdot \text{ (primary radical formation)} \tag{74}$$

$$PSH\cdot \text{ or } S\cdot + M \longrightarrow \text{(polymer)} \tag{75}$$

$$2PSH\cdot \text{ or } 2S\cdot \longrightarrow \text{(mixed products, competitive reactions)} \tag{76}$$

For the following discussion $PI_1\cdot$, $PI_2\cdot$, $I\cdot$, $PSH\cdot$ and $S\cdot$ will be designated as primary radicals ($PR\cdot$).

The overall rate of a photopolymerization reaction can be expressed as a function of initiation of the chain radicals, propagation of chains and termination processes. The rate of initiation (R_i) can be described in the following manner:

$$\begin{aligned} R_i = {} & \text{(primary radical formation)} \\ & - \text{(primary radical interaction with vinyl monomers)} \\ & - \text{(primary radical competitive interactions leading to} \\ & \quad \text{non-polymeric products)} \end{aligned} \tag{77}$$

Primary radical ($PR\cdot$) formation is given by

$$(PR\cdot) = I_o \phi \ell \varepsilon [PI \text{ or } PS] \tag{78}$$

where I_0 = incident light intensity, ϕ = quantum yield for radical production (ϕ = 2 when 1 quantum absorbed results in 2 primary radicals having equal activity and ϕ < 2 is due to competitive processes), ℓ = optical path length of the system ϕ and ε = photoinitiator (PI) or photosensitizer (PS) molar extinction coefficient.

Now,

$$\text{primary radical initiation} = k_1[PR\cdot][M] \tag{79}$$

and,

$$\text{primary radical competitive processes} = k_{cp}2[PR\cdot]^2 \tag{80}$$

If we assume that in many cases primary radical competing processes are at a minimum then

$$\text{rate of initiation } (R_i) = I_0\phi\ell\varepsilon[\text{PI or PS}] = k_1[PR\cdot][M] \tag{81}$$

The overall rate of a photopolymerization reaction (R_p) can be described by the following equation:

$$R_p = \frac{d[M]}{dt} = \frac{k_p[M]R_i^{1/2}}{k_t^{1/2}} \tag{82}$$

where k_t = termination rate constant (liter/mol), k_p = propagation rate constant (liter/mol), M] = monomer concentration (mol/liter), and R_i = rate of initiation (mol/liter).

If the rate constants for k_r, k_p, k_q, k_I, k_{SH} are known then values of α_{PI}, α_{PS} (Eqns (50, (60) and (61)) can be calculated. Also, according to Eqn (82) the rate of photopolymerization (R_p) should be proportional to $\alpha_{PI}^{\frac{1}{2}}$ or $\alpha_{PI}^{\frac{1}{2}}$ if one assumes R_i to be proportional to α_{PI} or α_{PS}.

The quantum yield for the number of kinetic chains started per photon absorbed by the photoinitiator or photosensitizer is defined as follows:

$$\Phi_i = f_p \phi(\alpha_{PI} \text{ or } \alpha_{PS}) \phi_{(triplet)} \qquad (83)$$

where f_p = fraction of radicals starting kinetic chains, ϕ = quantum yield for number of primary radicals formed (in α-cleavage reactions, ϕ = 2) and $\phi_{(triplet)}$ = quantum yield of triplet formation.

The use of photochemical and photopolymerization reaction kinetic analysis techniques helps one to better understand fundamental concepts associated with various chemical structures for photoinitiator and photosensitizer systems.[39-42,45]

Polymeric Crosslinking Reactions

In conventional monofunctional vinyl unsaturated monomer polymerization reactions, the liquid monomer undergoes an initially slow reaction sequence to form a solid mass of material (Figure 7). About half way through the reaction sequence the monomer/polymer ratio reaches a critical value (gel point) and a rapid rise in solution viscosity is noticed along with an autoacceleration in the rate of polymerization reaction. The final stages of conversion are relatively slow in that the monomer/polymer ratio is very low and the low molecular weight monomer units must diffuse into large macroradical structures in order to terminate the polymerization process.

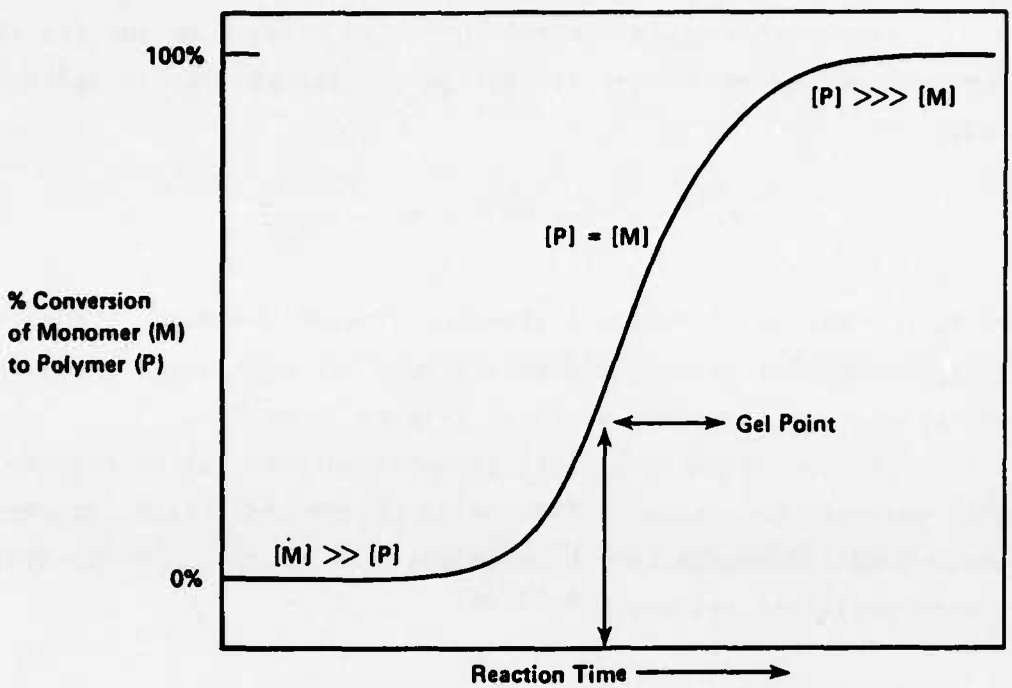

FIGURE 7. TIME SEQUENCE OF A TYPICAL VINYL POLYMERIZATION REACTION

Analysis of the overall rate equation for photoinduced polymerization reactions,

$$R_p = \frac{K\,[\text{monomer}][\text{photoinitiator}]^{1/2}}{k_t^{1/2}} \tag{84}$$

indicates that any substantial change in k_t (termination rate constant) strongly influences the rate of reaction. Since k_t has an indirect relationship to the monomer/polymer solution viscosity [$k_t = f\,(1/\eta)$ and $\eta = f$ (monomer/polymer)] then the % conversion of monomer to polymer can be accelerated under certain conditions directly related to monomer or polymer concentration effects.

The most efficient method of converting a liquid reactive monomer system to a solid polymer is through the use of multi-functional vinyl unsaturated monomers that are capable of quickly developing gel or network structures at very low percentages of conversion.

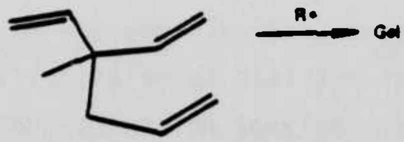

(85)

The photoinduced addition polymerization of multifunctional monomers proceeds in general in three stages: formation of linear ("primary") macromolecules with pendent functional groups, branching through these groups and, finally, intermolecular crosslinking leading to gelation, i.e., the occurrence of macromolecules of "infinite" molar mass.[46] In addition, intramolecular cyclization reactions may occur which, in special cases, lead to cyclopolymerizations and the absence of gelation.[47] Differences of opinion exist as to the relative extent of the three stages, the importance of intramolecular reactions, and the applicability of the various theories to the different polymerization stages, such as the classical statistical theories[48,50], the cascade theory[51,52], the percolation theory[53-55], and various kinetic approaches.[56,57]

Simple kinetic considerations show that primary molecules are already formed at very low monomer conversions. Free radical polymerizations reach their steady-state conditions for radical concentrations of approximately 10^{-8} mol/l. If the molar mass of the primary molecules is 10^5 g/mol and if the steady state is exclusively controlled by polymer radicals (which is approximately true for low initiator concentrations), then the steady state is reached for polymer concentrations of 10^{-3} g/l, i.e., at very low monomer conversions.

The pendant groups of primary molecules must be already subject to further reactions at these very low monomer conversions, regardless of whether all groups are equally accessible or only a fraction thereof, e.g., the groups on the periphery of the primary macromolecules. Pendent functional groups may be attacked by primary polymer radicals (or by initiator radicals if the initiator concentration is high) and the thus formed branched polymer radicals may add further monomer molecules. Since branching alone does not lead to gelation[48,58], addition of polymer radicals onto primary polymer molecules and recombination of branched polymer radicals are the two ways to achieve gelation. Other termination steps, such as the disproportionation reaction of polymer radicals or the termination by initiator radicals, neither increase the degree of polymerization nor the probability for intermolecular polymer/polymer reactions. An exception may be intermolecular chain transfer to primary or branched molecules since the newly formed polymer radicals may add further monomer molecules which in turn increases the molar mass. The probability of such transfer reactions is, however, small compared to addition of polymer radicals to primary or branched molecules.

Regardless of the mechanism associated with gelation of multifunctional vinyl unsaturated monomers their rates of conversion (liquid to solid) are usually much greater than single vinyl unsaturated compounds.

Solid-state photoinduced polymeric crosslinking reactions have only been of interest in thin film photoresist technologies, and this concept usually does not involve a propagation reaction in that it is a single-event-related phenomenon:

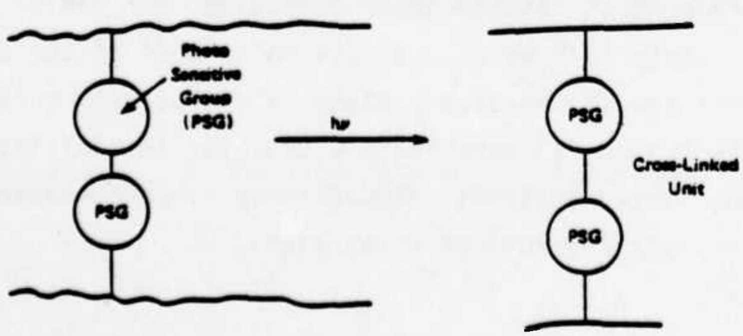

(86)

Combination of the multifunctional unsaturated monomer gelation oncepts (initiation, propagation and termination) with solid state hotopolymerization reactions should show a dramatic increase in quantum ield for crosslinked site formation.

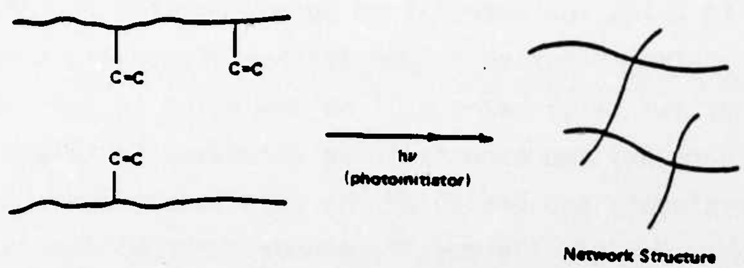

(87)

In this study it was of prime importance to develop a unique photoinitiator system; hence, the preliminary experiments were carried out in a well-characterized single vinyl unsaturated monomer system such as methyl methacrylate.

The actual photosensitive catalyst/polymer systems studied during this phase of the research program involved singlet-triplet (S-T), triplet-triplet (T-T) energy transfer reactions, free radical intermediates and unsaturated (methylmethacrylate) vinyl monomer-polymer substrates.

Two-Beam Irradiation Studies

An important goal of this program has been to discover processes that will allow the production of polymeric materials by selectively polymerizing materials at particular points internal to the container surface in which the material to be polymerized resides. Our experimental studies of the selective polymerization of acrylic monomers at the intersection of two laser beams will be described in this section of the report. There are two aspects to be discussed in this. First, the experimental rationale and design of the experiments done in this phase will be described. Second, the results of our tests will be given, along with our recommendations for the steps to be taken in subsequent studies toward making this two-photon process a commercially feasible reality.

By selective excitation of the material with two different wavelengths, it is expected that selective polymerization at a particular spot can be achieved, inside the outer surfaces of the prepolymer. The expectation is that the action of either single wavelength laser will not polymerize the material while the action of the two specified wavelengths will produce the selective energy transitions required to polymerized. It has been the goal of this research to develop the knowledge of the material and the steps in the process necessary to produce this selection.

Experimental Design

The primary design criterion for these experiments has been the use and its intermediate triplet state. Preliminary screening of sensitizers, initiators, and polymers was often carried out using focused Eimac 150 W high pressure Xenon arc lamps with appropriate Corning cut-off filters. Final characterization of each sample system, however, was carried out using crossed laser beams, with a computer-controlled three-axis translation stage being used to move the sample, while keeping the focal point of each beam fixed. While this is not an optimum procedure, it is far simpler experimentally than moving the beams would be, and it provides a valid and convenient technique for laboratory studies.

Figure 8 shows the setup of the lasers and the positioning of the material in the system. The laser beams are crossed at their focused position. The beams are focused by quartz lenses at a single spot in the sample cuvette. The beam from the singlet exciting laser is then directed in such a way as to be colinear with the beam from the second laser. The signal is then detected with a photomultiplier observed on an oscilloscope. In this way, the timing of the two signals can be controlled. Strong continuously radiating energy sources could also be used, but pulsed laser sources provide higher upper state populations in controlled periods of time such that the chances for an absorption of the second wavelength has a higher probability of occurring. Pulsing also reduces the problems associated with heating the samples as compared to a continuous source.

The laser used to excite the sensitizer was a Phase-R DL-1200 V flashlamp-pumped dye laser operating in the 630 nm region of the spectrum. For the porphyrin sensitizers, with which most of the laser experiments conducted, the dye used to produce this excitation was Kiton Red S ($5x10^{-3}$ M in methanol) which was excited as it flowed through the cavity of the flash lamp. The dye was kept cool by means of a circulating fluid temperature controller. The energy of the beam of the exciting laser was about 100 mJ, and had a half width of 2 nm. The energy, the time during the pulse, and the beam cross section determine the intensity of the light which for the Phase-R laser was 8 MW/cm^2. Data for making calculations can be found in Table 6.

The second laser was a Molectron UV24-DL14 nitrogen pulsed dye laser which we tuned to 730 nm; this was thought to be optimum for exciting the upper triplet states. The energy of this laser was in the range of 200 microjoules per pulse for the dyes Rhodamine B Perchlorate and Oxazine 1 Perchlorate, each at a concentration of $5x10^{-3}$ M (Molectron

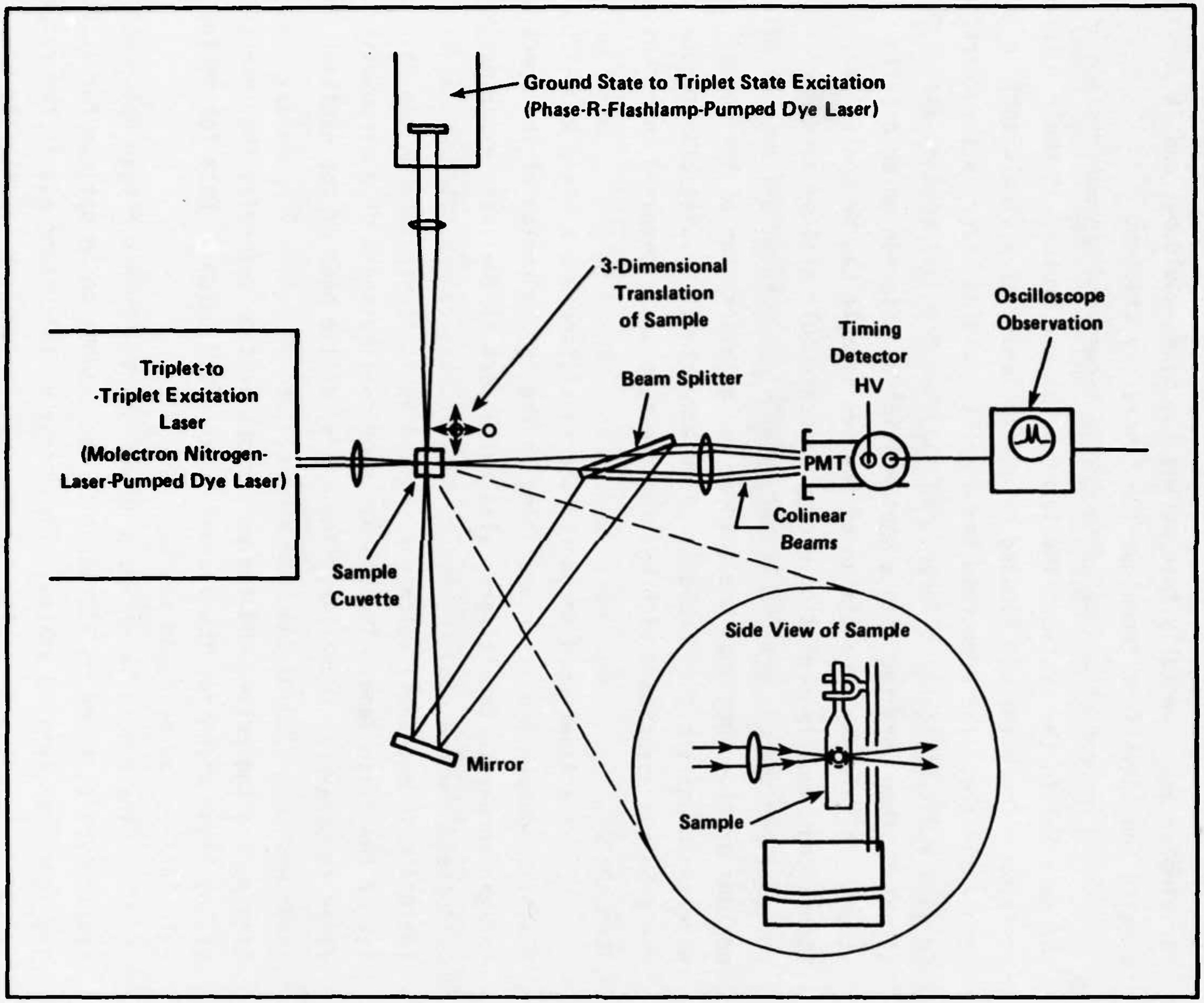

FIGURE 8. SCHEMATIC ILLUSTRATION OF TWO-BEAM LASER IRRADIATION SYSTEM

TABLE 6. DATA ON LASERS AND MATERIALS INTERACTIONS USED IN TWO-PHOTON EXPERIMENTS ON POLYMERIZATION OF METHYL METHACRYLATE WITH PORPHYRIN SENSITIZATION

	Laser 1 Phase-R DL1200V		Laser 2 Molectron UV24-OL14	
Pulse Energy	E_1	100 mJ	E_2	0.2 mJ
Area of Beam	A_{b1}^2	5×10^{-2} cm^2	A_{b2}^2	5.0×10^{-3} cm^2
Time of Pulse	τ_1	250 ns	τ_2	8 ns
Repetition Rate (Pulses per Second)		0.33 Hz		0.33 Hz
Wavelength	λ_1	590-620 nm	λ_2	730-780 nm
Bandwidth	$\Delta\lambda_1$	$\pm$ 2 nm	$\Delta\lambda_2$	$\pm$ 0.1 nm
Effective Optical Path Length at Intersection Point	ℓ_1	0.07 cm	ℓ_2	0.25 cm
Estimated Absorptivity of Porphyrin Sensitizer times concentration	$(\alpha_1 C_1)$	0.2 cm^{-1} at 620 nm	$(\alpha_2 C_2)$	0.4 cm^{-1} at 730 nm

Dye 19). The pulse duration of the second laser is only 8ns, however, and this energy must be controlled in time to arrive at the sample just after the pulse from the first laser. The cross-sectional area of the Molectron laser beam is also smaller than that from the Phase-R laser. With these data, a light intensity of 1.5 MW/cm^2 is found in the beam during a pulse which is similar to the Phase-R laser. In the case of the porphyrin photoinitiator, the timing of the triplet excitation pulse can be placed any time after 50 ns and up to a few microseconds because the triplet lifetime in the ground state is estimated to be in the tens of microseconds after the first beam has been absorbed.

Considerable effort was needed to synchronize the two systems so that both of the lasers fired at the same time. This was only partially accomplished due to jitter between the two instruments in timing. Figure 9 shows a schematic diagram of the triggering scheme used in our experiments to control this timing. By varying the delay in the trigger of the Molectron laser, the laser outputs of the two could be synchronized. The Molectron output seemed to be steady within 20 ns as compared to the trigger in put driving the two systems. However, the Phase-R laser seemed to jitter in a distribution around the Molectron laser by as much as 1-2 microseconds when this work was first begun. We estimate that this effect substantially reduced the number of shots in which the two lasers were actually synchronized in time. Subsequent improvements in the triggering of the Phase-R laser, and a complete overhaul of this laser (including replacement of the original coaxial flashlamp with a newer triaxial flashlamp design and replacement of both the power transformer and high-voltage flashlamp capacitor), greatly improved the stability and overall performance of the laser.

The accuracy and repeatability of sample irradiations was improved substantially during the past year by the development of a computer-controlled, 3-axis translation stage which allows the sample to be moved reproducibly in a pre-determined pattern, while keeping the laser beams fixed and synchronized. While this procedure is somewhat slower and

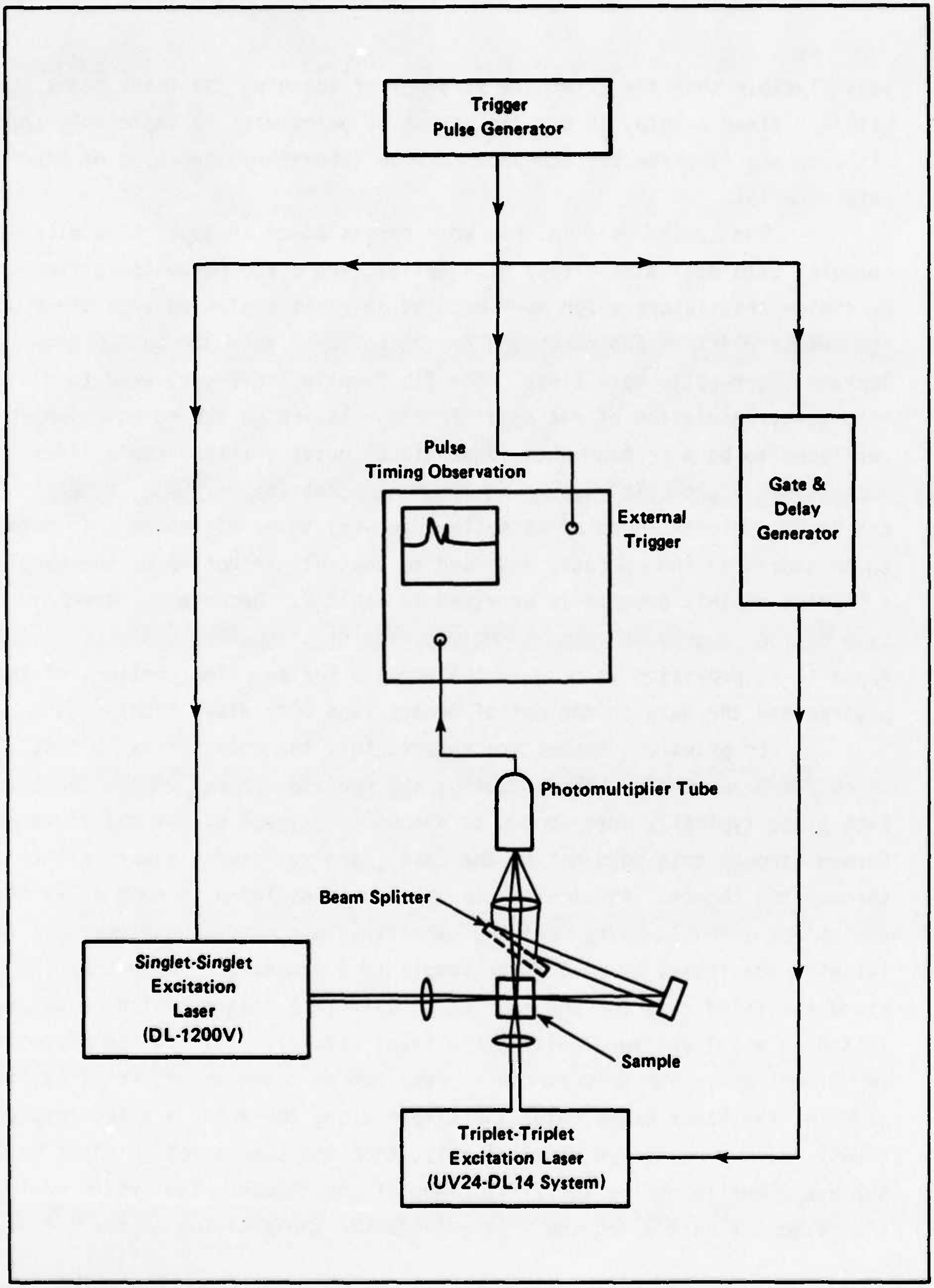

FIGURE 9. SCHEMATIC ILLUSTRATION OF LASER TRIGGERING SCHEME

less flexible than the alternate strategy of scanning the laser beams within a fixed sample, it has the virtue of being easy to implement, and its accuracy is perfectly adequate for the laboratory screening of candidate materials.

The system used in this work consisted of an Apple II-E microcomputer with dual mini-floppy disk drives, and 3 stepper-motor-driven precision translators which were mounted at right angles to each other on the sample platform and connected to the computer by means of Hewlett-Packard fiber-optic data links. The fiber-optic links were used to minimize the transmission of r-f noise from the lasers to the computer which was found to be a problem when conventional metal shielded-cable links were used. A Basic language program was written (by Warren E. Nicholson and Dan R. Grieser, both of Battelle-Columbus) to permit shape information to be stored in the computer and used to control the motion of the sample; a listing of this program is provided in Table 7. Because the combined size of the program and data sometimes exceeds the memory capacity of the Apple II-E, provision is made in the program for swapping portions of the program and the data in and out of memory (and onto disk) as needed.

In practice, shapes are entered into the computer as "planes", which are drawn on the CRT monitor by appropriate motions of the cursor. Each plane typically corresponds to one monitor image of the object to be formed (though this need not be the case), and represents a vertical slice through the object. Physically, the system is designed in such a way that the object is built up by "writing" the first plane in the polymer material with the lasers by moving the sample in 2 dimensions, then stopping along the third axis for one resolution unit (the size of which canbe adjusted at will) and then writing the shape specified for the new plane in two dimensions. The process can be repeated as often as desired. If, for example, the laser beams enter the sample along the x and y axes, respectively, with z being the vertical axis, then the sample motion might be in the x-z plane to define the first plane of the object. The system would then step one unit along the y axis to define the position of the second

TABLE 7. LISTING OF "3D-PCM" COMPUTER PROGRAM

```
]LIST

100  REM   <XYZTRANS>
103  IF  PEEK (104) = 8 THEN  NEW : END
105  POKE 214,255
110  GOTO 380
130 N = NS: POKE  - 16295,1
140  GOTO 170
160 N = NS: POKE  - 16296,0
170 NL = PX:NH = XP: GOTO 300
190 N = NS: POKE  - 16295,1
200  GOTO 230
220 N = NS: POKE  - 16296,0
230 NL = PY:NH = YP: GOTO 300
250 N = NS: POKE  - 16295,1
260  GOTO 290
280 N = NS: POKE  - 16296,0
290 NL =  - 16290:NH =  - 16289: GOTO 300
300  IF N <  = 0 THEN  RETURN
310  POKE NL,ZE: POKE NH,ZE:N = N - 1: GOTO 300
330  REM  22FEB84, DAN GRIESER
380  REM
385 PX =  - 16294:XP =  - 16293:PY =  - 16292:YP =  - 16291
390  IF  PEEK (2560) <  > 1 OR  PEEK (2561) <  > 0 THEN  GOTO 410
400  IF  PEEK (2590) = 45 AND  PEEK (2591) = 0 THEN  GOTO 420
410  PRINT  CHR$ (4);"BLOAD CURS,A2560,D1"
420  POKE 232,0: POKE 233,10:MX = 254
430  DIM XX%(MX),YY%(MX),ZZ%(MX),A$(80)
440  DIM FL$(30)
450  GOSUB 910: REM  INITIALIZE.
460  GOSUB 1050: REM  RESET DEFAULTS
470  TEXT : HOME
480  PRINT "CURRENT POSITION RELATIVE TO 'HOME':"
490  PRINT : GOSUB 1090
500  PRINT "    X=";XX;"       Y=";YY;"       Z=";ZZ: PRINT
510  HTAB HT: PRINT "***    MAIN MENU    ***"
520  PRINT
525  HTAB HT: PRINT " 0 = QUIT PROGRAM "
530  HTAB HT: PRINT " 1 = RESET DEFAULTS"
540  HTAB HT: PRINT " 2 = DISPLAY & REVISE DEFAULTS"
550  HTAB HT: PRINT " 3 = RESET 'HOME' POSITION"
560  HTAB HT: PRINT " 4 = 'HOME' THE DRIVES"
570  HTAB HT: PRINT " 5 = SLEW TO NEW POSITION"
580  HTAB HT: PRINT " 6 = JOG TO NEW POSITION"
590  HTAB HT: PRINT " 7 = ENTER NEW PATH"
600  HTAB HT: PRINT " 8 = TRACE CURRENT PATH"
610  HTAB HT: PRINT " 9 = DISPLAY CURRENT PATH"
615  HTAB HT: PRINT "10 = AUTO-TRACE PLANES"
617  HTAB HT: PRINT "11 = EXCHANGE X-Y AXIS"
620  VTAB 18: PRINT
630  HTAB HT: PRINT "CHOICE ?";: INPUT "";A$:FE =  FRE (0)
635 AA =  VAL (A$)
640  IF AA < 0 OR AA > 11 THEN  GOTO 620
650  IF AA = 0 THEN  PRINT : PRINT "FINIS!": POKE 214,0: POKE 103,1: POKE 104,8:
 NEW : END
655  SCALE= 1
660 AA =  VAL (A$)
670  ON AA GOSUB 1050,1140,1000,1300,1470,730,1820,2420,1760,4100,690
680  GOTO 470
690 TP = PX:PT = XP:PX = PY:XP = YP:PY = TP:YP = PT: RETURN
730  TEXT : HOME
740 NS = 1
```

TABLE 7. (Continued)

```
750  PRINT "PRESS 'J' = X CCW"
760  PRINT "      'K' = X CW"
770  PRINT "      'I' = Y CCW"
780  PRINT "      'M' = Y CW"
790  PRINT "      'U' = Z CCW"
800  PRINT "      'D' = Z CW"
810  PRINT "   <ESC> = TO LEAVE JOG MODE"
820  GET A$:FE =  FRE (0)
830  IF A$ =  CHR$ (27) THEN  RETURN
840  IF A$ = "J" THEN  GOSUB 130: GOTO 820
850  IF A$ = "K" THEN  GOSUB 160: GOTO 820
860  IF A$ = "I" THEN  GOSUB 190: GOTO 820
870  IF A$ = "M" THEN  GOSUB 220: GOTO 820
880  IF A$ = "U" THEN  GOSUB 250: GOTO 820
890  IF A$ = "D" THEN  GOSUB 280: GOTO 820
900  GOTO 820
910  POKE 33,40: HGR : TEXT : HOME
914 FT$ = "FILE NAME=":D$ =  CHR$ (4):VF$ = "VERIFY "
915 PL$ = "PLANE-":H$ = "-":HD$ = "HEADER":DK$ = "DISK-"
916 OP$ = "OPEN ":CL$ = "CLOSE ":RD$ = "READ ":WR$ = "WRITE "
920 ST = 3.175:HT = 5
930  POKE  - 16293,1: POKE  - 16291,1: POKE  - 16289,1
940  GOSUB 980
950  GOSUB 1000
960  GOSUB 1030
970  RETURN
980 ZE = 0:XF = ZE:YF = ZE:ZF = ZE
990  RETURN
1000 XO = ZE:YO = ZE:ZO = ZE: REM    "HOME" POSITIONS.
1010  GOSUB 1030
1020  RETURN
1030 XC = XO:YC = YO:ZC = ZO: REM  CURRENT POSITIONS.
1040  RETURN
1050 DV(1) = 32: REM   STEP SIZE=101.6 UM.
1055 SC = 430
1060 DV(2) = SC * 2: REM   TIME DELAY= 2 SEC.
1070 DV(3) = TS
1080  RETURN
1090 XX =  INT (XC * ST * 10 + .5) / 10:YY =  INT (YC * ST * 10 + .5) / 10:ZZ =
 INT (ZC * ST * 10 + .5) / 10
1100  RETURN
1110 XX =  INT (XF * ST * 10 + .5) / 10:YY =  INT (YF * ST * 10 + .5) / 10:ZZ =
 INT (ZF * ST * 10 + .5) / 10
1120  RETURN
1140  HOME
1150  HTAB HT: PRINT "DEFAULT VALUES:"
1160  PRINT " 1   STEP SIZE(MICRONS)=";DV(1) * ST
1170  PRINT " 2   TIME DELAY PER STEP (SECONDS)=";DV(2) / SC
1180  PRINT " 3   CURRENT TOTAL STEPS=";DV(3)
1190  PRINT " PRESS <ESC> TO RETURN"
1200  PRINT
1210  VTAB 10: HTAB HT: PRINT "CHOICE ?";: GET A$:FE =  FRE (0)
1220  IF A$ =  CHR$ (27) THEN  RETURN
1230  IF A$ < "1" OR A$ > "2" THEN 1210
1240 AA =  VAL (A$)
1250  PRINT : PRINT "NEW VALUE FOR '";AA;"'=";: INPUT NV
1260  IF AA = 1 THEN DV(1) =  INT (NV / ST + .5)
1270  IF AA = 2 THEN DV(2) =  INT (NV * SC + .5)
1280  GOTO 1140
1300 XD = XO - XC:YD = YO - YC:ZD = ZO - ZC
1310  GOSUB 1360
1320  GOSUB 1030
1330  GOSUB 1720
1340  RETURN
1360  IF XD = 0 THEN  GOTO 1390
1370  IF XD < 0 THEN NS =  ABS (XD): GOSUB 130: GOTO 1390
1380 NS = XD: GOSUB 160
1390  IF YD = 0 THEN  GOTO 1420
1400  IF YD < 0 THEN NS =  ABS (YD): GOSUB 190: GOTO 1420
1410 NS = YD: GOSUB 220
1420  IF ZD = 0 THEN  GOTO 1450
1430  IF ZD < 0 THEN NS =  ABS (ZD): GOSUB 250: GOTO 1450
1440 NS = ZD: GOSUB 280
```

TABLE 7. (Continued)

```
1450  RETURN
1470  HOME
1480  GOSUB 1710
1490  GOSUB 1730
1500  HOME : PRINT "CURRENT POSITION:"
1510  GOSUB 1090
1520  PRINT "X=";XX;"   Y=";YY;"   Z=";ZZ: PRINT
1530  PRINT "FUTURE POSITION:"
1540  GOSUB 1110: PRINT : PRINT "X=";XX;"   Y=";YY;"   Z=";ZZ
1550  PRINT : HTAB HT: PRINT "'S'=SLEW"
1560  HTAB HT: VTAB 12: PRINT "WHICH COORDINATE ?";: GET A$:FE =  FRE (0)
1570  IF A$ =  CHR$ (27) THEN  GOSUB 1730: RETURN
1580  IF A$ = "S" THEN  GOSUB 1740: GOTO 1470
1590  IF A$ < "X" OR A$ > "Z" THEN  GOTO 1560
1600  PRINT : PRINT
1610  IF A$ <  > "X" THEN  GOTO 1640
1620  GOSUB 1700
1630 XF =  INT (NV / 3.175 + .5): GOTO 1500
1640  IF A$ <  > "Y" THEN  GOTO 1670
1650  GOSUB 1700
1660 YF =  INT (NV / 3.175 + .5): GOTO 1500
1670  IF A$ <  > "Z" THEN  GOTO 1500
1680  GOSUB 1700
1690 ZF =  INT (NV / 3.175 + .5): GOTO 1500
1700  PRINT "NEW '";A$;"' VALUE (MICRONS)=";: INPUT NV: RETURN
1710 XD = ZE:YD = ZE:ZD = ZE: RETURN
1720 XF = XC:YF = YC:ZF = ZC: RETURN
1730 XC = XF:YC = YF:ZC = ZF: RETURN
1740 XD = XF - XC:YD = YF - YC:ZD = ZF - ZC: GOSUB 1360
1750  GOSUB 1730: GOSUB 1710: RETURN
1760  GOSUB 1780
1770  GET A$:FE =  FRE (0): RETURN
1780  POKE  - 16300,0: POKE  - 16304,0: POKE  - 16297,0: PRINT
1790  GOSUB 2360
1800  RETURN
1820  TEXT : HOME : PRINT " *** PATH ENTRY ROUTINE ***"
1830 DD = DV(1)
1840  PRINT : HTAB HT: PRINT " 1 = START AFRESH"
1850  HTAB HT: PRINT " 2 = CONTINUE CURRENT PATH"
1860  HTAB HT: PRINT " 3 = START IN MIDDLE"
1862  HTAB HT: PRINT " 4 = STORE CURRENT PATH"
1864  HTAB HT: PRINT " 5 = RECALL STORED PATH"
1870  HTAB HT: PRINT " <ESC> TO RETURN"
1880  VTAB 10: PRINT : PRINT "   CHOICE?";: GET A$:FE =  FRE (0)
1890  IF A$ =  CHR$ (27) THEN  RETURN
1900  IF A$ < "1" OR A$ > "5" THEN  GOTO 1880
1910 AA =  VAL (A$)
1920  ON AA GOSUB 1970,2030,1940,3100,3200
1930  GOTO 1820
1940  PRINT : PRINT "STARTING NUMBER=";: INPUT SN
1945 SN =  INT (SN) + 1
1950  IF SN > TS THEN  RETURN
1960  GOTO 2000
1970  TEXT : HOME : PRINT "*** FRESH START ***"
1980  PRINT "ZEROING THE PATH ARRAYS"
1985 NP = 1
1990 SN = 1:XL = 100:YL = 100
2000  FOR J = SN TO DV(3)
2010 XX%(J) = ZE:YY%(J) = ZE:ZZ%(J) = ZE
2020  NEXT J:TS = SN - 1
```

TABLE 7. (Continued)

```
2025  XDRAW 1 AT XL,YL
2030  PRINT : PRINT " READY TO DRAW PATH..."
2040  PRINT "USE 'JOG' KEYS TO DRAW PATH!"
2050  VTAB 14: PRINT : PRINT "   PRESS 'S' TO START..."
2055  PRINT : INVERSE : PRINT "TO STORE A PLANE USE CTRL 'S'..": NORMAL
2060  GET A$:FE =  FRE (0)
2070  IF A$ =  CHR$ (27) THEN  RETURN
2080  IF A$ <  > "S" THEN  GOTO 2050
2085  IF NP > 1 THEN  HGR
2090  GOSUB 1780
2100  IF AA <  > 1 THEN  GOTO 2136
2110 DV(3) = ZE:TS = ZE
2120  HGR : HCOLOR= 3:XL = 100:YL = 100
2130  ROT= 8: SCALE= 1
2136  IF AA = 3 THEN  GOSUB 3000
2140  GOSUB 2370
2150  GET A$:FE =  FRE (0)
2160  IF TS =  > MX THEN DV(3) = TS: RETURN
2170  IF A$ =  CHR$ (27) THEN DV(3) = TS: RETURN
2175  IF A$ =  CHR$ (19) THEN DV(3) = TS: GOTO 3300
2180  IF A$ <  > "K" THEN  GOTO 2220
2190 TS = TS + 1:XX%(TS) = XX%(TS - 1) + DD
2200 YY%(TS) = YY%(TS - 1):ZZ%(TS) = ZZ%(TS - 1)
2210  GOSUB 2610: GOTO 2140
2220  IF A$ <  > "J" THEN  GOTO 2240
2230 TS = TS + 1:XX%(TS) = XX%(TS - 1) - DD: GOTO 2200
2240  IF A$ <  > "I" THEN 2280
2250 TS = TS + 1:YY%(TS) = YY%(TS - 1) + DD
2260 XX%(TS) = XX%(TS - 1):ZZ%(TS) = ZZ%(TS - 1)
2270  GOSUB 2610: GOTO 2140
2280  IF A$ <  > "M" THEN 2300
2290 TS = TS + 1:YY%(TS) = YY%(TS - 1) - DD: GOTO 2260
2300  IF A$ <  > "U" THEN  GOTO 2340
2310 TS = TS + 1:ZZ%(TS) = ZZ%(TS - 1) + DD
2320 XX%(TS) = XX%(TS - 1):YY%(TS) = YY%(TS - 1)
2330  GOSUB 2610: GOTO 2140
2340  IF A$ <  > "D" THEN  GOTO 2140
2350 TS = TS + 1:ZZ%(TS) = ZZ%(TS - 1) - DD: GOTO 2320
2360 J = TS
2370  VTAB 21: CALL  - 868
2380 XX% =  INT (XX%(J) * ST + .5):YY% =  INT (YY%(J) * ST + .5):ZZ% =  INT (ZZ%
(J) * ST + .5)
2390  VTAB 21: PRINT "STEP #=";J;"   X=";XX%;"   Y=";YY%;"   Z=";ZZ%
2400  RETURN
2420  PRINT : PRINT "STARTING STEP=";: INPUT SN
2430  IF SN = 0 THEN  RETURN
2440 SN =  INT (SN): IF SN < 1 THEN SN = 1
2450  IF SN > DV(3) THEN  GOTO 2420
2455  XDRAW 1 AT XL,YL
2456  HGR
2460  GOSUB 1780
2465 TS = DV(3)
2470  FOR J = SN TO TS
2480 XF = XX%(J):YF = YY%(J):ZF = ZZ%(J)
2490  GOSUB 1740
2500  GOSUB 2620
2510  GOSUB 2370
2520  IF J = SN THEN  PRINT "PRESS 'S' TO START...";: GET A$: GOTO 2540
2530  GOTO 2560
2540  HOME : IF A$ = "S" THEN  GOTO 2560
2550  IF A$ =  CHR$ (27) THEN J = TS: GOTO 2590
2560  FOR T = 1 TO DV(2): NEXT T
2570 KY =  PEEK ( - 16384): IF KY < 128 THEN  GOTO 2590
2580  POKE  - 16368,0: IF KY = 155 THEN J = TS
2590  NEXT J
2600  RETURN
2610 J = TS
2620  IF J > SN THEN  XDRAW 1 AT XL,YL
2630 XP = 100 +  INT ((XX%(J) - .866025 * YY%(J)) / 30)
```

TABLE 7. (Continued)

```
2640 YP = 100 -  INT ((ZZ%(J) + .5 * YY%(J) + .5) / 30)
2650  IF XP < 0 THEN XP = 0
2660  IF XP > 279 THEN XP = 279
2670  IF YP > 159 THEN YP = 159
2680  IF YP < 0 THEN YP = 0
2690  XDRAW 1 AT XP,YP
2700 XL = XP:YL = YP
2710  HPLOT XP,YP
2720  RETURN
3000  HGR
3010  FOR J = 1 TO SN
3015  IF J > 1 THEN  XDRAW 1 AT XL,YL
3020  GOSUB 2630
3030  NEXT J
3040  RETURN
3100  HOME : PRINT "STORAGE ";FT$;: INPUT FL$
3110  IF  LEN (FL$) = 0 THEN  RETURN
3130  PRINT D$;OP$;FL$: PRINT D$;WR$;FL$
3140  PRINT DV(3)
3150  FOR J = 1 TO DV(3)
3160  PRINT XX%(J): PRINT YY%(J): PRINT ZZ%(J)
3170  NEXT J
3180  PRINT D$;CL$;FL$
3190  RETURN
3200  HOME : PRINT "RETRIEVE ";FT$;: INPUT FL$
3210  IF  LEN (FL$) = 0 THEN  RETURN
3220  PRINT D$;VF$;FL$
3230  PRINT D$;OP$;FL$: PRINT D$;RD$;FL$
3240  INPUT DV(3)
3250  FOR J = 1 TO DV(3)
3260  INPUT XX%(J): INPUT YY%(J): INPUT ZZ%(J)
3270  NEXT J
3280  PRINT D$;CL$;FL$
3290  RETURN
3300  IF NP = 1 THEN  TEXT : HOME : PRINT "TYPE A NAME FOR THE PLANES (9 CHAR. M
AX)": INPUT "";PN$
3310  IF NP = 1 AND  LEN (PN$) > 9 THEN  GOTO 3300
3320 FL$ = DK$ + HD$
3325  ONERR  GOTO 4500: PRINT
3327  PRINT D$;"VERIFY ";FL$;",D2"
3328  POKE 216,0
3330  PRINT : PRINT D$;OP$;FL$
3340  PRINT D$;RD$;FL$
3350  INPUT XD
3360  PRINT D$;CL$;FL$
3370  IF XD < 100 THEN  GOTO 3400
3380  HOME : VTAB 10: FLASH : PRINT "DATA DISK IS FULL. INSERT NEW!! DISK": NORM
AL
3385  PRINT : PRINT "PRESS ( ";: FLASH : PRINT "ESC";: NORMAL : PRINT " ) KEY TW
ICE TO CONFIRM!!": GET QA$: IF QA$ <  >  CHR$ (27) THEN  HOME : VTAB 11: GOTO 33
85
3390  GET QA$: IF QA$ <  >  CHR$ (27) THEN  HOME : VTAB 11: GOTO 3385
3395 XD = 1: GOSUB 4000
3400 FL$ = HD$ + H$ + PN$
3410  PRINT D$;OP$;FL$: PRINT D$;WR$;FL$
3420  PRINT NP
3430  PRINT D$;CL$;FL$:FE =  FRE (0)
3440  IF NP < 2 THEN XD = XD + 1: GOSUB 4000
3445  CALL 1002
3450 FL$ = PL$ + PN$ + H$ +  STR$ (NP):FE =  FRE (0)
3460  PRINT D$;OP$;FL$: PRINT D$;WR$;FL$
3470  PRINT DV(3): PRINT YY%(DV(3))
3480  FOR J = 1 TO DV(3): PRINT XX%(J): PRINT ZZ%(J): NEXT J
3490  PRINT D$;CL$;FL$
```

TABLE 7. (Continued)

```
3500 XD = XD + 1: GOSUB 4000
3510 NP = NP + 1:DQ = DV(3):XX%(1) = XX%(DQ):ZZ%(1) = ZZ%(DQ):YY%(1) = YY%(DQ)
3520  FOR J = 2 TO DQ:XX%(J) = ZE:YY%(J) = ZE:ZZ%(J) = ZE: NEXT J
3530 SN = 2:AA = 2:TS = 1
3540  TEXT : HOME : GOTO 2030
4000  PRINT : PRINT D$;OP$;DK$;HD$;",D2": PRINT D$;WR$;DK$;HD$
4010  PRINT XD
4020  PRINT D$;CL$;DK$;HD$
4030  PRINT : RETURN
4100  TEXT : HOME : POKE 43624,2: CALL 42350
4105 KY = 0
4110  PRINT : PRINT "NAME OF PLANE TO AUTO-TRACE? ";: INPUT "";PN$
4120  IF  LEN (PN$) < 1 THEN  THEN  POKE 43624,1: RETURN
4125 FL$ = HD$ + H$ + PN$:FE =  FRE (0)
4130  PRINT : PRINT D$;"VERIFY ";FL$
4140  PRINT : PRINT D$;OP$;FL$: PRINT D$;RD$;FL$
4150  INPUT NP: PRINT D$;CL$;FL$
4160  HOME : VTAB 10: PRINT "PLANE NUMBER TO START TRACE (1-";NP;") ";: INPUT ""
:SP
4170  IF SP < 1 OR SP > NP THEN  GOTO 4160
4180  PRINT : PRINT "LAST PLANE NUMBER TO TRACE (";SP;"-";NP;") ";: INPUT "";EP
4190  IF EP < SP OR EP > NP THEN  HOME : GOTO 4180
4200 EP =  INT (EP):SP =  INT (SP)
4203  GOSUB 1140: HOME
4205  IF NP > 100 AND U = 101 OR U = 201 THEN  TEXT : HOME : VTAB 19: PRINT "INS
ERT NEXT DISK FOR MORE PLANE DATA     HIT ANY KEY TO CONTINUE!": GET QA$: PRINT
: HOME
4210  FOR U = SP TO EP
4220 FL$ = PL$ + PN$ + H$ +  STR$ (U):FE =  FRE (0)
4230  PRINT : PRINT D$;OP$;FL$: PRINT D$;RD$;FL$
4240  INPUT DV(3): INPUT YY%(1)
4250  FOR J = 2 TO DV(3):YY%(J) = YY%(1): NEXT J
4260  FOR J = 1 TO DV(3): INPUT XX%(J): INPUT ZZ%(J): NEXT J
4270  PRINT D$;CL$;FL$
4275  IF U = SP THEN  SCALE= 1: ROT= 8: HCOLOR= 3
4280 SN = 1: GOSUB 2450
4282  IF KY = 155 THEN U = EP: GOTO 4290
4285 KY =  PEEK ( - 16384): IF KY < 128 THEN  GOTO 4290
4287  POKE  - 16368,0: IF KY = 155 THEN U = EP
4290  NEXT U
4295 KY = 0
4300  RETURN
4500  POKE 216,0: DATA     104,168,104,166,223,154,72,152,72,96
4501  FOR U = 0 TO 9: READ W: POKE 4096 + U,W: NEXT U: CALL 4096
4503 RL =  PEEK (218) + ( PEEK (219) * 256)
4505 RR =  PEEK (222): IF RR <  > 6 THEN  TEXT : HOME : PRINT "ERROR=";RR: END
4517  IF RL > 4099 THEN  GOTO 4550
4520  PRINT : PRINT D$;OP$;FL$: PRINT D$;WR$;FL$: PRINT ZE: PRINT D$;CL$;FL$
4530  POKE 216,0: GOTO 3330
4550  TEXT : HOME : PRINT "THAT PLANE NOT ON THIS DISK!! TRY AGAIN."
4560  FOR U = 1 TO 1000: NEXT U: POKE 216,0: GOTO 4100
```

ıne, and this plane would be "written" in the x and z directions as be-re. This process is shown schematically in Figure 10. Note that the ject coordinates are the inverse of the coordinates of motion, since in der for the laser beams to appear (to the object) as though they are ving in one direction, it is necessary for the sample to be moved in the posite direction. As Figure 11 illustrates for the simple case of a taircase" structure, the shapes in successive planes may or may not erlap, and can vary in shape and size as desired. Indeed, for complex apes which require many steps to describe, it is possible to use several lanes" of program/disk memory to describe a single physical plane of the ject. This is accomplished simply by retaining the same value of y for ch of the program planes until the first plane of the physical object d been described completely; the value of y would then be incremented on solution unit, and a new series of program planes begun, using this new lue. It should be pointed out that this procedure has been adopted as a ans of circumventing the problems posed by the limited memory capacity the Apple II-E system used, and that is may not be necessary to do this th computer systems having larger internal memory.

Samples were contained in 1 cm square Pyrex cuvettes, and were gassed either by purging with a flow of solvent-saturated argon gas for -30 minutes or by repeated freeze-pump-thaw cycles under vacuum (with a ass vacuum manifold evacuated by an oil diffusion pump) using custom-de sample cells of the type shown in Figure 12. In practice, the cell uld initially be positioned vertically, and the sample placed in the gassing bulk by means of a disposable pipet. The cell would then be nnected to the vacuum manifold in this position, and the sample degassed repeated freeze-pump-thaw cycles. After degassing, the high-vacuum opcock on the sample cell would be closed, s the apparatus could be moved from the manifold and tilted to pour the sample into the cuvette. te that the use of a male-to-female joint on the cuvette helps to mini-ze the probability of contaminating the sample with stopcock grease.

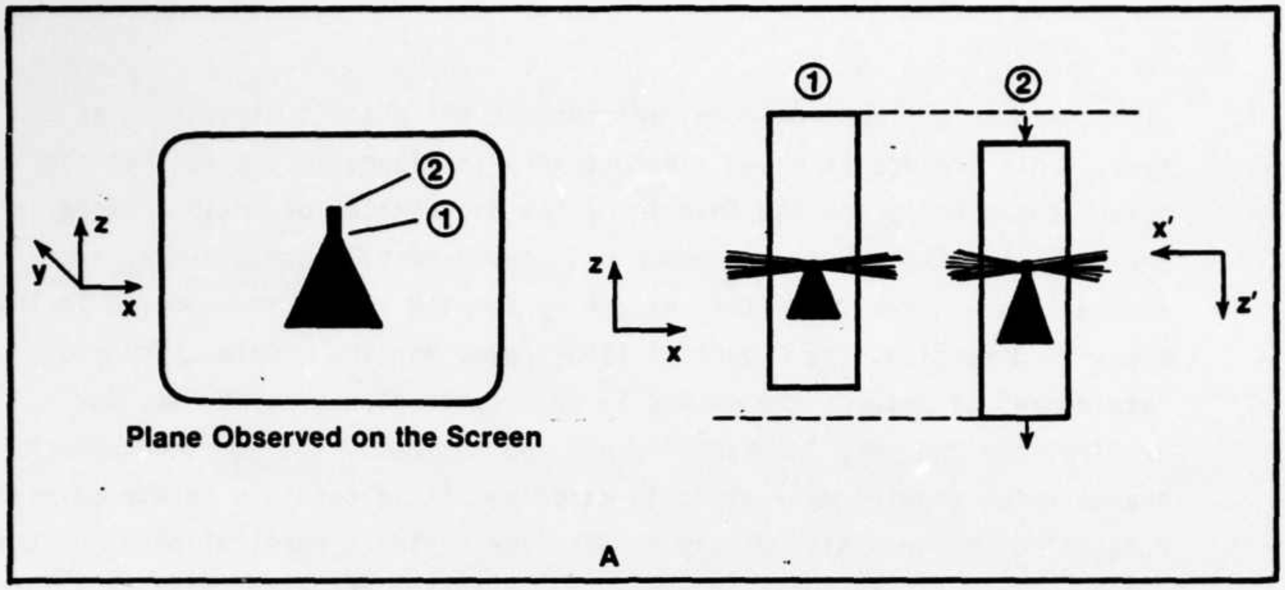

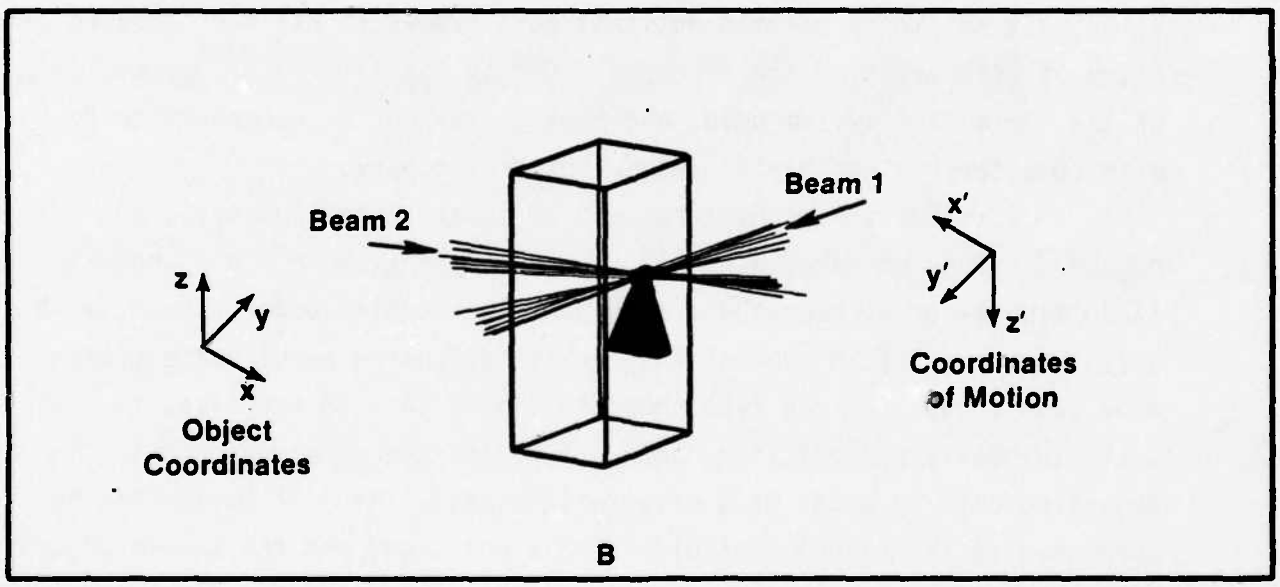

FIGURE 10. PRODUCTION OF ONE PLANE OF A POLYMERIZED SHAPE USING THE TWO PHOTON PROCESS, AS OBSERVED FROM DIFFERENT VIEWPOINTS:

A. FABRICATION OF A VERTICAL PIECE BY MOTION ALONG THE Z AXIS;

B. COMPARISON OF OBJECT COORDINATES WITH COORDINATES OF MOTION

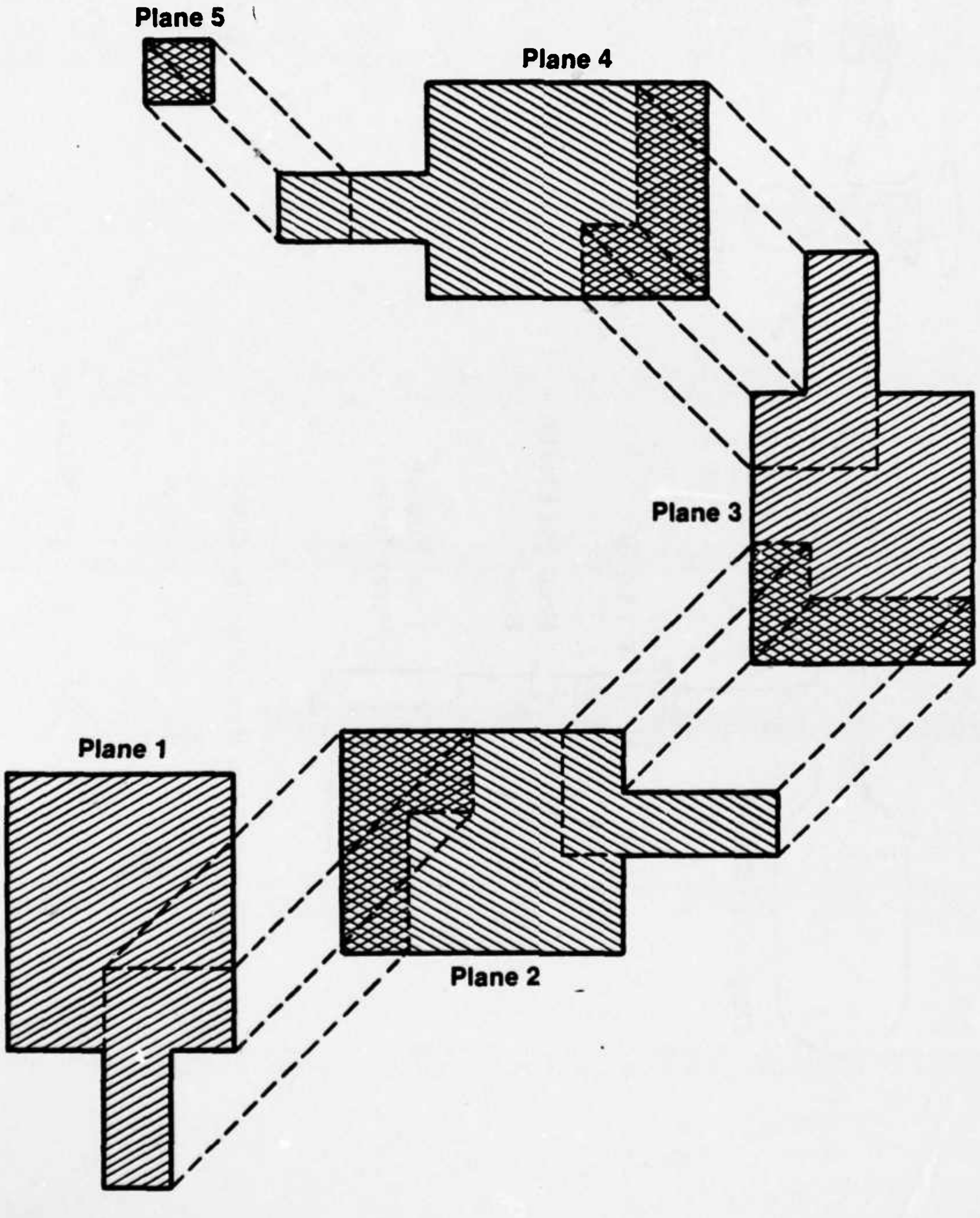

FIGURE 11. SCHEMATIC FABRICATION OF A "STAIRCASE" STRUCTURE IN SUCCESSIVE PLANES

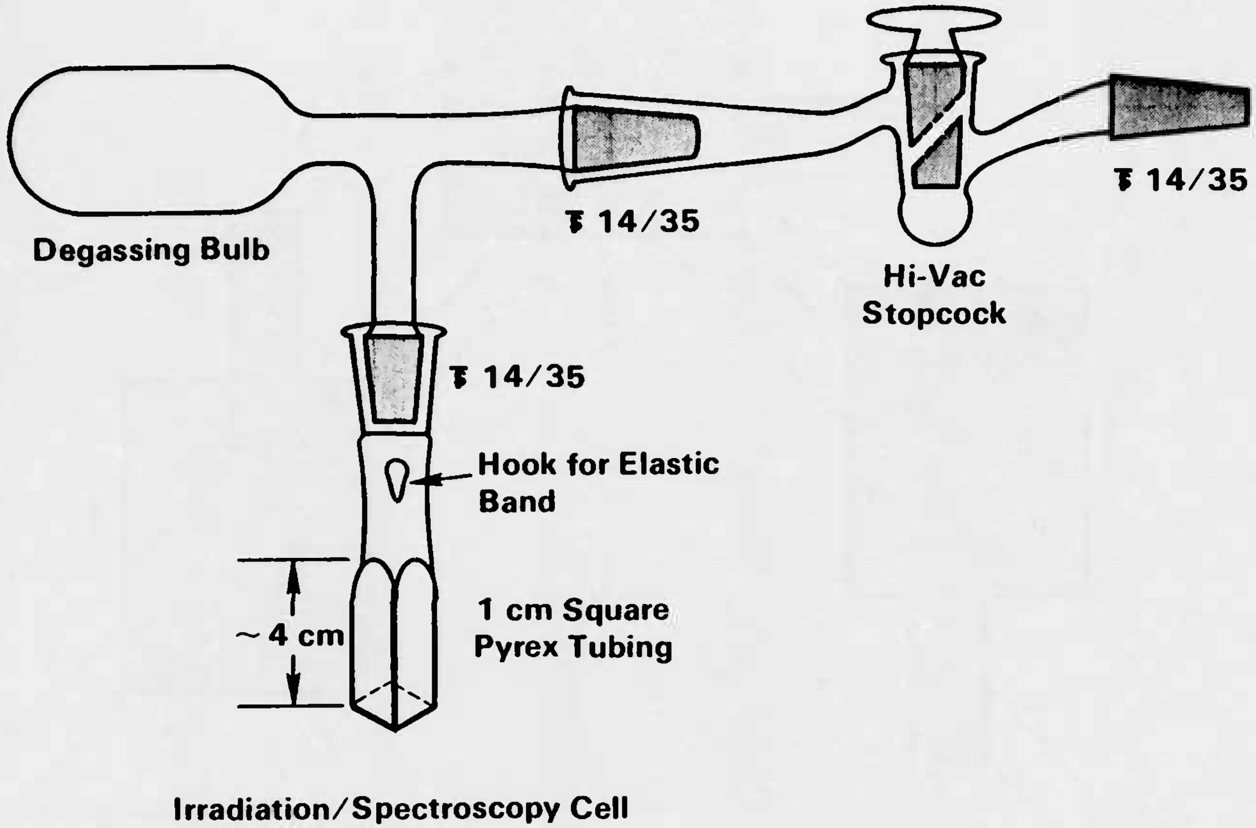

FIGURE 12. SAMPLE CELL CONFIGURATION

Many of the experiments performed during the first year of the project utilized solutions of candidate initiators and photosensitizers in methyl methacrylate (MMA). Since MMA is a highly fluid monomer which crosslinks rather inefficiently, little if any polymer formation could be observed directly after irradiation; instead, the polymer was precipitated with an excess of methanol, and then filtered and weighed. Subsequent experiments have used a variety of polymer blends designed to promote efficient crosslinking, forming hard, insoluble polymers. Oligomers have been added to increase the viscosity of the solution, and a variety of initiator systems have been tried. One of the most successful mixtures used to date contains the components shown in Figure 13, with weight ratios of MMA : TMPTA : PS169 Resin typically in the range of 1:3:6. The Irgacure 651 (or other) initiator is typically added at a concentration of 2-5% by weight, with the concentration of photosensitizer adjusted to maintain at least a 10-100 fold mole excess of initiator over the photosensitizer.

Estimated Amount of Polymerization Expected from Two-Beam Laser Experiments

An approximate calculation of the amount of polymerized material we are likely to form can be done using some material assumptions along with the data on the lasers and materials which were summarized in Table 6. These data were compiled from measurements made on our system in several different experiments. It must be noted, however, that the pulse energy varies with time, and the actual pathlength for beam 2 is very difficult to measure. Therefore, this calculation should be regarded as an estimate rather than as an accurate prediction.

In order to do these calculations on polymerization we must first characterize the laser beams at their intersection point: Their pulse energies are different and their cross sectional areas and times of lasing of the beams are also different. The times of interest are the

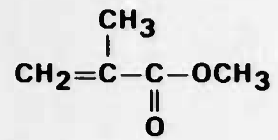

Methyl Methacrylate (MMA)

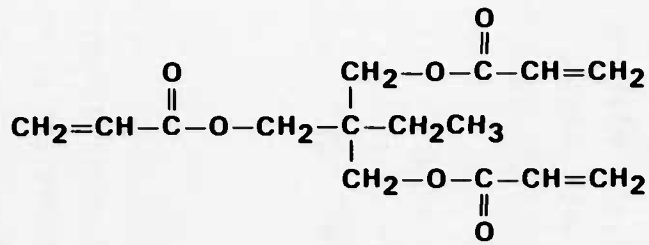

Trimethylolpropane Triacrylate (TMPTA)

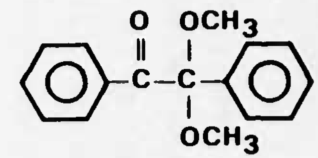

IRGACURE 651 Initiator

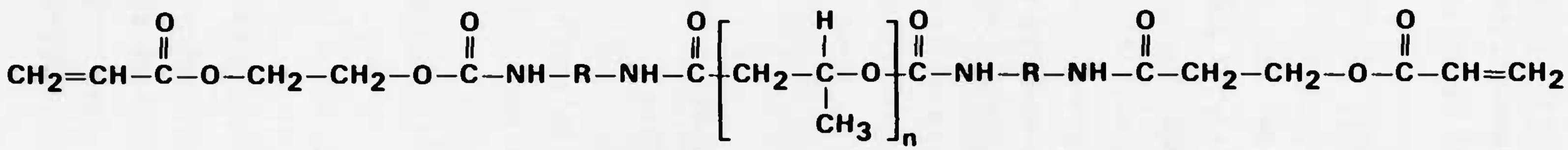

(R = low molecular weight propylene glycol oligomer)

PS 169 Resin

FIGURE 13. REPRESENTATIVE POLYMER SYSTEMS COMPONENTS

times during which the beams are lasing and affecting the sample. This gives the intensity during firing:

$$I = \frac{E}{\tau A} \tag{88}$$

where the symbols are as defined in Table 6 for each laser.

For the Phase R-laser, $I = 8.0\ \text{MW/cm}^2$
For the Molectron laser, $I = 5.0\ \text{MW/cm}^2$

The Phase-R laser fires for a much longer pulse duration than the Molectron laser, so the total amount of energy put into the sample is larger for the first laser. Since the porphyrin material is expected to have a lifetime in this system of tens of microseconds, we would like to set the timing of the second pulse to occur 250 ns after the first pulse. In this way, we take advantage of the full effect of the first beam, and yet relatively few of the excited sensitizing molecules will have decayed to the ground state. The relationship between the number of photons available and beam energy is just

$$E = \frac{Nhc}{\lambda} \quad \text{or} \quad N = \frac{E\lambda}{hc} \tag{89}$$

where E is the beam pulse energy
- λ is the beam wavelength
- h is Planck's constant (6.62×10^{-34} J-s)
- c is the speed of light
- N is the number of photons

This gives $N_{p1} = 3.17 \times 10^{17}$ photons from the Phase-R laser. Not all of N_{p1} are effective, however, because only 35% of the photons cross through the volume of beam 2 as shown in Figure 14.

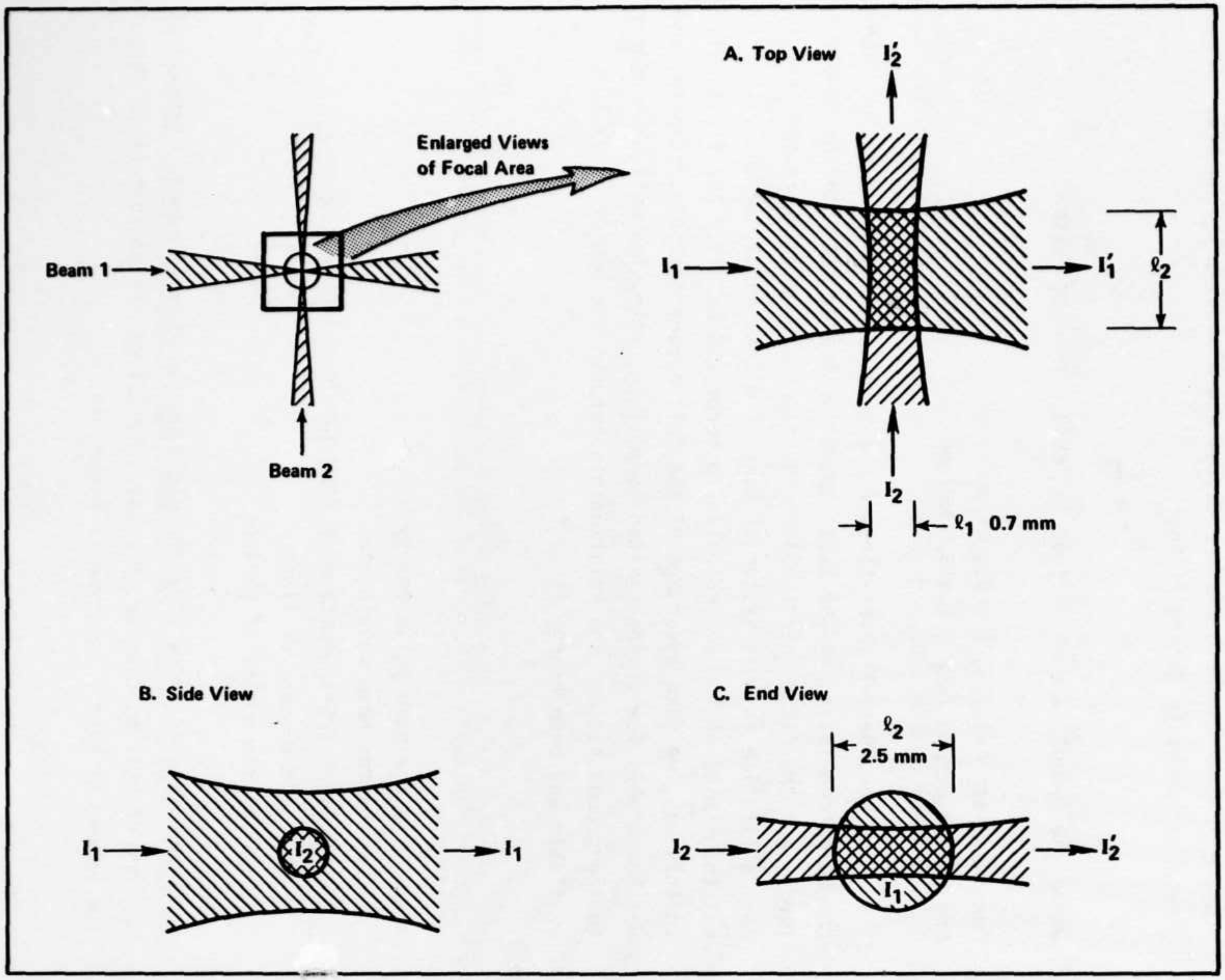

FIGURE 14. VIEWS OF FOCUSED BEAM INTERSECTIONS

Effectively,

$N_{p1} = 1.1 \times 10^{17}$ photons/pulse
$N_{p2} = 7.4 \times 10^{14}$ photons/pulse

Using Beer's Law, we can get an estimate of the number of molecules excited to the S1 state, as shown in Equation (90).

$$\ln\left(\frac{I_1}{I_1'}\right) = (\alpha_1 C_1)\ell_1 \quad (90)$$

where

I_1 is the original intensity,
I_1' is the transmitted intensity,
ℓ_1 is the length of beam 1 in the crossed beam volume, and
$(\alpha_1 C_1)$ is the product of the absorption cross section times the concentration of the sensitizer (α is base e).

This last quantity $\alpha_1 C_1$ has been determined to be $0.2\ \text{cm}^{-1}$ at the position of excitation. The wavelength of choice is at a position which allows absorption but not so much absorption that the beam is appreciably absorbed between entering and leaving the cuvette. For this case

$$\left(\frac{I'}{I}\right) = 0.8 \text{ through the cuvette} \quad (91)$$

The fraction of photons that send molecules to the S_1 state from the ground S_0 state is (1-T) where T is the transmittance, I'/I.

$$(1-T) = (1 - \frac{I'}{I}) \quad (92)$$

$$= (1 - \exp(-\alpha_1 C_1 \ell_1)) \quad (93)$$

$$= 0.014$$

Therefore, $$M_{Si} = (1-T)\ N_{pi} \tag{94}$$

where N_{pi} is the number of photons in the pulse of laser 1.

$$M_{Si} = 1.5 \times 10^{15}/\text{pulse} \tag{95}$$

We estimate 80% of these go the triplet state

$$M_{T_0} = 0.8\ M_{Si} = 1.2 \times 10^{15}/\text{pulse} \tag{96}$$

To estimate the number of excited T_1 molecules that go to the upper triplet state we must know what is relative concentration C_3 is present as compared to C_1 and make an estimate of α_3. By knowledge of the available molecules for absorbing the original beam and the volume in which this interaction takes place, we can estimate the number of molecules in the ground state in the beam intersection. The data are as follows:

Volume Sample (V)	= 3 ml
Sample Density =	= 0.85 gm/ml
Molecular Weight, W	= 90 (Molecular weight of the Methyl Methacrylate)
Available Material	= 2.55 gm
	= 0.028 moles
	= 1.75×10^{22} molecules of MM
Sensitizer Concentration in MMA	= 10^{-3} moles/liter

M_{So} = (Beam Volume)(Relative Sensitizer Concentration) (MMA molecules/cm^3)

$M_{So} = 5.7 \times 10^{15}$ molecules

This indicates that the triplet state concentration after the original pulse is about 20% of the original concentrations of sensitizer molecules on the MMA. α_3 is chosen to be close to what we hope is the peak of the triplet absorbance which we estimate to be ~8X stronger than the absorption band edge which was used for the excitation in the ground state. We need not worry about absorbance in the sample at any point but the intersection point because no molecules in the path of the second laser are in the triplet state except at that point. In contrast, the singlet excitation must occur at a point where some, but not too much, absorption will occur. Hence, the need for excitation away from the absorption band maximum.

Therefore, $\alpha_3 C_3 = 0.4$ (97)

Using the same method as with M_{S1}, M_{T1} can be calculated with ℓ_2 = 0.2 cm, using Beer's law:

$$\begin{aligned} M_{T_1} &= (1-T_3)\ (N_{p2}) \\ &= (1-0.9)\ (7.4\times10^{14}) \\ M_{T_1} &= 7.4 \times 10^{13} \end{aligned} \tag{98}$$

where T_3 is the transmittance, N_{p2} is the number of photons from the second laser, and M_{T_1} is the number of molecules in the excited triplet state after the second laser fires. It is assumed that 50% of these molecules, M_I, become dissociated, so $M_I = 4 \times 10^{13}$. We estimate that the number of linking events per dissociated molecule is approximately 500, based on previous experience. Therefore, we can say that the number of crosslinks initiated, M_c, is approximately

$M_c = 2 \times 10^{16}$ events per pulse. (99)

In our experiments, up to 10,000 synchronized pulses were fired, but because of jitter and loss of output power near the end of the dye lasing periods we feel have effectively seen about 5000 effective pulses. Linking this with the typical conditions of the sample,

$$\text{Percent of Molecules} = \frac{100\ (\text{Number of Pulses})(\text{Molecules Linked per pulse})}{(\text{Number of Molecules Available to Line})}$$

$$= 0.5\ \% \tag{100}$$

Thus, we should have polymerized about 0.5% of the material in our sample under the conditions assumed for this estimate. While this may not have been detectable for the MMA system, because of the solubility of the polymer, the results in TMPTA suggest that this estimate is conservative; at least, in those experiments, up to 10% of the sample was polymerized in a much shorter time. As will be seen shortly, subsequent results have shown that it is possible to achieve much higher efficiencies in photosensitized systems of this type.

Two-Photon Triplet Sensitized Photopolymerization Using Dibromoanthracene and Naphthalenesulfonylchloride

It is known from the literature that anthracene derivatives, especially 9,10 dibromoanthracene (DBA), have the unique ability to be excited at 400 nm to a high S_1 state which can then intersystem cross to a relatively high T_2 state followed by radiationless transition to a lower T_1 state (Figure 15)[7]. The anthracene derivatives alone are

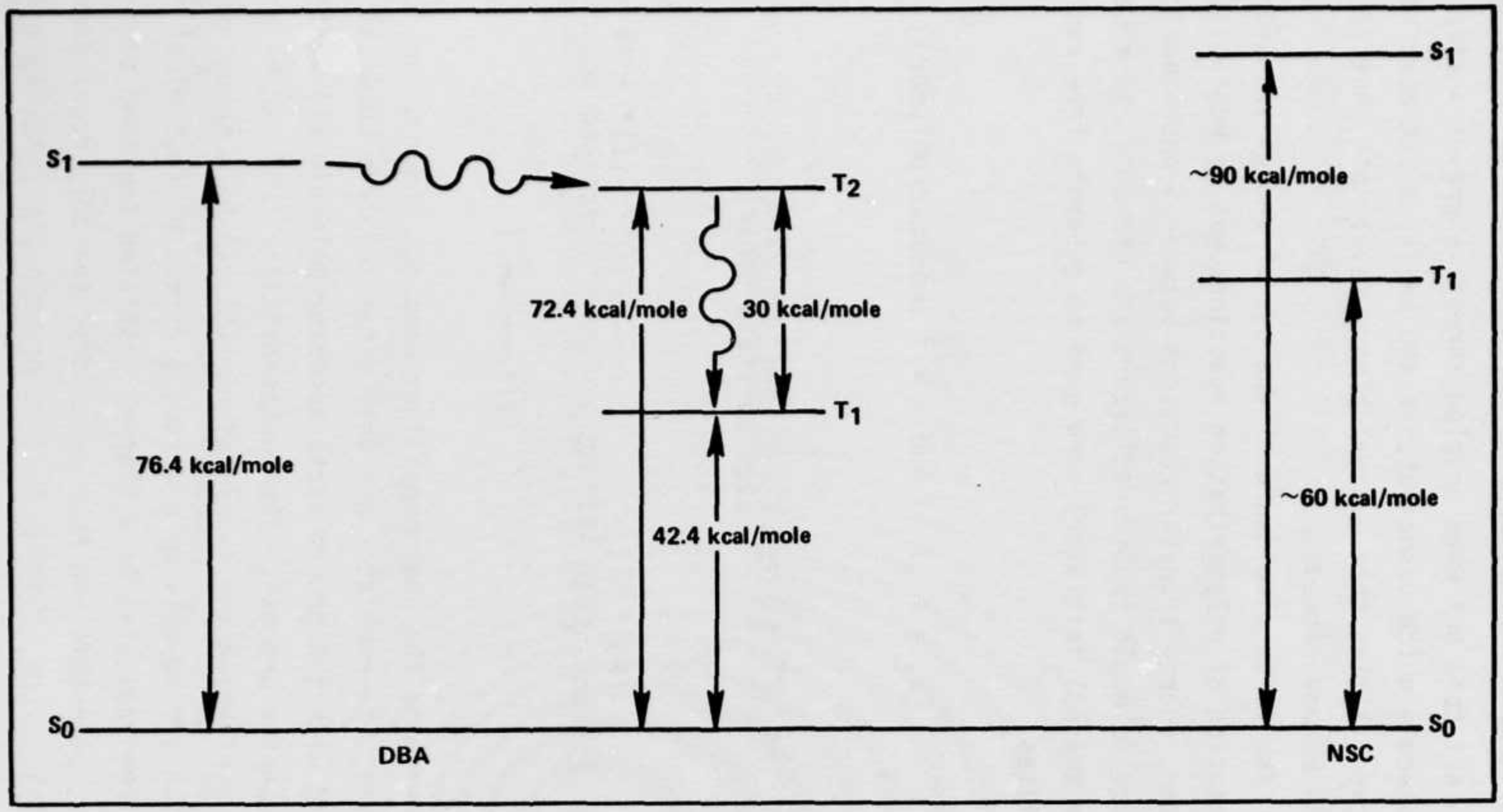

FIGURE 15. ENERGY-LEVEL DIAGRAM FOR 9,10-DIBROMOANTHRACENE (from Reference 7)

ot photoinitators but when coupled through energy transfer with a different molecule which cannot absorb 400 nm light but does have photoinitiation capabilities then a novel binary wavelength photoactive catalyst ystem can be envisioned.

The first disclosure of the use of energy transfer in the hotoinitiation of polymerization reactions was by McGinniss.[59] In his system, energy transfer reactions between a photochemically excited tate donor molecule (photosensitizer) and ground state acceptor molecule photo or thermal initiator) were used to generate free radical ntermediates:

$$[k_t = f\ (1/\eta) \text{ and } \eta = f\ (\text{monomer/polymer})] \tag{101}$$

$$PS \xrightarrow{h\nu} \underset{\text{(excited state donor)}}{(PS)^*} \tag{102}$$

$$\underset{\text{(ground state acceptor)}}{(PS)^* + I} \longrightarrow \underset{\text{(excited acceptor)}}{(I)^* + PS} \tag{103}$$

$$(I)^* \longrightarrow I\cdot \tag{104}$$

In these systems the photosensitizer does not undergo chemical change, and free radical intermediates are only generated from chemical changes ssociated with the ground state acceptor molecule (I) during or after the energy transfer process. The photosensitizer (PS) can be an aromatic carbonyl derivative and the initiator (I) can be a photoinitiator (molecules which are capable of undergoing direct photochemical reactions to produce free radicals) or a thermal initiator compound such as the diacyl peroxides, peresters and hydroperoxides; the only requirement for the reaction is that the excited state donor molecule (usually triplet excited state, but a high level excited singlet manifold reaction is also possi-

e) should have a higher energy level value than the ground state accep-
ɪr molecule, for efficient transfer of energy.[22]

The photosensitized decomposition of benzoyl peroxide with ·omatic carbonyl compounds is representative of an energy transfer free ɪdical generation process in that the peroxide (non-light absorbing re- ;tion conditions) is decomposed only in the presence of the photosensi- Izer (light absorbing species) but without any detectable change in the ɪotosensitizer chemical structure. The ability of the photosensitizer ɪromatic carbonyl compounds such as benzophenone, acetophenone, aceto- ɪphthone) to effect decomposition of benzoyl peroxide depends on the riplet energy levels of the photosensitizer aromatic carbonyl compound. ɪose aromatic carbonyl compounds having triplet energy values in excess f 55 kcal/mol demonstrate their ability to effect benzoyl peroxide de- omposition reactions while those aromatic carbonyl photosensitizers hav- ng triplet energy levels below 55 kcal/mol do not exhibit this energy ransfer free radical generation process.[60]

In the following type of energy transfer reaction, thioxanthone TX) is the only active light absorbing species (cut-off filters or ti- anium pigments strongly absorb all radiation below 360 nm) contained in he light-filtered reactive monomer system. Thioxanthone alone does not hotoinitiate polymerization of vinyl unsaturated monomers. Naphthalene ulfonyl chloride (NSC), chloromethylnaphthalene (CMN) and quinoline sul- onyl chloride (QSC) absorb light at approximately 310-330 nm which re- ults in homolytic cleavage of the sulfonyl chloride bond or chloromethyl ond to produce initiating free radical species, which can in turn effec- ively polymerize vinyl monomers. In this filtered or pigmented adiation-curable vinyl monomer coating system, all light in the 310-330 m range is absorbed by the filters or pigment, so direct absorption or xcitation by QSC, NSC, or CMN is not allowed. The only way photochemical nitiation can take place is through the light absorption of energy (370- 80 nm) by TX which can then transfer its absorbed energy to a ground tate QSC, NSC, or CMN molecule and result in free radical formation.[20,59]

AD-A154 711 THREE-DIMENSIONAL PHOTOCHEMICAL MACHINING WITH LASERS 2/3
(U) BATTELLE COLUMBUS LABS OH R E SCHWERZEL ET AL.
28 DEC 84 AFOSR-TR-85-0456 F49620-82-C-0077

UNCLASSIFIED F/G 13/8 NL

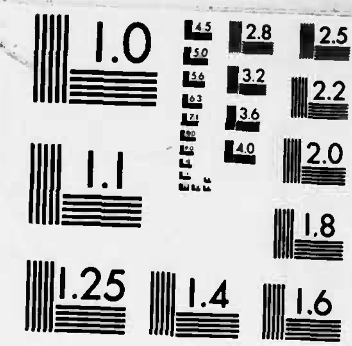

MICROCOPY RESOLUTION TEST CHART
NATIONAL BUREAU OF STANDARDS-1963-A

$$(TX)_0 \text{ (donor) } \xrightarrow[\text{(filter)}]{h\nu} (TX)_3^* \text{ (excited state donor)} \qquad (105)$$

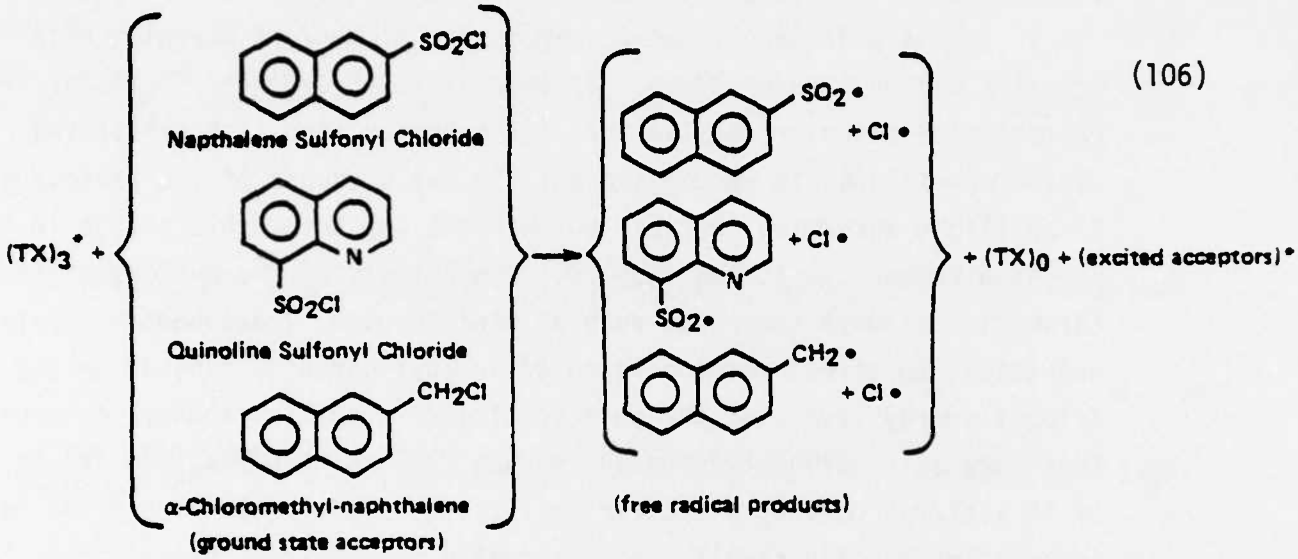

(106)

The triplet energy for TX is 65 kcal/mol and the triplet energies for NSC, QSC or CMN are approximately 60 kcal/mol (E_T = 5 kcal/mol excess) which meets one of the basic requirements for efficient energy transfer, i.e. E_T of donor (TX) > E_t of acceptor (QSC, NSC, CMN).(22)

In this present study the T_1 triplet energy value for NSC [E_T = 60 kcal/mole] lies below the T_2 level of DBA [$E_t \approx 72$ kcal/mole(7)] and above its T_1 level [E_T = 40 kcal/mole(7)]. Only excess energy coming from the T_2 level of DBA can couple with the T_1 level of NSC and cause photoinitiation (Figure 15).

The other major feature of the unique DBA photoactive catalyst systems is its ability to undergo readily allowable $T_1 \longrightarrow T_2$ transitions via utilization of a second light source (λ max > 500 nm) thus increasing the population of the upper T_2 state (Figure 15). This special feature of DBA allows one to construct a binary wavelength photoactive catalyst system.

$$DBA_{S0} \xrightarrow[(400\ nm)]{h\nu 1} DBA^{*}_{S_1} \qquad (107)$$

$$DBA^{*}_{S_1} \longrightarrow DBA^{*}_{T_2} \qquad (108)$$

$$DBA^{*}_{T_2} \longrightarrow DBA^{*}_{T_1} \qquad (109)$$

$$DBA^{*}_{T_1} \xrightarrow[\text{(greater than 500 nm)}]{h\nu 2} DBA^{*}_{T_2} \qquad (110)$$

$$DBA^{*}_{T_2} + NSC \longrightarrow NSC^{*}_{T_1} \qquad (111)$$

$$NSC^{*}_{T_1} \longrightarrow \text{Free radical intermediates} \qquad (112)$$

Another variation on this concept is the added ability of DBA to be sensitized through its lower level T_1 state through use of another photosensitizer molecule (λ_{max} 400 nm or greater but with λ_{max} larger than the ε of DBA) having its T_1 level higher than the T_1 level of DBA (Figure 16). A possible mechanistic scheme can be generated as follows, using benzil as a representative photosensitizer:

$$(B)_{S_0} \xrightarrow{h\nu 1} B^{*}_{S_1} \qquad (113)$$

$$B^{*}_{S_1} \longrightarrow B^{*}_{T_1} \quad (E_T = 53\ \text{kcal/mole}^{(22)}) \qquad (114)$$

$$B^{*}_{T_1} + DBA \longrightarrow B + DBA^{*}_{T_1} \quad (E_T = 42\ \text{kcal/mole}) \qquad (115)$$

$$DBA^{*}_{T_1} \xrightarrow{h\nu 2} DBA^{*}_{T_2} \qquad (116)$$

$$DBA^{*}_{T_2} + NSC \longrightarrow NSC^{*}_{T_1} \qquad (117)$$

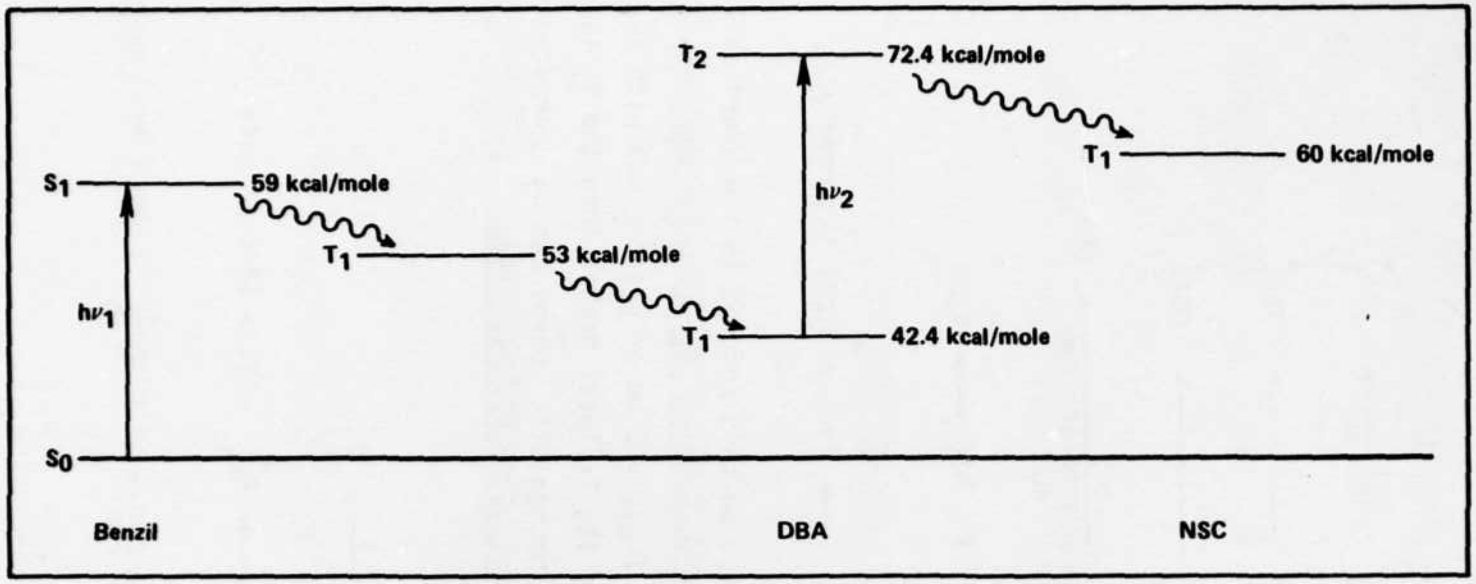

FIGURE 16. SCHEMATIC ENERGY-LEVEL DIAGRAM FOR TRIPLET-SENSITIZED EXCITATION OF DIBROMOANTHRACENE BY BENZIL

$$NSC^*_{T_1} \longrightarrow \text{free radical intermediates} \tag{118}$$

$$B^*_{T_1} + NSC \longrightarrow \text{no reaction} \tag{119}$$

$$NSC_{T_1} > B_{T_1} > DBA_{T_1}$$

60 53 42.4 kcal/mole

A major advantage to this scheme is the elimination of the direct $DBA_{S0} \longrightarrow DBA_{S1}{}^*$ transition followed by intersystem to DBA_{T_2} and interaction with NSC.

All of the chemicals for this series of experiments were purchased from Aldrich Chemical Company except for the TMPTA and PS169 resin. The naphthalene sulfonyl chloride was recrystallized from chloroform; the inhibitor (65 ppm methoxyhydroquinone) was removed from methylmethacrylate by base extraction and the other materials were used as received. Ultraviolet spectra of the photosensitized monomer solutions were obtained on a Cary 17 and photochemical irradiations (10 ml sample sizes) were carried out with filtered and nonfiltered Eimac 150 W high pressure Xenon arc lamp light sources. Polymer formation was determined gravimetrically via methanol precipitation of irradiated monomer-polymer solutions. Filters were obtained from the Corning Glass Company. Irradiations of the cross-linking polymer systems were carried out with the laser apparatus described previously.

The concentrations of dibromoanthracene (DBA) and naphthalene sulfonyl chloride (NSC) were adjusted so that the NSC concentration was in excess for efficient energy transfer (Figure 16). DBA does have absorption bands beyond 380 nm, but it was still necessary to include a sharp 410 cut-off filter so that direct absorption of the NSC (λ_{max} 310 nm) would be prevented (Figure 17). The filter (CS-3-74) does allows about 35% of the light from the source into the 415 nm region, which was sufficient to excite the $S_0 \rightarrow S_1$ transition region of DBA. The results in

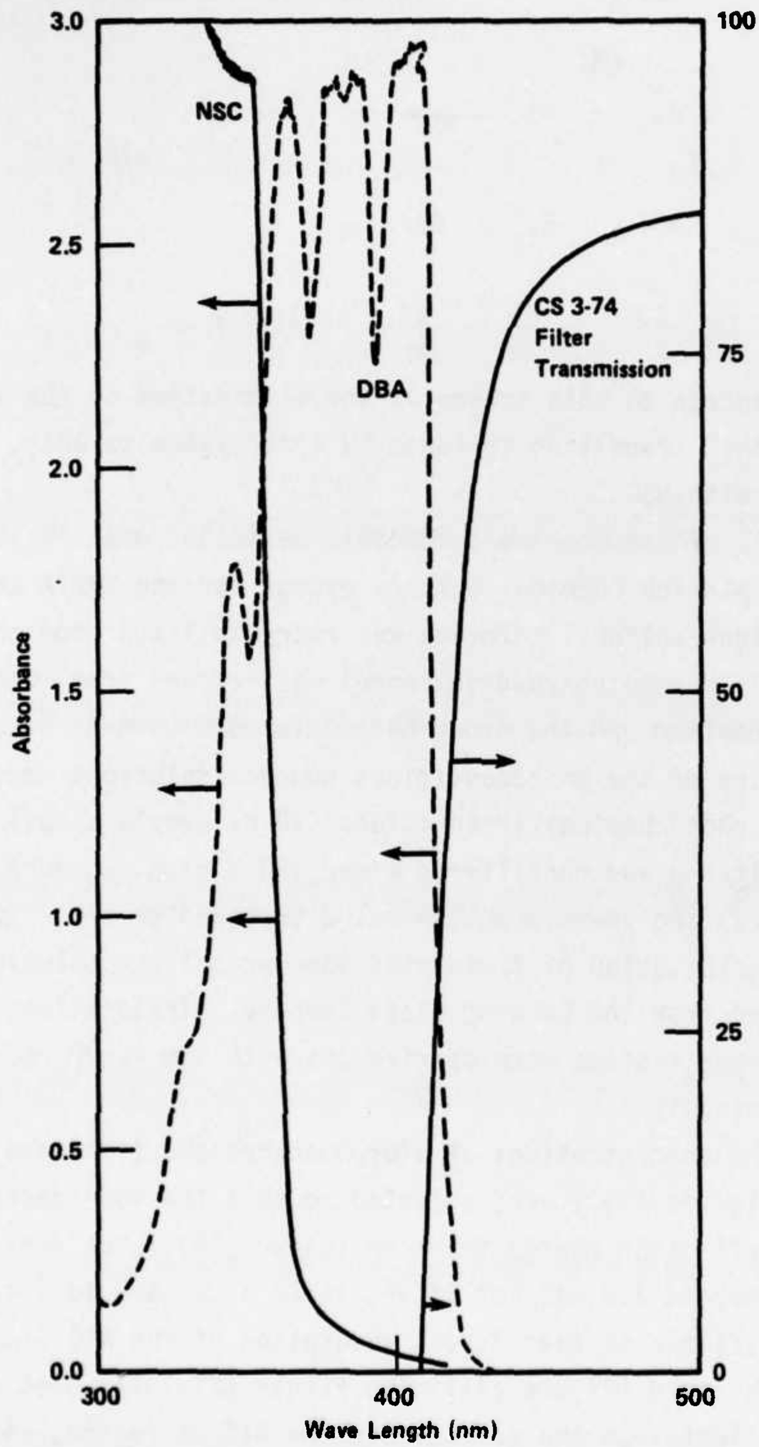

FIGURE 17. EXPERIMENTAL ABSORPTION SPECTRA FOR DBA (dashed line) AND FOR NSC (solid line) IN METHYL METHACRYLATE, SHOWING TRANSMISSION CURVE FOR CORNING CS 3-74 FILTER

Table 8 show that unfiltered NSC/MMA solutions polymerize without the benefit of energy transfer from DBA but filtered (CS-3-74) NSC solutions do not produce polymer unless the DBA is present for light absorption and for the $S_1 \rightarrow T_2$ (DBA) $\rightarrow T_1$ (NSC) energy transfer process depicted in Figure 17.

A graphical presentation showing the weight of polymer formed versus exposure time for filtered DBA/NSC/MMA solutions is shown in Figure 18.

The light source used in these experiments had considerable output in the 700 nm to IR wavelength range, and it is possible that readily allowable $T_1 \rightarrow T_2$ DBA transitions could be occurring at the same time as $S_0 \rightarrow S_1 \rightarrow T_2$ DBA and $T_2 \rightarrow T_1$ DBA, thus resulting in a more efficient population of the T_2 DBA state necessary for energy transfer to NSC (T_1 DBA << T_1 NSC). If any of the excess electronic energy from the T_2 level of DBA fell to the T_1 level of DBA without transferring to the T_1 level of NSC, then this would result in a less efficient photoinitation process. To test this concept, a combination of filter experiments were carried out in order to isolate certain wavelengths of light energy calculated to excite or prohibit the $T_1 \rightarrow T_2$ DBA transition (E_T = 30-32 kcal/mole, 850-900 nm wavelength range). Filter 1 (CS-3-74) cuts off all light below 400 nm but does allow the $S_0 — S_1$ DBA transition to occur; Filter 2 (CS-1-59) transmits 380 to 700 nm but has approximately 35% absorption in the IR radiation range; Filter 3 (CS-4-96) transmits 360 to 600 nm and strongly absorbs 660 to 1.5 microns. Monomer samples containing DBA and NSC exposed to the light source containing only filters 1 and 2 ($S_0 \rightarrow S_1 \rightarrow T_2$ DBA $\rightarrow T_1$ NSC and $T_1 \rightarrow T_2$ DBA $\rightarrow T_1$ NSC) showed significant levels of polymer formation in 1 hour. An identical experiment using filters 1, 2 and 3 ($S_0 \rightarrow S_1 \rightarrow T_2$ DBA $\rightarrow T_1$ NSC only and not $T_1 \rightarrow T_2$ DBA $\rightarrow$ T_1 NSC) resulted in almost half as much polymer formed in the 1 hour time period as was obtained with filters 1 and 2 (Table 8).

From these experiments one can conclude that the DBA $S_0 \rightarrow S_1$ $T_2 \rightarrow$ NSC T_1 is a viable single-wavelength photoinitiator system, but even

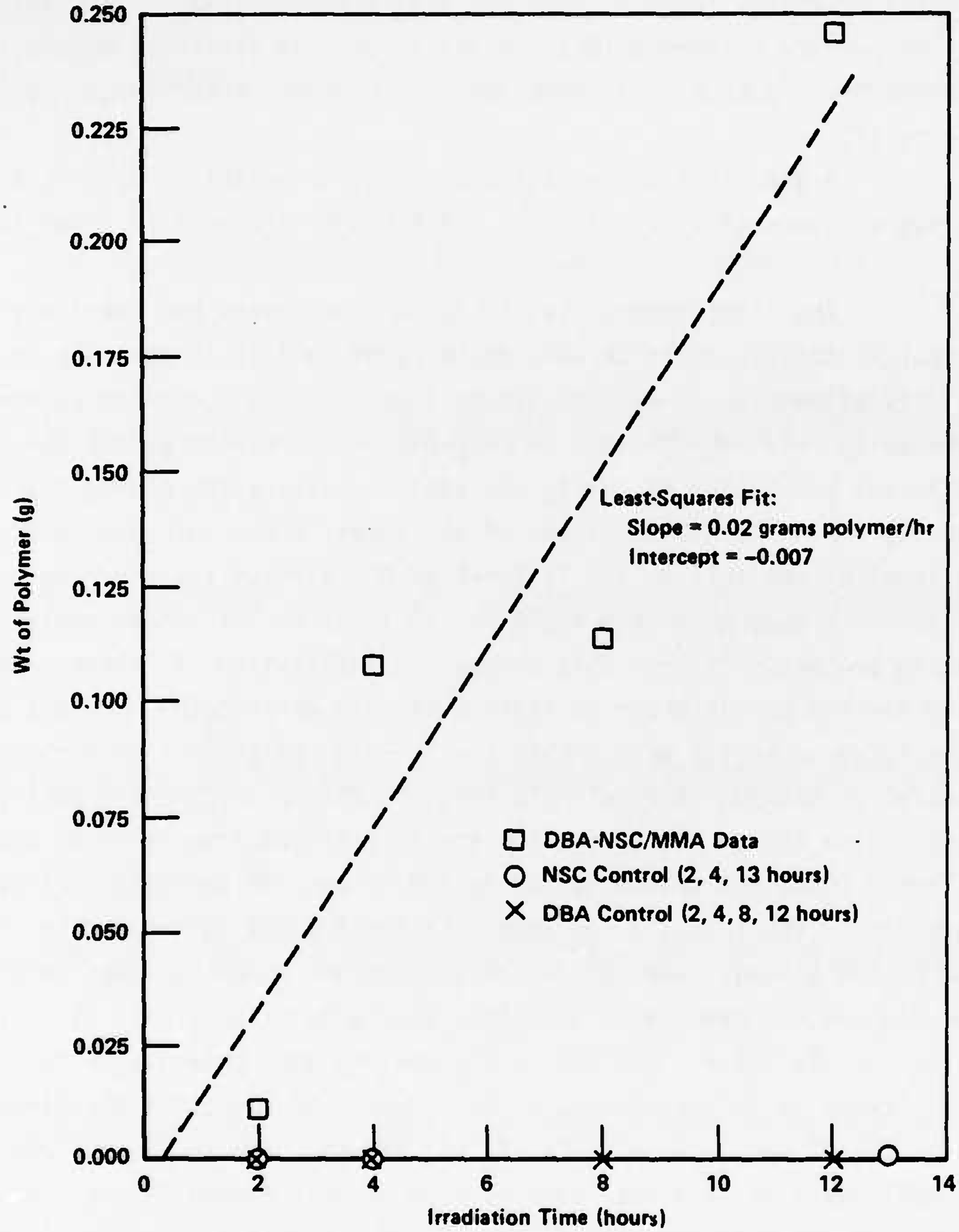

FIGURE 18. PHOTOPOLYMER FORMATION IN THE DBA/NSC/MMA SYSTEM

TABLE 8. SUMMARY OF DBA/NSC IRRADIATION EXPERIMENTS

MMA	DBA	NSC	Filter 1 CS-3-74	Filter 2 CS-1-59	Filter 3 CS-4-96	Results
+	1%	--	--	--	--	no polymer formed
+	--	2%	--	--	--	polymer formed in 20 minutes
+	1%	2%	--	--	--	polymer formed in 1 hour
+	--	--	--	--	--	no polymer formed
+	0.2%	--	yes	--	--	no polymer formed after 3 hours
+	--	2%	yes	--	--	no polymer formed after 3 hours
+	0.2%	2%	yes	--	--	polymer formed after 3 hours
+	0.2%	2%	yes	yes	--	0.25 gms polymer formed in 1 hour
+	0.2%	2%	yes	yes	yes	0.15 gms polymer formed in 1 hour

more important for this project is the fact that DBA $T_1 \rightarrow T_2$ transitions can be selectively excited to create a very efficient binary wavelength photoactive catalyst system for photopolymerization reactions. A patent disclosure has been written for this facet of the project.

Subsequent experiments with the DBA-NSC initiator system in the crosslinkable MMA/TMPTA/PS169 polymer blends described previously have confirmed that this system does indeed give preferential, selective crosslinking at the intersection point of the two laser beams. However, significant amounts of clouding of the polymer at the intersection point have also been observed, a result of precipitation of the DBA from the crosslinked polymer. Since this effect has not been observed with the porphyrin-sensitized systems studied during this project, it appears that the porphyrins (in particular, meso-tetraphenylporphyrin, or TPP), are to be preferred over the DBA-NSC system for purposes of photochemical machining.

Experimental Confirmation of Sensitizer Triplet Formation

As described in detail in the Appendix, a number of experiments were carried out using TPP in conjunction with a variety of photoinitiators with various MMA/TMhTA/olipomer resin systems. TPP is an attractive molecule for this purpose, because its excited-state energetics give it an upper triplet state with enough energy to sensitize a number of possible initiators (Figures 19,20) and because the spectroscopic characteristics of similar porphyrins provide reasonably selective access to both the ground-state and triplet-triplet absorption spectra at several different wavelengths (Figure 21). In particular, there are "windows" to the ground state spectrum at several of the maxima around 510 nm, 550 nm, 600 nm, and 650 nm in Figure 21, and "windows" to the triplet manifold at around 455 nm and 785 nm. The 785 nm peak is particularly appealing, as there is virtually no ground-state absorption in this region. While enhanced polymerization at the intersection point was observed with a number of the

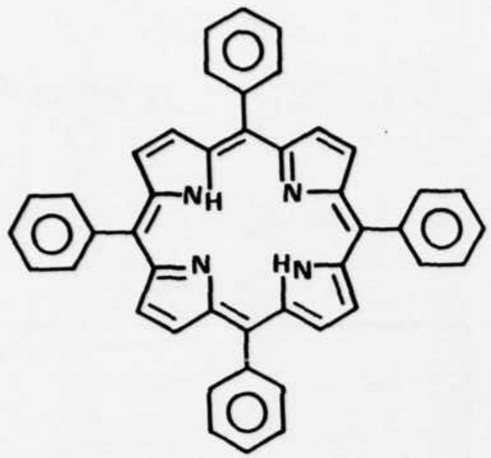

meso-Tetraphenylporphyrin

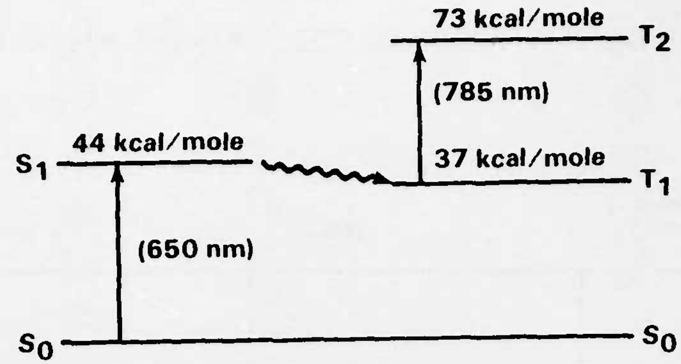

FIGURE 19. EXCITED-STATE ENERGETICS FOR meso-TETRAPHENYLPORPHYRIN

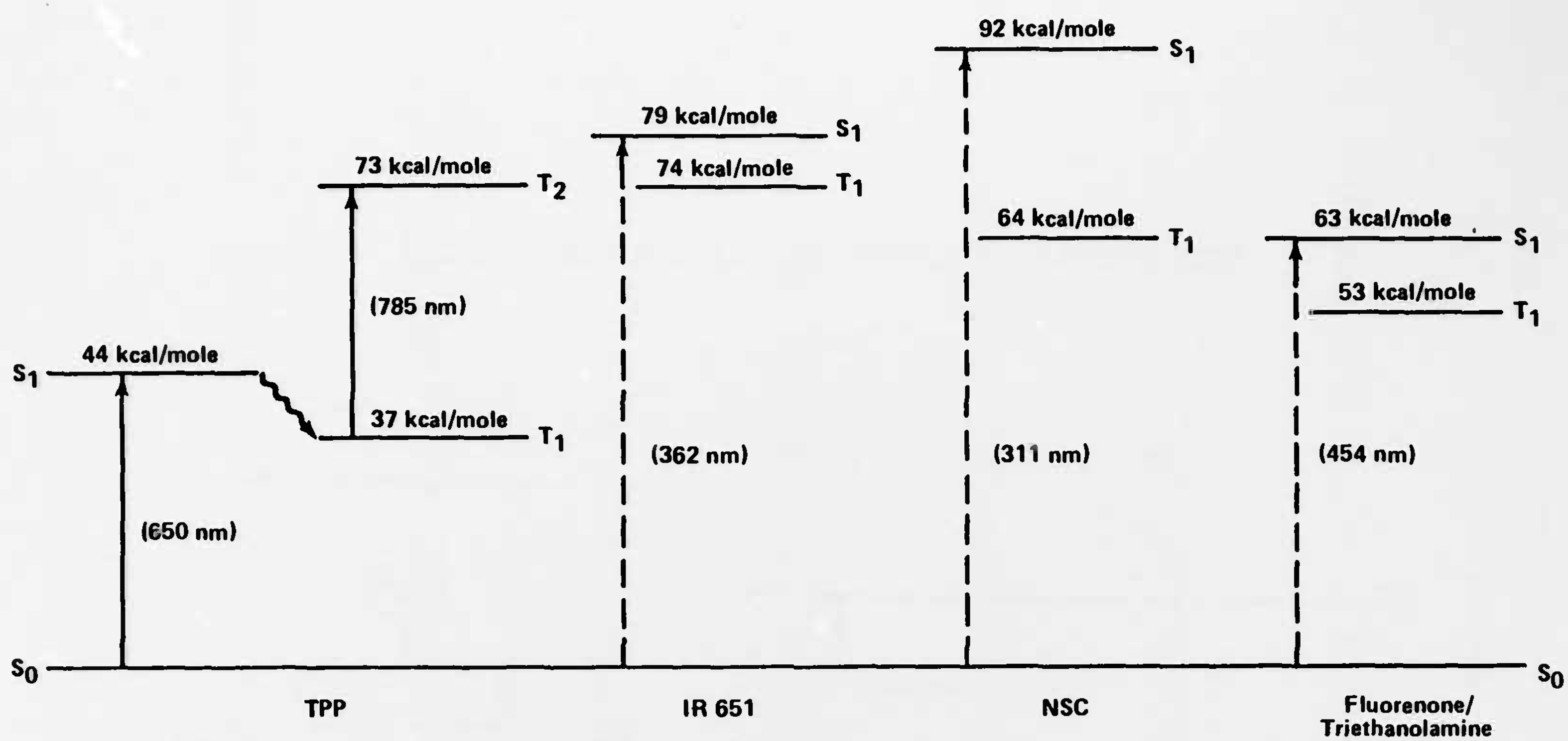

FIGURE 20. EXCITED-STATES ENERGETICS FOR TPP-SENSITIZED PHOTOINITIATOR SYSTEMS

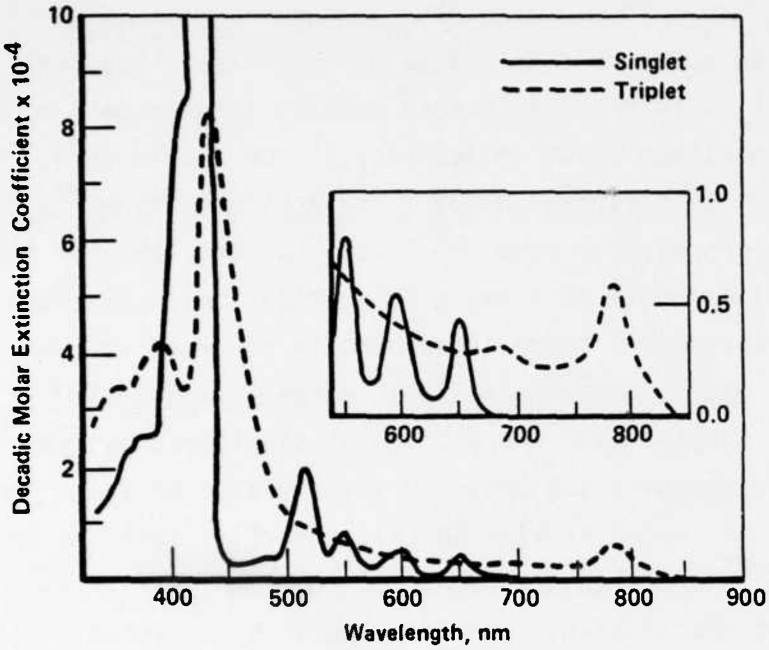

FIGURE 21. TRIPLET-TRIPLET ABSORPTION SPECTRUM OF *meso*-TETRAETHYLPORPHYRIN IN PYRIDINE (From Reference 10)

initiator systems used with TPP, single-beam polymerization was also often observed as a competing process. This is manifested as the growth of a slender, finger-like projection of polymer along the beam axis of one or both beams, and results from the fact that both ground-state and triplet have finite absorbance at that wavelength. Since the rate of polymerization is dependent on the light intensity (although not in a simple, linear way, since polymerization is a chain propagation process initiated, in this case, by the sequential absorption of two photons in the same laser pulse) the polymer forms most rapidly near the beam center. This results in a "self-lensing" effect, in which the tip of the optically clear polymer finger focuses the beam into the nearly polymer, causing further propagation of the finger. The beam is often so distorted by this process that no trace of the beam can be seen at the intersection point. This is, in fact, probably the most serious problem remaining to be solved; the crosslinked polymers obtained to date are hard, insoluble, and optically clear, but until the single-beam problem is overcome, it will be difficult to achieve either speed or accuracy in PCM fabrication. The single-beam process may have virtue, however, in applications of these materials to photolithography; the same non-linear optical behavior responsible for self-lensing should give rapid polymerization in the most intense portions of the lithographic image, resulting in theoretical resolution that exceeds the diffraction-limited resolution of conventional photoresists.

Coupled with the problem of single-beam polymerization is the problem of trapping the upper T_2 state with a separate photoinitiator molecule. As noted earlier in this Report, a large molar excess of initiator is required (and, indeed, a single molecule with covalently linked sensitizer and initiator moieties would be preferred). It occurred to us that it should be possible to probe the concentration and spectroscopic properties of the triplet-state species formed in our experiments by monitoring the intensity of beam 2 transmitted through the sample in the presence and absence of beam 1. The experiment is essentially a straightforward absorbance measurement, where the effective optical path length is the diameter of beam 1 at the intersection point and the concentration of absorber (in the vicinity of the 785 nm peak, which is unique to the triplet) is zero unless beam 1 has been turned on. It is particularly helpful in this case that the beam 2 (Molectron) pulse duration is very short compared to the probable lifetime of the T_1 triplet state.

The sample for this experiment consisted of a solution of 1.0×10^{-4} M TPP and $\sim 2.2 \times 10^{-3}$ M Irgacure 651 photoinitiator (an acetophenone derivative) in a mixture of trimethylolpropane triacrylate (TMPTA, a cross-linking acrylic additive), methyl methacrylate (MMA), and PS 169 (an acrylic oligomer, to increase viscosity) in relative proportions of 3:1:6 by weight, with a total volume of approximately 3 ml or so. The sample was degassed under red safe light <u>in vacuo</u> by a series of 5 or 6 repeated freeze-pump-thaw cycles, sealed with a high-vacuum stopcock, and stored in a dark freezer until just before use, when it was allowed to warm to room temperature.

With the sample clamped at the intersection point of the two focused laser beams, the "pump" beam from the Phase-R laser was kept at a constant wavelength of about 600 nm (using Rhodamine 6G in methanol) to excite the TPP selectively. The "probe" beam, from the Molectron laser, was tuned in 5 nm increments from 750 nm to 800 nm [using 3,3'-diethyloxatricarboncyanine iodide (DOTC) in DMSO], since the lowest-energy T-T absorption band was expected to occur in this wavelength range. The two laser pulses were triggered externally by a delay generator, such that the "probe" beam arrived about 1.5 sec after the "pump" beam had ended.

At each wavelength, one or the other (or both) of the laser beams was alternately blocked so we could record (a) background noise and (b) the intensity of the "probe" beam transmitted through the sample with and without the presence of the "pump" beam. A sensitive photomultiplier tube, protected by a Corning CS 7-59 IR-transmitting filter with a cutoff of about 700 um, was used as a detector, with its output amplified and displayed on an oscilloscope. The process of measuring noise, "probe" intensity alone, and "probe" intensity in presence of the "pump" beam was repeated 2 or 3 times for each wavelength; we then moved on to the next point.

The actual data, averaged over the several readings taken at each wavelength, are shown in Table 9 and Figure 22. While there is undoubtably a substantial amount of error built into the procedure used, it is significant that we succeeded in measuring a spectrum that is very similar to that reported by Sapunov, et al (Figure 21).[10]

Using our absorbance data and Sapunov's value for the molar decadic extinction coefficient of T_1 ($7x10^3$), we estimate that the concentration of TPP triplets formed along the path of the "pump" beam is roughly $6x10^{-5}$ M. Since the initial concentration of TPP is about $1x10^{-4}$ M, and since the quantum yield of triplet formation for TPP is

TABLE 9. REDUCED DATA FROM TRIPLET-TRIPLET ABSORPTION MEASUREMENT

λ, nm (molectron)	Average Intensities Molect.	Molect. + Phas-R	Noise	Io [(Molect.) - (Noise)]	I [(Mol. + Phas-R) - (Noise)]	T (I/Io)	A [-log(I/Io)]
750	0.175	0.175	0.100	0.075	0.075	1.000	0.000
755	0.200	0.200	0.100	0.100	0.100	1.000	0.000
760	0.200	0.200	0.100	0.100	0.100	1.000	0.000
765	0.250	0.250	0.100	0.150	0.150	1.000	0.000
770	0.250	0.248	0.100	0.150	0.148	0.987	0.006
775	0.225	0.220	0.100	0.125	0.120	0.960	0.018
780	0.200	0.190	0.085	0.115	0.105	0.913	0.040
785	0.225	0.200	0.085	0.140	0.115	0.821	0.085
790	0.225	0.200	0.085	0.140	0.115	0.821	0.085
795	0.200	0.188	0.085	0.115	0.103	0.896	0.048
800	0.200	0.190	0.085	0.115	0.105	0.913	0.040

(All values of I and I_0 are probably good to $\pm$ 0.02 or so)

- Sample #1 (7/2/84): (Total Vol ~3 ml) ~1×10^{-4} M TPP + 2.2×10^{-3} M IR 651 (Initiator) in TMPTA/MMA/PS169 (3:1:6 by weight)

- Concentration of TPP* (T_1) Formed: $A = \varepsilon \ell c$; $c = A/\varepsilon \ell$

A_{785nm} ~ 0.085

ℓ ~ 0.2 cm (Phase-R beam diameter in cell ~ 2 mm)

ε_{785} ~ 7×10^3 M^{-1} cm^{-1} (V. V. Sapunov, et al., Reference 10).

$$\boxed{C(T_1) \approx 0.085/1,4000 \approx 6 \times 10^{-5}\ M}$$

Active volume ~ 5×10^{-4} ml (Molectron probe beam ~ 0.5 mm diam.)

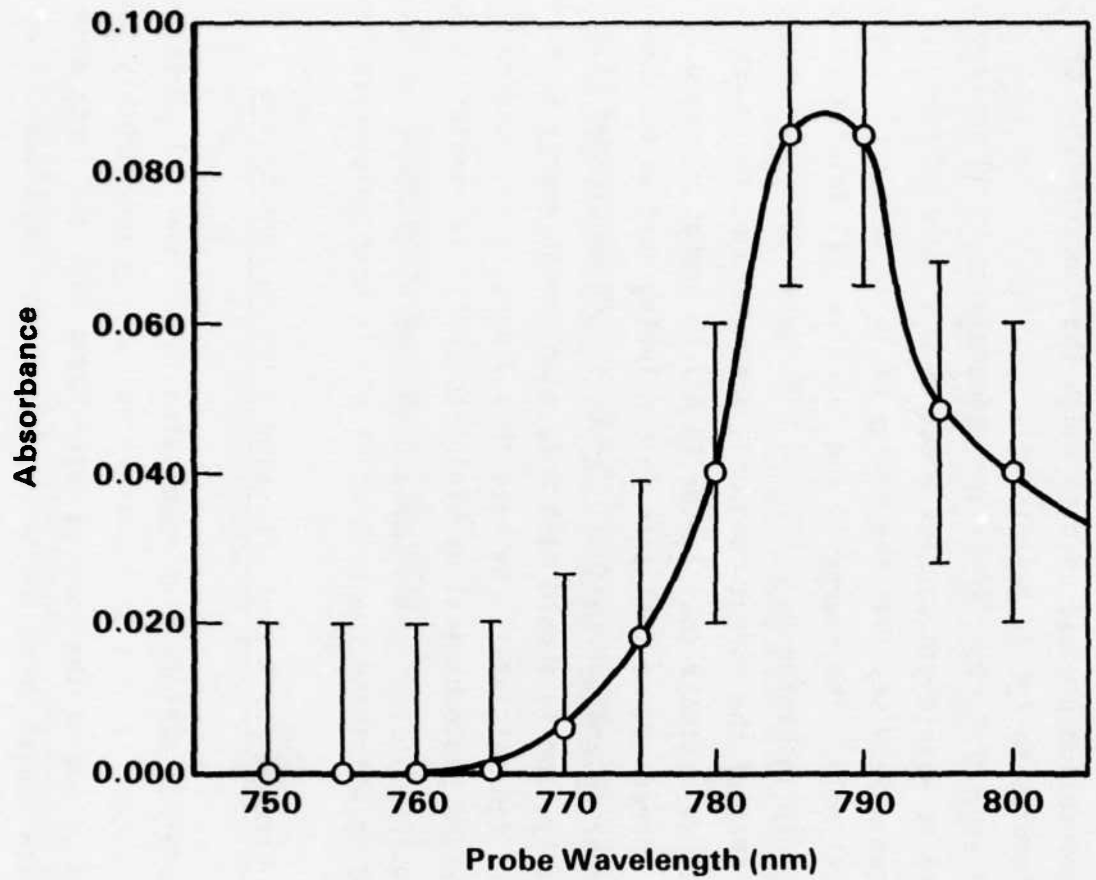

FIGURE 22. TRIPLET-TRIPLET ABSORPTION SPECTRUM OF meso-TETRAPHENYLPORPHIN IN POLYMER

about 0.7, the maximum concentration of triplets we could expect is about 7×10^{-5} M. This suggests that over 80% of the theoretical concentration of triplets is formed with each "pump" pulse under our experimental conditions. Furthermore, since this number is based on an optical absorption measurement, virtually all of those T_1 molecules are being excited to T_2 (that is, the absorption process used to gauge the concentration of T_1 excites the molecules to T_2, by definition).

The energy of T_1 for TPP is approximately 38 to 40 kcal/mole and light of 785 nm wavelength carries about 36 kcal/mole of energy. Therefore, we can safely say that the energy of T_2 in this system must be around 74-76 kcal/mole. The energy of the reactive (T_1) triplet state of the Irgacure 651 initiator is not known precisely, but it is probably a bit lower than that of the parent compound, acetophenone, for which T_1 is at 74 kcal/mole; we estimate that T_1 for IR 641 is probably around 71 or 72 kcal/mole. Therefore, we feel safe in concluding that we have designed a system with appropriate energetics: S_0 and T_1 can be excited selectively and cleanly, and T_2 should have more than enough energy to excite than T_1 state of the initiator. We have thus demonstrated technical feasibility for the photochemical machining concept. It remains to demonstrate the successful fabrication of a high-resolution shape in three dimensions, and to eliminate the problem of single-beam polymerization.

New Concept For A Rapid-Focusing Rotating Lens System

In order to achieve high resolution in a commercial photochemical machining system, it will be necessary to rapidly and smoothly move the focal point of one of the focused laser beams back and forth over a considerable path length along the beam propagation direction. Doing this by moving elements of a set of lenses relative to one another involves linear or rotatory motions that are not constant in time and which frequently involve sharp accelerations and decelerations, leading to wear or slippage of the mechanical components used to effectuate the lens motions.

As an alternative, we suggest the use of a rotating lens whose focal length varies with the angle of rotation, illuminated by a beam displaced from, but parallel to, the axis of rotation. Such a lens could be fabricated along conventional lines, either by casting an appropriately shaped mold or by careful turning, using equipment developed for fabricating radially symmetric aspherics, but a more practical and versatile realization would seem to be in the form of a Fresnel lens. The rake angle of the Fresnel gooves can be varied with angle around the lens in order to move the focal distance back and forth (or, if desired, in a "sawtooth" pattern, with a jump back from the longest to the shortest focal distance every 180 or 360 degrees) either linearly with time or according to any desired schedule, as indicated in Figure 23.

It is easy to allow time for moving either the beam or the object transversely at the end of each scan by adding an opaque sector with a bit of black paint, yielding a focal-length/time characteristic as in Figure 23(d). At the same time that the rake angle is changed, the Fresnel groove width and depth can be gradually modified so that beams passing through adjacent facets interfere constructively, insuring a sharp focus and one which does not change with focal distance. If the image space has a refractive index different from that of air, as is likely for PCM applications, this can be allowed for in the design of the lens. A suggestion of how such a lens might appear is given in Figure 24. We emphasize that whatever the desired focal distance/time characteristic, it can be maintained, with appropriate lens designs, by rotating the lens at constant angular velocity. The angular rotation may be produced electrically, or, as indicated in Figure 24, through impulse of a fluid on vanes attached to the lens. An interesting possibility for forming the lens is laser machining. It is possible that a suitable variable-transmission mask could be made photolithographically, which would enable the grooves to be made either by exposure to a uniform beam, or, more likely, by rotating the lens blank under a cylindrically focused beam passing through the photomask. Direct cutting along a spiral path is also feasible, using

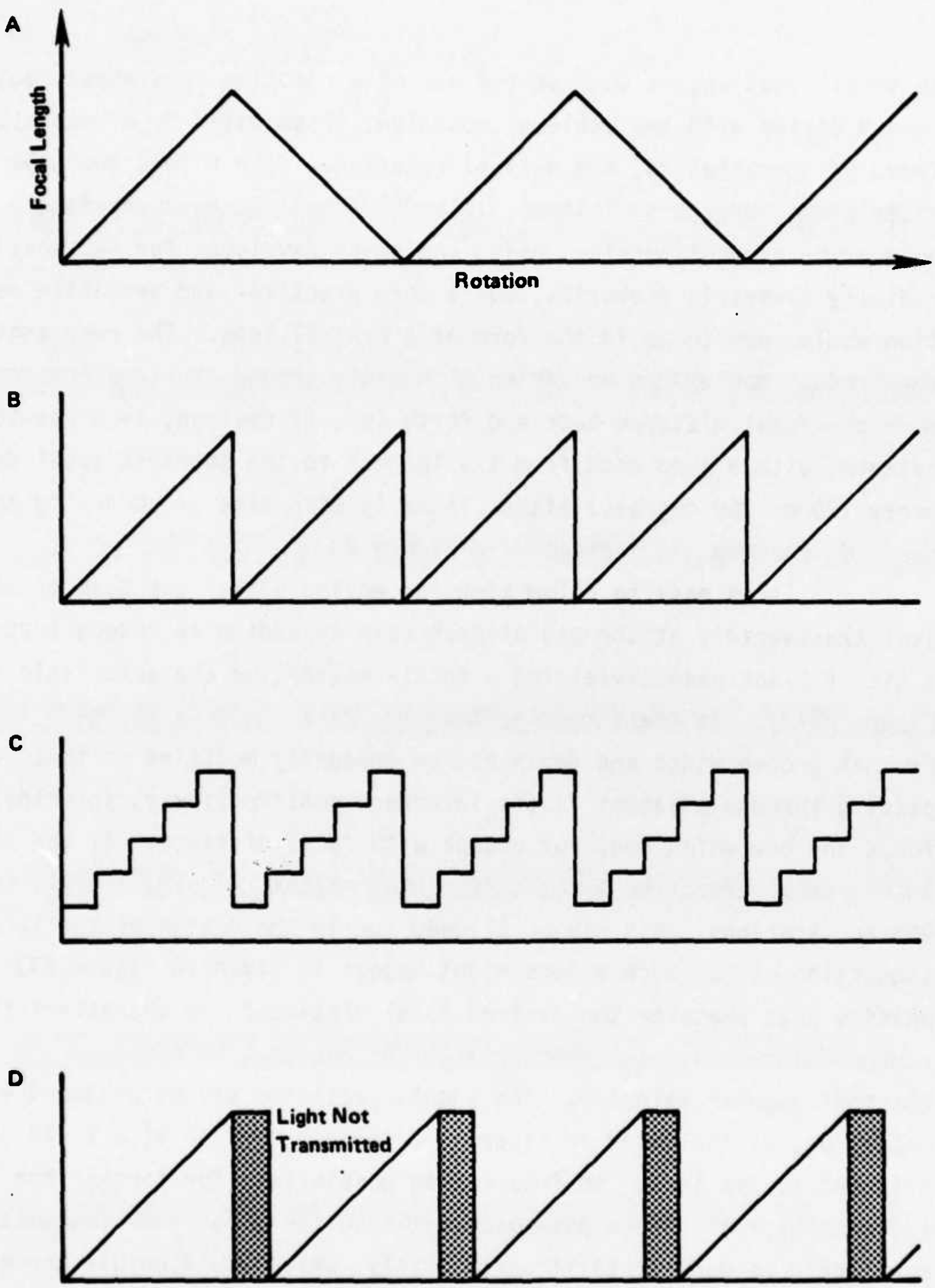

FIGURE 23. POSSIBLE FOCAL-LENGTH DEPENDENCE ON ROTATION FOR REPRESENTATIVE VARIABLE-FOCUS FRESNEL LENS DESIGNS: (a) RECIPROCATING; (b) SMOOTH SAWTOOTH; (c) STEPPED SAWTOOTH; SMOOTH SAWTOOTH WITH OPAQUE INTERVALS

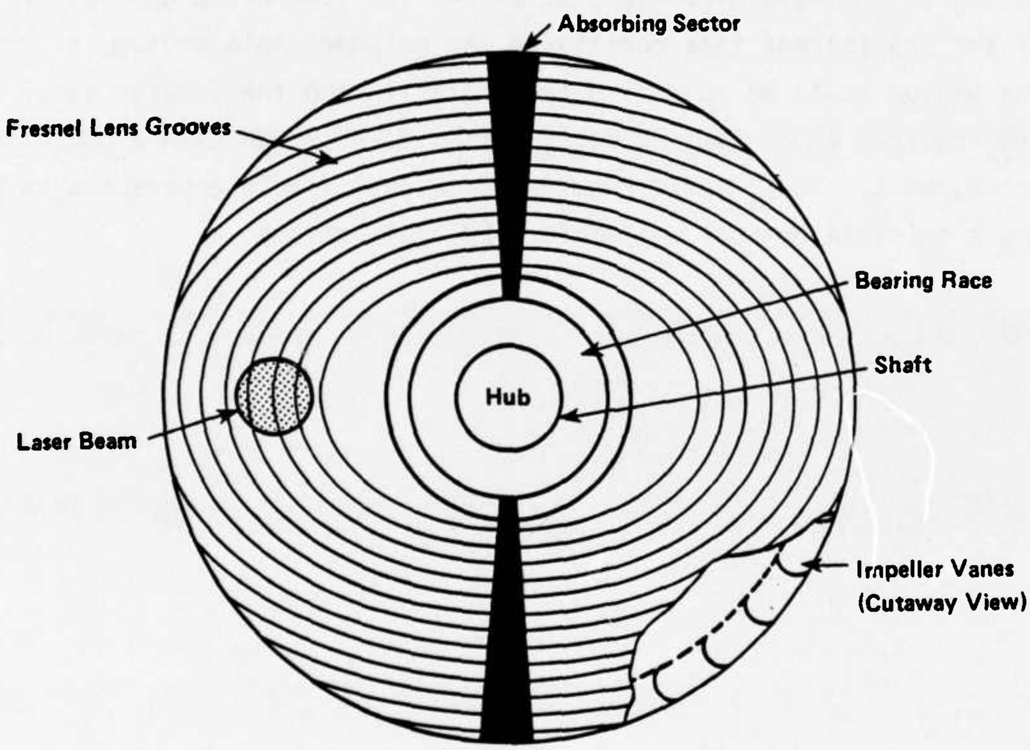

FIGURE 24. CONCEPTUAL ILLUSTRATION OF A VARIABLE - FOCUS FRESNEL LENS

an industrial CO_2 or excimer laser. There are likely to be additional advantages to laser-machining Fresnel lenses, compared to the usual stamping process for their manufacture, in that one is not necessarily constrained to groove shapes which can be easily removed from a stamping mold.

Modifications and extensions of the Fresnel lens and rotating elements concept enable one to focus the beam anywhere within a rectangular region, rather than just along a line. Thus, with uniform linear motion in a single direction, of either the lasers and optical system or of the transparent tank containing the polymerizable medium, all points in the medium could be addressed sequentially with the focused laser beam. The required linear motion could easily be provided with a jackscrew arrangement. Thus, there seem to be several viable approaches to designing a suitable optical system for PCM applications.

RECOMMENDATIONS FOR FUTURE RESEARCH

As noted before, the research performed on this project during the past two years has succeeded in demonstrating the technical feasibility of photochemical machining, and has identified several promising materials for use as photosensitizers, initiators, and polymer components. A novel concept for a rapid-focus optical system has also been conceived, and it has been found that several of the same basic polymer/sensitizer/initiator systems which are useful for PCM may also have applications as high-contrast photoresist materials.

Two major materials problems remain to be addressed: the single-beam polymerization observed with many of the more reactive polymer combinations studied, and the relatively slow polymerization observed in those systems which did not exhibit single-beam hardening. We suggest that it may be possible to attack both problems simultaneously by developing unimolecular photoinitiators consisting of derivatized TPP molecules with appropriate initiator moieties linked covalently to the porphyrin ring system. It will be recalled that this approach was tried at the outset of the project (although with limited success), using brominated or sulfonated porphyrin and rubrene derivatives. These attempts were unsuccessful because of a poor match of energetics (the upper excited triplet states turned out to have too little energy to cleave the molecule and initiate polymerization) and because of difficulties of purifying the photoporphyrin IX derivatives that were synthesized. It seems likely that approaches based on derivatization of TPP with either benzoin ether groups or fluorenone-like groups will be more successful. By having the initiator moiety linked to the TPP sensitizer, one can be ensured of having the high local concentration of initiator required to trap the short-lived upper T_2 state of TPP. This should permit efficient photopolymerization to be obtained with irradiation in the 600-650 nm and 780-790 nm wavelength regions, respectively, making it possible to avoid the shorter wavelengths where single-beam polymerization is more of a problem. The crosslinking acrylate polymers used for the research in this project seem well suited to PCM applications without much further modification.

In addition to the materials problem discussed above, additional work is required to develop the optical system and computer system for true PCM operation. It will be necessary to develop a self-aligning optical system which will automatically maintain focus and synchromization while scanning the two beams throughout the volume to be polymerized. Also, a more flexible computer system will be needed to permit the facile description of shapes to be made; it is likely that a straightforward modification of existing CAD/CAM technology will provide the needed improvements here.

In summary, there appear to be no fundamental barriers to the successful development of an operational PCM system. Additional R&D efforts will be required, of course, but with sustained diligence, it should be only a matter of a few years until the PCM concept becomes a reality.

REFERENCES

1. Rice , O. K.,J. Chem. Phys. 12, 1 (1944).

2. Sloane, N. J. A., Scientific American 250, #1, 116 (1984).

3. Wood, V. E., Amer. J. Phys. 34, 645 (1966).

4. Hirschfelder, J. O., C. F. Curtiss and R. B. Bird, Molecular Theory of Gases and Liquids (John Wiley, 1954), pp. 1037-8.

5. Wiley, J. O. and Seman, J. A., Bell Syst. Tech. J. 49, 355 (1970).

6. Labhart, H. and Heinzelmann, E., in "Organic Molecular Photophysics", Vol. I, J. B. Birks, Ed., John Wiley and Sons, London, England (1973), Chapter 6.

7. (a) Liu, R.S.H. and Gale, D. M., J. Amer Chem. Soc., 90, 1897 (1968);
(b) Liu, R.S.H., ibid., 90, 1900 (1968).

8. Yildiz, A., et al, J. Chem. Phys., 49, 1403 (1968).

9. Tsvirho, M.P., et al, Opt. Spectrosc., 34, 635 (1973).

10. Sapunov, V.V., et al, Zh. Prikl. Spektrosk., 21, 667 (1974).

11. The preparation of rubrene dibromide is described by Keszthelyi, C. P. and Bard, A. J., J. Org. Chem., 39, 2936 (1974).

12. Oster, G. and Yang, N. L., Chem. Reviews, 68, 125 (1968).

13. Kinstle, J. F., Paint Varn. Prod., 63 (6), 17 (1973).

14. Labana, S. S., J. Macromol. Scis. Reviews in Macromolecular Chemistry, 11(2), 299 (1974).

15. Pappas, S. P., Progr. Org. Coatings, 2 (4), 333 (1974).

16. Rabek, J. F., Photochem. Photobio., 7, 5 (1968).

17. Pappas, S. P. and McGinniss, V. D., in: "UV Curing Science and Technology", Pappas, S. P., Ed., Technology Marketing Corp., Connecticut, USA (1975).

18. Amivi, S. M., Bamford, C. H. and Mullik., J., J. Poly. Sci., Poly. Symp., 50, 33 (1975).

19. McGinniss, V. D., SME technical paper, FC76-486 (1976).

20. McGinniss, V. D., Photographic Science and Engineering, 23 (3), 124 (1979).

21. Rabek, J. E., Photopolymers - Principles, Processes and Materials, Technical papers, SPE, Mid-Hudson Section, October, No. 27 (1973).

22. Turro, N. J., Modern Molecular Photochemistry, Benjamin/Cummings, California, USA (1978).

23. Knowles, A., Chemistry and Industry, 17, 1058 (1973).

24. McGinniss, V. D., J. Radiation Curing, 2, 3 (1975).

25. Cohen, S. G., Parola, A. and Parsons, G. H., Chem. Reviews, 73, 141 (1973).

26. Rust, J. B., "Photopolymers - Principles, Processes and Materials," Technical papers, SPE, Mid-Hudson Section, October, No. 55 (1970).

27. Rollefson, G. K. and Burton, M. (Eds.), "Photochemistry and the Mechanism of Chemical Reactions," Prentice-Hall, New York, N.Y. (1942).

28. Jenkins, A. D. and Ledwith, A. (Eds.) "Reactivity, Mechanism and Structure in Polymer Chemistry", John Wiley, New York, N.Y. (1974).

29. Leermakers, P. A. and Weissberger, A. (Eds.) Technique of Organic Chemistry, Vol. XIV, Interscience, new York (1969).

30. Turro, N. J., Chem. Eng. News, 45, 8 (1967).

31. Cundall, R. B., J. Oil Col. Chemists Assoc., 59, 95 (1976).

32. Wells, C.H.J., "Introduction to Molecular Photochemistry," Chapman and Hall, London (1972).

33. (a) Simons, J. P., "Photochemistry and Spectroscopy", Wiley-Interscience, London (1971).
    (b) Hulme, B. E., Paint Manufacture, 9, March (1975).

34. McGinniss, V. D., in "Developments in Polymer Photochemistry", Vol. 3, N. S. Allen, Ed., Applied Science Publishers, Ltd., Essex, England (1981), Chapter 1.

35. (a) Murov. S. L. (Ed.), Handbook of Photochemistry, Marcel Dekker, New York (1973),
    (b) Heine, H. G. and Trankneker, H. J., Progr. Org. Coatings, 3, 115 (1975).

36. (a) McGinniss, V. D., Provder, T., Kuo, C. Y., and Gallopo, A., Macromol., 11, 405 (1978).
(b) Jaffe, H. H. and Orchin, M. (Eds.), "Theory and applications of Ultraviolet Spectroscopy", John Wiley, New York, N.Y. (1966).

37. Labana, S. S., Ed., "Ultraviolet Light Induced Reactions in Polymers", ACS Symposium Series No. 25, American Chemical Society, Washington, DC (1976).

38. Calvert, J. G. and Pitts, J. N., Jr., Photochemistry, John Wiley, New York, N.Y. (1966).

39. Schnabel, W., Photographic Science and Engineering, 23 (3), 154 (1979).

40. DeSchryver, F. C., Pure Appl. Chem., 34, 213 (1973).

41. Delzenne, G., Ind. Chim. Belg., 24, 739 (1959)

42. Delzenne, G., Ind. Chim. Belg., 30, 679 (1965).

43. Hutchison, J. and Ledwith, A., Advances in Polymer Science, 14, 49 (1974).

44. Rudolph, H., Rosenkranz, H. J. and Heine, H. G., ACS Polymer Preprints, 16 (1), 399 (1975).

45. McGinniss, V. D. and Dusek, D. M., J. Paint Technol., 46 (589), 23 (1974).

46. Carothers, W. H., Chem. Rev., 8, 402 (1931).

47. See, e.g., Aso, C., Kunitake, T., and Tagami, S., Prog. Polym. Sci. Jpn., 1, 149 (1971); Corfield, G. C., Chem. Soc. Rev., 1, 523 (1972); Butler, G. B., Corfield, G. C., and Aso, C., Prog. Polym. Sci., 4, 71 (1975).

48. Flory, P. J., J. Am. Chem. Soc., 63, 3083, 3091, 3096 (1941); J. Phys. Chem., 46, 132 (1942); Principles of Polymer Chemistry, Cornell University Press, Ithaca, New York, 1953.

49. Stockmayer, W. H., J. Chem. Phys., 11, 45 (1943); 12, 125 (1944).

50. Walling, C., J. Am. Chem. Soc., 67, 441 (1945).

51. Gordon, M., Proc. R. Soc. London, Ser. A, 268, 240 (1962); Dobson, G. R. and Gordon, M., J. Chem. Phys., 41, 2389 (1964); 43, 705 (1964); Butler, S., Gordon, M., and Malcolm, G. N., Proc. R. Soc. London, Ser. A, 295, 29 (1966); Gordon, M. and Scantlebury, G. R., J. Polym. Sci., Part C, 16, 3933 (1968); Gordon, M., Kucharik, S., and Ward, T. C., Collect. Czech. Chem. Commun., 35, 3252 (1970).

52. Dusek, K. and Ilansky, M., J. Polym. Sci., Polym. Symp., 53, 57, 75 (1977).

53. Hammersley, J. M.. Proc. Cambridge Philos. Soc., 53, 642 (1957).

54. Kirkpatric, S., Rev. Mod. Phys., 45, 574 (1973).

55. Staufer, D., J. Chem. Soc., Faraday Trans., [2] 72, 1354 (1976).

56. Gordon, M., Proc. R. Soc. London, Ser. A, 201 569 (1951); J. Chem. Phys., 22, 610 (1954).

57. Soper, B., Haward, R. N., and White, E.F.T., J. Polym. Sci., Polym. Chem. Ed., 10, 2545 (1972).

58. Kast, H. and Funke, W., Makromol. Chem., 180, 1335 (1979).

59. McGinniss, V. D., in Reference 37, p. 135.

60. (a) Farenholtz, S. R. and Trozzollo, A. M., J. Amer. Chem. Soc., 93, 251 (1971);
(b) Walling C. and Gibian, M.J., ibid, 87, 3413 (1965).

APPENDIX

MASTER'S DEGREE THESIS OF DEAN R. JOHNSON
THE OHIO STATE UNIVERSITY
1984

THREE-DIMENSIONAL PHOTOPOLYMERIZATION

A Thesis

Presented in Partial Fulfillment of the Requirements
for the Degree Master of Science

by

Dean Ronald Johnson, B.A., Ch.

The Ohio State University
1984

Approved by

Kent S. Knaebel
Adviser

Robert E Schwegel
Adviser

Department of Chemical Engineering

To my loving wife Betty,

for her understanding,

patience and support.

TABLE OF CONTENTS

Page

TABLES

I. SUMMARY

Design of a photopolymerization system with the capability to build three dimensional shapes within given boundaries was undertaken. Such a system required the development of new photoinitiators or photosensitizer systems, which, when used with an appropriate monomer solution, resulted in a clear hard polymer.

The primary requirement of the photoinitiators was that they form free radical initiators when irradiated by two light beams of different wavelengths. The absorbed energy of beam 1 excited the photoinitiator to a singlet which underwent intersystem crossing to a relatively long-lived triplet. Beam 2 was absorbed by the triplet and provided enough energy to cause bond scission and formation of a free radical initiator. The approach taken to obtain photoinitiators with such characteristics required the synthesis of new photoinitiator molecules.

Parent molecules were selected which had desirable absorption characteristics in the visible region as well as the ability to form triplets efficiently. To these molecules a known initiating group of either bromine or sulfonyl chloride was added. A total of seven new photoinitiators were prepared. Irradiation trials of the seven photoinitiators in monomer, indicated that they all were capable of photoinitiating polymerization. Analyses of the photoinitiators to obtain molecular formulas were inconclusive as were proton NMR and ^{13}C NMR analyses. It should be noted that this information was not necessary for successful completion of this study. From a series of

photochemical and thermal stability studies one photoinitiator was selected for further study. This was a polybrominated tetraphenyl porphine ($TPPBr_X$). Attempts to obtain a triplet-triplet absorption spectrum of $TPPBr_X$ were only partially successful.

The monomer selected for the initial photopolymerization trials was trimethylolpropane triacrylate (TMPTA) which was known to be an efficient crosslinking monomer. A recurring problem with the $TPPBr_X$/TMPTA system was single beam polymerization. To control this undesirable reaction methylmethacrylate (MMA) was added to the TMPTA monomer solution. Study of the $TPPBr_X$ photoinitiator system was discontinued when two-beam photopolymerization was not achieved.

The light sources and wavelength distribution used for beams 1 and 2 were changed during the course of this research study. The final system incorporated two pulsed dye lasers, which provided high radiant power to each beam and allowed selective control of the wavelength of each beam.

The photosensitizer system studied used tetraphenyl porphine (TPP) as the photosensitizer and naphthalene sulfonyl chloride (NSC) as the initiator. TPP was chosen based on its known singlet-singlet and triplet-triplet absorption spectra which indicated two possible wavelength selections for beam 2. One was 460nm where there was only a small amount of singlet-singlet absorption and the other was 785nm where there was no singlet-singlet absorption.

Different mole ratios of TPP:NSC were studied using a TMPTA+MMA monomer solution. Two-beam polymerization was achieved using a TPP:NSC molar ratio of 1:20 in a monomer solution composed of 3:1

TMPTA to MMA by volume. The occurrence of single-beam polymerization was also present in this system. Use of a large mole excess of NSC to TPP (100:1) resulted in polymerization prior to sample irradiation.

To increase the mass of polymer formed within a given irradiation time period, an oligomer was added to the monomer solution. This would increase the mass of polymer formed for each cross-link event. Study of this type of monomer system is being continued and there have been indications that two-beam polymerization is occurring.

This study provided much valuable information toward the development of a two-beam polymerization system. Problems encountered in sample preparation, irradiation conditions, and irradiation techniques were identified and successfully solved. Two-beam polymerization was achieved and many ideas for further study were generated.

II. INTRODUCTION

Photopolymerization has received much attention and research effort over the past 15 years. Primary emphasis has been on the development of applications such as pollution-free coatings, inks, and films using ultraviolet-initiated polymerization.[1] This has led in turn to the development of many new photopolymerization initiators, whose reactivity is dependent upon exposure to light of specific wavelengths and intensity. The concept of two-beam photopolymerization presents a basis for greatly increasing the control over the polymerization process as well as opening new avenues of application, such as making models for investment casting.

For the two-beam polymerization process to work effectively, polymerization must occur only at the intersection of the two beams' paths within a solution of monomer and photoinitiator or photosensitizer. Polymerization by either beam by itself is undesirable and, therefore, the selection of photoinitiators, photosensitizers, wavelength content of the two light beams and monomers are all areas that require consideration.

Development of this concept has been a part of the research effort at Battelle's Columbus Laboratories and at the Formigraphic Engine Corporation in California. Early research at Battelle resulted in the development of a system based on the use of intersecting light beams to produce a fluorescent spot. Movement of the spot was controlled by movement of the light beams and hence their point of intersection. Application efforts were directed toward a three-dimensional oscilloscope-type fluorescent display. Such three-dimensional control is one of the basic premises on which this photopolymerization study is based, since this enables one to define a shape or solid form within given boundaries.

The second and perhaps more important premise is the ability to obtain polymerization at the point of intersection of the two light beams. To this end, new photoinitiators have been and are presently being developed primarily, if not exclusively, at Battelle. Along with the new photoinitiators, compatible monomers must be selected to complete the system. The ultimate system will allow control over the location and rate of polymerization and yield a polymer that is useful in the specific application.

This study has been one of the key initial steps in the development of such a system, and, as such, has provided information to aid in the selection of system components, and has helped to identify the conditions necessary for two-beam polymerization to occur.

III. PRINCIPLES OF PHOTOCHEMISTRY

A. Basic Concepts

A basic understanding of photochemistry begins with an understanding of the behavior of light. For this purpose, it is most useful to consider that a beam of light consists of a stream of particles, called photons. Molecules or chromophoric groups within a molecule will selectively absorb photons of a particular range of wavelengths and energy content. When a photon is absorbed, its energy is transferred to the molecule by which it is absorbed, causing structural or chemical changes within the molecule.

Photochemistry is therefore the study of the chemical reactions of molecules which have been "excited" by the absorption of light.

The probability of absorption is expressed by a constant known as the molar extinction coefficient, ϵ . Large values of ϵ indicate a high probability of absorption by a molecule at a given wavelength and low values of ϵ represent less probability of absorption. ϵ cannot be measured directly, but can be obtained from an absorption spectrum when the concentration and optical path length are known. The relationship between ϵ and absorption, A, is given as:

$$A = \log (I_o/I_t) = \epsilon lc \qquad (1)$$

I_o = intensity of the incident light

I_t = intensity of the transmitted light

l = optical path length (cm.)

c = concentration (mole/l.)

ϵ is a fundamental molecular property and is independent of concentration and path length if Lambert's and Beer's laws hold.

Lambert's law: The proportion of light absorbed by a medium is independent of the initial intensity I_o[2]

Beer's law: The amount of light absorbed is proportional to the concentration of absorbing molecules in the light path.[2]

A molecule's absorption spectrum indicates what wavelengths of light the molecule absorbs as well as the variation of ϵ with wavelength.

B. Photoexcitation

Molecules in their normal energy state are said to be in their ground state. When a molecule in its ground state absorbs a photon, the energized molecule is said to be in an excited state. A molecule in an excited state is best regarded as a completely new entity, only remotely related to the same molecule in its ground state.[3] In addition to undergoing a change in electron configuration, the excited molecule will possess a different geometry and react quite differently than the molecule in its ground state.

An excited molecule can exist in one of two different types of electronic states, referred to as singlet (S_n) or triplet (T_n) states. The relationship between these two types of states can best be explained with the aid of a state energy diagram (see Figure 1). If a molecule at ground state S_o absorbs a photon, it is increased in energy to the S_n level. In the S_n level the excited molecule retains the paired (antiparallel) spin configuration of the S_o state (Figure 2). The S_n levels are represented by a series of parallel lines, because within each electronic state there are many different vibrational energy levels. The excess energy of molecules excited to upper vibrational levels is rapidly lost through thermal relaxation, as the molecule seeks its lowest excited energy level. Thermal relaxation also occurs rapidly from the upper S_n levels to the S_1 level. In solution, the relaxation energy lost is transferred as heat to the solvent surrounding the excited molecules.

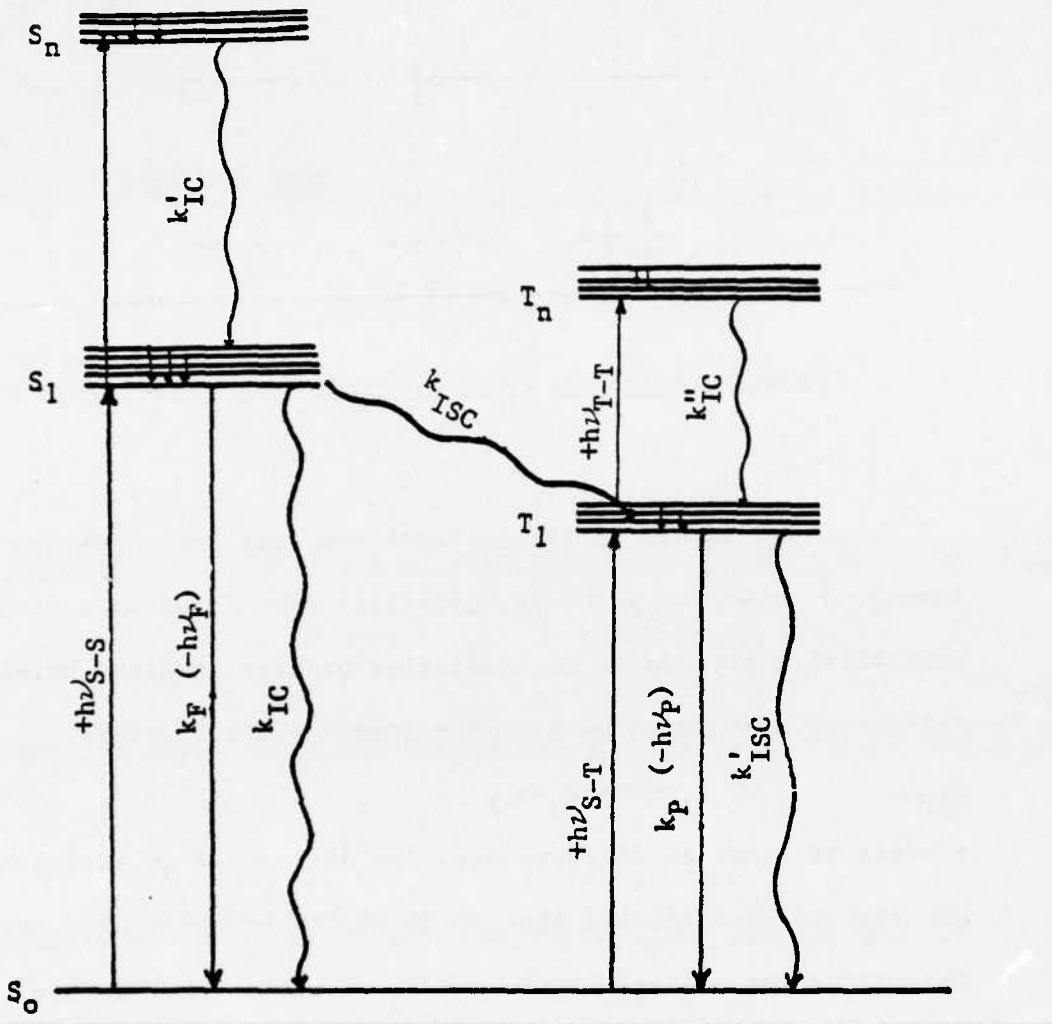

S_o - ground state energy level

S_1 - 1st excited singlet energy level, lowest vibrational level

T_1 - 1st excited triplet energy level, lowest vibrational level

k_F - fluorescence rate constant

$k_{IC}, k'_{IC}, k''_{IC}$ - internal conversion rate constant

k_{ISC}, k'_{ISC} - intersystem crossing rate constant

k_P - phosphorescence rate constant

FIGURE 1: ENERGY STATE DIAGRAM

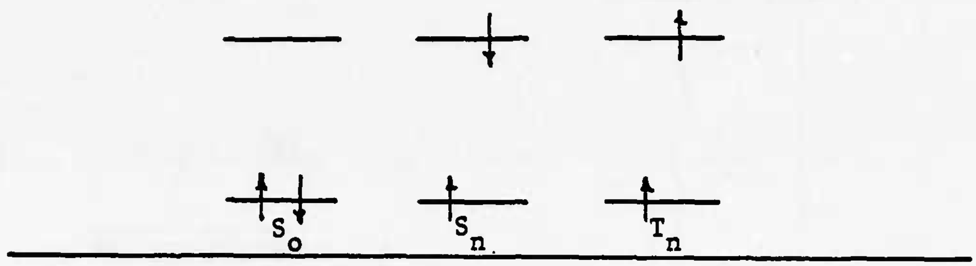

FIGURE 2: EXCITED STATE ELECTRON SPIN CONFIGURATIONS

A molecule in its S_1 level can release its excess energy through a number of pathways, generally classified as radiative or nonradiative processes. The radiative process involves release of a photon and conversion back to the ground state S_o. This

$$S_1 \longrightarrow S_o + h\nu_F \tag{2}$$

process is known as fluorescence. The difference in energy between the absorbed and emitted photons is due to energy lost as heat during the relaxation process from upper S_n or vibrational levels to the lowest S_1 vibrational level. This decrease in energy causes a shift in the fluorescence spectrum of the molecule to less energetic longer wavelengths relative to the molecules absorption spectrum.

Nonradiative processes involve thermal relaxation to a S_n level from a S_{n+1} level or from a S_n level to the corresponding triplet, T_n, energy level. The

$$S_{n+1} \longrightarrow S_n + \text{heat} \tag{3}$$

transition is known as internal conversion (IC) and the

$$S_n \longrightarrow T_n + \text{heat} \tag{4}$$

transition is known as intersystem crossing (ISC). Of the two processes, internal conversion is often the path of least resistance because intersystem crossing also requires that the excited electron undergo a change in spin direction, known as a spin flip (Figure 2).

The triplet state also has multiple vibrational and electronic (T_n) levels and, as in the singlet state, seeks to relax to the lowest triplet, T_1, and vibrational level. The nonradiative transition from T_1 to S_o is referred to as intersystem crossing (eq. 5) whereas the radiative transition (eq. 6) is called phosphorescence.

$$T_1 \longrightarrow S_o + \text{heat} \tag{5}$$

$$T_1 \longrightarrow S_o + h\nu_P \tag{6}$$

The thermal relaxation from upper vibrational or S_n, T_n levels to S_1 or T_1 generally occurs in the order of 10^{-12} sec. Consequently, fluorescence (eq. 2) and phosphorescence (eq. 6) will almost always occur between the lowest vibrational level of S_1 or T_1 and the ground state S_o.[2]

The sequential absorption of a second photon by a molecule in its excited T_1 state allows a molecule to reach upper triplet, T_n, levels. The wavelength and energy of the second absorbed photon is dependent upon a molecule's triplet absorption spectrum. Excitation to upper triplet levels by photon absorption at T_1 was first suggested in 1944 by Lewis and Kasha.[4] They proposed that the triplet state was a likely candidate for the metastable intermediate observed in spectroscopic studies of certain aromatic molecules.[5] It was not until 1963 that the existence of a photochemical process involving sequential absorption of two photons was established.[6]

Although the excitation from ground state to triplet state, $S_o \longrightarrow T_1$, may seem to be easily attainable because of the lower energy level of T_1, this process rarely occurs because it requires a simultaneous photon absorption and electron spin flip.

It is helpful to examine the time scales involved in the just mentioned series of events, from photon energy absorption to energy releases. Figure 3 presents a comparison of photochemical events.

	Time Scale (sec)	Event
	10^{-15} (femto-)	Absorption or emission of light
		Electronic motion
		Electron transfer
	10^{-12} (pico-)	Vibrational motion
		Bond cleavages (weak)
		Rotational and translational
	10^{-9} (nano-)	Motion (small molecules, fluid)
Fluorescence		Singlet lifetime
		Bond cleavage (strong)
		Spin-orbit coupling
	10^{-6} (micro-)	liquid at R.T. (25°C)
	10^{-3} (milli)	Triplet lifetimes - very cold solutions
Phosphorescence		
	10^{0}	glasses

FIGURE 3: COMPARISON OF TIME SCALES OF PHOTOCHEMICAL EVENTS[a]

(a) From Reference 2, pg. 7

The rate constants for the individual processes which occur during molecular excitation and de-excitation are designated on Figure 1 by the letter k with the appropriate subscript. The quantum yield, or efficiency, of an individual process is defined as the ratio of the rate constant of the process to the sum total of all the rate constants which serve to populate or depopulate the excited state in question. Equation 7 is an example of quantum yield of fluorescence.

$$\phi_F = \frac{k_F}{k_F + k_{IC} + k_{ISC}} \tag{7}$$

IV. PRINCIPLES OF PHOTOPOLYMERIZATION

Polymerization generally occurs via addition reactions of alkene monomers or condensation reactions of monomers which result in intermolecular elimination of small molecules such as water or alcohols. More specifically, addition polymer reactions occur through free-radical, cationic or anionic mechanisms. Of primary interest in this study is the free-radical mechanism of polymerization.

Photopolymerization incorporates photoinitiator or photosensitizer molecules to initiate the polymerization process. The primary difference between a photoinitiated or a photosensitized system lies in the function of the initiator or sensitizer molecule. A photoinitiator molecule is the source of the free radical initiator; whereas, in a photosensitized system, the photosensitizer molecule acts as an agent to facilitate the transfer of absorbed energy to an initiator molecule. The initiator molecule becomes the primary free radical initiator. Photoinitiator or photosensitizer molecules can be organic, organometallic or inorganic compounds.[7]

The wavelength or energy of light absorbed by either a photoinitiator or photosensitizer, to accomplish free radical formation, is primarily dependent upon the molecular structure of the molecules.[8-11] Some of the key properties of these compounds are described in the following sections.

A. Photoinitiators

A photoinitiator can be described as being a molecule which, upon absorption of light energy of appropriate wavelength and intensity, undergoes a bond rupture (homolytic scission) to form free radical intermediates.

The primary photochemical reactions for a photoinitiator in a 2-beam system are as follows (subscript S or T denotes singlet or triplet):

$PI + h\nu \xrightarrow{I_{o1} \epsilon_1} (PI)^*_S$ (absorption of beam 1 to form excited singlet) (8)

$(PI)^*_S \xrightarrow{k_{ic}} PI + \text{heat}$ (internal conversion) (9)

$(PI)^*_S \xrightarrow{k_f} PI + h\nu_F$ (fluorescence) (10)

$(PI)^*_S \xrightarrow{k_{isc}} (PI)^*_T$ (intersystem crossing) (11)

$(PI)^*_T + h\nu_2 \xrightarrow{I_{o2} \epsilon_2} (PI)^*_{T2}$ (absorption of beam 2 to form upper level triplet (12)

$(PI)^*_T \xrightarrow{k'_{isc}} PI + \text{heat}$ (intersystem crossing) (13)

$(PI)^*_T \xrightarrow{k_p} PI + h\nu_P$ (phosphorescence) (14)

$(PI)^*_T + Q \xrightarrow{k_q} PI$ (quenching) (15)

$(PI)^*_{T2} \xrightarrow{k_r} PI^{\cdot}_1 + PI^{\cdot}_2$ (bond scission to form free radical initiators) (16)

As can be seen in the processes presented above, there are numerous competitive paths which may be taken prior to formation of the free radical initiators. It is desirable to be able to influence the sequence of events to maximize the efficiency of free radical production. The first set of competitive paths is eqs. 9,10,11. Of these three the most desirable is eq. 11, intersystem crossing, to form triplets. Triplet quantum yields for molecules can often be found in the literature or in sources such as Handbook of Photochemistry.[12] Based on reported triplet quantum yields, the initial photoinitiator selection is the primary way to insure a high rate of intersystem crossing. Additional control over triplet formation can be accomplished through chemically changing the molecule or the solvent environment to exploit the so-called "heavy atom effect."[13,14] This principle states that the addition of a so-called "heavy atom" (i.e. Br,Cl) to a molecule or to the solvent surrounding the molecule, will increase its rate of intersystem crossing.

The second set of competitive paths is comprised of eqs. 12,13,14,15. Absorption of beam 2 by the molecules T_1 triplet is the most desirable process in this set. Maximizing the formation of upper triplets, T_n, is dependent upon selection of the wavelength of beam 2 and the time interval between beam 1 and beam 2 irradiations.

Quenching, eq. 15, is the process through which an excited triplet molecule loses its energy to a molecule in the reaction medium known as a quencher. The result is a nonproductive energy transfer in terms of the product or process desired. This reduces the population of triplet molecules present and correspondingly reduces the chances of the desired reaction occurring. A quencher commonly found dissolved in liquids is oxygen. Oxygen exists in the ground state as a triplet and has been shown experimentally to quench both singlet[15] and triplet[16] states. Therefore the elimination of oxygen in the reaction solution is one important step if efficient photopolymerization is desired. In addition to oxygen, certain monomer chemical structures can behave as quenchers.

For a system to attain maximum efficiency the desired sequence of processes would be 8, 11, 12, 16, followed by a high rate of reaction of the free radicals ($PI_1^\bullet$ and $PI_2^\bullet$) with monomer to initiate chain growth and hence polymerization. Assuming that the triplet species absorbs beam 2 and that the singlet is transparent to beam 2, an expression can be derived for the rate of change of free radical formation from equations 8 to 16, as follows, where the rate of change of excited singlet concentration is given by $d[PI]_S^*/dt$:

$$d[PI]_S^*/dt = [PI]\ (Io_1 \epsilon_1) - [PI]_S^*\ k_{ic} - [PI]_S^*\ k_f - [PI]_S^*\ k_{isc} \qquad (17)$$

at steady state $d[PI]_S^*/dt = 0$, solving for $[PI]_S^*$

$$[PI]_S^* = \frac{[PI]\ (Io_1 \epsilon_1)}{k_{ic} + k_f + k_{isc}} \qquad (18)$$

assuming $k_f \simeq 0$, $k_{ic} \simeq 0$ gives

$$[PI]_S^* = \frac{[PI]\ (Io_1 \epsilon_1)}{k_{isc}} \qquad (19)$$

The rate of change of triplet concentration, $d[PI]_T^*/dt$, is given by

$$d[PI]_T^*/dt = [PI]_S^* k_{isc} - [PI]_{T2}^* (Io_2 \in_2) - [PI]_T^* k'_{isc} - [PI]_T^* k_p - [PI]_T^* [Q] k_q \qquad (20)$$

At steady state $d[PI]_T^*/dt=0$, solving for $[PI]_T^*$ and substitution of eq. 19 into 20, gives

$$[PI]_T^* = \frac{[PI] (Io_1 \in_1) - [PI]_{T2}^* (Io_2 \in_2) k_{isc}}{k_{isc} (k'_{isc} + k_p + [Q] k_q)} \qquad (21)$$

Rate of change for PI_{T2}^* concentration $d[PI]_{T2}^*/dt$

$$d[PI]_{T2}^*/dt = [PI]_T^* (Io_2 \in_2) - [PI]_{T2}^* k_r \qquad (22)$$

at steady state $d[PI]_{T2}^*/dt = 0$ solving for $[PI]_{T2}^*$

$$[PI]_{T2}^* = \frac{[PI]_T^* (Io_2 \in_2)}{k_r} \qquad (23)$$

subst. eq. 21 into 23, solving for $[PI]_{T2}^*$ gives

$$[PI]_{T2}^* = \frac{[PI] (Io_1 \in_1) (Io_2 \in_2)}{k_{isc} k_r (k'_{isc} + k_p + [Q] k_q) + (Io_2 \in_2)^2 k_{isc}} \qquad (24)$$

Rate of formation of PI;

$$\frac{d[PI^\cdot]}{dt} = [PI]_{T2}^* k_r \qquad (25)$$

subst. eq. 24 into eq. 25 gives

$$\frac{d[PI^\cdot]}{dt} = \frac{[PI] (Io_1 \in_1) (Io_2 \in_2) k_r}{k_r k_{isc} (k'_{isc} + k_p + [Q] k_q) + (Io_2 \in_2)^2 k_{isc}} \qquad (26)$$

It follows that for $k_q > k_p > k'_{isc} > k_{isc} > k_r$, the nonproductive processes will be the controlling paths, resulting in inefficient free radical production. This confirms what was previously stated and shows the need to reduce quenching, phosphorescence and $T_1 \longrightarrow S_o$ intersystem crossing.

This free radical formation process results in the destruction of the photoinitiator molecule, thereby reducing the concentration and therefore the efficiency of the photoinitiator solution. In selecting a photoinitiator for the two beam system proposed, the following characteristics are desired:

1. A fast rate of intersystem crossing relative to other deactivation paths of S_1 (i.e. $\phi_{isc} \simeq 1.0$).
2. Visible or near ultraviolet light absorption to produce a photochemically active intermediate species (triplet).
3. A long triplet lifetime, to maximize the opportunity of further absorption at the triplet level.
4. The presence of a chromophoric group which is known to form free radicals.
5. A mimimum amount of overlap between the singlet and triplet absorption spectra to eliminate competition between the two excited states.
6. A strong triplet absorbance at wavelengths of sufficient energy to cause bond cleavage.
7. Undergo efficient irreversible crosslinking only upon irradiation of the reactive intermediate (triplet).

The process to be accomplished is shown schematically in Figure 4.

As can be seen in Figure 4, a molecule is excited to its lowest singlet state S_1 with photons from beam 1 having an energy below the dissociation threshold of the molecule. It then rapidly undergoes intersystem crossing to its lowest triplet excited state T_1. In the absence of beam 2 the excited state will revert back to its initial ground state. Excitation of the reactive intermediate species at T_1

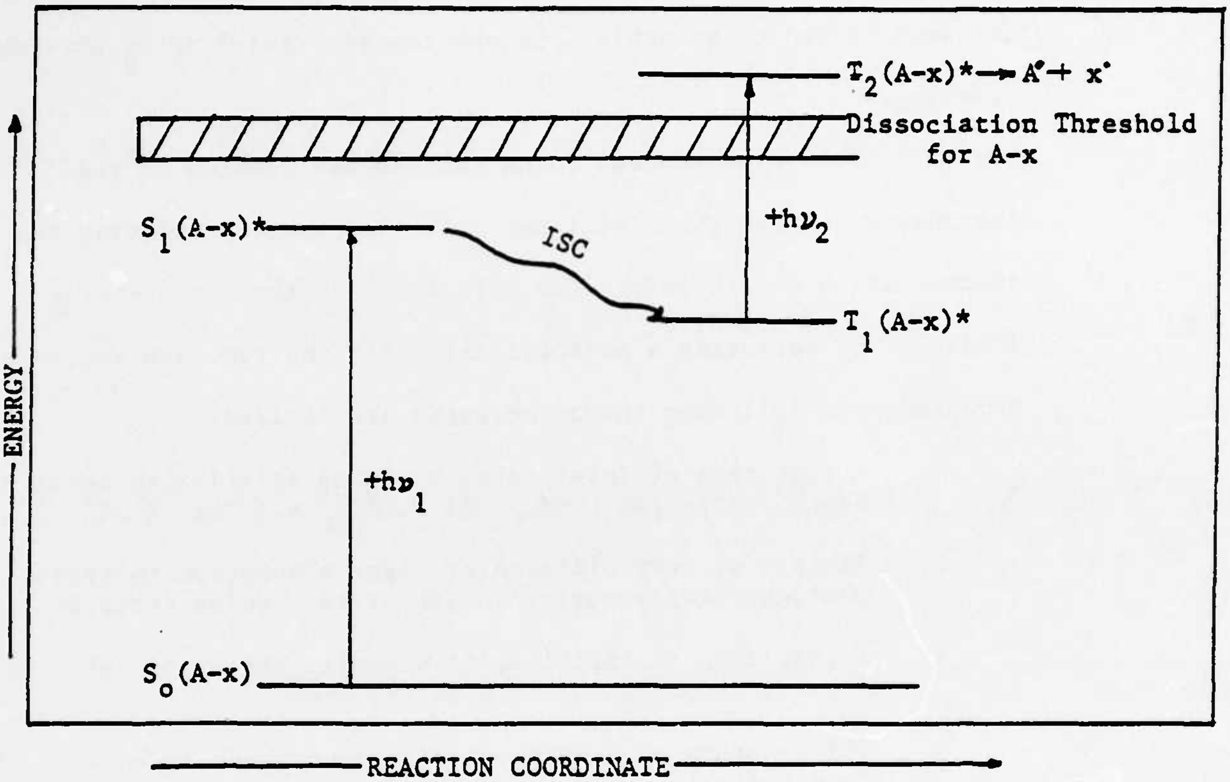

FIGURE 4: GENERAL STRATEGY FOR PHOTOINIATIATOR DESIGN

with beam 2, of proper wavelength and energy content, will cause the triplet T_1 to absorb energy in excess of the dissociation energy needed to fragment the molecule into reactive free radicals. These free radicals are the initiators for the polymerization process.

The approach selected to identify candidates to be synthesized was based on their containing two distinct functional groups: a light-absorbing moiety, or chromophore, and a labile initiating group that can be fragmented with high efficiency once sufficient energy is contained in the molecule.[17]

Two proven initiator groups were chosen for the candidate materials; these are the aryl sulfonyl chlorides and the benzylic bromides, as shown generically below.[17] There is ample precedent for the use of these initiating groups in commercial polymerization systems.[17]

$$Ar\text{-}SO_2Cl \xrightarrow{\text{60-65 Kcal/Mole}} ArSO_2^{\cdot} + Cl^{\cdot} \tag{27}$$

$$Ar\text{-}CH_2Br \xrightarrow{\text{65-70 Kcal/Mole}} ArCH_2^{\cdot} + Br^{\cdot} \tag{28}$$

65 Kcal/mole = energy at 440nm

70 Kcal/mole = energy at 408nm

The remaining problem then was to identify "Ar" groups which would give the required absorption characteristics and intersystems crossing requirements.

An additional advantage of selecting sulfonyl chloride and bromide as the free radical supplier is the presence of the "heavy atoms", Br and Cl. The effect of their presence has been discussed previously (pg 13).

B. Photosensitizers

A photosensitizer is a molecule which, upon absorption of light of the proper wavelength and energy content, undergoes intersystem crossing to its triplet state, followed by energy transfer to an acceptor by intermolecular collision. Depending upon the conditions desired, the energy acceptor may be a monomer or initiator (photo or thermal) which, following energy transfer, produces free radical intermediates.

The advantage of using a photosensitized system over a photoinitiated system is that it permits a greater selection of candidate molecules, the primary requirement being a T_1 energy level higher than the T_1 level of the initiator selected. The main disadvantage is the introduction of another molecule into the free radical production process. There are now two steps dependent upon diffusion and collision.

The primary photochemical reactions for a photosensitizer in this two-beam system are:

$$PS + h\nu \xrightarrow{Io_1 \epsilon_1} (PS)^*_S \quad \text{(beam 1 absorption to excited singlet)} \qquad (29)$$

$$(PS)^*_S \xrightarrow{k_{ic}} PS + \text{heat (internal conversion)} \qquad (30)$$

$$(PS)^*_S \xrightarrow{k_f} PS + h\nu_F \quad \text{(fluorescence)} \qquad (31)$$

$$(PS)^*_S \xrightarrow{k_{isc}} (PS)^*_T \quad \text{(intersystem crossing)} \qquad (32)$$

$$(PS)^*_T + h\nu \xrightarrow{Io_2\epsilon_2} (PS)^*_{T2} \quad \text{(beam 2 absorption to upper triplet)} \tag{33}$$

$$(PS)^*_T \xrightarrow{k_p} PS + h\nu_p \quad \text{(phosphorescence)} \tag{34}$$

$$(PS)^*_T \xrightarrow{k'_{isc}} PS + \text{heat (intersystem crossing)} \tag{35}$$

$$(PS)^*_T + Q \xrightarrow{k_q} PS \quad \text{(quenching)} \tag{36}$$

$$(PS)^*_{T2} + PI \text{ (photo or thermal initiator)} \xrightarrow{k_t} PS + (PI)^*_T \tag{37}$$

$$(PS)^*_{T2} \xrightarrow{k'_{ic}} (PS)^*_T + \text{heat (internal conversion)} \tag{38}$$

$$(PI)^*_T \xrightarrow{k_r} PI^{\cdot}_1 + PI^{\cdot}_2 \quad \text{(free radical formation)} \tag{39}$$

Using equations 29-39 and the same arguments as for the photoinitiator process yields:

$$[PS]^*_S = [PS]\ (Io_1\epsilon_1)/k_{isc} \tag{40}$$

$$[PS]^*_T = \frac{[PS]\ (Io_1\epsilon_1)}{k_p + k'_{isc} + [Q]k_q + Io_2\epsilon_2} \tag{41}$$

$$[PS]^*_{T2} = \frac{[PS]\ (Io_1\epsilon_1)\ (Io_2\epsilon_2)}{(k_p + k'_{isc} + [Q]k_q + Io_2\epsilon_2)([PI]k_f + k'_{ic})} \tag{42}$$

$$[PI]^*_T = \frac{[PS]\ (Io_1\epsilon_1)\ (Io_2\epsilon_2)\ [PI]\ k_f}{(k_p + k'_{isc} + [Q]k_q + Io_2\epsilon_2)\ ([PI]k_f + k'_{ic})\ k_r} \tag{43}$$

Rate of free radical formation

$$\frac{d[PI^{\cdot}]}{dt} = \frac{[PS]\ (Io_1\epsilon_1)\ (Io_2\epsilon_2)\ [PI]\ k_f}{(k_p + k'_{isc} + [Q]k_q + Io_2\epsilon_2)\ ([PI]\ k_f + k'_{ic})} \tag{44}$$

The effect of k_p, k'_{isc}, k_q, k'_{ic} is again apparent in the rate of free radical formation.

A photosensitizer system does not result in the destruction of the photosensitizer molecule because it is returned to its ground state. A good photosensitizer for this two-beam system should possess the following characteristics.

1. High degree of intersystem crossing (i.e. $\phi_{isc} \simeq 1.0$)
2. T_1 energy level below T_1 level of initiator molecule
3. T_2 energy level above T_1 level of initiator molecule
4. Long triplet lifetime in order to maximize the efficiency of the energy transfer process
5. Strong absorption in region of the spectrum where the initiator does not absorb.
6. Nonreactive with initiator molecule.

The process to be accomplished is shown in Figure 5.

As can be seen in Figure 5, the photosensitizer is excited by beam one and from its S_1 level intersystem crosses to its lowest triplet level T_1. The T_1 intermediate absorbs beam 2 to reach an upper triplet level which then transfers its energy to a ground state initiator molecule. The resulting bond cleavage produces the desired free radical. An initiator should have the following characteristics:

1. Noncompetitive absorption spectrum in the regions of beams 1 and 2
2. T_1 energy level greater than the dissociation energy necessary for radical production
3. T_1 energy level greater than T_1 of the photosensitizer, but less than T_2 of photosensitizer

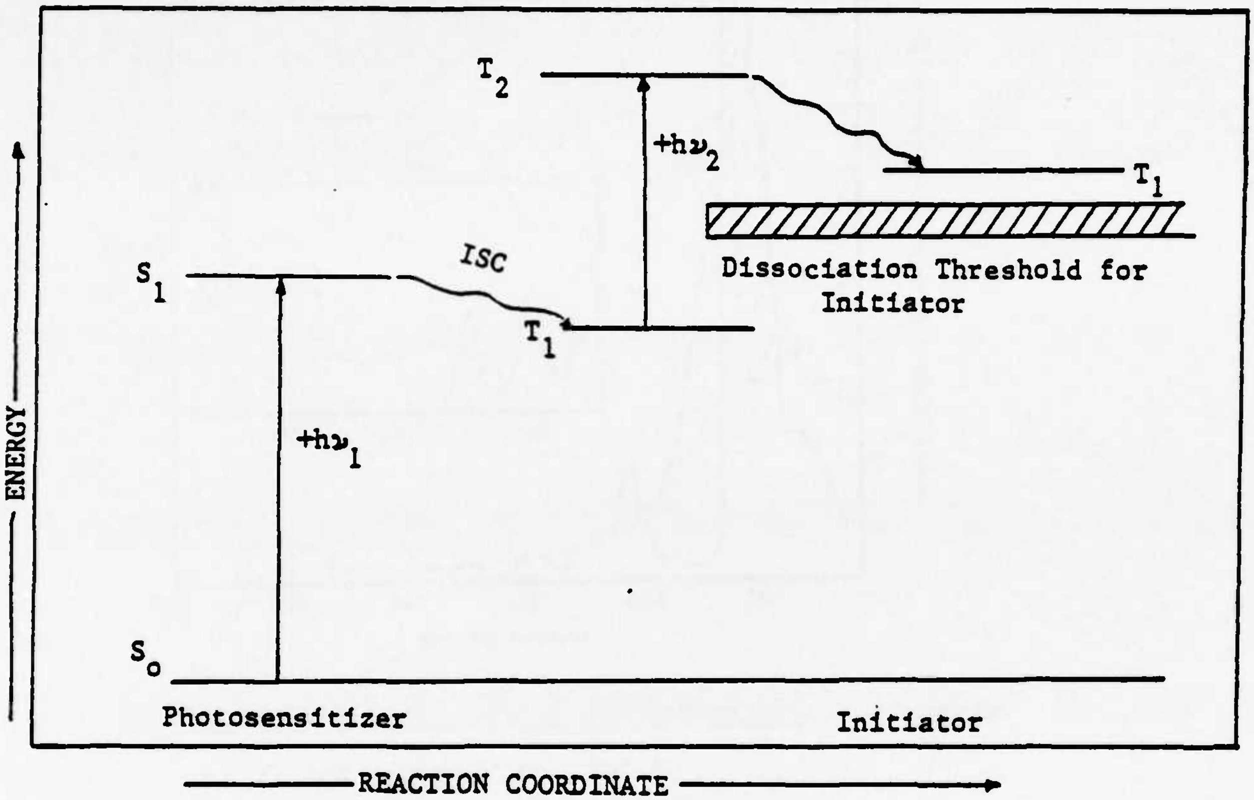

FIGURE 5: GENERAL STRATEGY FOR PHOTOSENSITIZER SYSTEM

It was decided to base a photosensitizer/initiator system on proven initiators. The ones chosen were napthalene sulfonyl chloride (NSC) and chloromethylnapthalene (CMN). The triplet energies for NSC and CMN are approximately 60 kcal/mol.[17] In selecting a photoinitiator molecule, Tetraphenylporphine was selected based on its known singlet and triplet absorption characteristics (see Figure 6). The "window" in the ground state absorption spectrum of TPP at 450-470 nm and the strong triplet absorption in this region make it an excellent candidate. Figure 7 illustrates the TPP+NSC photosensitized system.

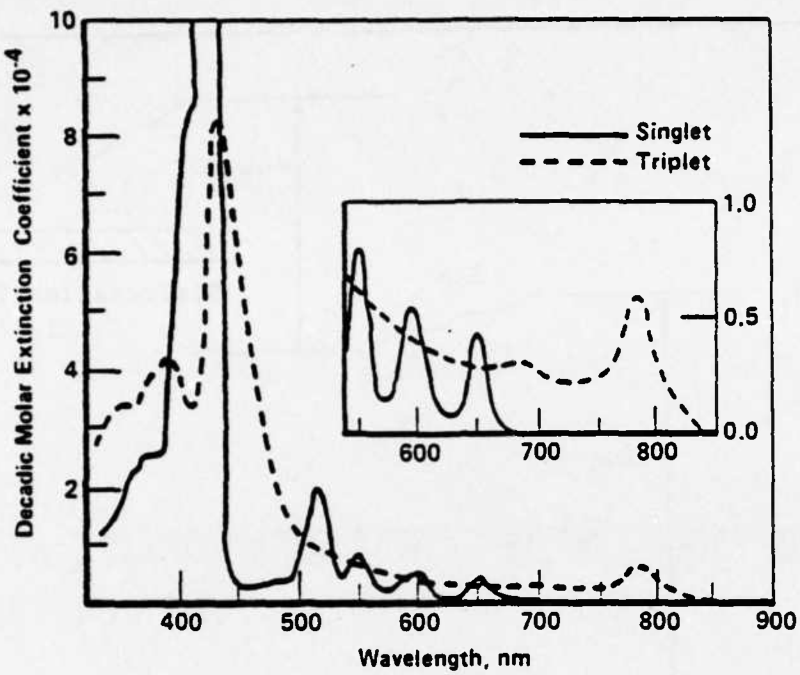

FIGURE 6 : SINGLET-SINGLET AND TRIPLET-TRIPLET ABSORPTION OF MESO-TETRAPHENYL PORPHINE

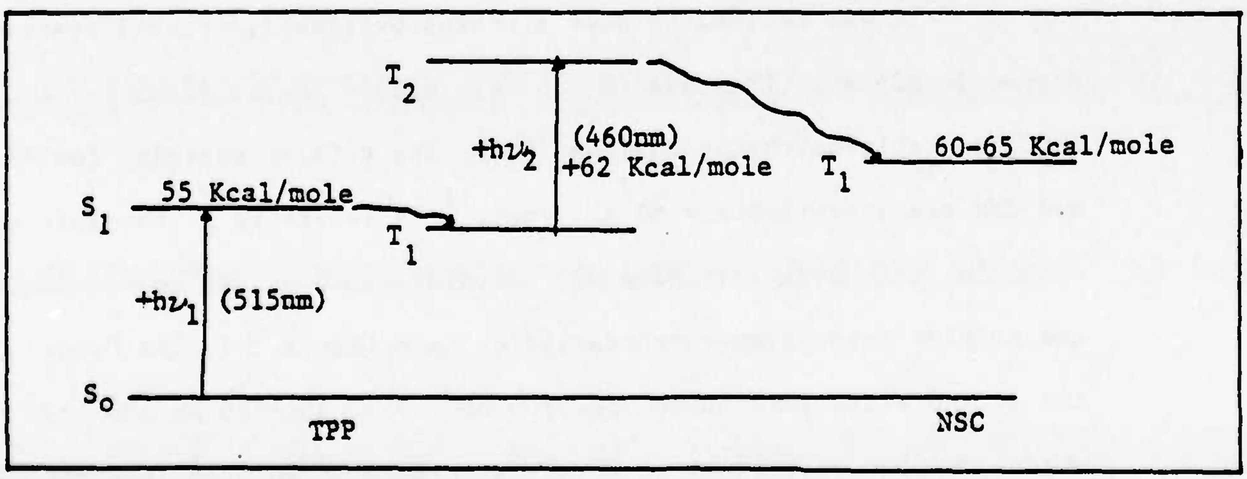

FIGURE 7 : TPP/NSC PHOTOSENSITIZER SYSTEM

C. Free Radical Reactivity

The overall rate of polymerization within a system is determined by the efficiency of radical production coupled with the effect of competitive interactions between free radicals and vinyl monomer. There are a number of factors which may affect the actual fraction of free radicals which may become primary initiators.

1. Certain structures may be incapable of starting kinetic chain growth of a vinyl monomer.
2. The chemical structure of the monomer may determine whether or not a primary radical intermediate undergoes initiation or termination kinetic processes.
3. Free radical intermediate structures may only participate in termination reactions with a growing chain.
4. Solvent factors can also interfere with the polymerization process.

V. EXPERIMENTAL

A. Purpose of Investigation

The purpose of this experimental investigation was twofold:

(1) Identification and characterization of molecules to act as photoinitiators or photosensitizers for two-beam photopolymerization.

(2) Identification of monomers which, when coupled with the photoinitiators or photosensitizers, will achieve the desired polymerization under controlled conditions.

B. Plan of Experimentation

The experimental plan required the synthesis of molecules which had previously been proposed as photoinitiators. Synthesis involved attaching proven groups, known to form free radicals, to parent molecules which had the desired absorption characteristics. Once the syntheses were completed, it became necessary to determine whether the molecules were in fact capable of inducing photopolymerization. If the molecules exhibited the ability to induce photopolymerization, further identification and characterization was pursued. This included molecular weight determination as well as more complete spectral and NMR analysis, to find where the photoactivated groups were located on the molecules. Additional characterization of the photoinitiator candidates included temperature and irradiation stability tests.

Next, a series of irradiation experiments was undertaken using various samples of photoinitiator/monomer and photosensitizer/initiator/monomer. This involved single and double beam irradiations with light sources of varying intensity and selectivity.

Samples were also sent to the Solar Energy Research Institute in Golden, Colorado, for the measurement of triplet-triplet absorption spectra.

C. Materials

The following reagents and solvents were used in the preparation of the photoinitiator compounds and were used as obtained with no further purification.

$C_{36}H_{38}N_4O_4$ - Protoporphyrin IX Dimethyl Ester (PPDME), 95% (Sigma)

$C_{42}H_{28}$ - 5,6,11,12 - Tetraphenylnaphthacene (Rubrene), 97% (Aldrich)

$C_{44}H_{30}N_4$ - Tetraphenylporphine (m-TPP), 97-99%, (Aldrich)

Br_2 - Bromine, 100%, reagent grade (Baker)

$CHSO_3H$ - Chlorosulfonic Acid, 99%, (Aldrich)

$CHCl_3$ - Chloroform, 100%, reagent grade (Baker)

The following chemicals and solvents were used in the analysis and characterization of the photoinitiator molecules.

CH_3OH - Methanol, 99%, distilled in glass, (Burdick & Jackson)

C_2H_5OH - Ethanol, 100%, distilled in glass, (Burdick & Jackson)

CH_3COCH_3 - Acetone, 99.5%, reagent grade, (Baker)

C_6H_6 - Benzene, distilled in glass, (Burdick & Jackson)

C_6H_{12} - Cyclohexane, 100%, distilled in glass, (Burdick & Jackson)

C_7H_9 - Toluene, 99.8%, reagent grade, (Baker)

CH_2Cl_2 - Methylene chloride, 99%, (MCB reagents)

EtOAc - Ethyl acetate, distilled in glass, (Burdick & Jackson)

Petroleum Ether - distilled in glass, (Burdick & Jackson)

$ZnCl_2$ - Zinc chloride, 97%, analytical reagent, (Mallinckrodt)

$MgSO_4$ - Magnesium sulfate, anhydrous powder, reagent grade, (Baker)

$NaHCO_3$ - Sodium bicarbonate, powder, reagent grade, (Baker)

The following chemicals were used as initiators in the photosensitizer systems.

NSC - 1-Napthalenesulfonyl chloride, 97%, (Aldrich)

CMN - 1-Chloromethylnaphthalene, practical, (Eastman Kodak)

The following monomers were used in the photopolymerization experimental study.

TMPTA - Trimethylolpropane triacrylate, 97.9%, (Sartoma, used as received from manufacturer, 100-150 ppm Hydroquinone inhibitor)

MMA - Methyl methacrylate (Aldrich, redistilled)

PS169 - Urethane-acrylic oligomer, 100%, (Polymer Systems Corp.)

1. Monomer Selection

Characteristics. In selecting the monomers to be used in these experimental trials two primary characteristics were of concern.

1) The monomer should crosslink efficiently and relatively rapidly.

2) The polymerization product should be a hard, clear solid.

The most efficient way of converting a liquid reactive monomer system to a solid polymer is through the use of multi-functional vinyl unsaturated monomers that are capable of quickly developing gel or network structures at very low percentages of conversion.[18]

Monomer Candiates. The monomer originally suggested to use in this study was trimethylolpropane triacrylate (TMPTA). As can be seen in Figure 8 the TMPTA molecule contains three vinyl groups which are readily accessible for free radical addition reactions.

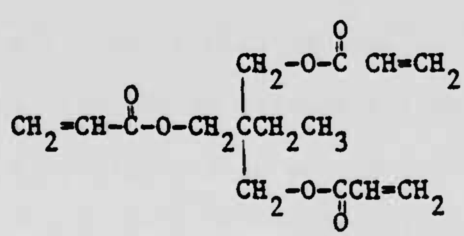

FIGURE 8: TRIMETHYLOLPROPANE TRIACRYLATE MONOMER

Another monomer which had previously been used in two-beam photopolymerization trials was methyl methacrylate (MMA). Figure 9 shows the structure of the MMA molecule. Polymethylmethacrylate is used as an investment material in the casting industry,[19] and is widely used elsewhere as Lucite™ and Plexiglas™.

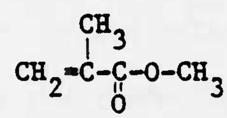

FIGURE 9: METHYLMETHACRYLATE MONOMER

Because of its single vinyl group, the reactivity of MMA is less than for TMPTA, as can be expected. The difference in reactivity between TMPTA and MMA was used to advantage by making solutions of the two monomers to control the rate of polymerization.

A third material employed in this study was PS169, which is a urethane-acrylic oligomer, Figure 10. An exact molecular formula was not available because the R group and a value for n in the formula below are unknown. The n is thought to be in the range of 1,000-3,000, resulting in a monomer with a viscosity of 250,000 cps as compared to TMPTA at 85-92 cps. This monomer was used to increase the mass of polymer formed per cross link event.

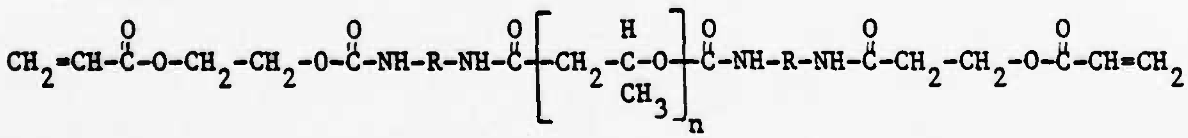

FIGURE 10: PS169

2. Preparation of Photoinitiators

The structures of the parent molecules used for the preparation of the photoinitiators are shown in Figures 11-13.

Preparation of Brominated Protoporphyrin IX Dimethyl Ester: Selective bromination of PPDME was reported by M. Goutermann[20] using the mild brominating agent, pyridinium bromide perbromide. The product, after purification by column chromatography, was stated to be $PPDMEBr_4$ with bromination on the two vinyl side chains.

To achieve maximum bromination of the PPDME molecule, the use of neat Br_2 was attempted. The reasons for maximizing the number of bromines attached to PPDME in this study were twofold: 1) to increase the degree of intersystem crossing ($S_1 \longrightarrow T_1$), by the so-called "heavy atom" effect, and 2) to provide more possible sites for free radical formation. The bromination was accomplished by the dropwise addition of a bromine/chloroform solution to the PPDME dissolved in chloroform. The reaction took place at -20°C. For more complete procedures see Appendix I, page116. After removal of the solvent and unreacted bromine, the product was obtained by scraping the inside of the flask with a metal spatula. The product was a dark iridescent purple solid. Because the number of Br attached to the parent PPDME molecule was unknown, the polybrominated compound was referred to as $PPDMEBr_X$.

Goutermann's[20] preparation of $PPMEBr_4$ included a step where the initial reaction product was purified by column chromatography to yield the $PPDMEBr_4$. This same procedure was used in this study to

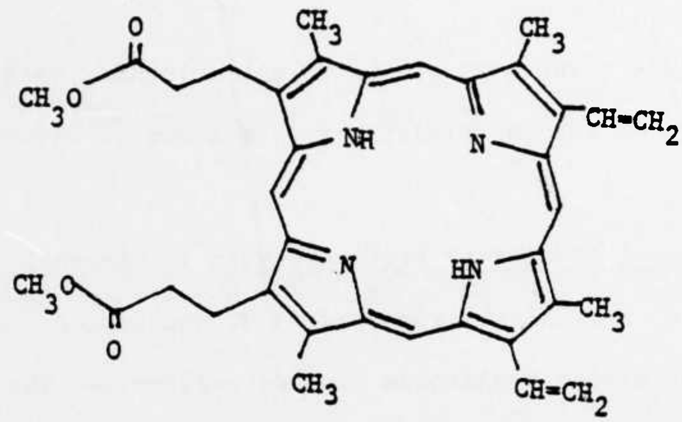

FIGURE 11: PROTOPORPHYRIN IX DIMETHYL ESTER (PPDME)

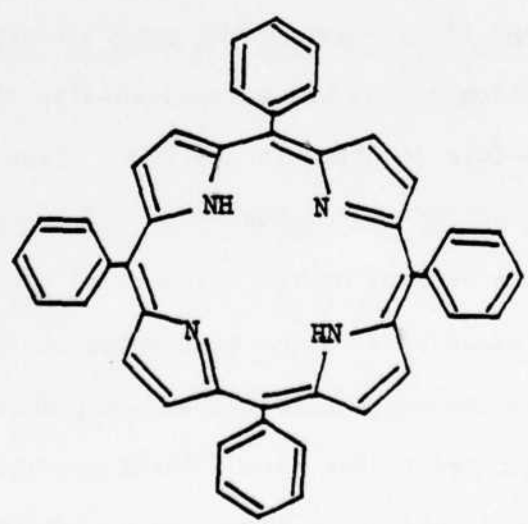

FIGURE 12: m-TETRAPHENYLPORPHINE (m-TPP)

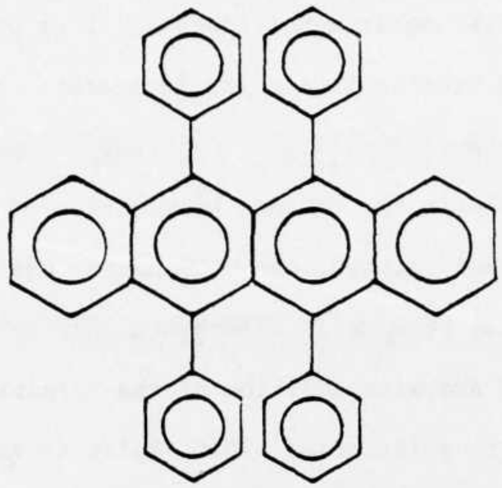

FIGURE 13: 5,6,11,12 - TETRAPHENYL-TETRACENE (RUBRENE)

obtain $PPDMEBr_4$. Using either a silica gel or alumina column, $PPDMEBr_X$ was dissolved in a minimal amount of $CHCl_3$. This was placed on top of the column and was eluted with $CHCl_3$. A number of different bands appeared on the column, but when they were collected they all had the same visible spectra. The solvent was evaporated, and the final product was a very viscous dark substance, $PPDMEBr_4$.

Elemental analysis and spectroscopic data for this and the other compounds prepared are presented in a later section of this thesis.

Preparation of Brominated meso-Tetraphenylporphin: The bromination of m-TPP has been reported by Samuels, et al.[21] Using a solution of m-TPP in $CHCl_3$ and N-bromosuccinimide they obtained a monobromotetraphenylporphin. By doubling the amount of N-bromosuccinimide, the product obtained was dibromotetraphenylporphin. They used a different procedure, and bromine in a chloroform-acetic acid solution to produce tribromotetraphenylporphin.

To obtain the maximum bromination of the m-TPP, for the reasons previously stated, the bromination was carried out using a solution of neat bromine in chloroform. The bromination was accomplished by the dropwise addition of the bromine solution to an m-TPP/chloroform solution at -20°C. Refer to Appendix A.1, page 118 for the complete procedure. The bromination product was a purple solid. Because the number of Br attached to the parent TPP molecule was unknown, the polybrominated compound was referred to as $TPPBr_X$.

Samuels, et al[21] included a chromotographic step in their preparation of $TPPBr_3$. Using this procedure and the $TPPBr_X$ product dissolved in a minimal amount of $CHCl_3$, the sample was chromatographed on alumina. After the $CHCl_3$ was evaporated from the collected solution, the product remaining was a purple solid, $TPPBr_3$. (See Table 8 for visible absorption data.)

Preparation of Chlorosulfonated Tetraphenylporphin: Chlorosulfonation of m-TPP consisted of the dropwise addition of a solution of m-TPP in methylene chloride to chlorosulfonic acid in a reaction flask. The addition was done at a reduced temperature of -20°C. See Appendix A.1, page 119, for the complete procedure. The final product was a purple solid. Because of the extremely low product yield, this procedure was not acceptable.

A second more involved synthesis procedure was performed by Dr. Jerry Jenkins of Otterbein College. The product was highly hygroscopic and could not be isolated in a solid form. It was maintained in a solution of methylene chloride over anhydrous $MgSO_4$. No further work was done on the chlorosulfonation of m-TPP and it was eliminated as a photoinitiator candidate.

Preparation of Chlorosulfonated Rubrene: The chlorosulfonated rubrene used in this study was prepared by Dr. Jenkins. The preparation involved the addition of chlorosulfonic acid to a solution of rubrene in methylene chloride at a reduced temperature of 0°C. The procedure can be found in Appendix A.1, page 118, and is included as a reference for the chlorosulfonation of m-TPP. The product was a light yellow powder, $Ru(SO_2Cl)_6$. The addition of six SO_2Cl groups to the rubrene parent molecule was substantiated through an elemental microanalysis performed on samples sent to the Galbraith Laboratories, Inc., of Knoxville, Tennessee. The results are presented in Table 1.

Table 1

Elemental Analysis of Ru $(SO_2Cl)_6$
(Hexachlorosulfonated Rubrene)

Element	Analysis (%)[1]	Calc. % for $Ru(So_2Cl)_6$
C	44.88	44.88
H	2.44	1.98
S	17.14	17.11
Cl	18.72	18.95
O	(16.82)[2]	(17.08)[2]
Total %	100.00	100.00

1) values represent an average of duplicate analyses
2) values obtained by difference

D. Apparatus

To obtain light beams of a specific wavelength content, various light sources and control systems were used. These are schematically illustrated in Figures 14 to 17. Different combinations of these systems were also used, i.e., xenon arc lamp with monochromator or laser.

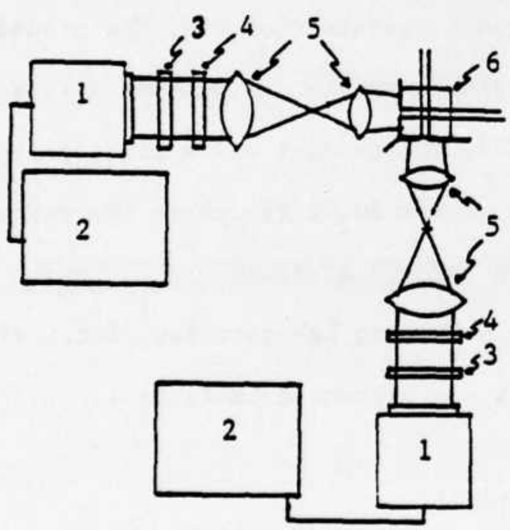

1 Xenon arc lamp
2 Power supply
3 UV cut off filter
4 Sharp cut filter
5 Lens
6 Sample cell with foil mask

FIGURE 14: XENON ARC LAMP IRRADIATION CONFIGURATION

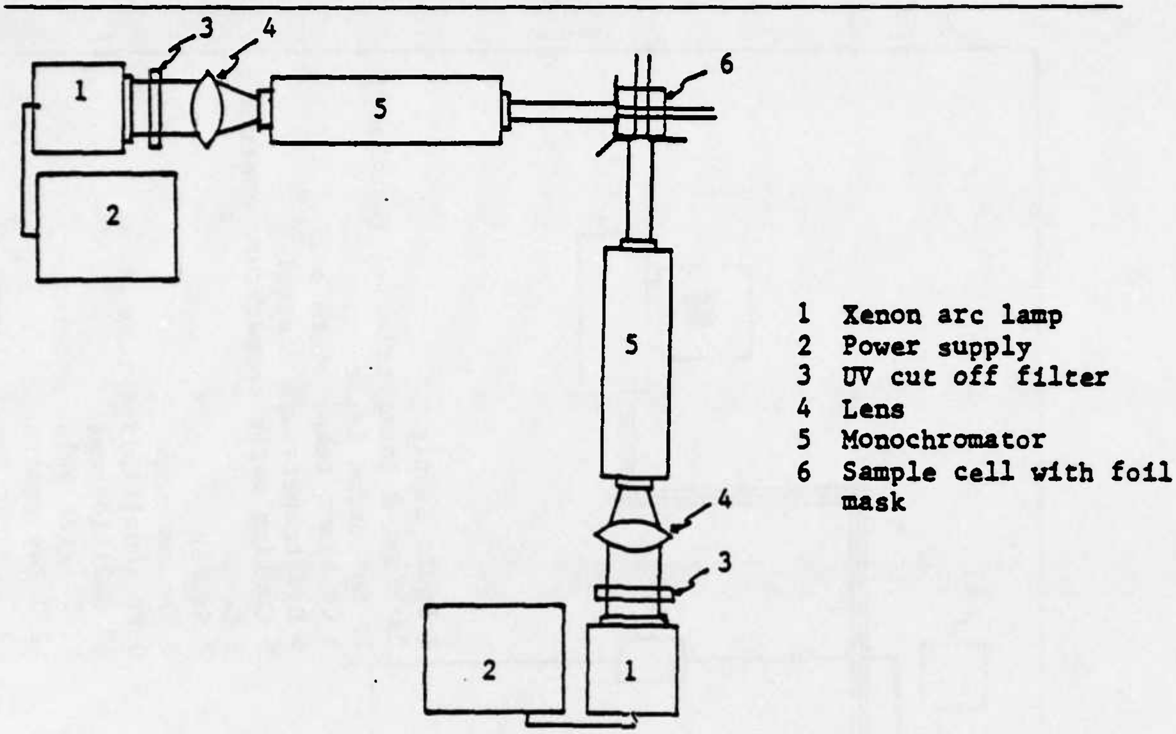

FIGURE 15: MONOCHROMATOR IRRADIATION CONFIGURATION

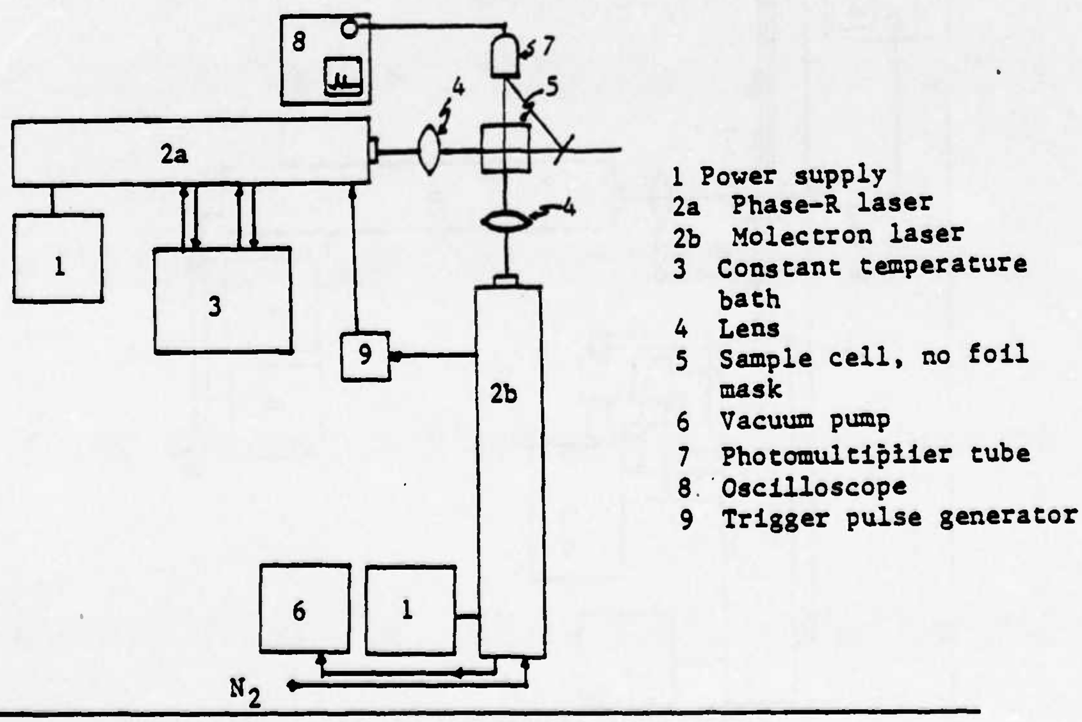

FIGURE 16: LASER IRRADIATION CONFIGURATION

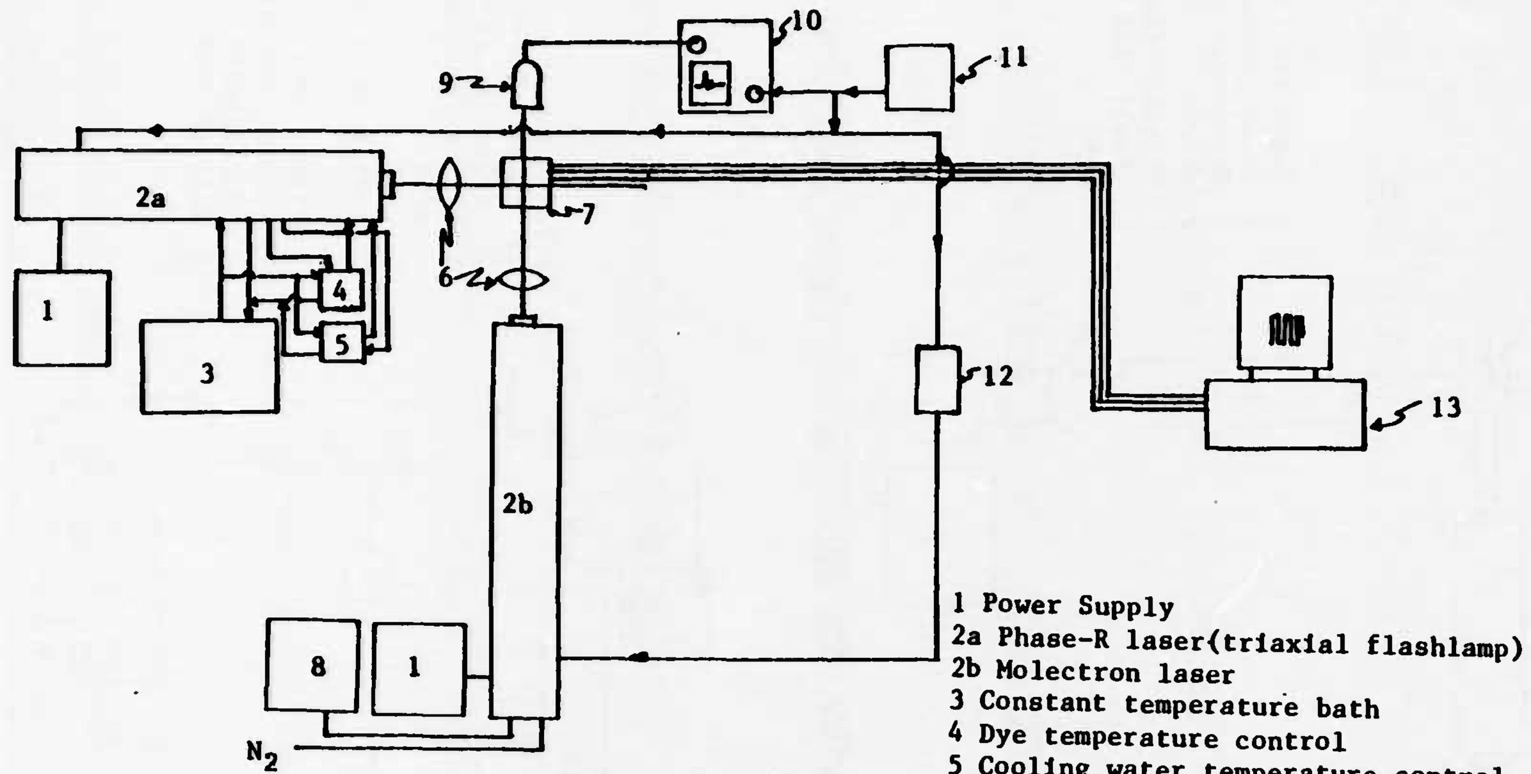

1 Power Supply
2a Phase-R laser(triaxial flashlamp)
2b Molectron laser
3 Constant temperature bath
4 Dye temperature control
5 Cooling water temperature control
6 Lens
7 Sample
8 Vacuum pump
9 Photomultiplier tube
10 Oscilloscope
11 Trigger pulse generator
12 Delay generator
13 Computer for 3-dimensional translational control of sample

FIGURE 17: LASER IRRADIATION CONFIGURATION

Light Sources: The light sources used for the lamp irradiations were Eimac high pressure, short-arc, 150 watt xenon illuminators, Models R-150-2 and R-150-8. Beam intensity was controlled using Eimac power supplies P250S-1 and P5150-8 respectively. These illuminators are capable of 18 watts of radiation, 6 watts of which is in the visible range, 400nm-800nm.

Filters: To control the light energy of the radiated beams, 2" x 2" glass filters were used in series. The filters were manufactured by Corning Glass Works or Melles Griot. Combinations of ultraviolet cut off and sharp cut visible and infrared transmitting filters were generally used. Selection of the filters to be used was based on the absorption spectrum of the molecule to be irradiated.

Monochromators: More specific beam control was obtained by using a Xenon arc lamp and monochromator in line with the UV cut off filter. The monochromators used were manufactured by Instruments SA, Inc. and Bausch & Lomb.

Lasers: Two different lasers were used, a Phase-R DL-1200V dye laser and Molectron DL-II nitrogen pulsed tunable dye laser. The Phase-R was initially used with a coaxial flashlamp and later was operated with a triaxial flashlamp. The triaxial flashlamp permitted much better dye temperature control which increased the power output of the laser and the dye lifetime. The laser pulse rates were controlled by an external trigger. Beam 2 was pulsed approximately .5 μ sec after beam 1.

E. Experimental Procedures

Sample Preparation: At the start of the project all photoinitiator/monomer solutions were prepared by dissolving the photoinitiator directly in the monomer. Because of the relative insolubility of the photoinitiators or photosensitizers in the monomer solution, it was impossible to know the actual compositions of the solutions obtained. To solve this problem, the photoinitiators or photosensitizers were initially dissolved in a minimal amount of chloroform. Aliquots of this solution were then added to the monomer and mixing was accomplished by bubbling an argon stream through the solution. Using this method, it was possible to obtain solutions of known weight percent compositions of photoinitiator or photosensitizer. In solutions of the photoinitiators $PPDMEBr_X$ and $TPPBr_X$, molar concentrations could not be obtained because of the inconclusive molecular weight results of the elemental analysis. The use of photosensitizers of known molecular weights, however, permitted the calculation of molar concentrations.

Another factor which was considered in solution preparation was the desire to have the sample solution absorption in the range of .3-.5 at the wavelengths used for beam 1 excitation. This was done to ensure that the strength of the beam would be ample throughout the beam path in the sample solution to create a significant singlet and hence triplet population. For the sample sizes used in this study approximately .1-.2 mg of photoinitiator or photosensitizer were dissolved in approximately 3.0 g of monomer. After dissolving the photoinitiator or photosensitizer in the monomer, the sample solution was degassed.

The purpose of the degassing operation was to eliminate dissolved O_2 in the sample and consequently minimize quenching. Three different degassing procedures were tried before a system which gave consistent results was found.

The first procedure consisted of bubbling a stream of argon through the sample. A pipet was placed into the sample cell with the outlet close to the bottom. Argon was introduced through tygon tubing connecting the pipet and control valve on a gas tank. Bubbling was allowed to occur at a rather vigorous rate, 3-4 bubbles/sec. A foil cap or "tent" was placed over the top of the cell to keep out particulate contaminates in the air. At the end of the degassing period, usually 30 minutes, the pipet was slowly removed while continuing to purge with argon. When the pipet was completely removed, the cell was immediately sealed with a teflon plug and teflon tape. Prior to irradiation or spectrometric analysis the sample was allowed to stand for 10 minutes to get rid of bubbles suspended in the sample solution.

The second degassing procedure involved the removal of dissolved O_2 through repeated freezing (liquid N_2) and thawing cycles. This was accomplished using a roughing vacuum pump and diffusion vacuum pump apparatus. Briefly, the steps of this procedure were: 1) freezing the sample, 2) evacuating the sample flask, 3) isolating the sample from the vacuum line with a stopcock and 4) thawing the sample to permit the dissolved gases to diffuse from the sample into the evacuated space above the sample.

After four cycles the final vacuum was broken with argon gas. The sample flask was capped and removed to an argon atmosphere where the sample solution was transferred, under a stream of argon, to a square pyrex irradiation cell. The cell was immediately sealed with a teflon plug and teflon tape. Sample irradiations after this degassing procedure continued to give inconsistent results.

The third degassing procedure followed the same freeze/thaw operation previously described. The sample flask used for the degassing was designed to permit irradiation of the sample without transferring the solution to a separate irradiation cell (see Figure 18). This method made it possible to keep the sample under vacuum during irradiations and gave reproducible results.

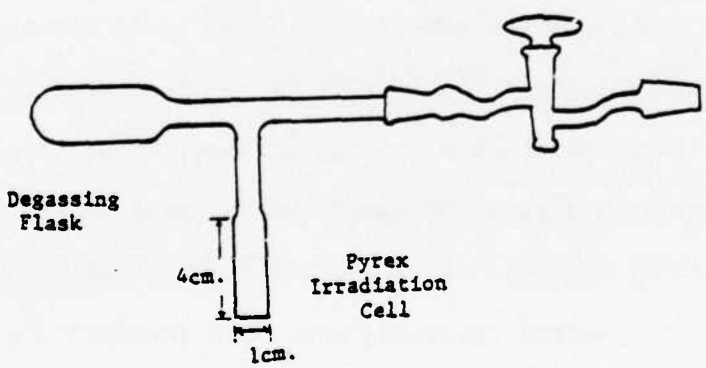

FIGURE 18: SAMPLE SOLUTION DEGASSING APPARATUS

VI. THEORETICAL CALCULATIONS

To better understand what is occurring from the photon absorption to polymerization steps in this process it is best to consider a simplified example. The concentrations, absorption intensities, and irradiation conditions are taken from experimental irradiation trials.

The physical arrangement during the irradiation is illustrated in fig. 19. The windows in the sample cell are .25cm on a side and the incident beams are approximately 1cm. in diameter. Therefore the beams within the photoinitiator/monomer solution are .25cm square and their intersection forms a volume of .0156 cm^3. This is the volume of interest. The calculations will be based on a photoinitiator molecular formula of $TPPBr_6$ (M.W.=1048).

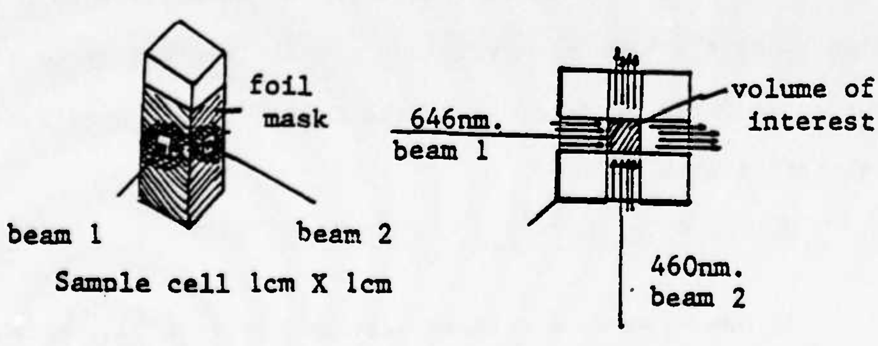

FIGURE 19: SAMPLE CELL IRRADIATION SCHEME

The sample solution is comprised of .12 mg (1.2×10^{-4} mmole) a photoinitiator (PI) in 3 ml of monomer for a 4.0×10^{-5} M solution. To calculate the number of PI molecules in the irradiated volume is a matter of multiplying molar concentration, irradiated volume and Avogadro's number to give 6.1×10^{14} PI molecules.

To calculate the number of photons in the incident beams 1 and 2 it is necessary to have power measurements of the beams. These are generally measured in watts or volts and then are converted to photons/sec. (eq. 6, Appendix II). For this example, the incident photon rates are:

beam 1 (646nm) = 2.11×10^{16} photons/sec

beam 2 (460nm) = 1.51×10^{16} photons/sec

The number of photons actually entering the intersection volume is dependent on the absorption spectrum of the sample as recorded on the CARY 17DX. Equation 1 is used for this calculation. For

$$A = \epsilon c l \qquad (1)$$

a given system ϵc is constant, therefore the absorption at a specific location along the beam path within the cell is given by eq. 45. The absorption at 646nm as recorded on the CARY 17DX was 0.59 for an optical path length of 1 cm.

$$A_2 = \frac{A_1 l_2}{l_1} \qquad (45)$$

If one assumes a triplet quantum yield of 90%, which is realistic for the molecules we are considering, this gives a total triplet population of 2.88×10^{15} triplets/sec. This is the population of molecules which is subject to irradiation by beam 2.

Ideally beam 2 is absorbed only by the triplets formed within the intersection volume. For these calculations that will be assumed to be the case. An absorption of .10 by T_1 over the .25 cm path length gives 2.9×10^{14} photons absorbed per second which will cause an equal number of bond cleavages and twice that number, 5.8×10^{14}, free radicals per second. The number of propagation or polymerization steps which occur as a result of the free radical formation is not known and is dependent upon the competitive routes present within the photo-initiator/monomer solution as well as the rate of collision between the free radical and monomer.

The use of a photosensitizer, initiator and monomer system introduces additional competitive routes in the process of free radical production. The controlling step in this system will be the rate of transfer of energy from photosensitizer T_2 to initiator T_1. In a three-part system it is important to have a considerable excess of initiator molecules to photosensitizer molecules to facilitate the transfer of triplet energy.

The use of lasers as light energy sources in this 2-photon system brings with it some additional considerations and expectations. In comparison to using two continuous beam sources as was done in the example presented above, the use of pulsed lasers greatly increases the power input to the reaction solution and thereby increases the total number of triplets formed in a given period of time. To efficiently make use of this increased triplet yield, the two lasers must be synchronized, so that the second laser fires within the triplet lifetime, which is typically in the microsecond range, see Figure 20. Goutermann and Khalil[20] reported triplet lifetimes of 4.6±1, 4.5 and 6.6±1 microseconds for PPDME, $PPDMEBr_4$ and TPP respectively.

Some typical pulse characteristics of the Phase-R DL 1200V and Molectron UV24-0L14 lasers used in this study are presented in Table 2.

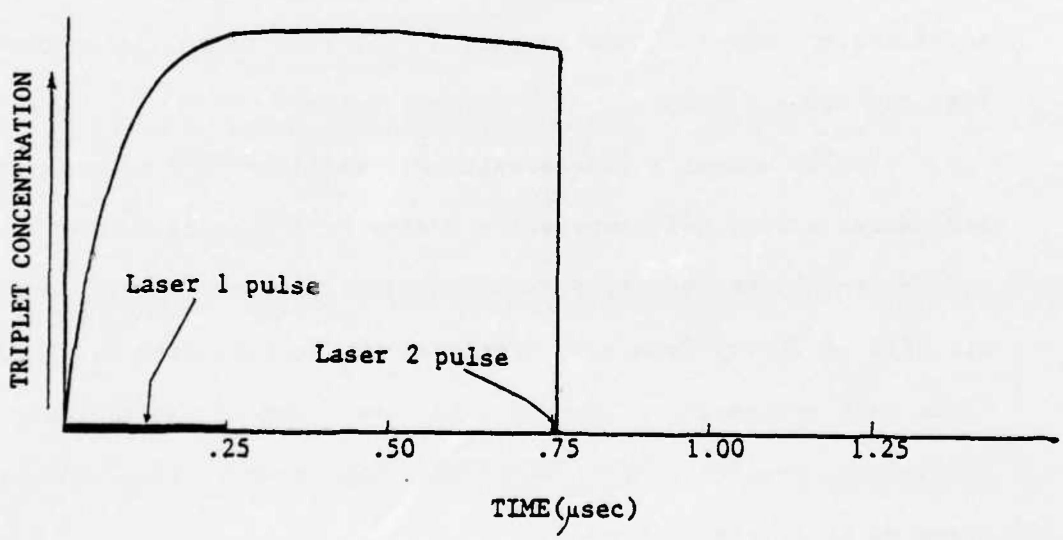

FIGURE 20: TRIPLET CONCENTRATION VS LASER PULSE TIMING

For the Phase-R DL 1200V with the triaxial flashlamp the pulse energy is dependent upon many variables; 1) dye lifetime, 2) dye temperature, 3) cooling water temperature, 4) pulse rate, and 5) flow rate through the flashlamp. Problems encountered in optimizing all these variables makes it difficult to maximize the pulse energy output. The Molectron UV24-OL14 pulse energy is mainly controlled through dye lifetime and internal alignment adjustments.

The area of the beam and the optical path length at the intersection point are controlled by the beam focus. Ideally both of the beams focus at the point of intersection to maximize the energy entering that spot.

TABLE 2: Laser Pulse Characteristics

	Phase-R DL1200V (R6G dye)	Molectron UV24-OL14 (Molectron dye #8)
Pulse Energy	112uJ	75uJ
Area of Beam	$5x10^{-2}cm^2$	$5.0x10^{-3}cm^2$
Time of Pulse	250ns	8ns
Repetition Rate (Pulses per Second)	1.0-2.0	1.0-2.0
Wave length selected	584nm (max.)	460nm
Band width (no grating) (with grating)	570nm-618nm ±2nm	±0.1nm
Optical Path length at Intersection Point	0.07cm	0.25cm

VII. CHARACTERIZATION OF PHOTOINITIATORS & PHOTOSENSITIZERS

Characterization of the photoinitiator molecule candidates involved a number of steps. They were performed as follows:

1. Observable physical characteristics
2. Spectral analysis - VIS spectrum
3. Solubility and recrystallization
4. Temperature stability
5. Irradiation stability
6. Elemental analysis

A. Physical Characteristics

The physical characteristics of the photoinitiator candidates and parent molecules are presented in Table 3.

TABLE 3: Physical Characteristics

	Color	Form
$TPPBr_X$	purple green (recrystallized)	iridescent crystals powder-like solid
$TPPBr_3$	purple	powder-like solid
$PPDMEBr_X$	purple	iridescent crystals
$PPDMEBr_4$	purplish	viscous material
$Ru(SO_2Cl)_6$	pale yellow	powder-like solid
TPP	purple	solid
PPDME	purple	solid

B. Elemental Analysis

An elemental quantitative microanalysis of the products $PPDMEBr_X$ and $TPPBr_x$ was performed by Galbraith Laboratories, Inc. The other two photoinitiator candidates, $PPDMEBr_4$ and $TPPBr_3$, were not analyzed because of the close agreement of their absorption spectra with values reported in the literature. Two separate sets of samples of $PPDMEBr_X$ and $TPPBr_X$ were analyzed. The second sample set differed from the first set in that 1) the second set had been washed with benzene to remove any $PPDMEBr_4$ or $TPPBr_3$ which possibly was present in their respective samples and 2) the samples were dried overnight in a vacuum descicator prior to being sealed in glass vials and shipped.

The results of the $PPDMEBr_X$ elemental analyses are presented in Table 4. For comparison, Table 5 contains some calculated elemental percentage values for proposed molecular formulas. Assuming that the second analysis is the more accurate of the two, because of the additional sample preparation steps, the results indicate a value for X in $PPDMEBr_X$ in the range of 6 to 7. The inconsistencies between the analyzed and calculated element percentage values is possibly the result of a mixture of brominated products in the samples analyzed.

The results of the $TPPBr_X$ elemental analyses are presented in Table 6. Table 7 contains some calculated elemental percentage values for proposed molecular formulas. Again, assuming that the additional preparation steps of sample two resulted in a purer sample, the results indicate a value of X very close to 7. Agreement between the elements C,H,N is quite good, so the major discrepancy is in the Br analysis. It

Table 4

Elemental Analysis of $PPDMEBr_x$
(Brominated Protoporphyrin 1X Dimethyl Ester)

Element	Analysis 1 (%)[1]	Analysis 2 (%)[1]
C	34.78	38.02
H	3.48	5.61
N	4.23	4.45
Br	46.40	47.76
O	(11.11)[2]	(4.17)[2]
Total %	100.00	100.00

1) values represent an average of duplicate analyses
2) value obtained by difference

Table 5

Calculated Elemental % Values for Selected
X Values in $PPDMEBr_X$

	Calculate % Value for X =		
Element	6	7	8
C	39.60	36.90	34.55
H	3.50	3.20	3.04
N	5.10	4.78	4.48
Br	44.00	47.85	51.18
O	5.90	5.47	5.12

Table 6
Elemental Analysis of $TPPBr_X$
(Brominated m-Tetraphenylporphine))

Element	Analysis 1 (%)[1]	Analysis 2 (%)[1]
C	47.46	44.85
H	2.94	2.91
N	4.71	4.57
Br	33.76	43.15
Total %	88.87	95.47

1) values represent an average of duplicate analyses

Table 7

Calculated Elemental % Values for Selected
X Values in $TPPBr_X$

	Calculated % Value for X =			
Element	4	5	6	7
C	56.49	52.03	48.23	44.90
H	3.21	2.96	2.74	2.60
N	5.99	5.52	5.12	4.80
Br	34.23	39.42	43.85	47.70

is probable that the $TPPBr_X$ analyzed contains a mixture of brominated products and isomers.

Proton NMR and ^{13}C NMR

Attempts to further describe the molecular structures of the $PPDMEBr_X$, $PPDMEBr_4$, $TPPBr_X$ and $TPPBr_3$ molecules included NMR analysis. These analyses were performed by personnel at the University's Johnston Laboratory. The proton NMR were run on a Nicolet 300 MHz instrument and the ^{13}C NMR were run on a Nicolet 500 MHz instrument. Interpretation of the spectra obtained from these analyses was inconclusive, since the highly complex spectra indicated the presence of a mixture of brominated compounds in all the brominated products.

It should be noted that knowledge of the location of the bromines on the $PPDMEBr_X$, $PPDMEBr_4$, $TPPBr_X$ and $TPPBr_3$ molecules as well as the number of bromines on the $PPDMEBr_X$ and $TPPBr_X$ molecules is not essential for this study. More important are the spectral characteristics of the molecules and their photochemical behavior upon irradiation.

C. Spectral Analysis

Absorption spectra were taken on a CARY 17DX recording spectrophotometer in the visible region at room temperature. The samples were dissolved in $CHCl_3$ and were scanned at 2nm/second versus a reference cell of $CHCl_3$ (see Figures 21 to 28). The cells used were matched 10mm quartz cells. The peak absorption wavelengths in nanometers and their relative intensities are recorded in Table 8. Literature values are included for comparison, when available.

TABLE 8: Visible (VIS) Absorption Spectra for Photoinitiators and Parent Compounds

Compound	Wavelength (Relative intensity)				
PPDME	420 (12.5)	506 (1.0)	541 (.77)	578 (.44)	632 (.37)
$PPDMEBr_X$	423 (5.8)	568 (1.0)	585 (.46)(s)	609 (.40)	
$PPDMEBr_4$	403 (11.9)	505 (1.0)	540 (.70)	574 (.45)	627 (.29)
(ref. 17)		502 (1.0)	534 (.79)	573 (.43)	627 (.29)
m-TPP	420 (31.9)	515 (1.0)	549 (.48)	589 (.35)	646 (.29)
$TPPBr_X$	421 (3.83)	454 (5.44)	522(s)	672 (1.0)	
$TPPBr_3$	420 (17.2)	522 (1.0)	595 (.27)	662 (.29)	
(ref. 20)	429 (1.3)	526 (1.0)	601 (.89)	662 (.94)	
Rubrene	430(s)	458 (.53)	487 (.96)	522 (1.0)	
$Ru(SO_2Cl)_6$	355 (1.35)	413 (1.0)	440(s)		

1. (s) denotes a shoulder

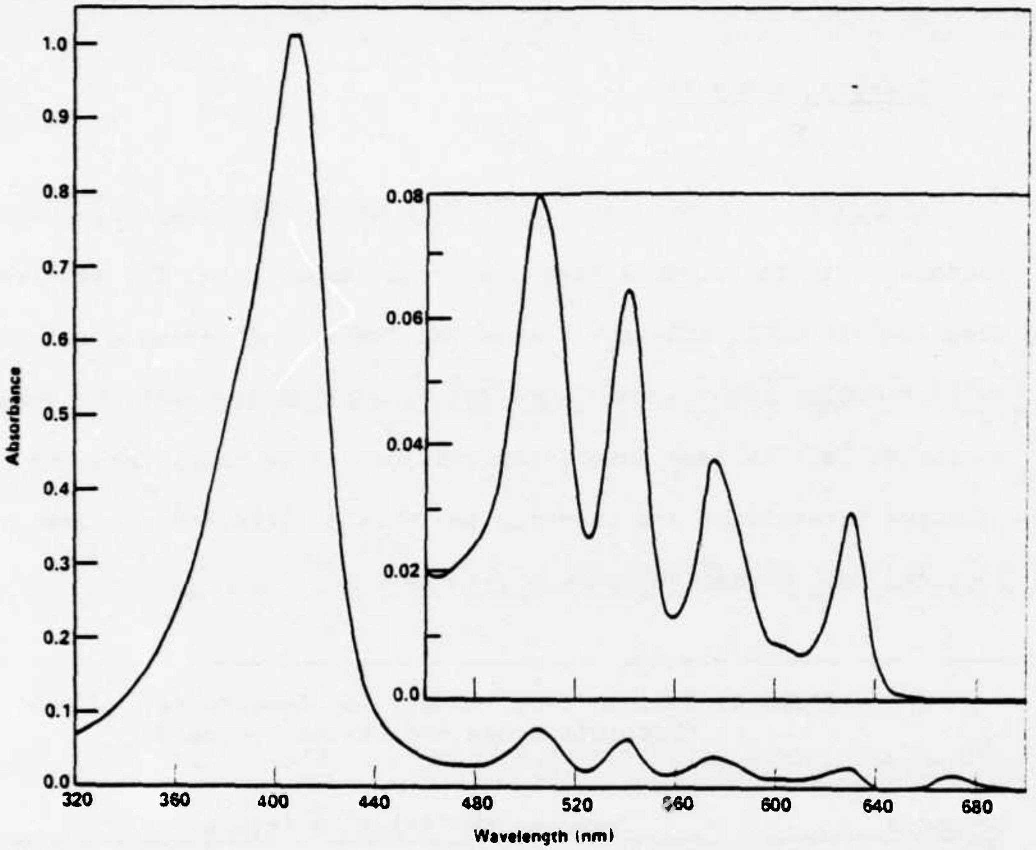

FIGURE 21: VISIBLE SPECTRUM OF PROTOPORPHYRIN IX DIMETHYL ESTER, PPDME

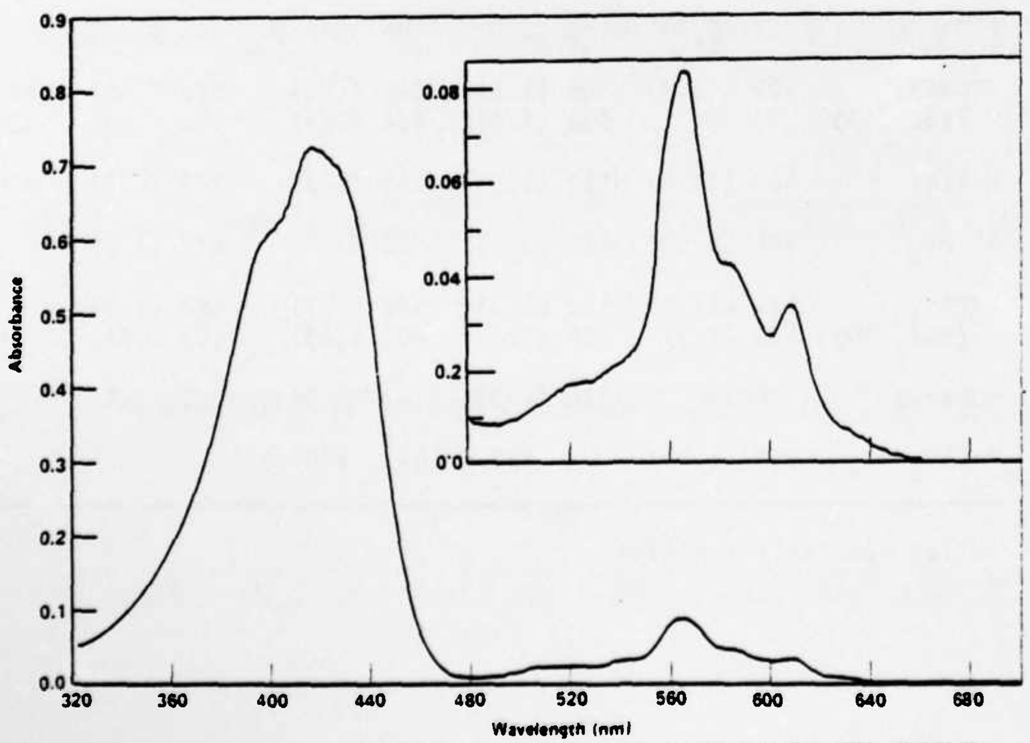

FIGURE 22: VISIBLE SPECTRUM OF POLYBROMINATED PPDME

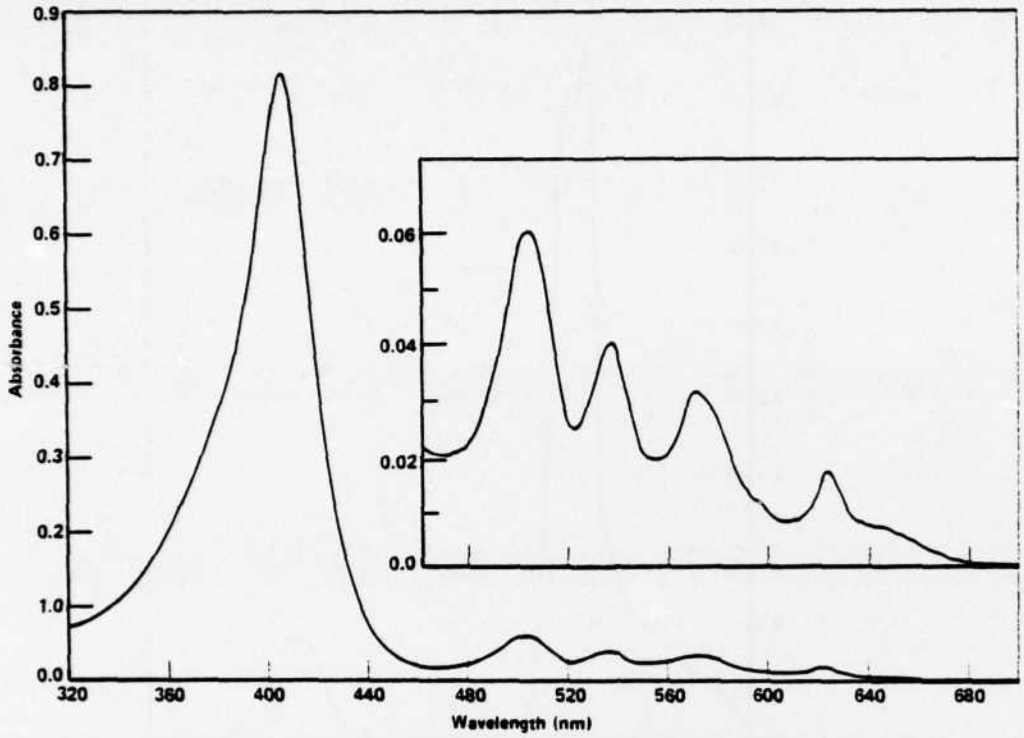

FIGURE 23: VISIBLE SPECTRUM OF TETRABROMINATED PPDME

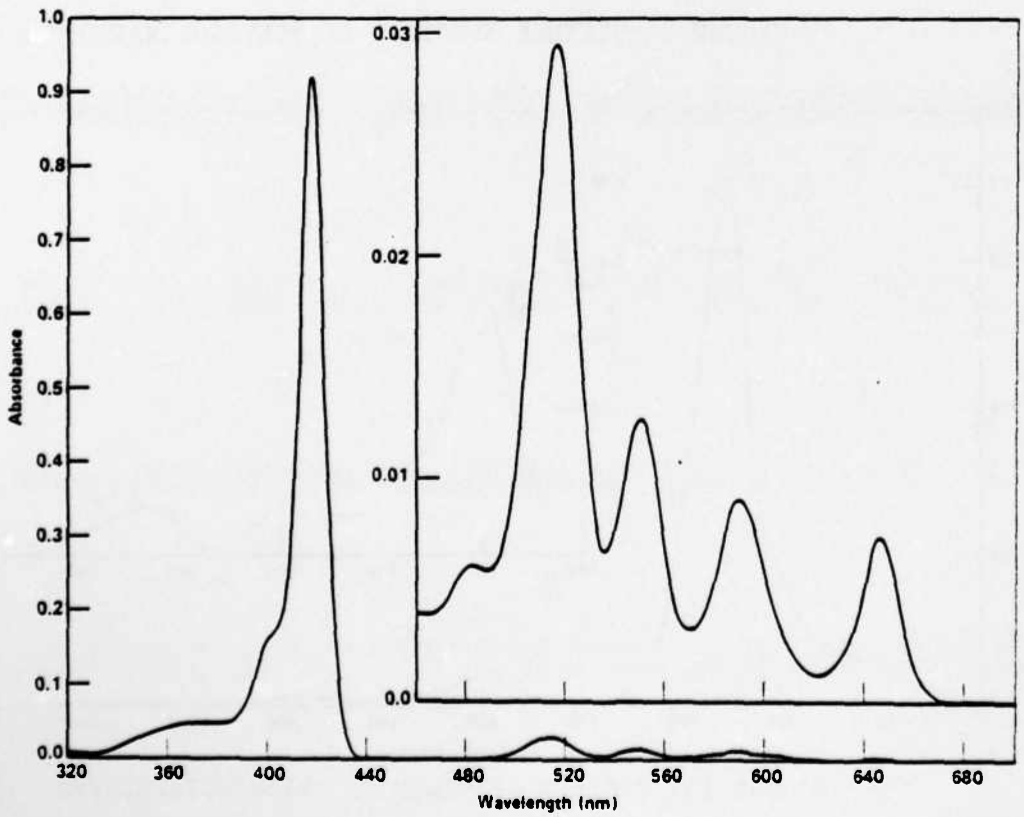

FIGURE 24: VISIBLE SPECTRUM OF MESO-TETRAPHENYL PORPHINE,TPP

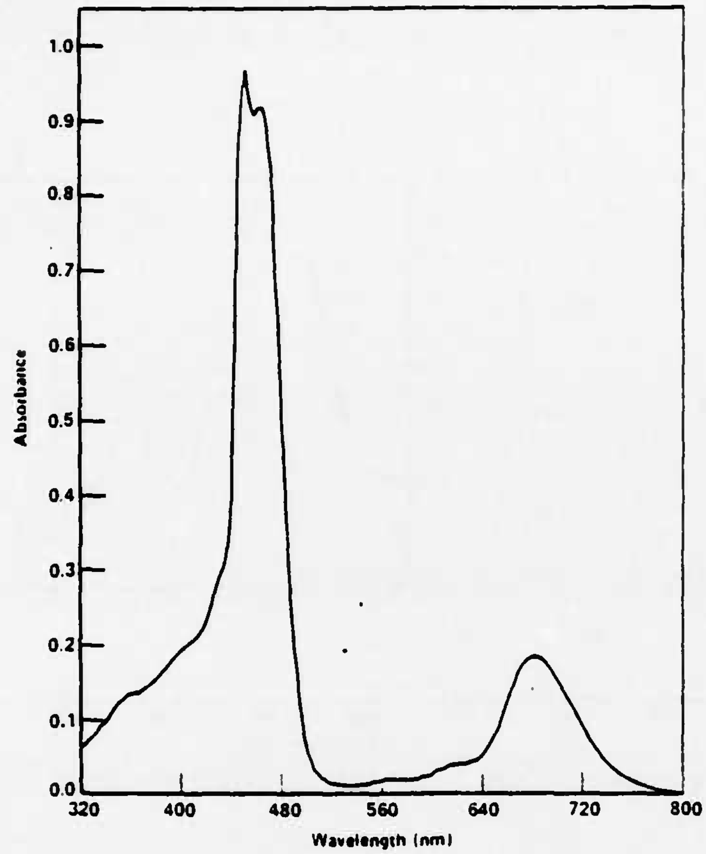

FIGURE 25:VISIBLE SPECTRUM OF POLYBROMINATED TPP

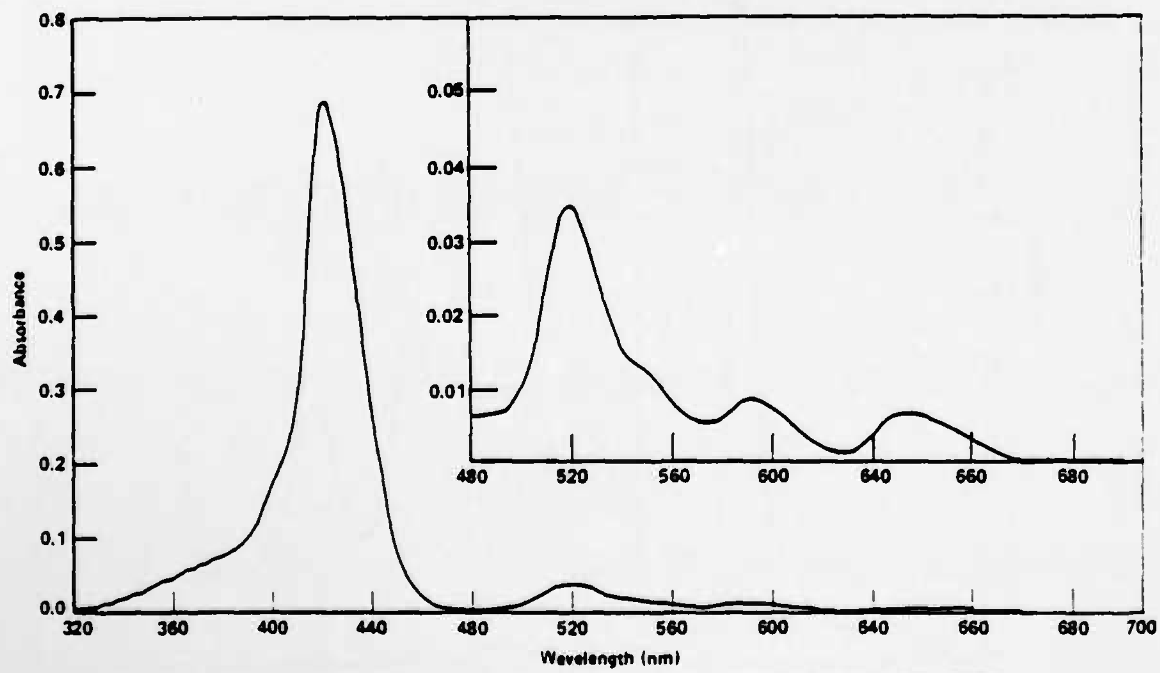

FIGURE 26: VISIBLE SPECTRUM OF TRIBROMINATED TPP

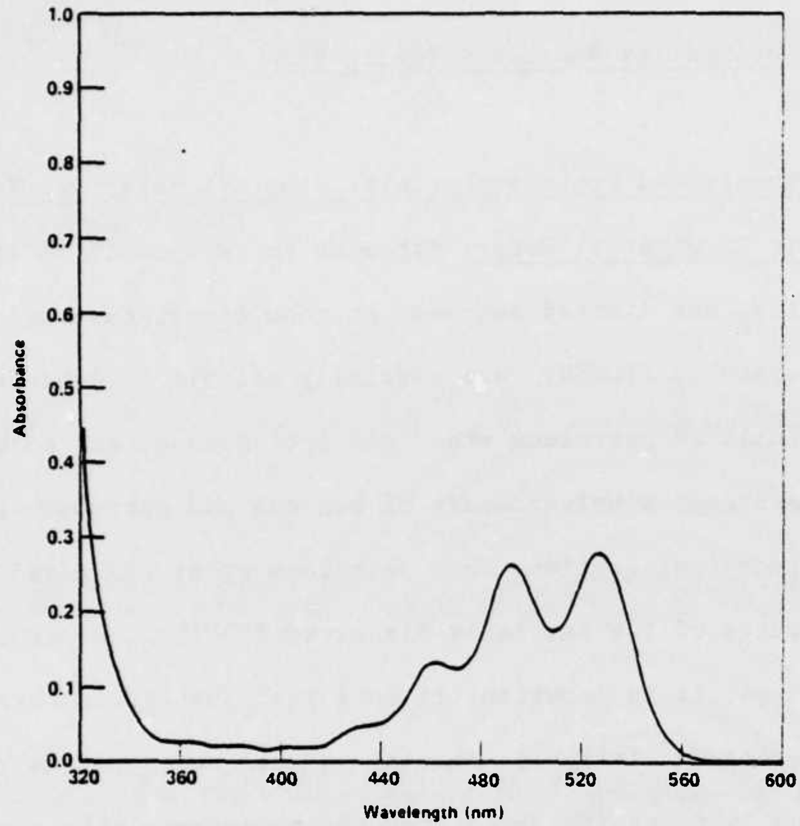

FIGURE 27: VISIBLE SPECTRUM OF RUBRENE

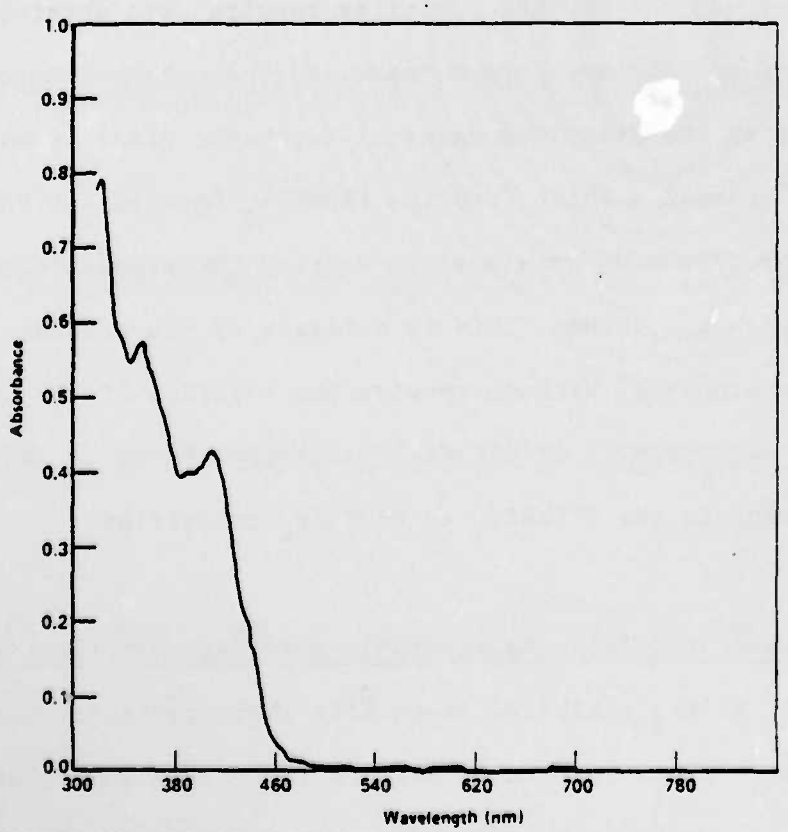

FIGURE 28: VISIBLE SPECTRUM OF HEXACHLOROSULFONATED RUBRENE

D. Solubility and Recrystallization

Polybrominated Protoporphyrin IX Dimethyl Ester and Tetrabromoprotoporphyrin IX Dimethyl Ester: Attempts to recrystallize the product $PPDMEBr_X$ had limited success. At room temperature and elevated temperatures $PPDMEBr_X$ was partially soluble in benzene and toluene, insoluble in petroleum ether and cyclohexane, and soluble in methanol and acetone; a solvent pair of benzene and petroleum ether was selected for recrystallization. When petroleum ether was added to the benzene supernate of the partially dissolved $PPDMEBr_X$, a purple precipitate appeared. It is important to note that the precipitate obtained had a VIS spectrum similar to the initial product, whereas the VIS spectrum of the filtrate indicated that the benzene-soluble portion of the product was the $PPDMEBr_4$. Similar results were obtained with the solvent pair toluene/cyclohexane. Further study showed that the act of filtering the dissolved material (sintered glass or Whatman filter paper) caused a shift from the $PPDMEBr_X$ form to the $PPDMEBr_4$ form. A similar result was achieved by passing the product through an alumina or silica gel column. This is evidence of the presence of some very labile bromines. Without knowing the location of the bromines on the parent molecule it is difficult to speculate as to what exactly is occurring in the $PPDMEBr_X$ to $PPDMEBr_4$ transition.

Polybrominated Tetraphenylporphin and Tribromotetraphenylporphin: The product $TPPBr_X$ exhibited solubility characteristics similar to the $PPDMEBr_X$. It was partially soluble in benzene and toluene, insoluble in petroleum ether, ethyl acetate and cyclohexane and soluble in methanol, acetone and chloroform. When petroleum ether was added to the supernate of a $TPPBr_X$/benzene solution, a greenish precipitate appeared. The precipitate exhibited visible spectral characteristics similar to the $TPPBr_X$ reaction product. However, the visible spectrum of the filtrate was similar to the $TPPBr_3$ spectrum reported.[21] Also noted was a color change of the filtrate, from yellow-green to amber-red, which coincided with the change in spectrum.

Based on the apparent solubility of the $TPPBr_3$ in benzene and the insolubility of the $TPPBr_X$ in benzene, a quantitative study was undertaken in an attempt to establish the relative weight percent of $TPPBr_3$ in the reaction product $TPPBr_X$. This was done by stirring a $TPPBr_X$/benzene solution in a preweighed test tube for 30 min. The supernatant was carefully transferred to a second test tube where approximately a 2:1 (volume) amount of petroleum ether was added; the mixture was stirred and placed in an ice water bath, a small amount of precipitate was present.

The remaining solvent in the undissolved portion of the original $TPPBr_X$ sample was evaporated with an argon stream and the amount of $TPPBr_X$ remaining was determined by weighing. The mixture in the ice bath was separated by vacuum filtration. By weighing the green solid precipitate $TPPBr_X$, the amount of $TPPBr_3$ present in the filtrate was determined by difference:

$$\underset{\text{(orig. sample)}}{TPPBr_X} - \underset{\text{(undis. sample)}}{TPPBr_X} - \underset{\text{(ppt.)}}{TPPBr_X} = \underset{\text{in solution)}}{TPPBr_3} \qquad (46)$$

AD-A154 711 THREE-DIMENSIONAL PHOTOCHEMICAL MACHINING WITH LASERS 3/3
(U) BATTELLE COLUMBUS LABS OH R E SCHWERZEL ET AL.
28 DEC 84 AFOSR-TR-85-0456 F49620-82-C-0077

UNCLASSIFIED F/G 13/8 NL

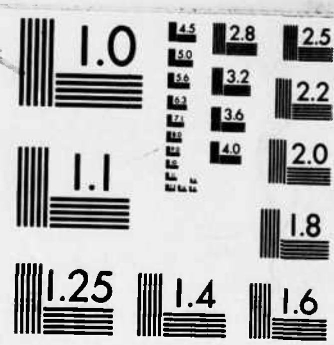

MICROCOPY RESOLUTION TEST CHART
NATIONAL BUREAU OF STANDARDS-1963-A

This procedure was repeated three times using the undissolved portion of the previous sample as the beginning sample for each trial. With each successive trial more $TPPBr_3$ was left in the final filtrate, which led to a suspicion that something was occurring in the dissolving/ filtration process to produce $TPPBr_3$. A calculation of the total amount of $TPPBr_3$ present in the original sample based on the difference formula above resulted in a high weight percent of $TPPBr_3$. If this were the case, it would be reasonable to expect indications of $TPPBr_3$ to show up in the visible spectrum of the reaction product $TPPBr_X$. Further trials confirmed that the filtration step was indeed changing the $TPPBr_X$ to the $TPPBr_3$ form. When something as gentle as Whatman filter paper would cause the $Br_X \longrightarrow Br_3$ transition it was concluded that there also must be some very labile bromines present on the $TPPBr_X$ molecule. Unfortunately, these bromines did not seem to contribute to rapid polymer formation when the compound was irradiated in a monomer solution.

<u>Chlorosulfonated Rubrene</u>: Recrystallization of the chlorosulfonated rubrene was accomplished using a hot ethyl acetate and pentane solvent pair. See Appendix A.1, pg.118.

E. Thermal Stability

The projected increases in temperature of the monomer/ photoinitiator solutions due to light absorption are expected to be relatively minor. Ideally the absorbed energy is not released as heat, through internal conversion, but is retained by the formation of the T_1 species and subsequently results in bond cleavage. Likewise the heat release due to the polymerization of MMA[22] and TMPTA[23] is minor. The thermal stability of the initiator would become an important factor if the temperature of the reaction mixture were to become a parameter in the control of the rate of polymerization.

Thermal stability was determined by preparing a $CHCl_3$ solution of each photoinitiator molecule. The solutions were transferred to square pyrex cells which fit into the CARY 17DX spectrometer sample holders. The cells were then placed in copper mesh baskets and were suspended in the fluid (50/50 Peak antifreeze: water) resevoir of a Lauda K2/R constant temperature controller. At 30-minute intervals the samples were removed from the resevoir and quenched by swirling them for 1 min. in an ice water bath. Thermal stability was monitered by taking a visible absorption spectrum at each 30-minute interval. A reduction or change in the absorption intensity at the absorption peak wavelengths would indicate a proportional decrease in the concentration or reactivity of the photoinitiator solution.

From the results, it was observed that over the time periods considered, up to 2 hrs., there was no decrease in the intensity of the absorption spectra of any of the photoinitiator molecules. During the 60°C trial there was, however, an increase (5%-15%) in the intensity of absorption but this was due to evaporation of the $CHCl_3$ solvent and the consequent increase in concentration.

F. Photochemical Stability

The necessity for having the photoinitiators stable to irradiation by the wavelengths they strongly absorb does not imply that they will not undergo the desired bond cleavage. What is required is that as the two light beams pass through the monomer/photoinitiator solution prior to intersecting, the photoinitiator molecules within the beam paths must not be destroyed or altered. If the photoinitiator molecules were altered, this would not only result in a reduction in concentration of photoinitiators in the solution but the resulting altered molecules may have absorption spectra which are similar to that of the photoinitiator and therefore compete with the photoinitiator. The degradation products may also quench or scavenge the triplets or free radicals which are produced by the desired process.

In the two beam system which was being studied here, the initial excitation beam was the one of primary concern. The second beam was positioned in a "window" of the photoinitiator absorption spectrum, and therefore was only slightly absorbed, if at all, by the photoinitiator molecule. In selecting the wavelengths for these irradiation stability trials, one first considered the absorption spectrum of each photoinitiator. It was decided to use an irradiation beam which included wavelengths of the entire visible area of interest for each photoinitiator being considered. This obviously was not representative of the use of a laser of a single wavelength or narrow band width but was comparable to the most general situation which was encountered in the experiments performed during this study.

Irradiation stability was determined by irradiating a chloroform solution of each photoinitiator with a light beam comprised of the visible wavelengths of interest for each candidate molecule. The light source was a xenon arc lamp (Eimac R150-8) using an Eimac P5150-8 power supply. The wavelengths of the beam incident on the sample cell were controlled by using Corning or Melles Groit 2" x 2" glass filters in series. The beam was focused to approximately a 1 cm. diameter spot on the cell. Because the complete sample was not being irradiated, the actual degree of change, if any, is also dependent upon diffusion and mixing within the cell during the irradiation period. What was important in these trials was to see if there existed an obvious degradative process due to irradiation. The samples were analyzed at hourly intervals. If no change was noted after the initial interval, the irradiation was discontinued. The results can be seen in Figures 29 to 33.

All the photoinitiators exhibited some degree of photochemical instability. The polybrominated compounds, $TPPBr_X$ and $PPDMEBr_X$, were the most stable with decreases in absorption of 1.1% and 9.9% respectively, over the first hour. In contrast, the $TPPBr_3$ and $PPDMEBr_4$ compounds exhibited significant decreases in absorption of 43.4% and 58.3% respectively, over the first hour. Absorption of $Ru(SO_2Cl)_6$ decreased 30.7% over the first hour.

Based on these results, the $TPPBr_X$ photoinitiator displayed the highest degree of photochemical stability and appeared to be the best photoinitiator candidate of the five compounds considered.

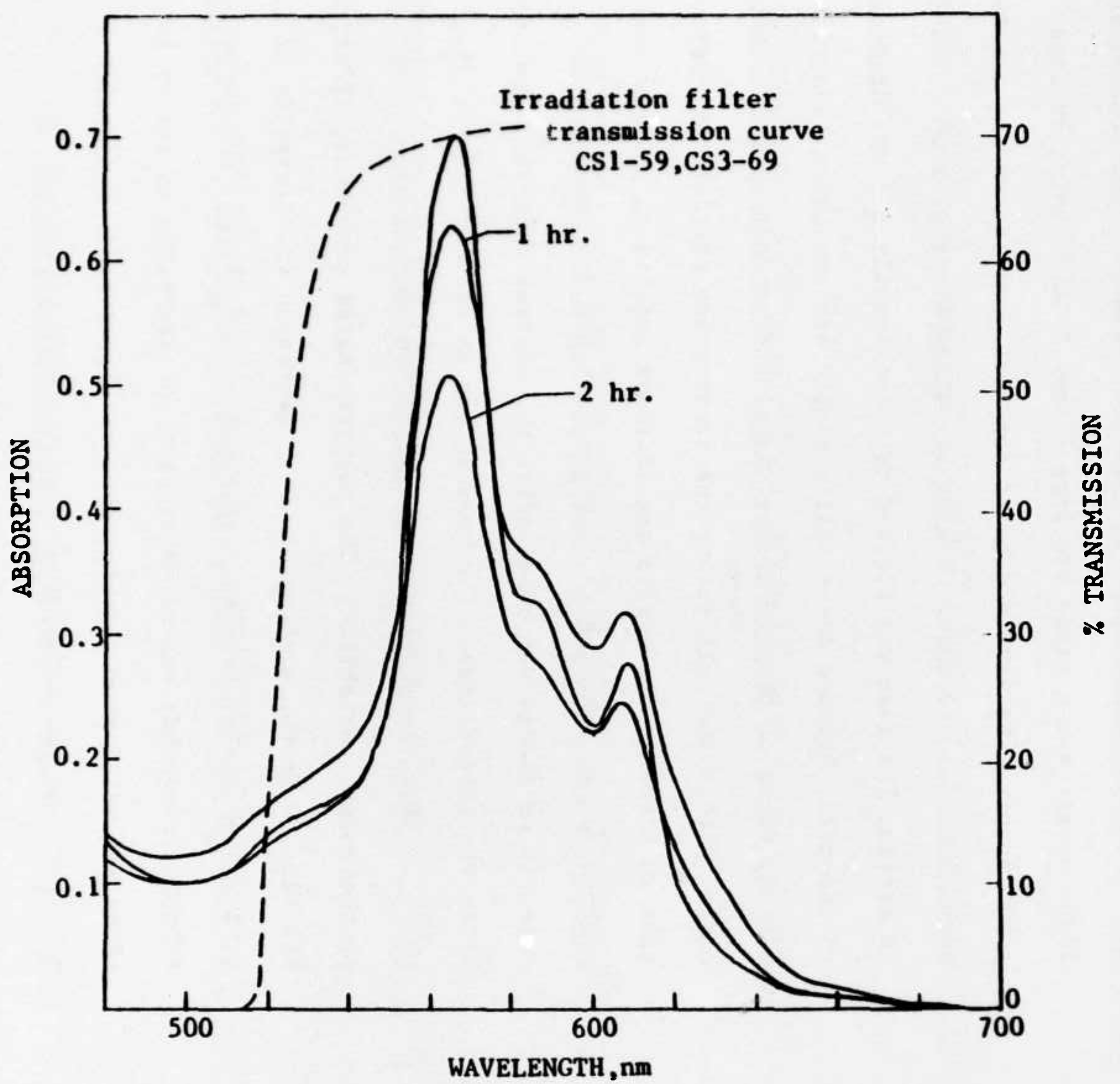

FIGURE 29: IRRADIATION OF $PPDMEBr_X$ IN $CHCl_3$

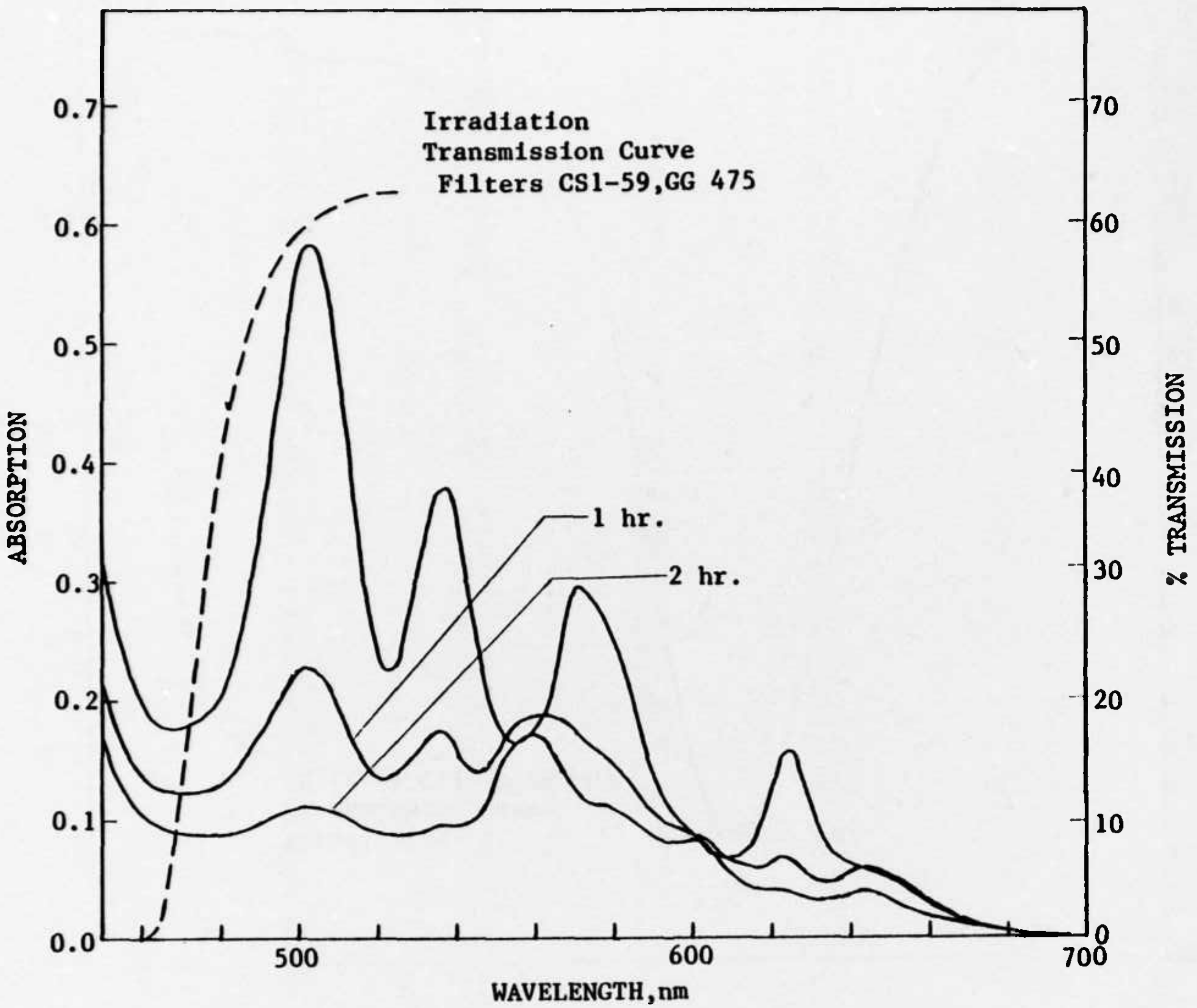

FIGURE 30: IRRADIATION OF $PPDMEBr_4$ IN $CHCl_3$

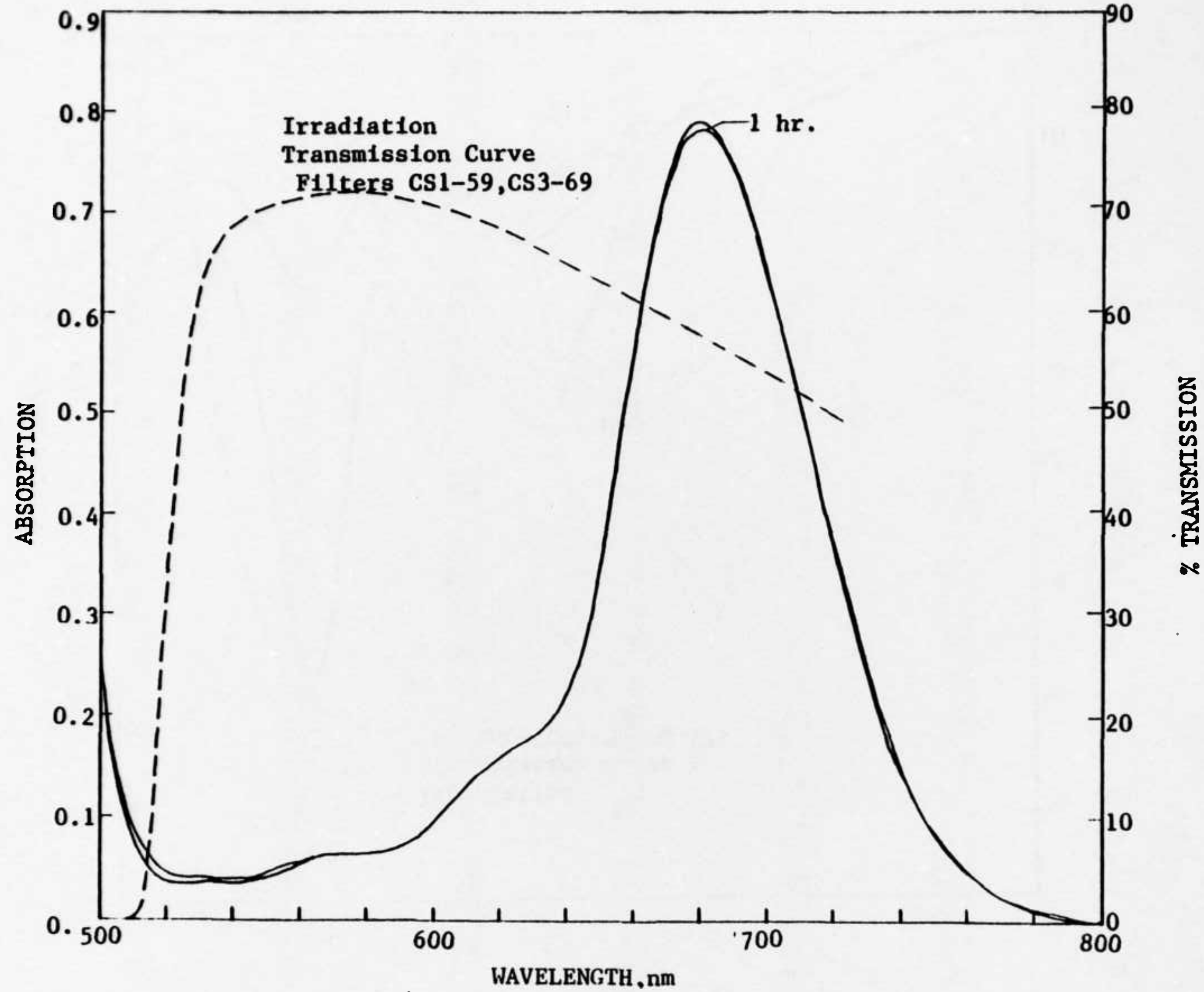

FIGURE 31: IRRADIATION OF $TPPBr_X$ IN $CHCl_3$

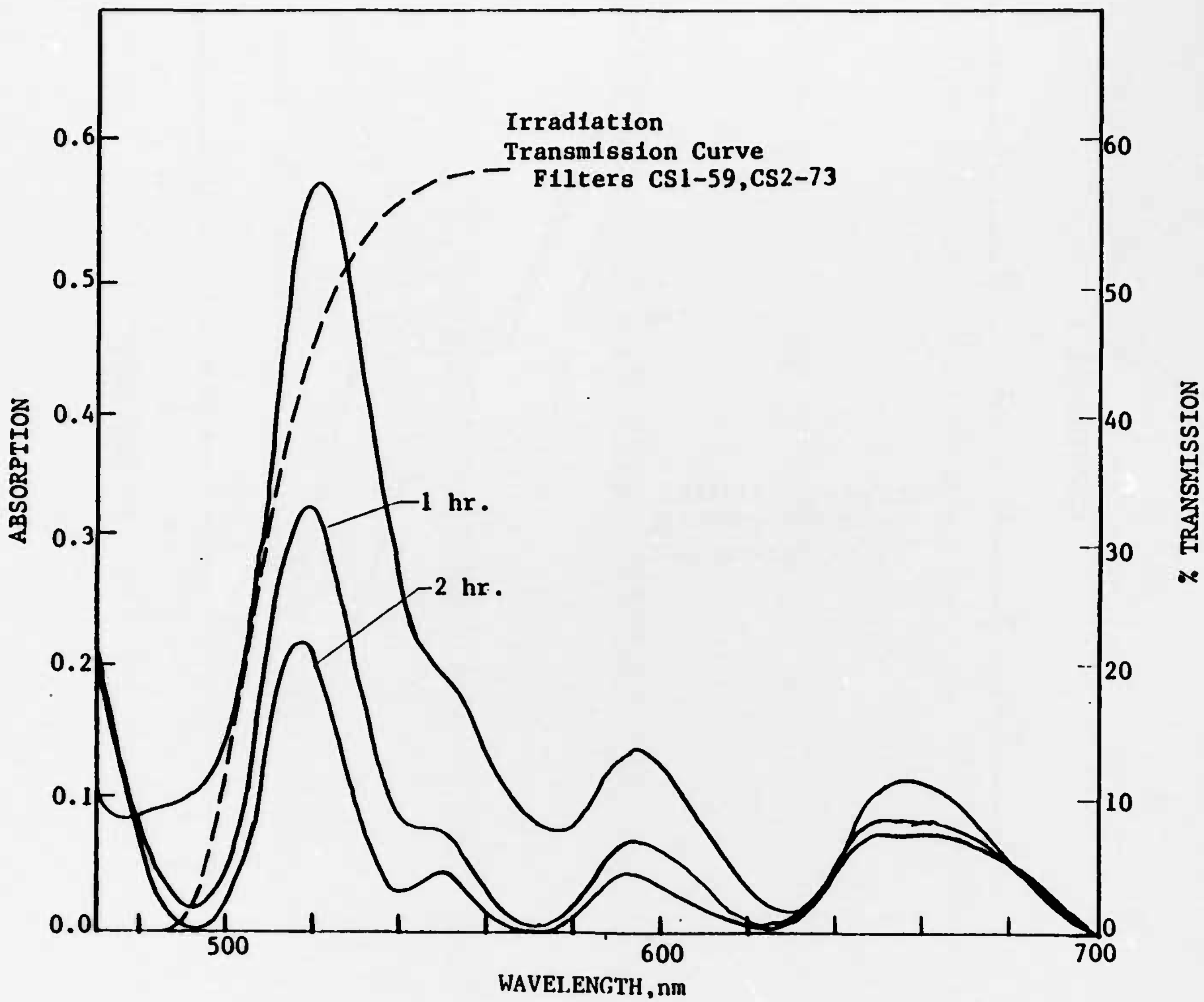

FIGURE 32: IRRADIATION OF $TPPBr_3$ IN $CHCl_3$

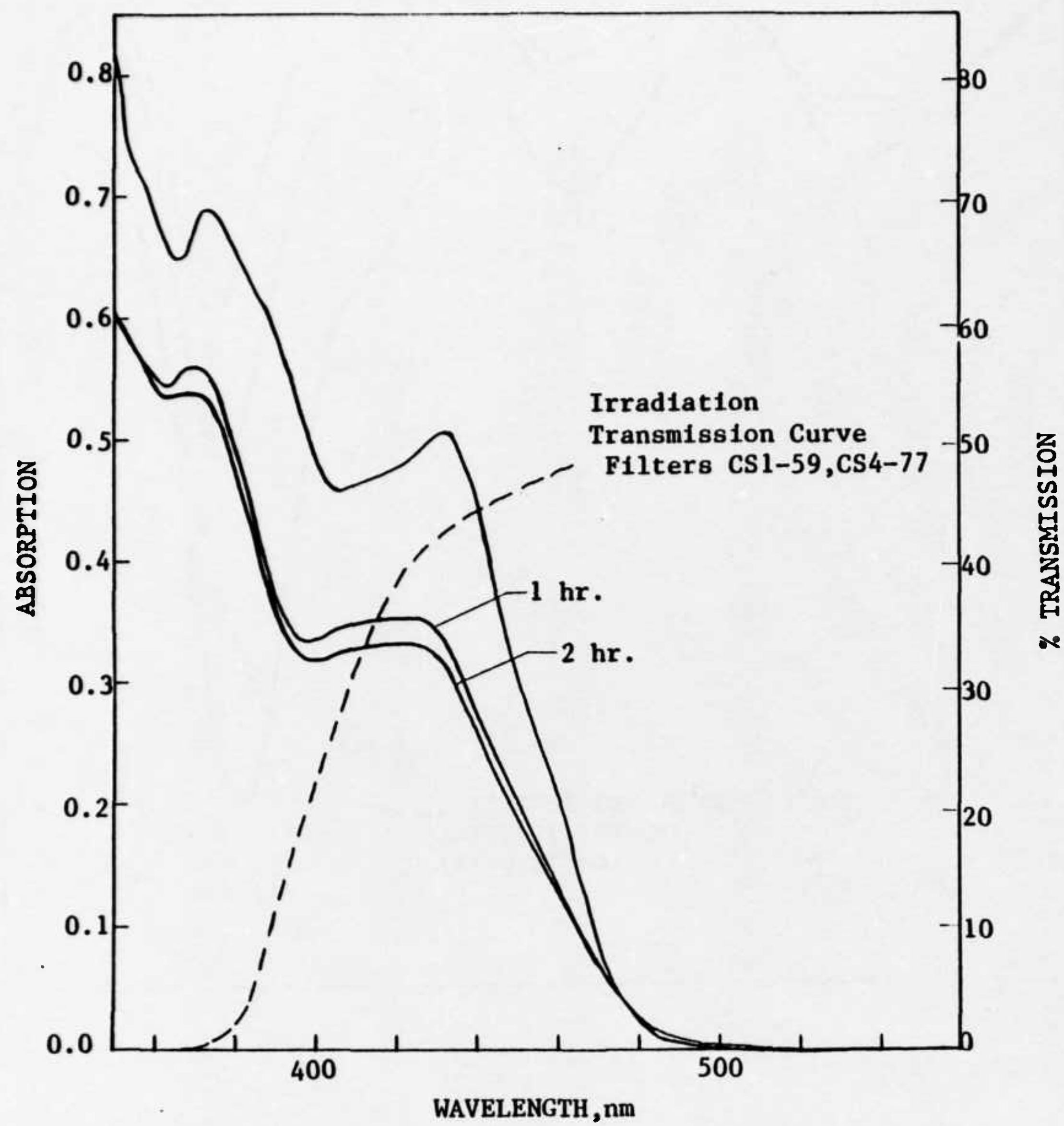

FIGURE 33: IRRADIATION OF $Ru(SO_2Cl)_6$ IN $CHCl_3$

VIII. RESULTS AND DISCUSSION

Rather than compiling a single table which summarizes all the experimental irradiation trials performed, the trials are presented according to the photoinitiator or photosensitizer system being considered. The intent of the individual trials is stated and the results will be noted.

A. Photoinitiator Candidate Irradiations

After the photoinitiator (PI) molecules had been synthesized it was necessary to ascertain whether they were capable of initiating polymerization upon absorption of light. The photoinitiators were dissolved in the monomer TMPTA and irradiated by a Xe arc lamp with no light filtration. Pyrex test tubes (13mm x 100mm) were used to hold the sample solutions. The amount of PI dissolved in the TMPTA was unknown and the samples were degassed with argon for 30 min. Irradiation of all three photoinitiator compounds; $TPPBr_X$, $PPDMEBr_X$, and Ru $(SO_2Cl)_6$, in their respective solutions resulted in polymerization. This confirmed the assumption that bromination of tetraphenyl porphine (TPP) and protoporphyrin IX dimethyl ester (PPDME) and chlorosulfonation of rubrene would result in compounds which would be suitable as photoinitiators.

B. Irradiation Trials with $TPPBr_X$

The irradiation trials of $TPPBr_X$ are presented in Table 9 and the irradiation beam wavelength content is shown in Figure 34. Without knowing the formula weight the concentration of $TPPBr_X$ in the monomer TMPTA can only be given on a weight percent basis. Sample solutions were irradiated in disposable 1cm x 1cm cuvettes. These cuvettes were selected for two primary reasons, 1) they presented flat surfaces to the incident irradiation beams and 2) they could be used directly in the CARY 17DX spectrometer for absorption spectra.

The first series of irradiations using $TPPBr_X$ were runs 1 to 4. Their purpose was to identify combinations of 2" x 2" colored glass filters which could be placed in series in the path of beams 1 and 2 to restrict or promote polymerization. With no triplet absorption information available for $TPPBr_X$, the approach was to first find a filter combination for beam 1 which would not allow polymerization to occur. The second requirement was that removal of one of the filters would cause the sample solution to polymerize. Using the beam 1 filter series which did not cause polymerization, beam 2 would be selected so that the two beams together would initiate polymer formation.

In selecting the filters for beam 2, the triplet absorption information available for tetraphenyl porphine (TPP) was referenced (see Fig. 6). Based on the TPP triplet absorption in the near infrared, it was proposed that beam 2 should contain only those wavelengths beyond the visible range. Filter CS7-56 was selected because of its transmission of wavelengths above 800nm only.

Two sets of filters for beam 1 were selected, these are shown in Runs 2 and 4. The CS1-59, RG-665, CS4-77 series was more desirable because it permitted more energy to be absorbed by the singlet which correspondingly should result in more triplet formation.

Run 6 gave the first indications of a positive result when a block of polymer seemed to have been formed within the monomer solution as opposed to being attached to either side of the sample cell. It should be noted that this sample was degassed for a period of 150 min. and a cell mask (Figure 19) was used to better define the intersection volume of the two beams.

Runs 7 to 10 were performed to determine the relationship between length of the degassing period and irradiation time before the onset of polymerization. There were no indications that longer degassing times resulted in more rapid polymerization.

One possible cause for the inconsistent results may have been the cloudiness which developed on the inside walls of the disposable cubettes during the irradiation period. To eliminate this problem all future irradiations were done with the sample solutions in 1cm x 1cm pyrex cells.

Runs 12 and 13 used the Molectron DL-II laser @ 630nm for beam 1. Although $TPPBr_X$ does not absorb strongly at this wavelength, the wavelength distribution in the beam is much less than when the filter, Xe arc lamp system was used. This was intended to eliminate what seemed to be single beam polymerization taking place in beam 1, as evidenced by the polymer deposits on the beam 1 cell wall. By using a

Xe arc lamp/filter system for beam 2, a continual source of photons would be available for triplet absorption.

Run 12 resulted in polymer deposits on the interior cell walls from both beams. There was not enough refraction and beam diffusion within the cell to cause two beam polymerization on both surfaces. It was possible that thermal effects were causing the polymerization, but single beam polymerization was more likely the cause.

The sample in Run 13 may have reabsorbed enough O_2 to effectively quench the singlets and triplets formed, resulting in no polymerization.

Run 14 was an attempt to see if $TPPBr_X$ could act as a photosensitizer with naphthalene sulfonyl chloride (NSC) as the initiator. The irradiation resulted in small polymer deposits from the laser on the interior cell wall, again single beam polymerization.

Without knowledge of the $TPPBr_X$ triplet absorption spectrum, it was decided to discontinue irradiation trials of $TPPBr_X$/TMPTA. The apparent single beam polymerization with different irradiation conditions strongly suggests the possibility of singlet and triplet absorption spectra overlap. To more finely tune the wavelengths of beams 1 and 2 and eliminate or reduce the single beam polymerization, the triplet absorption spectrum of $TPPBr_X$ was necessary.

Table.9 : Irradiation of $TPPBr_x$[1] in THPTA[2] with Argon Degas[3]

Run	Beam 1[4]	Beam 2[4]	Time	Polymer	Comments
1	Xe arc CS1-59 CS2-59 CS4-77	--	15 min	no	Intent is to see if polymerization does not occur with this filter combination but does occur with removal of CS4-77. Weight % $TPPBr_x$ approx. $3.6x10^{-3}$ in solution.
	CS1-59 CS2-59		60 min	no	Irradiation conditions changed to increase the amount of light energy entering the sample solution.
	no filters		12 min	yes	Remove all filters to see if sample will polymerize as previously shown.
2	Xe arc CS1-59 CS2-59 CS4-77	--	15 min	no	Repeat Run 1, weight % of $TPPBr_x$
	CS1-59 CS2-59		15 min	no	
			45 min	yes	Slight deposit on cell wall
			60 min	yes	No apparent change in amount of polymer formed
			75 min	yes	Large amount of polymer is present
3	Xe arc CS1-59 CS2-59	--	15 min	no	
			30 min	yes	Small deposit on cell wall
			60 min	yes	Approx. 50% of sample polymerized
4	Xe arc CS1-59 RG-665 CS4-77	--	15 min	no	Degas period of 90 minutes
	CS1-59 RG-665		15 min	no	
			60 min	no	
	CS1-59 CS2-59		30 min	yes	Approx. 80% of sample polymerized
5	Xe arc CS1-59 CS2-59 CS4-77	Xe arc CS7-56	15 min	no	Intent is to see if addition of IR light by means of beam 2 will cause polymerization to occur. Excite triplet beyond 800nm.
			30 min	no	
			60 min	no	Degas period 60 minutes

Table 9 continued

6	Xe arc	Xe arc	15 min	yes	Mask used[5], degas period 150 min.
	CS1-59	CS7-56	30 min	yes	Block of polymer within cell, not attached to either wall
	RG-665				
7	Xe arc	Xe arc	15 min	no	Degas period of 120 min, repeat of Run 6
	CS1-59	CS7-56	45 min	no	
	RG-665				
8	Xe arc	Xe arc	9 min	yes	Degas period of 150 min, CS 7-56 filter cracked permitting some unfiltered light into sample. Repeat of Run 6
	CS1-59	CS7-56			
	RG-665				
9	Xe arc	Xe arc	15 min	no	Degas period 180 min, repeat of Run 6
	CS1-59	CS7-56	30 min	no	
	RG-665		45 min	yes	Viscosity of sample increased
10	Xe arc	Xe arc	15 min	no	Degas period 270 min, repeat of Run 6
	CS1-59	CS7-56	30 min	no	
	RG-665		45 min	yes	Viscosity of sample increased slightly after 75 min irradiation time
11	laser[6]	Xe arc	60 min	no	Sample moved at 10-minute intervals. Increase energy input by using a pulsing laser to form more triplets
	630nm	CS7-56			
12	laser	Xe arc	30 min	yes	Cell moved continuously during irradiation. polymer formed on cell walls of both beams
	630nm	CS7-56			
13	laser	--	30 min	no	Cell moved at 5-min. intervals. See if polymer formed in Run 12 could be from refraction of light entering cell and actually a 2-beam process or a single beam process from each beam.
	630nm				
	Xe arc		15 min	no	
	CS1-59		30 min		
	RG-665		60 min		

1. Polybrominated tetraphenylporphine, approx. .01 wt % solutions
2. Trimethylolpropane triacrylate monomer
3. Sample solutions are degassed with argon for 30 minutes unless otherwise noted
4. See fig.34 for filter combination transmission curves, CS (Corning Glass), RG (Melles Griot)
5. Foil mask was used on sample cell to control volume of cell irradiated by the two beams, see fig. 19 .
6. Molectron UV24-DL14 laser with Kiton Red dye

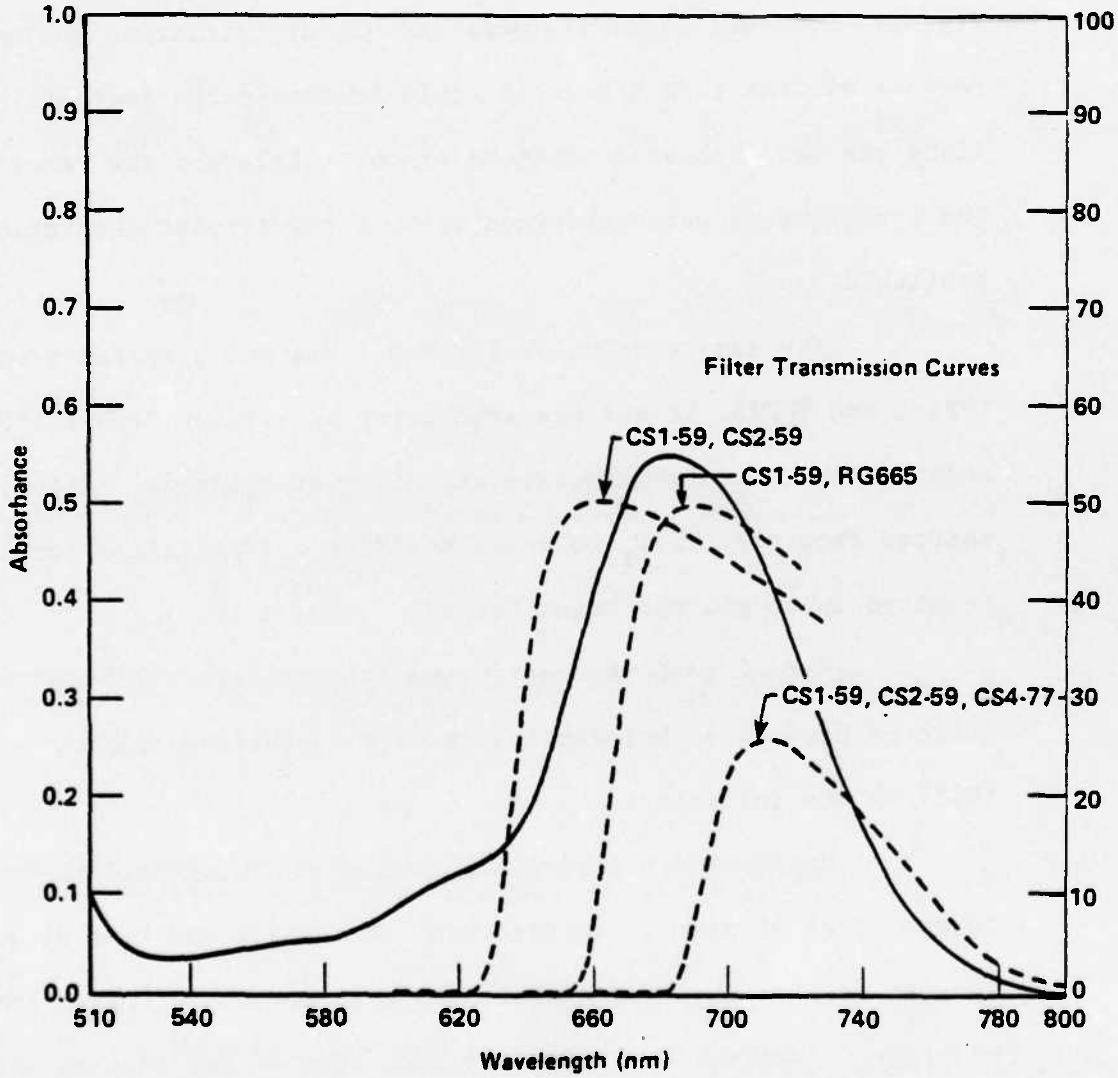

FIGURE 34: $TPPBr_X$ SPECTRUM + IRRADIATION FILTER CURVES

C. Irradiation Trials with $TPPBr_3$

The results of the irradiation stability tests indicated that $TPPBr_3$ would not be a good candidate for long irradiation periods, see Fig. 29. However, if $TPPBr_3$ were capable of initiating polymerization in periods of less than ½ hour it could be considered further. Table 10 lists the irradiation conditions of the trials and the results noted. The irradiations were performed without the triplet absorption spectrum available.

The sample solution for Run 1 was not prepared from solid $TPPBr_3$ and TMPTA. It was prepared using an aliquot from a $TPPBr_X$/TMPTA solution which, during storage at -8°C over a ten-day period, had shifted from the $TPPBr_X$ molecule to $TPPBr_3$. Irradiation for 30 min. resulted in no polymer being formed.

Runs 2 to 6 were conducted to see if the $TPPBr_3$ compound could be used as a photosensitizer with napthalene sulfonyl chloride (NSC) as the initiator.

Run 2 used a 20:1 molar excess of NSC:$TPPBr_3$, no polymer was formed after 30 min. of irradiation. The sample was then stored in the freezer for two days, redegassed and used for Run 3. After Run 3, with no polymer formed, a VIS spectrum was taken of the sample, and showed a peak shift to approximately 680nm where the peak for $TPPBr_X$ is found. An experiment was tried and it was found that the peak shift occurs with the addition of the NSC to the $TPPBr_3$/TMPTA solution, prior to irradiation. The peak shift indicates either chlorosulfonation or chlorination of the $TPPBr_3$ molecule. Whatever chemical reaction was

Table 10: Irradiation of $TPPBr_3$[1] in THPTA[2] with Argon Degas[3]

Run	Beam 1	Beam 2	Time	Polymer	Comments: foil mask used for all irradiation trials. Runs 2 to 6, NSC+$TPPBr_3$[4]
1	Xe arc CS1-59 CS2-73	--	15 min 30 min	no no	No polymer or indications of polymer.
2	Xe arc CS1-59 CS2-73	--	15 min 30 min	no no	Sample solution contains 20:1 excess NSC:$TPPBr_3$. Look at $TPPBr_3$ as a photosensitizer.
3	Xe arc CS1-59 CS2-73	Xe arc CS7-56	30 min	no	Sample from Run 2 redegassed for 30 min. Visible spectrums taken after irradiation shows shift toward polybrominated molecule NSC:$TPPBr_3$ 20:1
4	Xe arc CS1-59 CS2-73	Xe arc CS7-56	15 min	yes	NSC:$TPPBr_3$, 5:1. Polymer formed in beam 1 side. Concentration of $TPPBr_3$ is twice that in Runs 1 to 3.
5	Xe arc CS1-59 CS2-73	Xe arc CS7-56	15 min	no	NSC:$TPPBr_3$, 5:1
6	Xe arc CS1-59 CS2-73	Xe arc CS7-56	15 min	yes	NSC:$TPPBr_3$, 2.5:1. Polymer formed on beam 1 side. Concentration of $TPPBr_3$ is same as Run 4.

1. Sample solutions approx. 10^{-5} M in $TPPBr_3$
2. Trimethylolpropane triacrylate monomer
3. Argon degas for 30 minutes unless otherwise noted
4. Ratios of NSC:$TPPBr_3$ are mole ratios

occurring did not form primary initiators or at least not in a quantity necessary to initiate polymerization.

Some polymer was found in Runs 4 and 6, but again it was on the beam 1 side only and was apparent after 15 min. of irradiation.

Because of the shifts in the absorption spectrum of the $TPPBr_3$/NSC/TMPTA solution, this system was not considered to be useful for our photopolymerization process.

D. Irradiations Trials with $PPDMEBr_X$

After the instability of $TPPBr_X$ in TMPTA was observed, the stability of $PPDMEBr_X$ in TMPTA was examined. A previously prepared solution of $PPDMEBr_X$ in TMPTA was removed from -8°C storage, allowed to come to room temperature and an absorption spectrum was taken. The resulting spectrum showed a complete shift from the $PPDMEBr_X$ compound to the $PPDMEBr_4$ compound. This solution did not exhibit an increase in viscosity so apparently the chemical reaction taking place does not involve free radical or ion intermediates, which initiate polymerization.

Knowing that $PPDMEBr_X$ undergoes the shift to $PPDMEBr_4$ at a reduced temperature over a 10-day period, a study of the effect of temperature and irradiation on $PPDMEBr_X$ in TMPTA was undertaken.

To minimize the effect mixing may have on the bromination change, the solid $PPDMEBr_X$ was not dissolved directly in the TMPTA as was the normal procedure. An alternate method of first dissolving the $PPDMEBr_X$ in a small amount of chloroform, and then using aliquots of

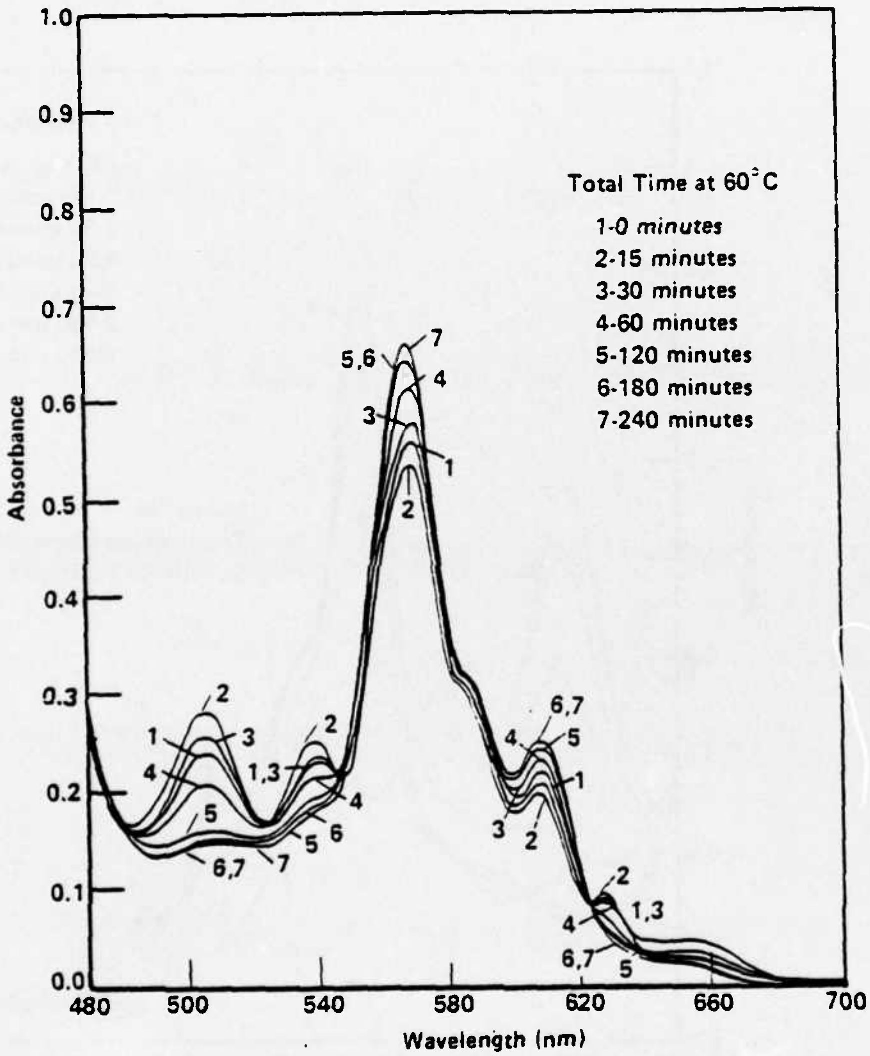

FIGURE 36: PPDMEBr$_X$/TMPTA AT 60 C

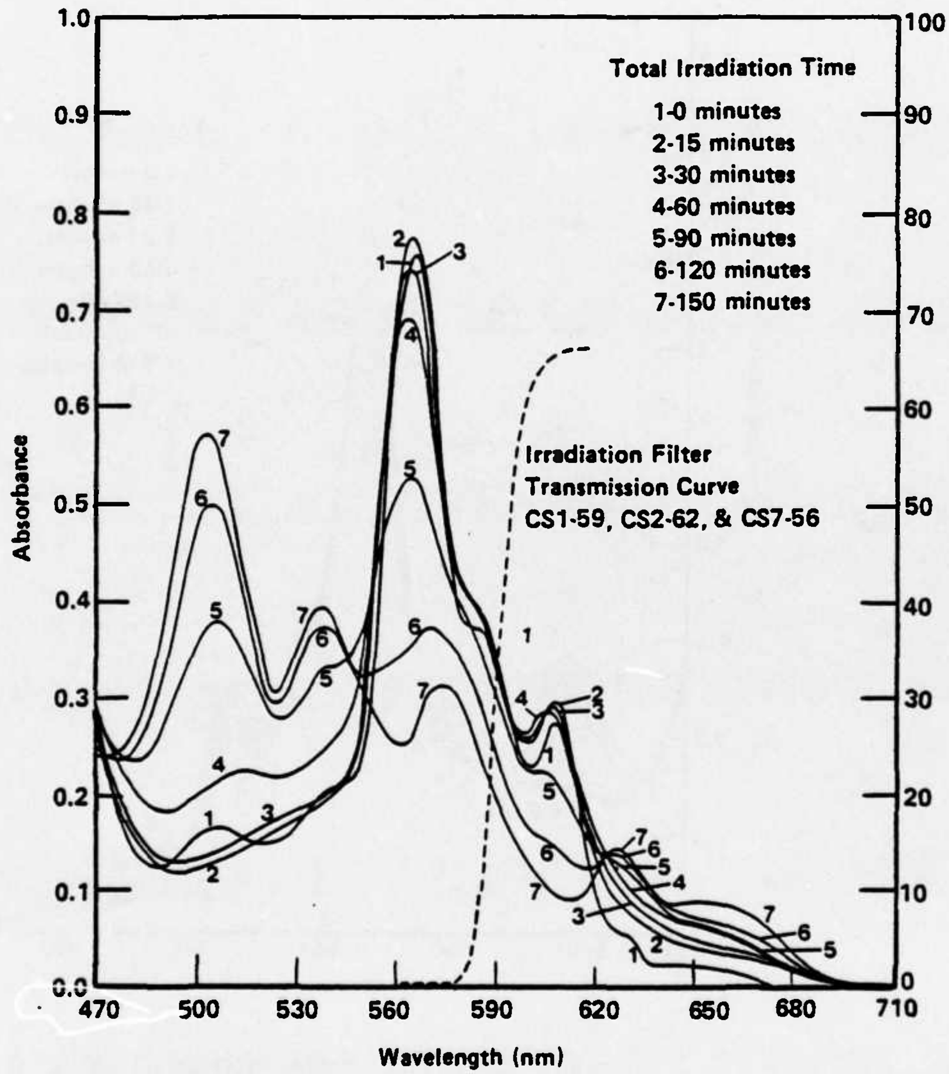

FIGURE 36: IRRADIATION OF $PPDMEBr_X$ IN TMPTA

this solution in the TMPTA made it possible to reduce the mixing time to a few minutes.

The effect of temperature on the $PPDMEBr_X$/TMPTA solution was studied by placing a sample solution in a 60°C constant temperature bath. See Fig. 36 for the spectra taken during the study.

Irradiation stability was studied by irradiating a $PPDMEBr_X$/TMPTA sample solution using two Xe arc lamp beams with different filter combinations. The results and filter transmission curves are shown in Fig. 37.

Comparing Figures 36 and 37 it can be seen that the thermal effects are less severe and within 30 minutes the $Br_X \longrightarrow Br_4$ shift is reversed. Irradiation of $PPDMEBr_X$/TMPTA readily promotes a complete Br_X to Br_4 shift.

Some irradiation trials were run for $PPDMEBr_X$/TMPTA using varying filter combinations but due to the instability of $PPDMEBr_X$ in TMPTA the results were inconsistent. When polymer was formed it was always a result of beam 1 only.

E. Irradiation Trials of Tetraphenyl Porphine (TPP) and Naphthalene Sulfonyl Chloride (NSC) as a Photosensitizer/Initiator System

When the decision was made to discontinue work on the photoinitiator systems, the next step was to study systems using tetraphenyl porphine as a photosensitizer. The basis for selecting TPP and NSC has been previously explained. An absorption spectrum of TPP + NSC and the glass filter transmission curves is shown in Figure 38. Table 11 is a compilation of the trials conducted, and as can be seen

Table 11: Irradiation of TPP[1] + NSC[2] in TMPTA[3] with 30 min. Argon Degas

Run	NSC:TPP[4]	Beam 1[5]	Beam 2[5]	Time	Polymer	Comments
1	260:1	Xe arc CS1-59 CS3-66	laser[6] 450nm	3 min	yes	Sample was moved continuously during irradiation, large amount of polymer formed apparently from beam 1.
2	260:1	XE arc CS1-59 CS3-66	--	2 min	yes	Sample moved continuously during irradiation,. See if polymer formed in Run 1 was single beam process. Large amount of polymer formed.
3	260:1	--	laser 450nm	3 min 25 min	no	Sample moved continuously for 3 min. then remained stationary for 25 min. Polymer not formed by beam 2 alone.
4	260:1	Xe arc CS1-59 CS2-59	laser 450nm	3 min	yes	Repeat Run 1 with change in beam 1. Small polymer deposit on beam 1 side.
5	260:1	Xe arc CS1-59 CS2-59	--	3 min	yes	Repeat Run 2 with change in beam 1. Large amount of polymer on beam 1 side.
6	234:1[7]	Xe arc CS1-59 CS2-59	laser 450nm	2 min	no	Sample moved continuously during irradiation
7	234:1	Xe arc CS1-59 CS2-59	laser 450nm	4 min	no	NO argon degas, sample moved continuously
8	234:1	Xe arc CS1-59 CS2-59	laser 450nm	7 min 12 min	yes	For the initial 7 min the sample was moved every 15 sec. the remaining 12 min the sample was moved every 2 min. When methanol was added to sample solution and mixed, string-like polymer pieces were present
9	234:1	Xe arc CS1-59 CS2-59	--	15 min	yes	Mask used to better define irradiated area. Polymer formed in shape of mask opening and projects into sample cell.

Table 11 continued

10	234:1	Xe arc CS1-59 CS2-59	laser 450nm	20 min	yes	See if addition of second beam increases the amount of polymer formed. Polymer formed same as Run 9
11	234:1	Xe arc CS1-59 CS2-59	laser 450nm	20 min	no	NO argon degas
12	234:1	Xe arc CS1-59 CS2-59	laser 450nm	20 min	no	Repeat Run 10.

1. Tetraphenyl porphine, solutions approx. 9×10^{-5} M TPP
2. Naphthelene sulfonyl chloride
3. Trimethylolpropane triacrylate monomer
4. Ratio shown is mole ratio
5. See fig 38 for filter transmission curves
6. Molectron UV24-OL14 laser with Molectron #8 dye
7. Sample solution approx. 2×10^{-5} M TPP

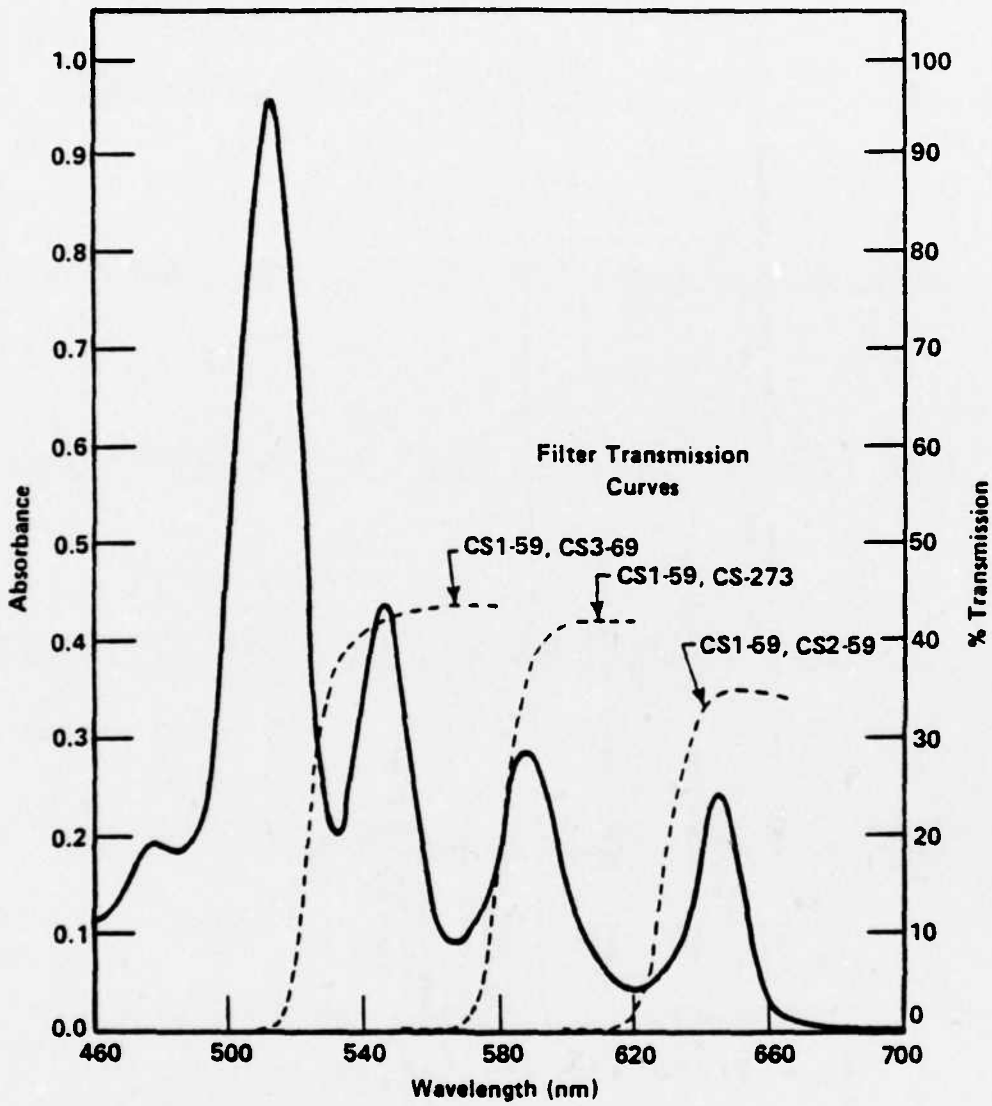

FIGURE 37: TPP+NSC IN TMPTA ABSORPTION SPECTRUM + IRRADIATION FILTER TRANSMISSION CURVES

the irradiation system consisted of a filtered Xe arc lamp beam and a laser beam. Beam 1 will essentially be producing a constant population of triplets (T_1). The concentrated energy of the laser of beam 2 will maximize the number of upper triplets (T_n) formed which can then transfer their energy to the NSC initiator.

Runs 1 to 3 were made to determine if polymerization of TMPTA would occur by 2 beam irradiation. The short run times and continuous sample movement were to serve as an indicator as to how efficient the system was. There was a large excess of NSC to TPP as well which would also help facilitate the energy transfer process. Runs 4 and 5 repeated runs 1 and 2, using a different filter series for beam 1. The results from all 5 runs indicated that the polymer formed was the result of irradiation by beam 1 only, although the amount of polymer formed in run 4 was much less.

Run 7 showed that the degassing step was definitely a factor in the polymerization process. Elimination of the argon degassing step caused no polymerization to occur.

Runs 8 to 12 were repetitious of the previous runs, but the molarity of the TPP was reduced by a factor of 4.5 and a foil mask was used, see Figure 32. These changes were to decrease the amount of single beam polymerization as well as better define the volume where the 2-beam process is taking place. No solid polymer was observed within the beam intersection volume, and there was a decrease in the amount of single beam 1 polymer formed, as was anticipated.

A control was run using a single beam irradiation of a solution of TPP in TMPTA with no NSC initiator present. This resulted in polymer being formed on the cell wall similar to the results of irradiation of TPP in the presence of NSC. It was proposed that the TMPTA was undergoing polymerization via a process other than free radical initiation such as charge transfer. Efforts to control this process led to a series of irradiations of TPP + NSC in methyl methacrylate (MMA). MMA is a slow crosslinking monomer, which is known to polymerize in a 2 beam photosensitized system. It was suggested that perhaps MMA could be used in solution with TMPTA to control the single beam process. Irradiation trials showed no single beam polymerization in a TPP+NSC/MMA system. It was then necessary to establish the relative polymerization rates of TMPTA/MMA solutions of different compositions.

Irradiation of TPP+NSC in TMPTA/MMA. This series of trials is presented in Table 12. The purpose was to identify a sample solution of a known TMPTA/MMA composition which shows some indications of polymerization within a 60 min. time period. The irradiation beams are of the same light content used for previous TPP+NSC trials. For Runs 4 and 5 distilled MMA was used to reduce the amount of inhibitors present in the sample solution. Run 5 was the first of the trials to exhibit polymerization. A small polymer deposit was found on the beam 1 side of the cell and additional polymer precipitated out of the solutions when methanol was added. This was the composition of TMPTA/MMA (3:1 by vol.) selected for the ensuing trials.

Table 12: Irradiation of TPP+NSC[1] in Mixture of TMPTA[2] and MMA[2] with 30 min. Argon Degas

Run	Component	Vol %	Beam 1[3]	Beam 2[4]	Time	Polymer[5]	Comments -- foil mask used, see fig 19.
1	TMPTA MMA	10 90	Xe arc CS1-58 CS3-69	mono 460nm	60	no	The purpose of these runs is to attempt to control the rate of polymerization by addition of MMA, a relatively slow crosslinker, to TMPTA
2	TMPTA MMA	35 65	Xe arc CS1-58 CS3-69	mono 460nm	60	no	
3	TMPTA MMA	50 50	Xe arc CS1-58 CS3-69	mono 460nm	60	no	
4	TMPTA MMA	50 50	Xe arc CS1-58 CS3-69	mono 460nm	60	no	MMA used in this Run is distilled to reduce the amount of inhibitors present
5	TMPTA MMA	75 25	Xe arc CS1-58 CS3-69	mono 460nm	60	yes	A small deposit of polymer is visible on beam 1 cell side, precipitation of remaining solution with methanol results in a very cloudy solution.

1. Mole ratio of tetraphenyl porphine: napthalene sulfonyl chloride is 1:20
2. TMPTA - trimethylolpropane triacrylate, MMA - methyl methacrylate
3. See fig. 38 for filter transmission curve
4. Light source is Xe arc lamp, beam wavelength content controlled by a monochromator
5. The check for polymer was made visually as well as by precipitation with methanol

Irradiation of TPP+NSC in TMPTA/MMA (3:1). Table 13 shows this series of irradiation trials. Run 1 gave results which were both expected and unexpected. The irradiation time was increased to allow for more 2-beam polymerization to occur, and the resulting polymer formed gave indications that 2-beam as well as single beam polymerization was occurring. An unexpected change in color of the polymer also was present. In all previous trials the polymer formed was either colorless or the color of the sample solution. The polymer from this irradiation was a yellow/green color in contrast to the pinkish color of the sample solution. Because the polymerized portion of sample was a solid, attempts at getting an absorption spectrum were not successful. The volume of the sample solution was approx. 1 ml compared to approx. 2 ml of previous samples. Runs 2 and 3 were attempts to find the effect on volume on polymerization but the results were inconclusive. Runs 4 and 5 were also for the purpose of finding the effect of sample volume on polymerization. Run 4 was the first trial to result in an unattached piece of yellow/green polymer in addition to some colorless polymer deposits on the cell walls. This is the first result in the TPP+NSC system which gave concrete evidence of the 2-beam polymerization process taking place. Attempts to reproduce this result with Runs 7 and 8 were unsuccessful however.

This series of trials introduced some new questions. The inconsistency of the results and nonreproducibility may be the result of the degassing procedure and treatment after the degassing. Although the cells are plugged and sealed with teflon tape, because of the variations in fit of the plugs into the cells it is quite possible that

Table 13: Irradiation of TPP+NSC[1] in TMPTA/MMA[2] with Argon Degas[3]

Run	Beam 1[4]	Beam 2[5]	Time	Polymer	Comments[6]: foil mask used on sample cell
1	Xe arc CS1-58 CS3-69	mono 460nm	120 min	yes	Shape of polymer formed indicates that there is perhaps both one and two beam polymerization occurring. Polymer is a yellow/green color compared to pinkish color of solution. 1 ml sample
2	Xe arc CS1-58 CS2-73	mono 460nm	120 min	no	2 ml sample
	CS1-58 CS3-69		120 min	no	
	CS1-58 CS3-69		120 min	no	Sample redegassed for 60 min with argon prior to this irradiation. Solution checked by ppt. with methanol -- no evidence of polymer
3	Xe arc CS1-58 CS3-69	mono 460nm	75 min	yes	Sample approx. 90% polymerized. 1.5 ml sample
4	Xe arc CS1-58 CS3-69	mono 460nm	60 min	yes	Small deposits on both beam sides of cell, also on unattached piece of polymer within the solution. Polymer yellow/green. 1 ml sample
5	Xe arc CS1-58 CS3-69	mono 460nm	60 min	yes	Large amount of polymer. 2 ml sample
6	--	mono 460nm	60 min	no	Beam 2 alone does not cause polymerization. 2 ml sample
7	Xe arc CS1-58 CS3-69	mono 460nm	60 min	yes	Large amount of polymer
8	Xe arc CS1-58 CS3-69	mono 460nm	60 min 60 min 30 min	no no yes	 Add additional TPP/NSC solution, degas for 30 min.

1. Tetraphenyl porphine, napthalene sulfonyl chloride mole ratio 1:20, solutions approx. 3×10^{-5} M
2. TMPTA - trimethylolpropane triacrylate, MMA - methyl methacrylate, volume ratio TMPTA/MMA (3:1)
3. Argon degas period is 30 min, unless noted otherwise
4. See fig 38 for filter transmission curves
5. Light source is a Xe arc lamp, beam wavelength content is controlled by a monochromator
6. Foil mask used for all irradiations (see fig 19)

varying amounts of O_2 were diffusing back into the sample solution during the irradiation.

Another question concerns the presence of the yellow/green coloring of the polymer formed. Is the 2-beam polymerization the result of this color change or does the change occur after the polymer has been formed?

The concern over the degassing procedure was considered first. Degassing the samples with a bubbling stream of argon was discontinued.

Irradiation of TPP+NSC in TMPTA/MMA with Vacuum Degas I. The most effective way to eliminate dissolved gases from the sample solutions was to use the freeze /thaw cycles described earlier (pg. 44).

Beam 2 was changed to a laser tuned to 460 nm, which allowed for reduced irradiation times, see Table 14. In anticipation of the increased polymerization which would occur because of the vacuum degassing, Runs 1-4 were performed to reestablish a TMPTA/MMA ratio for further trials. Contrary to what was expected no polymerization occurred in any of the samples. In Run 5 the sample was stationary for the entire 60 min. irradiation period, still no polymer, not even single beam. The sample solution for Run 6 was degassed using argon for 60 min. After 45 min. irradiation time, a yellow/green color was apparent in the sample. At the end of the 60 min. there was a large amount of yellow/green polymer formed, the remaining solution was also yellow/green.

Table 14: Irradiation of TPP+NSC[1] in TMPTA/MMA[2] with Vacuum Degas[3] 1

Run	Component	Vol %	Beam 1[4]	Beam 2[5]	Time	Polymer[6]	Comments
1	TMPTA MMA	35 65	Xe arc CS1-58 CS3-69	laser 460nm	30 min	no	Runs 1-4 sample movement was approx. 25 microns every sec. for first 30 min. followed by 30 min. of beam 1 irradiation only. Laser beam dia. approx. 100 microns. Small bubbles could be observed rising in beam 1 path through the sample solution.
				--	30 min	no	
2	TMPTA MMA	45 55	Xe arc CS1-58 CS3-69	laser 460nm	30 min	no	
				--	30 min	no	
3	TMPTA MMA	65 35	Xe arc CS1-58 CS3-69	laser 460nm	30 min	no	
				--	30 min	no	
4	TMPTA MMA	75 25	Xe arc CS1-58 CS3-69	laser 460nm	30 min	no	
				--	30 min	no	
5	TMPTA MMA	75 25	Xe arc CS1-58 CS3-69	laser 460nm	60 min	no	Sample stationary for entire 60 min.
6	TMPTA MMA	75 25	Xe arc CS1-58 CS3-69	laser 460nm	60 min	yes	Argon degas for 45 min. After 45 min. yellow-green color apparent. At end of run, large amount of polymer formed. Polymer as well as remainder of solution is yellow-green.

1. Tetraphenyl porphine : naphthalene sulfonyl chloride mole ratio 1:20. Solution approx. 3×10^{-5} M TPP
2. TMPTA - trimethylolpropane triacrylate, MMA-methyl methacrylate monomers
3. Degas using 4 freeze (L.N.)/thaw cycles, followed by transfer of sample to irradiation cell
4. Refer to fig. 38 for filter transmission curves
5. Molectron UV24-)L14 laser with Molectron #8 dye. Approx. 75 μJ/pulse @ 24 pps

The rising bubbles seen in the beam 1 path through the sample are indications that there were probably convection currents being set up within the sample solution. These currents could be responsible for depleting the triplet population within beam 1, thereby reducing the effectiveness of beam 2.

The results of Run 6 seemed to indicate that O_2 played a positive role in the polymerization process and may also be responsible for the change in color of the solution. It remains to be determined if the color change causes the polymerization. Results of an absorption spectrum taken of the yellow/green liquid from Run 6 are presented in Figure 38. The peak shift from 646nm to 658nm, accompanied by the increase in absorption is indicative of some chlorosulfonation or chlorination of the TPP or possibly the formation of a TPP/NSC complex. The shift is towards the 680nm peak found in $TPPBr_X$ and $TPP(SO_2Cl)_X$.

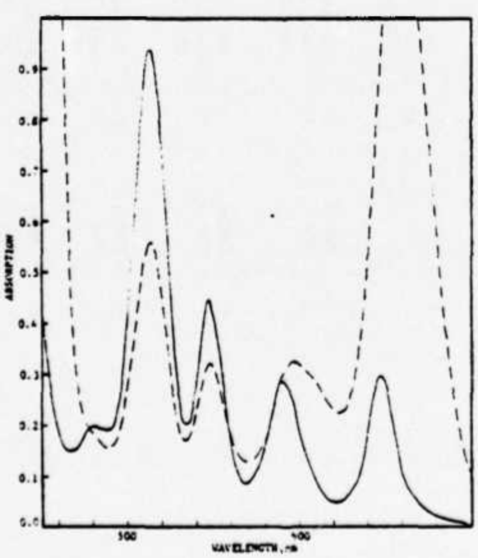

FIGURE 38: ABSORPTION SPECTRUM SHIFT FOR TPP+NSC

Despite the apparent benefit from the presence of some O_2 in the sample solution, the change in absorption spectrum is unpredictable as well as undesirable for our system. Rather than trying to control the amount of O_2 in the sample solution, it is better to have a polymerization system which works in the absence of O_2. To accomplish this objective the sample solutions were degassed using the freeze/thaw procedure and were maintained under vacuum during the irradiation period.

Irradiation of TPP+NSC in TMPTA/MMA Under Vacuum. Irradiations of samples in the absence of O_2 are presented in Table 15. Runs 1 and 2 were essentially repeats of runs from the last section. The significant differences were the use of a foil mask to further reduce the size of beam 1 entering the sample and in Run 2, air streams were directed at the sides to provide cooling where the beams entered the sample cell.

Bubbles were still observed to be rising within beam 1, in the solution, bubbles were also produced by beam 2. These bubbles could be the result of vaporization of solvent within the sample solution. After the irradiation periods were completed similar results from Run 1 and 2 were noted. Both samples were yellow/green in color and both had become gel-like. The color change and accompanying polymerization was not due to the presence of O_2 in the sample solution, but must rather be caused by the amount of energy present in beam 1.

For Run 3 a monochromator replaced the filter system of previous trials. Beam 1 was set at 550nm and during the 30 min. irradiation period no visible currents were produced within the sample,

Table 15: Irradiation of TPP + NSC[1] in TMPTA/MMA[2] with Vacuum Degas II[3]

Run	Beam 1[4]	Beam 2[5]	Time	Polymer	Comments -- Computer controlled movement 50 μ steps/sec/step 1. Mask used for 1,2,3
1	Xe arc CS1-58 CS3-66	laser 460nm	47 min	yes	Bubbles still apparent in sample during irradiation. There were 2 visible polymer areas on beam 2 side. Solution in sample cell is yellow/green, very viscous gel-like, some solid material.
2	Xe arc CS1-58 CS3-66	laser 460nm	45 min	yes	Air stream directed at sides of cell to reduce the amount of heat from beams. Solution color still changes; very viscous gel-like. Less bubble movement during irradiation.
3	mono[6] 550nm	laser 460nm	30 min	yes	No bubbling in solution. Time at each step reduced to .5 sec. Only polymerization is small deposits on rear beam 1 cell wall and beam 2 cell wall. No color change.
4	laser[7] 584 nm max	laser 460nm	60 min	yes	Pulse rate approx. 5 pps. beam 2 @ 62 μJ . beam 1 @ 5 μJ. Polymer formed from beam 2, string-like appendage.
	--	laser 460nm	60 min	yes	Same as result of previous 60 min. trial
		laser 460nm	60 min	yes	Beam attenuated with neutral density filters
5	laser 584nm max	laser 460nm	52 min	yes	Pulse rate 1.4 pps. Beam 2 @ 75 μJ, beam 1 @ 22 μJ/pulse. Polymer formed from beam 2. No beam 1 polymerization
6	laser 584nm max	laser 460nm	27 min	no	Cell angled in attempt to attach polymer to rear wall. Five sec/step, 100 μ/step. Beam energy same as Run 5
7	laser 584nm max	laser 460nm	53 min	no	Repeat Run 6, change to 10 sec/step
8	--	laser[8] 785nm	60 min	no	New dye for beam 2, IR dye at triplet peak approx. 785nm. No polymer, 1.8 pps
	laser 584nm max		30 min		Add beam 1, difficult to know intersection. No polymer evident

1. Tetraphenylporphine : naphthalene sulfonyl chloride mole ratio 1:20. Solution approx 3×10^{-5} $\underline{M}$ TPP
2. TMPTA - trimethylolpropane triacrylate: MMA - methyl methacrylate - vol. ratio 65:35
3. Degas using 4 freeze (LN_2)/thaw cycles, sample solution remains under vacuum for irradiation
4. See fig 38 for filter transmission curve
5. Molectron UV24-DL14 laser with Molectron dye #8, approx. 75 μJ @ 24 pps
6. Light source is a Xe arc lamp, beam wavelength content controlled by a monochromator
7. Phase R DL1200V laser with R6G dye. .5 μ sec delay between pulse 1 and pulse 2
8. Molectron UV24-DL14 laser with IR dye @ 785nm.

no bubbling occurred from either beam, and no solution color change resulted. The only polymer formed were a small deposit on the far beam 1 cell wall and on the incident beam 2 cell wall.

Using a monochromator greatly reduces the amount of energy available during any fraction of a second within the beam. Another laser was installed to supply beam 1. The two lasers were synchronized so beam 2 was produced approximately .5 microsec. after beam 1. This delay is well within the reported triplet lifetime for TPP (pg48). Runs 4 to 7 were performed to observe the effects changes in pulse rate and lasing time had on the formation of polymer. The results indicated that a single beam polymerization step was occurring from beam 2. This can be explained by the overlap of singlet and triplet absorption at 460nm. for TPP. No beam 1 polymerization was evident, but no two beam polymerization was evident either. This may be the result of the comparatively low energy output of laser 1.

To resolve the beam 2 polymerization problem, the 460nm dye in laser 2 was replaced by Exciton DOTC Iodide, a dye lasing at 785nm. Run 8 shows that this change did eliminate beam 2 polymerization, however it is also at a cost of beam 2 energy and being in the IR region of the spectrum the beam is not visible, which complicates attempts to focus and align the intersection of the two beams. Fortunately there is also a visible pulse which is produced by laser 2 so the IR beam location is predictable. The relative positioning of the two beams from laser 2 was determined by using a fiber optic and spectrometer to measure the energy at different locations.

Increasing the power of beam 1 was accomplished by improving the efficiency of the cooling system of laser 1 and further optimization of the laser itself.

The lack of visible amounts of polymer being formed by the two beam process is a continuing problem. For this two beam polymerization process to be acceptable, ample polymer should be formed, within the 5 min. irradiation times at each step, to have a visible amount of polymer present. One approach suggested to solve this problem was to include in the sample solution a large molecular weight molecule which has already undergone some cross linking. Materials which are comprised of 2 to 10 moles of a monomer are referred to as oligomers.[24] The purpose of the oligomer in solution is to increase the mass of polymer formed for each cross link event. Therefore if free radical formation is less than expected, the mass of polymer formed can be increased. One consideration which must also be noted is that introduction of large molecules which contain few vinyl groups also reduces the concentration of C=C per volume of solution as well as reducing the opportunity for TPP T_n collision with NSC. The oligomer selected for this study was PS169 (see pg. 33).

Irradiation of TPP+NSC in TMPTA+MMA+PS169: Due to the very viscous nature of PS169, the sample solutions were prepared on a weight basis as compared to a volume basis as was previously done. Considerable mixing with a glass stir rod was needed to obtain a uniform mixture of these three components. This mixing was done prior to addition of the TPP+NSC/$CHCl_3$ aliquots. Further mixing employed an argon stream.

Two different solutions were originally prepared for study. These were MMA:TMPTA:PS169 in weight ratios of 35:65:35 and 35:65:65. See Table 16 for irradiation results. Runs 1 to 3 used the first solution composition and Runs 4 to 6 the latter.

The irradiation conditions for Runs 1 and 2 were essentially the same, with the major difference in the time spent on each irradiation point within the sample solution. Neither run resulted in any visible polymer formed although when methanol was added to the solution and it was mixed vigorously some polymer 'strings' (approx. .5cm in length) were seen within the solution. Whether this was the actual shape of the polymer formed or was the result of the mixing is not known. Generally, when no deposit is evident on the incident cell wall surfaces the appearance of polymer 'strings' has been the result of mixing. This does however indicate that some two beam polymerization may have occurred.

In Run 3 the TPP:NSC ratio was changed to 1:100 to increase the probability of the energy transfer collisions occurring between TPP T_n and NSC. Another physical change within the sample cell was the addition of pyrex beads. The purpose of the beads was to present a surface to which the polymer may be attached, thus eliminating the necessity to angle the sample cell or work near the bottom of the cell where there is much refraction. The energy content of both beam 1 and beam 2 had been substantially increased. Despite all these changes which should promote polymerization, no polymer was visible.

The sample solution remained in the dark for the following 6 days and when the solution was next observed the color had changed from

Table 16: Irradiation of TPP+NSC[1] in TMPTA[2]+MMA[2]+PS169 with Vacuum Degas II[3]

Run	Beam 1[4]	Beam 2[5]	Time	Polymer	Comments: Sample cell movement approx. 100μ/step. Laser 2 delay approx. 5 μsec
					Runs 1 and 2 same sample. MMA:TMPTA:PS169 (35:65:35 by wt)
1	laser 584nm max	laser 785nm	5 min	no	1.2pps, beam 1 approx. 25μJ, beam 2 approx. 4μJ, 10 sec/step. build polymer from rear cell wall. No single two-beam polymer apparent
2	laser 584nm max	laser 785nm	60 min	no	1.5pps, beam 1 approx. 3μJ, beam 2 approx. 4μJ, 5 min/step. build polymer from bottom of cell. No single or two-beam polymer apparent
					After Runs 1 and 2, methanol added to sample solution, some fine polymer "strings" evident.
3	laser 584nm max	laser 785 nm	60 min	no	1.4pps, beam 1 approx. 112μJ, beam 2 approx. 14μJ, 5 min/step. NSC:TPP 100:1 build polymer on beads. After six days storage in dark, color change from pinkish to yellow.
					Runs 4 to 6 same sample. MMA:TMPTA:PS169 (35:65:65 by wt.)
4	laser 584nm max	laser 785nm	15 min	no	1.2pps, beam 1 approx. 25μJ, beam 2 approx. 4μJ, 30 sec/step. build polymer from rear cell wall. No single or two-beam polymer apparent
5	laser 584nm max	laser 785nm	60 min	no	1.5pps, beam 1 approx. 35μJ, beam 2 approx. 4μJ, 5 min/step. build polymer from bottom of cell. No single or two-beam polymer apparent
6	laser 584nm max	laser 785nm	60 min	yes	1.3pps, beam 1 approx. 112μJ, beam 2 approx. 9.5μJ, 5 min/step. build polymer from bottom of cell. Polymer deposit on bottom of cell appears to be from beam 1 only.
					Runs 7 and 8 are same sample solution, Runs 9 and 10 are same sample solution.
7	--	laser 490nm	10 min	yes	3pps, beam 2 only, MMA:TMPTA:PS169 (1:1:2 by wt.) NSC:TPP, 100:1. Polymer formed, seems to be more than other beam 2 in MMA+TMPTA solutions
8	laser 584nm max	laser 785 nm	90 min	no	1.5pps, beam 1 approx. 110μJ, beam 2 approx. 7.5μJ, 5 min/step. No single or two-beam polymer apparent.
9	--	laser 490nm	10 min	yes	3pps, beam 2 only, MMA:TMPTA (1:1 by wt.) NSC:TPP, 100:1 polymer formed, less than in Run 7. Sample solution green
10	laser 584nm max	laser 785nm	90 min	no	1.5pps, beam 1 approx. 110μJ, beam 2 approx. 7.5μJ, 5 min/step. No single or two-beam polymer apparent

1. Tetraphenyl porphine: Naphthalene sulfonyl chloride mole ratio 1:20 unless stated otherwise. Sample solution 3×10^{-5} M in TPP.
2. TMPTA - trimethylolpropane triacrylate, MMA - methyl methacrylate, PS169 - see page 33.
3. Degas using 4 freeze (LN_2)/thaw cycles, sample solution remains under vacuum for irrotion.
4. Phase-R laser, triaxial flashlamp, R6G dye
5. Molectron UV24-OL14 laser

pinkish to yellow. A visible spectrum indicated a change similar to that shown in Figure 39. This result should answer the question as to whether O_2 is necessary for this change to occur. The presence of O_2 does not induce this color change, but a large excess of NSC does seem to promote a chemical change within the sample solution. Again there is no indication of polymerization accompanying the color change.

Runs 4 and 5 were also unsuccessful as far as two beam polymerization. An increase in the weight fraction of PS169 in the solution does not noticeably affect the polymerization rate. Run 6 however did result in some polymer being formed but it was from beam 1 only.

New sample solutions were prepared for the last 4 runs. A control solution of MMA+TMPTA (1:1 by weight) was compared to a solution of MMA+TMPTA+PS169 (1:1:1 by weight). Again the mole ratio of TPP:NSC was 1:100. After the solutions had been degassed they remained in a dark cabinet for 4 days.

Prior to the start of irradiation trials on the samples, a change in color was noticed in the control solution. The solution was green and approximately 80% of the sample had polymerized. No color change had occurred within the sample containing the PS169. Further study with solutions of TPP+NSC (1:100 mole ratio) in MMA, TMPTA, MMA+TMPTA and MMA+TMPTA+PS169 showed that the spectra of the first three solutions were similar and displayed a shift in intensity of the peaks as noticed before. The MMA+TMPTA+PS169 solution had a spectrum the same as TPP itself. This further supports the idea that the presence of a large excess of NSC in the presence of TPP causes the formation of a

TPP+NSC complex or TPP chlorination. What role the PS169 plays in counteracting this occurrence is not known. This also raises the question as to how useful the TPP/NSC photosensitizer system is for the two beam process being studied.

F. Summary of Experimental Results.

The photoinitiators used for the photopolymerization studies all exhibited the same undesirable characteristic of single-beam polymerization. An exact cause for this cannot be stated without knowing the triplet-triplet absorption spectra of the photoinitiator compounds. The parent compounds, tetraphenyl porphine (TPP) and protoporphyrin IX dimethyl ester (PPDME), both have considerable overlap of their singlet-singlet and triplet-triplet absorption spectra so it was probable that the brominated compounds have this overlap as well.

An additional problem with the $TPPBr_X$ and $PPDMEBr_X$ photoinitiators was the shift to the $TPPBr_3$ and $PPDMEBr_4$ forms when in solution with the monomer trimethylolpropane triacrylate (TMPTA). The results of the photochemical irradiation stability tests indicated that this shift did not occur in the solvent, $CHCl_3$, so it was a result of the presence of the TMPTA monomer.

These findings limited the value of the photoinitiators synthesized for the particular monomer systems considered in this study. The photoinitiators should not, however, be eliminated from further consideration with different monomer systems.

The TPP+NSC photosensitized system in the monomer TMPTA also gave single-beam polymerization. Adjustment of the monomer solution composition with methyl methacrylate (MMA) and changes in the irradiation source eliminated this problem. One cause of inconsistent results was the presence of O_2 in the sample solution. This problem was controlled by degassing the sample solution and maintaining it under vacuum during the irradiation trials.

In order to increase the efficiency of the energy transfer from the photosensitizer to the initiator, an excess of initiator is required. In the TPP+NSC system studied, it was found that a 20:1, NSC:TPP, mole excess did not cause any changes in the sample solution but a 100:1, NSC:TPP, mole excess caused a change in the spectral properties (color change) of the solution. In the TMPTA/MMA monomer solution the color change was followed by polymerization, prior to irradiation. Addition of the oligomer PS169 to the TMPTA/MMA solution inhibited the color change, and provided a high molecular weight material in the sample solution to increase the mass of polymer formed per each cross-link event.

Two-beam polymerization was accomplished with the TPP+NSC system, resulting in a yellow-green polymer from the pinkish sample solution. However, additional trials repeated under the same conditions, resulted in no two-beam polymerization.

IX. SINGLE-BEAM POLYMERIZATION RATE STUDY

The inability to attain two-beam photopolymerization on a measurable scale eliminated the possibility of obtaining any polymerization rate information. However, with the TPP+NSC photosensitized system and knowledge of the TPP singlet-singlet and triplet-triplet absorption spectra (Fig. 6) some information could be obtained from the single-beam photopolymerization at 460nm. The purpose was to determine whether the mechanism of the single-beam polymerization reaction was the result of the absorption of one or two photons by the TPP system, because of the overlap of the S-S and T-T spectra, as well as to obtain some polymerization rate information.

The Molectron UV24-OL14 pulse dye laser was used as the beam source because of its capability to be more accurately tuned to a given wavelength and its consistent energy output. Sample preparation followed the procedures used in the previous irradiation trials. Because of the spontaneous polymerization which occurred with a TPP:NSC mole ratio of 1:100, the sample was comprised of 1:20 mole ratio TPP:NSC in TMPTA:MMA at a 65:35 volume ratio. For consistency with the previous polymerization studies it was necessary to eliminate O_2 in the sample, so the samples were degassed and maintained under vacuum as before.

A number of alternate approaches were considered for controlling the total irradiation of the sample. To measure the relationship between the amount of polymer formed and the total incident photon exposure, could be accomplished in the following ways:

1. For a selected laser pulse rate, the irradiation time period could be changed.

2. For a selected irradiation time, the laser pulse rate could be varied for different trials.

3. For a selected laser pulse rate and a constant irradiation time, attenuate the beam energy incident to the sample using combinations of neutral density filters.

Because of the small amounts of polymer formed, accurate quantitative results could not be achieved by weighing the polymer. The polymer formed by the single-beam irradiation is physically attached to the inside cell wall, and forms a "finger" which extends into the sample solution along the path of the beam. The relative amounts of polymer formed could be compared most easily by conducting the trials in close proximity to each other within the same sample cell and measuring the dimensions of the "fingers" formed in each case. The trials were conducted in a vertical sequence within the sample cell, with approximately 1mm separating the incident beam positions.

Initially, approach number 1 listed above was used. The purpose was to measure the amount of polymer formed as the solid propagated into the sample solution as a function of irradiation time. Time periods of 45, 30 and 15 minutes and a pulse rate of 2pps were used for these trials. The results indicated that there was a limit to the amount of polymer formed by this single-beam process. The 45 and 30 minute irradiation times resulted in approximately equal amounts of polymer being formed, and the 15-minute irradiation time polymerized very nearly the same amount. Rather than reducing the irradiation times to 5, 10 and 15 minutes, the pulse rate was reduced 1pps. This pulse rate proved to be near the lower limit of the Molectron laser and an unacceptably high rate of misfiring resulted.

Some interesting observations and conclusions resulted from these irradiation trials. One was the shape of the polymer "finger" formed. Rather than being a uniform cylindrical projection from the cell wall, the polymer formed in a shape which was indicative of polymerization in a radial direction as well as along the axis of the beam, as shown in figure 39 .

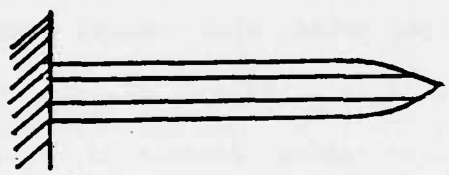

FIGURE 39: SHAPE OF POLYMER PROJECTION

A denser inner polymer core was surrounded by less dense polymer. The propagating end of the polymer formed was tapered, indicating that polymerization was occurring more rapidly in the center of the beam than at the edges of the beam.

A second observation was the relative amount of beam dispersion in the sample solution which was evident as the amount of polymer formed increased. More polymer resulted in more beam dispersion. This information was used subsequently to estimate the relative degree of polymerization achieved.

The second approach tried was to vary the pulse rate and maintain a uniform irradiation time. The irradiation time was reduced to 8 minutes and the pulse rates selected were 2pps, 3pps and 4pps. These trials gave the desired visual variations in length of polymer formed but they also displayed a variation in the beam diameters for different pulse rates, which was not desirable. The 4pps beam was the largest in diameter and the 2pps beam the smallest. These differences in diameter and the resulting photon density variations within the beams did not permit a valid comparison of the relative sizes of the polymer formed. The third approach was then tried and was found to be an acceptable method to obtain the information desired.

Using a laser pulse rate of 2pps with an energy content of approximately 56μJ per pulse, with neutral density filters to give beam energy attenuations of 20%, 50% and 75%, and an irradiation time of 12 minutes, the trials proceeded. Because of the noticeable changes in beam dispersion as the amount of polymer formed increases, an attempt was made to correlate the two variables. This was done by monitoring the power of the beam transmitted through the sample, I(t). A decrease in transmitted power would indicate an increase in polymer formed. To do this, a photomultiplier tube was located behind the sample and in line with the laser beam. A lens focused the beam leaving the sample cell onto the photomultiplier tube detector. The signal from the detector was sent to an oscilloscope from which the pulse power value was obtained. Readings were taken at 15-second intervals during the 12-minute irradiation time. The power readings were normalized to the energy transmitted through the sample at time equal zero. A plot of I(t)/I(o) vs. time is shown in Figure 40 for each amount of beam

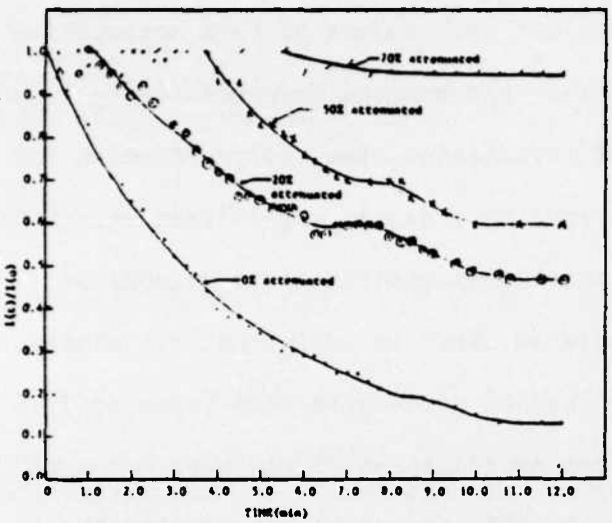

FIGURE 40: I(t)/I(o) VS. TIME

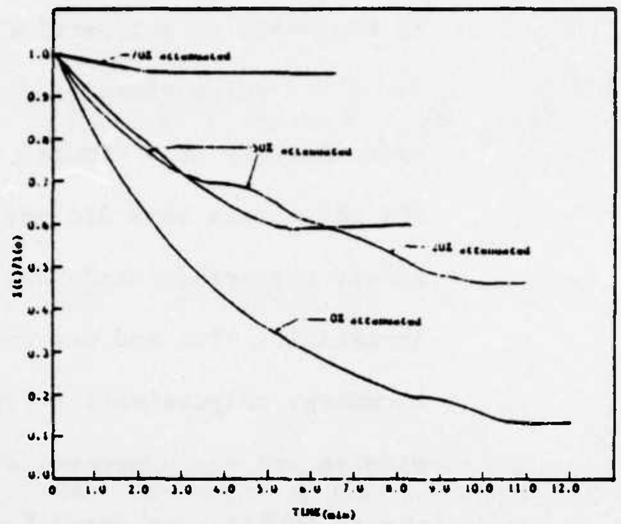

FIGURE 41: I(t)/I(o) VS. TIME NORMALIZED TO START OF POLYMERIZATION

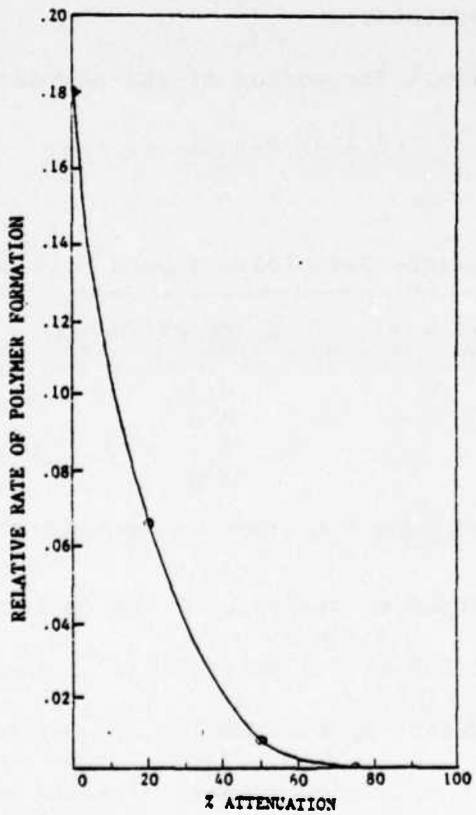

FIGURE 42 : RELATIVE RATE OF POLYMER FORMATION VS. % ATTENUATION

attenuation. Figure 41 shows the curve normalized to time equal zero, as the onset of polymerization for each amount of beam attenuation.

Polymerization for the unattenuated beam was completed after approximately 10.5 minutes of irradiation time. Polymerization for the 20% attenuated beam did not occur to a degree significant enough to affect the transmitted beam until approximately 1.25 minutes of irradiation time and was completed after an additional 9.5 minutes. Likewise, polymerization for the 50% attenuated beam began at 3.75 minutes and was completed after an additional 7 minutes. No significant change in I(t) was noted for the 75% attenuated beam during the 12 minute irradiation period. A plot of % attenuation vs. polymerization time showed an exponential correlation between the photon flux and the rate of polymerization.

A visual inspection of the polymer formed provided the physical data listed in Table 17.

Table 17: Single Beam Polymer Data - 12 min. Irradiation Time

% Attenuation	Diameter(mm)	Length(mm)
0	0.9	3.0
20	0.6	2.2
50	0.2	1.5
75	0.0	0.0

A graphical analysis of the individual curves in Figure 41 indicated that 50% of the polymerization that occurred during each experiment required approximately 2.0, 2.2, and 1.7 minutes for the 0%, 20% and 50% attenuations, respectively. An estimate of polymer formed based on the information in Table 17, gives relative quantities of polymer formed of .33 for 20% and .025 for 50% attenuation based the amount of polymer formed with 0% attenuation as 1.0. A plot of polymer formed per minute vs. % beam attenuation is presented in Figure 42. This shows how the relative rate of polymer formation was affected by % beam attenuation, for the conditions in this study.

If the single-beam photopolymerization process which occured was a two photon process, a reduction in incident beam energy by a factor of 2 should result in a reduction of the amount of polymer found by a factor of 4. The data collected indicates a reduction by a factor of 3 for the 20% attenuated beam and a factor of 40 for the 50% attenuated beam. The polymerization process occurring clearly is not solely a two-photon process.

X. CONCLUSIONS

1. Knowledge of a compounds singlet-singlet and triplet-triplet absorption spectra is of primary importance in studying molecules to act as photoinitiators or photosensitizers in this two-beam system. This is essential to reduce the amount of time spent in locating proper wavelengths for beams 1 and 2.

2. The two-beam polymerization system being considered is a viable system. Although limited success has been achieved in actually producing a two-beam polymerization process, much work has been done to better describe the requirements of such a system.

3. To better understand the single-beampolymerization process and develop ways to better control it, triplet-triplet spectra are necessary for the photoinitiators.

4. Problems associated with the sample solution preparation have essentially been eliminated. The ability to obtain consistent results by having the sample solution remain under vacuum during the irradiation period will be very beneficial to future irradiation trials.

5. The undesirable spectral shifts of the TPP/NSC photosensitized system make it a questionable candidate for further study. The effect of the presence of PS169 does however introduce another approach for controlling the TPP/NSC spectrum shifts.

XI. RECOMMENDATIONS FOR FUTURE WORK

Recommendations for future work are summarized as follows:

1. Increase energy input into the sample solution. Having identified wavelengths from beam 1 and beam 2 which apparently do not cause polymerization individually, further work should be done to optimize the laser energy output from each laser. For the Phase R DL1200V laser, this involves more completely controlling the dye temperature and flow conditions and the cooling water temperature and temperature differential between dye and cooling water. For the Molectron UV24-OL14 laser, optimizing internal alignment of the beam and increasing the quantity of dye in the curvettes are the main adjustments possible.

2. Study the possibility of arranging a set of mirrors to reflect the laser beams back into the sample to achieve multiple passes for each laser pulse. This would essentially increase the number of pulses without increasing the rate of degradation of the dye solutions.

3. Studies should be performed using chloromethylnaphthalene as an initiator with TPP as a photosensitizer. This would further elucidate the value of TPP as a photosensitizer.

4. Change the monomer composition of the sample solution. This has been suggested and some work has begun in this direction. The primary purpose is to add a large molecular weight digomer to the solution, thereby, more rapidly increasing the mass of polymer formed. More work should be done using different sample solution compositions as well as a range of TPP:NSC ratios.

5. Increase the concentration of TPP, to increase the population of triplets. Large increases in TPP concentration may also require that a method be devised to rotate the sample to compensate for the increase in absorption.

6. Additional photosensitizers and photoinitiators should be considered. Having identified some of the problems which are encountered in this two-beam system, new candidates can be selected with these considerations in mind.

APPENDIX

XII APPENDIX A.1 PHOTOINITIATOR PREPARATION PROCEDURES

The apparatus configuration used for the following photoinitiator preparations was the same for all synthesis and can be in Fig. 43. All procedures were performed in a fume hood and under red light illumination to avoid excitation of the product molecules.

Preparation of Brominated Protoporphyrin IX Dimethyl Ester.

100 mg. of PPDME was dissolved in 35 ml. of $CHCl_3$ in a 50 ml 3-neck round bottom flask equipped with a gas outlet adapter, thermometer, magnetic stir bar and a 10 ml chromatographic column. The flask was placed in a dry ice/propanol bath and the solution was chilled to -30°C to -20°C while being stirred. Prior to the reduction of temperature, the system was flushed with argon and was maintained in an argon atmosphere throughout the bromination reaction. A solution of Br_2 in $CHCl_3$ was added (25:1 mole excess Br_2:PPDME) dropwise over a period of 30 minutes. The reaction mixture temperature was maintained at -30°C to -20°C throughout the addition. After the Br_2 had been added the mixture was allowed to come to room temperature and was stirred for an additional 1 hour. At this point, the reacted solution was transferred from the reaction vessel to a 100 ml round bottom flask. The $CHCl_3$ and unreacted Br_2 were removed using a rotoevaporator and a slightly warm water bath. The remaining solid was redissolved in $CHCl_3$ and again rotoevaporated to remove the liquid. The dark purple

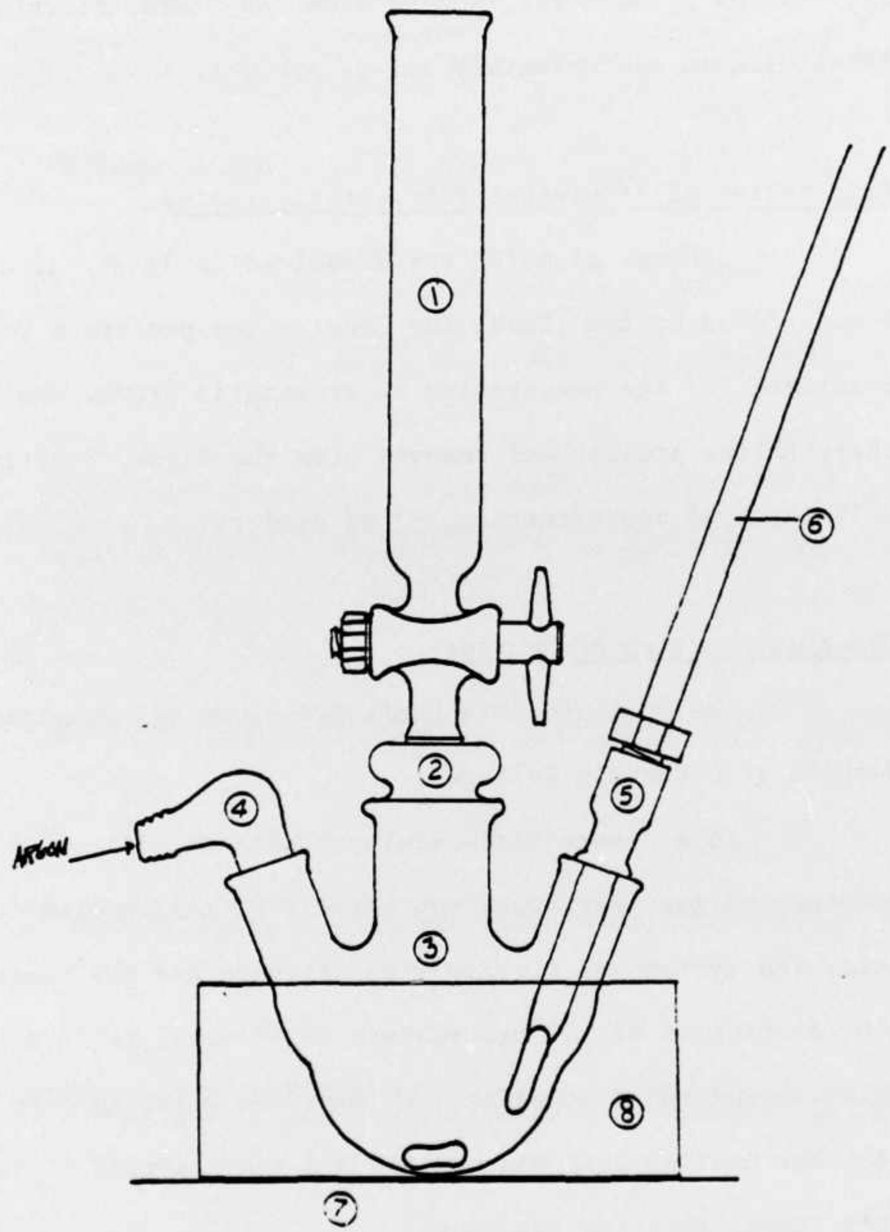

1. KONTES Bantam-ware 10 ml Chromatographic Column
2. 19/22 - 14/20 Bushing Adapter
3. KONTES Bantam-ware 50 ml 3-neck Flask
4. 14/20 Outlet Adapter
5. 14/20 Ace-Thread Adapter
6. -100°C to 50°C Thermometer
7. Corning PC 353 Magnetic Stirrer

FIGURE 43: SYNTHESIS APPARATUS

crystalline product was removed from the flask. Starting with 100 mg PPDME yielded approximately 217 mg product.

Preparation of Brominated Tetraphenylporphine.

100 mg. of m-TPP was dissolved in 35 ml. of $CHCl_3$ in a 50 ml 3-neck round bottom flask. The bromination procedure was the same as described for the preparation of brominated PPDME. The dark purple chrystalline product was removed from the flask. Starting with 100 mg m-TPP yielded approximately 137 mg product.

Chlorosulfonation of Rubrene.

The following synthesis procedure was provided by Dr. Jerry Jenkins of Otterbein College.

To a 3-neck flask equipped with an additional funnel, thermometer and gas inlet tube was added 3 ml (45 mmol) of chlorosulfonic acid. The system was flushed with nitrogen and the reagent coolec to 0°C. A solution of 100 mg. rubrene (0.19 mmol) in 10 ml of methylene chloride was added dropwise with magnetic stirring over a period of 25 min. The cooling bath was removed and the reaction mixture stirred at room temperature for two hours.

The mixture was quenched by slowly pouring onto crushed ice. The layers were separated and the aqueous layer was extracted several times with CH_2Cl_2 or EtOAc. The combined bright yellow crganic layers were dried over $CaSO_4$. Filtration and removal of solvent afforded a yellow-brown solid.

Recrystallization of crude material was accomplished by dissolving in a minimum of hot EtOAc and adding pentane to the cloud point.

Chlorosulfonation of Tetraphenylporphin.

Three ml. of $ClSO_3H$ were placed in a 50ml 3-neck round bottom flask. The flask was purged with argon and maintained under an argon atmosphere. The cooling bath temperature was reduced to -20°C using propanol/dry ice. A solution of 100 mg m-TPP in 35 ml. of CH_2Cl_2 was added dropwise, with continuous stirring. The addition was completed in 15 minutes and resulted in a deep green solution. The cooling bath was removed and the reaction mixture was stirred for an additional 2 hrs. The resulting mixture was quenched by cautiously pouring it onto approximately 25 g. of crushed ice. The organic layer was separated and the aqueous layer was washed with 3 portions of CH_2Cl_2. A large amount of emulsion-like material formed at the interface. This material was insoluble in EtOAc, $CHCl_3$ and benzene, but was very soluble in acetone. The combined organic layers were washed with a saturated aqueous $NaHCO_3$ solution, then dried over $MgSO_4$. Decanting and filtering the liquid was followed by removal of the solvent using a rotoevaporator. The final product was a very small amount of purple solid. A visible spectra was run, see table __. Due to the small amount of product formed this process was deemed not acceptable.

XIII. APPENDIX A.2 USEFUL RELATIONS IN ENERGY CALCULATIONS

$$E \text{ (energy of a single photon)} = h \ = \frac{hc}{\ } \tag{1}$$

where $h = 6.62\text{x}10^{-34}$ Joule sec (Planck's constant)

$c = 3.00\text{x}10^{8}$ m/sec (speed of light in vacuum)

$$\text{I Einstein} = 6.02\text{x}10^{23} \text{ photons} = 1 \text{ mole of photons} \tag{2}$$

$$E \text{ (kcal/mole)} = \frac{2.86\text{x}10^{4}}{\text{(nm)}} \tag{3}$$

$$E \text{ (k.j./mole)} = 4.184\text{x}E \text{ (Kcal/mole)} = \frac{1.19\text{x}10^{5}}{\text{(nm)}} \tag{4}$$

$$1 \text{ Watt} = 1 \text{ Joule/sec} \tag{5}$$

$$N \text{ (number of photons)} = \frac{\text{(nm)}}{1.986\text{x}10^{-16}} \text{ photons/Joule} \tag{6}$$

XII. BIBLIOGRAPHY

1. McGinniss, V.D., Provder, T., Kuo C. and Gallopo, A., "Macromolecules", 11, 393 (1978).

2. Turro, Nicholas J., Modern Molecular Photochemistry, Benjamin/Cummings Publishing Co., Inc., Menlo Park, Calif., 1978, pp. 628.

3. Hercules, D.M. (Ed), Fluorescence and Phosphoresence Analysis, Wiley-Interscience, New York, 1966, pp. 258.

4. Lewis, G.N. and Kasha, M., "J. Am. Chem. Soc.", 67, 1232 (1944)

5. Lesclaux, R. and Joussot-Dubien, J. in Organic Molecular Photophysics, Vol. I, ed. Birks, J.B., Wiley, New York, 1973, pp. 600.

6. Dorizon, P. and Ptak, M., "J. Chem. Phys.", 61, 1681 (1964)

7. McGinnis, V.D., in Developments in Polymer Photochemistry-3, ed., Allen, Norman S., Applied Science Publishers Ltd., Essex, England

8. Rust, J.B., "Photopolymers-Principles, Processes and Materials", Technical papers, SPE, Mid-Hudson Section, October, No. 55 (1970)

9. Rollefson, G.K. and Burton, M. (Eds.), Photochemistry and the Mechanism of Chemical Reactions", Prentice-Hall, New York (1942)

10. Jenkins, A.D. and Ledwith, A. (Eds.), Reactivity, Mechanism and Structure in Polymer Chemistry, John Wiley, New York (1974)

11. Leermakers, P.A. and Weissberger, A. (Eds.), Technique of Organic Chemistry, Vol. XIV, Interscience, New York (1969)

12. Murov, S.L. (Ed.), Handbook of Photochemistry, Marcel Dekker, New York (1973), pp. 272.

13. McClure, D.S., Blake, N.W. and Hanst, P.L., "J. Chem. Phys.", 22, 255 (1954)

14. Ermolavev, V.L. and Svitashev, K.J., "Opt. Spect.", 1, 399 (1959)

15. Gijman, O.L. et al, "Trans. Farad, Soc. II", 70, 708 (1973)

16. Merkel, P.B. and Kearns, D., "J. Chem. Phys.", 58, 398 (1973)

17. Schwerzel, R., in "Three-Dimensional Photochemical Machining with Lasers", Battelle Columbus Laboratory Technical Report, Nov. (1983).

18. McGinnis, V.D., in "Three-Dimensional Photochemical Machining with Lasers", Battelle Columbus Laboratory Technical Report, Nov. (1983)

19. Lady, E.L. Precision Investment Casting, Reinhold Pub. Corp., New York (1948)

20. Goutermann, M. and Khalil, G.E., "J. Molecular Spectroscopy", 53, 88 (1974)

21. Samuels, E. et al., "J. Chem. Soc. (c)", 145 (1968)

22. Brandrup, J. and Immergut, E.H., Polymer Handbook, Interscience Publishers, New York (1966)

23. Moore, J.E., Schrocter, S.H., Shultz, A.R. and Stang, L.D., "Colorimetric Analysis of Photopolymerization", in Ultraviolet Light Induced Reactions in Polymers, ed. Labana, S.S., ACS Symposium Series No. 25, American Chemical Society, Washington, D.C. (1976)

24. Solomons, T.W. Graham, Organic Chemistry, 2nd ed., John Wiley, New York, 1980, pp. 1066.

XV. ACKNOWLEDGEMENTS

The author wishes to thank Dr. Robert E. Schwerzel for his guidance in this research project, his valuable assistance in helping me understand the concepts contained in this thesis and his many helpful comments in preparing this manuscript.

Many thanks also to Dr. Kent Knaebel for his assistance in the organization of the thesis paper.

Dr. Jerry Jenkins is gratefully acknowledged for his guidance and assistance in organic synthesis and experimental techniques.

Many thanks to William Ivancic for his assistance and the availability of his laser laboratory for experimental work.

Thanks also to Dr. Vincent McGinnis for his suggestions and providing the monomer and photosensitizers used in this study.

The support from Battelle and the U.S.Air Force Office of Scientific Research and Ohio State University is gratefully acknowledged.

END

FILMED

7-85

DTIC